

**Optimizing epigenetic therapies
of hematological malignancies: identification of
novel epigenetic biomarkers and mechanistic
study of 5-aza-2'-deoxycytidine**

Dissertation

zur Erlangung des Grades des
Doktors der Naturwissenschaften

der Naturwissenschaftlich-Technischen Fakultät III Chemie,
Pharmazie, Bio- und Werkstoffwissenschaften der Universität des
Saarlandes

Vorgelegt von
Diplom Biologe Karius Tommy

Saarbrücken, im Oktober 2011

Datum des Kolloquiums: 24 April 2012
Dekan: Prof. Dr. W. F. Maier
Vorsitzender: Prof. Dr. M.J. Schmitt
Berichterstatter: Prof. Dr. J.E. Walter
Prof. Dr. E. Meese
Akad. Mitarbeiter: Dr. G.-W. Kohring

Acknowledgement

First and foremost I would like to express my sincerest gratitude to my supervisor Prof. Dr. Jörn Walter for his confidence in me and would like to thank him that he gave me the opportunity to do this thesis.

I would like to thank Prof. Dr. Eckart Meese who accepted without hesitation to evaluate my thesis.

I am very grateful that the head of the “Laboratoire de biologie moléculaire et cellulaire du cancer (LBMCC)” in Luxembourg Dr. Marc Diederich immediately agreed to do this external thesis and gave me the opportunity to work in his laboratory. This thesis would have not been possible without the encouragement, guidance and valuable assistance of my supervisor in Luxembourg Dr. Michael Schnekenburger.

This work would not have been possible without the financial support of: “Télévie Luxembourg”, “Fondation de recherche cancer et sang (FRCS)”, Recherches Scientifiques Luxembourg (RSL)”, the action “Lions vaincre le cancer Luxembourg”, “Een Häerz fir kriibskrank Kanner” and the National Research Fund Luxembourg.

Collective and individual acknowledgements are also owed to my colleagues at the LBMCC for their cooperation during this thesis. I would like to address special thanks to the epigenetics group (Cindy, Cristina, Carole and Guillaume) for stimulating scientific discussions, technical assistance and encouraging words during coffee breaks. Many thanks go also to all the LBMCC PhD students who were in one way or another supporting me at my work. Moreover, I would like to thank Estelle Henry for her important cell culture work and Anthoula Gaigneaux for her helping hand during the bioinformatical processing of the results.

Moreover, I would like to mention the members of the epigenetics laboratory at the University des Saarlandes in Saarbrücken and thank them for the warm welcomes at each of my numerous visits. To Dr. Sascha Tierling, thanks for the offer to do a practical training in Saarbrücken and to learn more about deep-sequencing. I would like to thank Nicole Jundel for her help with the paperwork that was necessary for this thesis.

Words fail me to express my appreciation to my girlfriend Anne Ruppert, whose dedication, love and persistent confidence in me allowed me to sustain the ups and downs during the last few years.

I would also like to thank my family for their assistance and support throughout all my studies at the University.

Finally, I offer my regards to all of those who supported me in any respect during the completion of this thesis.

Karius Tommy
Luxembourg, October 2011

**“Give every day the chance to become the most
beautiful day in your life”**

Mark Twain (* 30. 11. 1835 - † 21. 04. 1910)

ACKNOWLEDGEMENT	II
1. INTRODUCTION.....	1
1.1. EPIGENETICS HISTORY	1
1.2. EPIGENETICS	3
1.2.1. <i>Histone modifications</i>	3
1.2.2. <i>DNA modifications</i>	7
1.2.3. <i>RNA-mediated gene regulation</i>	12
1.2.4. <i>Cross talk of epigenetic modifications</i>	16
1.3. NORMAL AND MALIGNANT HEMATOPOIESIS	18
1.4. EPIGENETIC ALTERATIONS IN HEMATOLOGICAL MALIGNANCIES	22
1.5. DNA METHYLATION IN THE MANAGEMENT OF BLOOD CANCER.....	31
1.6. DNA METHYLATION AS A THERAPEUTIC TARGET	35
1.7. GLUTATHIONE S-TRANSFERASE P1	40
1.8. PROSTAGLANDIN-ENDOPEROXIDE SYNTHASE 2	43
2. HYPOTHESIS AND AIM OF THIS THESIS	48
3. MATERIAL.....	50
3.1. CHEMICALS.....	50
3.2. BUFFERS AND SOLUTIONS.....	52
3.2.1. <i>General buffers</i>	52
3.2.2. <i>Gel electrophoresis</i>	52
3.2.3. <i>Western Blot</i>	52
3.2.4. <i>Nuclear extraction</i>	53
3.2.5. <i>Acid extraction</i>	53
3.2.6. <i>Cross-linking chromatin immunoprecipitation</i>	53
3.3. KITS.....	54
3.3.1. <i>Extraction/Purification</i>	54
3.3.2. <i>Bisulfite conversion</i>	54
3.3.3. <i>Microfluidic Lab-on-a-Chip application</i>	55
3.3.4. <i>DNA quantification</i>	55
3.3.5. <i>Western Blot</i>	55
3.3.6. <i>Purification and separation of blood cells</i>	55
3.3.7. <i>Analysis of GST activity</i>	56
3.3.8. <i>Analysis of cell proliferation</i>	56
3.4. MEDIA	56
3.4.1. <i>Mammalian cell culture</i>	56
3.4.2. <i>Bacterial culture</i>	56
3.5. CELLS	57
3.5.1. <i>Mammalian cell lines</i>	57
3.5.2. <i>Prokaryotic cells</i>	57
3.5.3. <i>Patient samples</i>	57
3.6. ENZYMES	58
3.6.1. <i>Endonucleases</i>	58
3.6.2. <i>Polymerases</i>	58
3.6.3. <i>Other enzymes and proteins</i>	59
3.7. OLIGONUCLEOTIDES.....	59
3.8. ANTIBODIES	66
3.9. MARKERS	68
3.10. PLASMID/CONTROL DNA	68
3.11. DEVICES AND INSTRUMENTS	68
4. METHODS	71
4.1. BIOINFORMATION	71
4.1.1. <i>Oligonucleotide design</i>	71
4.1.2. <i>CpG island identification</i>	71
4.1.3. <i>Bisulfite sequencing data analysis</i>	71
4.1.4. <i>Image analysis</i>	72
4.1.5. <i>Heat map analysis</i>	72

4.1.6.	<i>Prediction of putative miRNAs targeting GSTP1 expression</i>	72
4.2.	MICROBIOLOGY.....	73
4.2.1.	<i>Bacterial cell culture</i>	73
4.2.2.	<i>Transformation</i>	74
4.3.	CELL CULTURE.....	74
4.3.1.	<i>Storage of eukaryotic cells</i>	74
4.3.2.	<i>Culturing of eukaryotic cells</i>	74
4.3.3.	<i>Trypan blue exclusion test</i>	75
4.3.4.	<i>Cell line treatments</i>	75
4.3.5.	<i>Purification of peripheral blood mononuclear cells</i>	75
4.3.6.	<i>Separation of CD34+ cells from umbilical cord blood</i>	76
4.4.	BIOLOGICAL CHEMISTRY.....	77
4.4.1.	<i>Whole cell extracts</i>	77
4.4.2.	<i>Nuclear protein extraction</i>	78
4.4.3.	<i>Histone acid extraction</i>	78
4.4.4.	<i>Protein quantification</i>	78
4.4.5.	<i>SDS-Page</i>	79
4.4.6.	<i>Western Blot</i>	80
4.4.7.	<i>GST activity assay</i>	81
4.5.	CELL BIOLOGY.....	81
4.5.1.	<i>Indirect immunofluorescence labeling</i>	81
4.5.2.	<i>Fluorescent nucleic acid staining</i>	82
4.5.3.	<i>Cell trace proliferation assay</i>	83
4.5.4.	<i>Flow cytometry</i>	83
4.5.5.	<i>Fluorescence microscopy</i>	85
4.6.	MOLECULAR BIOLOGY.....	85
4.6.1.	<i>Electrophoretic migration</i>	85
4.6.2.	<i>Ethidium bromide staining</i>	86
4.6.3.	<i>DNA extraction</i>	86
4.6.4.	<i>DNA quantification</i>	86
4.6.5.	<i>DNA precipitation</i>	87
4.6.6.	<i>Gel extraction</i>	87
4.6.7.	<i>RNA extraction</i>	87
4.6.8.	<i>RNA quantification</i>	88
4.6.9.	<i>Determination of RNA quality</i>	88
4.6.10.	<i>Simultaneous RNA and DNA purification</i>	88
4.6.11.	<i>DNA digestion</i>	88
4.6.12.	<i>Cloning, ligation and Blue/White colony screening</i>	89
4.6.13.	<i>PCRs</i>	90
4.6.14.	<i>Bisulfite treatment</i>	97
4.6.15.	<i>Bio-CoBRA</i>	99
4.6.16.	<i>Crosslinked chromatin immunoprecipitation (X-ChIP)</i>	100
4.7.	STATISTICAL ANALYSIS.....	103
5.	RESULTS	104
5.1.	EPIGENETIC REGULATION OF GSTP1 GENE EXPRESSION IN HEMATOLOGICAL MALIGNANCIES.....	105
5.1.1.	<i>Analysis of the constitutive GSTP1 expression in human leukemia/lymphoma cell lines</i>	105
5.1.2.	<i>Effect of DAC treatment on GSTP1 expression in human leukemia/lymphoma cell lines</i>	107
5.1.3.	<i>Effect of HDAC inhibitors on GSTP1 expression in human leukemia cell lines</i> 115	
5.1.4.	<i>DNA methylation analysis of GSTP1 promoter region</i>	117
5.1.5.	<i>Analysis of the chromatin structure of GSTP1 promoter</i>	126
5.1.6.	<i>Analysis of the DAC-induced acquisition of a GSTP1 transcriptional permissive state in GSTP1 non-expressing cells</i>	128
5.1.7.	<i>GSTP1 promoter methylation status in leukemia patient samples</i>	132
5.1.8.	<i>Involvement of micro RNAs in regulation of GSTP1 expression</i>	134

5.2. DNA HYPERMETHYLATION AS A KEY PLAYER IN PTGS2 EXPRESSION SILENCING IN HEMATOLOGICAL MALIGNANCIES	137
5.2.1. <i>PTGS2</i> expression in leukemia/lymphoma cell lines and healthy blood cells .	137
5.2.2. CpG density analysis of <i>PTGS2</i> promoter and gene body.....	139
5.2.3. Methylation status of <i>PTGS2</i> promoter in leukemia and lymphoma cell lines.	141
5.2.4. Effect of DAC treatment on <i>PTGS2</i> methylation and expression.....	143
5.2.5. Methylation analysis of <i>PTGS2</i> promoter in leukemia and lymphoma patient samples	145
5.2.6. Correlation between <i>PTGS2</i> methylation and expression in samples from patients with hematological malignancies.....	146
5.3. DNA METHYLATION FINGERPRINT OF BLOOD CANCER CELLS	148
5.3.1. Methylomic profiling of hematological malignancies.....	149
5.4. ANALYSIS OF DAC TREATMENT RESPONSE IN BLOOD CANCER CELL LINES	152
5.4.1. Effect of DAC treatment on leukemia/lymphoma cell survival.....	153
5.4.2. Influence of DAC treatment on global DNA methylation in leukemia/lymphoma cells	157
5.4.3. Analysis of DAC-induced growth inhibition by a single cell approach	162
5.4.4. Simultaneous analysis of DAC-induced <i>GSTP1</i> expression and cell proliferation	164
5.4.5. Analysis of the relationship between <i>GSTP1</i> expression and methylation pattern in DAC-treated RAJI cells	166
5.4.6. Analysis of gene-specific demethylation in DAC-treated RAJI cells.....	168
5.4.7. Analysis of <i>GSTP1</i> promoter methylation recovery after DAC treatment.....	172
6. DISCUSSION.....	174
7. CONCLUSIONS AND PERSPECTIVES	196
SUMMARY	201
ZUSAMMENFASSUNG	202
REFERENCES	203
LIST OF ABBREVIATIONS.....	VII
TABLE OF FIGURES.....	XIV
LIST OF TABLES	XVI
APPENDIX	XVII
CURRICULUM VITAE.....	XXVII

1. Introduction

1.1. Epigenetics history

The ancient world was already highly interested in development and inheritance mechanisms. Philosophers as Anaxagoras or Hippocrates hold the preformation theory and preached the *homunculus* (Latin for little human) as origin of all life. One hundred years later, Aristoteles challenged this maxim with his thesis of *epigenesis* (Greek for subsequent development). He thought that embryonic development was characterized by permanent formation of new structures. This idea was revived by William Harvey in 1651 and proved by Caspar Friederich in 1796 (Wolff 1759). Both showed that the human being is developed from one fertilized egg cell. This discovery motivated embryologists as well as developmental biologists to decrypt developmental embryonic processes with microsurgical and chemical methods. Remarkably, genetics was ignored until rediscovery of Mendel's laws in the 20th century. However, at that time, genetic knowledge was insufficient to explain the link between genotype and phenotype since the main focus was on genes behavior (Hortshemke 2005).

The British scientist Conrad Hal Waddington brought about a rebound by accentuating the importance of genetics in all domains of biological research and thus juggling genetics and developmental biology (Waddington 1942). He described inheritance and development as a discussion between the genetic information and environment. According to him, the one-dimensional interpretation of genes was insufficient to explain development. Thus, it must exist something '*epi*', over or upon genes (*genea*, greek for descent, race). From his point of view, the zygote possesses preformed characteristics that interact during early development to form through *epigenesis* an adult life form (Haig 2004). Therefore, Waddington joined the terms *epigenesis* and genetic to coin epigenetic. Hence, he defined for the first time the department of science that analyses the causal interaction between genes (genotype) and their products (phenotype) (Waddington 1942; Moch 2004). Attention should be paid to the fact that Waddington established this revolutionary idea without

the knowledge that genes encode proteins. Not until three years later, the paradigm of one gene-one enzyme was published (Beadle and Tatum 1941).

To illustrate his concept of epigenetics, Waddington published in 1957 the famous epigenetic map, showing a ball rolling down a plain. This ball represents an embryonic cell, curling irrevocably down the slope of development. The different channels, present on the surface, mark different developmental fates (Figure 1) (Burbano 2006).

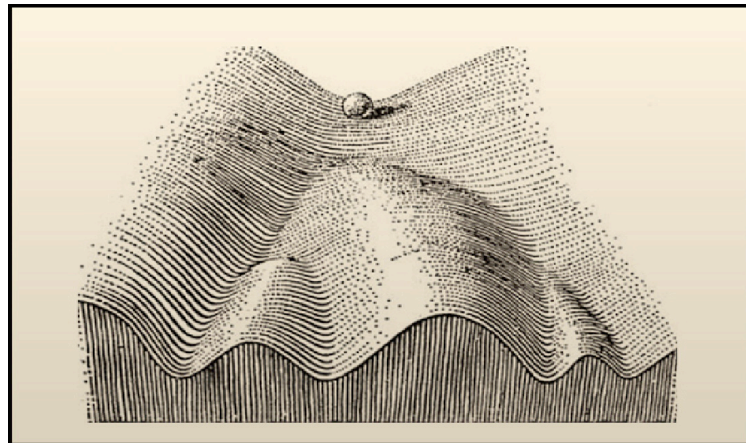


Figure 1: Conrad Hal Waddington's classical epigenetic landscape.

The ball is a metaphor for an embryonic cell in the process of differentiation. The inclined plan represents the different possible developmental possibilities, whereas canalizations stand for irrepealably developmental decisions, which were taken by the cell (Goldberg, Allis et al. 2007).

The term of DNA methylation was first mentioned in 1969 in a publication about long-term memory (Griffith and Mahler 1969). The association between DNA methylation, gene regulation and X-chromosome inactivation was established in 1975 (Holliday and Pugh 1975; Riggs 1975; Sager and Kitchin 1975). However, the word "epigenetic" did not appear in any of these publications (Haig 2004).

At the beginning of the nineties, epigenetic was defined as the study of modifications in gene expression occurring in differentiated cells, as well as the mitotic inheritance of this expression pattern. Then, it was referred to nucleus-mediated and DNA sequence-independent inheritance. Both definitions were not complete but complement each other (Holliday 2006). Afterwards, the scientist Hall combined both definitions and defined epigenetic

as the sum of genetic and not genetic factors that control gene expression and therefore, the phenotypic complexity during development (Hall 1992). Medawar and Medawar formulated epigenetic in 1988 as “Genetics proposes, epigenetics disposes”. Nowadays, molecular biologists define epigenetic as the study of mitotically and/or meiotically heritable changes that occur without DNA sequence changes (Berger, Kouzarides et al. 2009). In contrast, functional morphologists define epigenetic as a general series of interactions among cells and their products, resulting in differentiation and morphogenesis (Haig 2004).

1.2. Epigenetics

Epigenetic events are crucial in the control of both normal and defective (e.g. cancer-associated) cellular processes (Vaissiere, Sawan et al. 2008). The flexible and heritable epigenetic events include, at protein level, a bewildering array of post-translational modifications (PTMs) of histone proteins, at DNA level, a process in which enzymes add methyl groups onto cytosines (DNA methylation) or, at RNA level, an RNA-mediated gene silencing in form of RNA interference. To cope with their tasks such as gene regulation or transposon silencing, epigenetic mechanisms are interconnected and act in self-reinforcement.

1.2.1. Histone modifications

In the nucleus, eukaryotic genome is packed as chromatin, present under various levels of condensation from the lightly condensed and actively transcribed euchromatin to the compact and silenced heterochromatin. The nucleosome core particle forms the ‘heart’ of the chromatin structure. This nucleoprotein complex is composed of a histone octamer, consisting of two copies of each highly conserved core histone proteins H2A, H2B, H3, and H4 around which 146bp DNA are wrapped to form a superhelix (Figure 2) (Kornberg and Lorch 1999). Together these proteins form a globular domain

whereby their unstructured amino termini protrude flexibly on the surface of the chromatin polymer. Initially thought as a static and non-participating structural chromatin element, it became clear that histones are a dynamic and indispensable component of the gene regulation machinery.

The N-terminal histone tails comprise 25-30% of the mass of individual histones and are the sites of numerous PTMs (Figure 2) (Alfrey and Mirsky 1964; Wolffe and Hayes 1999).

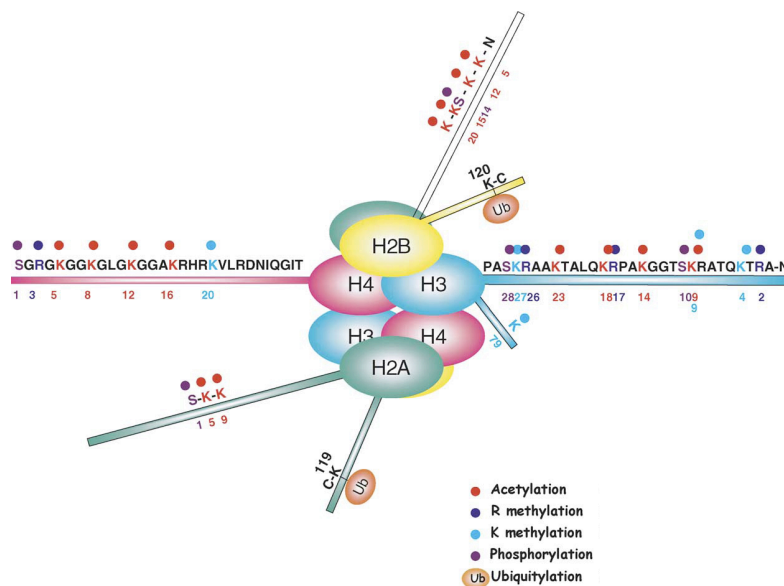


Figure 2: Schematic representation of post-translational modifications within N-terminal tail domains of the core histone octamer.

Colored dots over modified amino acids (K: lysine, R: arginine, S: serine) indicate the nature of post-translational modifications (*i.e.* acetylation, methylation, phosphorylation or ubiquitylation). Numbers refer to the positions on histone proteins (Strahl, Grant et al. 2002).

The panel of histone PTMs including acetylation, methylation, phosphorylation, ubiquitylation, deamination, proline isomerization, sumoylation or ADP-ribosylation codes for epigenetically relevant information at defined genetic loci (Figure 2) (Neff and Armstrong 2009). Indeed, one type of PTM can be applied on several amino acids in different histone tail positions and interacts with other PTMs. Moreover, in the case of methylation, lysine and arginine residues can be mono, di- or tri-methylated, adding another layer of complexity to the histone code. Hence, spatial distribution of

histone modifications allows to affect synergistically chromatin-interacting enzymes (Kurdistani, Tavazoie et al. 2004).

Functional consequences of histone modifications may be first the establishment of a specific global chromatin environment and second the orchestration of DNA-based biological tasks (Kouzarides 2007). Considering only electrostatic requirements for the chromatin polymer folding, histone acetylation and phosphorylation could synergistically unravel the negatively charged chromatin fiber by neutralizing positive and adding negative charges, respectively (Kouzarides 2007). However, effects of the myriad of histone PTMs are more complex, affecting the interaction of histones, DNA and the adjacent nucleosomes as well as the inter-nucleosomal contacts. Accordingly, gene promoter accessibility is changed and gene expression activated or silenced (Leone, D'Alo et al. 2008). The remarkable diversity and biological specificity of histone modifications coupled with distinct patterns of covalent histone marks let assume that a histone 'language' which may be encoded on these tail domains is far more complex than the genetic code.

For example, acetylation (ac) of specific lysines (K) in the N-terminal tail of the core histones H3 and H4 (e.g. H3K9ac, H3K4ac or H4K12ac) is a well-known histone modification, which plays a fundamental role in transcriptional activation (Figure 2) (Lennartsson and Ekwall 2009). In addition to their role in regulation of gene expression, histone PTMs partition genome into different distinct domains, associated with very local functions such as gene transcription and DNA repair, or to more genome-wide functions including DNA replication or chromosome condensation. For instance, during replication, histones are rapidly synthesized and assembled into newly synthesized DNA. In this process, pre-acetylated H3 and H4 are brought to replicating chromatin and become erased after complete replication and chromatin maturation (Turner and O'Neill 1995). Furthermore, phosphorylation of histone H3 on serine 10 (H3S10P) and the presence of the linker histone H1 have long been implicated in chromosome condensation during mitosis (Bradbury 1992; Koshland and Strunnikov 1996). Moreover, H3S10P correlates with the induction of early immediate response genes such as c-jun, c-fos and c-myc (Zippo, Serafini et al. 2009). Regarding lysine methylation, consequences depend on the position within histone tails. For

example, di- and tri-methylation of H3K4 and H3K26 are associated with open transcriptional active chromatin. In contrast, trimethylation of H3K9, H3K27 or H4K20 appears to be largely localized on promoters of repressed genes (Pan, Tian et al. 2007). In any case, these generalizations must be treated with care, since some modifications can exert different transcriptional outcomes depending on the surrounding microenvironment, the specific time point and the combination with other PTMs (Bernstein, Mikkelsen et al. 2006; Guenther, Levine et al. 2007).

Non-histone protein complexes with unique biological properties are in charge of reading histone modification patterns to mediate the recruitment of further docking proteins or complexes (e.g. NuRD, SIN3) leading to transcriptional activation or repression. For example, the repressive chromatin mark H3K9me3 is bound by the non-histone heterochromatin protein (HP) 1, forming a recruitment platform for histone methyltransferases (e.g. Suv family proteins), which is involved in chromatin condensation (Campos and Reinberg 2009). In addition, non-histone multiprotein complexes are composed of proteins involved in chromatin remodeling and formation of repressed chromatin structure such as histone deacetylases (HDACs), histone-binding proteins (e.g. RbAp48) as well as methylation-binding (MBDs) proteins and DNA methyltransferases (DNMTs) (Ahringer 2000). The dynamic modulation of chromatin structure is mainly realized by remodeling enzymes, *i.e.* histone methyltransferases (HMTs), histone acetyltransferases (HATs) and HDACs. HMTs and HATs generate particular arrays of methylation and acetylation marks on histones, respectively (Vaissiere, Sawan et al. 2008). Histone deacetylation is catalyzed by HDACs, which are classified in 4 classes depending on their sequence similarity, cellular localization, substrate specificity and zinc or NAD⁺ dependency (Minucci and Pelicci 2006; Ouaisi and Ouaisi 2006). Acetylation of histones is catalyzed by HATs, which are classified in three major families: general control non-derepressible 5 (Gcn5)-related N-acetyltransferase, p300/ CREB binding protein (CBP) and MYST proteins (Yang and Seto 2007). Furthermore, HATs and HDACs affect indirectly gene expression by modifying a growing list of non-histone substrates (Minucci and Pelicci 2006). Indeed, acetylation of specific lysine residues on transcription factors (e.g. p53 or STAT) affects their cellular

localization, stability, DNA binding activity and protein-protein interactions (Bruserud, Stapnes et al. 2006).

HMTs can be classified by their target specificity (Suv39h1 (H3K9), SET8 (H4K20), MLL1 (H3K4)) into three main groups that catalyze the transfer of a methylgroup from the methyl donor *S*-adenosylmethionine (SAM) to the ϵ -nitrogen in lysine or the guanidinium nitrogen in arginine. HMTs form large, multiprotein complexes that typically contain other histone modifier enzymes (HATs, HDACs), DNMTs, chromatin-binding subunits (chromo-like domains) or transcription factors recruiting epigenetic machinery to specific target promoters (Esteller 2006).

Similarly to protein kinases and phosphatases, short preferred consensus motifs are likely to exist, leading individual HATs and HDACs to their targets and thus helping to establish the final histone code (Kimura and Horikoshi 1998). Moreover, these histone modifying enzymes are tethered to their targets by cell-specific transcription factors, MBDs, chromatin-binding subunits or can even bind directly to DNA (e.g. activating transcription factor 2) and work in large multiprotein complexes (Cress and Seto 2000; Kawasaki, Schiltz et al. 2000).

1.2.2. DNA modifications

Enzymatic methylation of the cytosine base is an essential component of mammalian genome that neither influences the Watson-Crick base pairing nor the DNA polymerase processing during replication. Hence, DNA methylation has no impact on DNA sequence and the pattern is stably propagated during mitosis from the parent to daughter cells (Jeltsch 2002).

In eukaryotic cells, DNA methylation usually occurs within the context of the palindromic CpG dinucleotide at the fifth carbon atom of the cytosine ring, resulting in gene silencing (Gardiner-Garden and Frommer 1987; Hopkins, Burns et al. 2007). Over evolutionary time scale, spontaneous hydrolytic deamination of methylated cytosines has been responsible for cytosine to thymine transitional mutation. This genetic alteration leads to the under-representation of CpG dinucleotides with only about one quarter of the

expected general frequency in the human genome (Schulz and Goering 2011). Remaining CpGs are unequally distributed across the genome with long CpG-free or -poor DNA stretches separated by short CpG-rich regions. CpG islands (CGIs) are clusters that contain high frequency of CpG dinucleotides and overlap with 76% of putative human promoter regions. Marino-Ramirez *et al.* defined typical CGIs as a 500-bp long sequence with a GC percentage of over 50% and a ratio of CpG observed/expected that is greater than or equal to 0.6 (Marino-Ramirez, Spouge *et al.* 2004). Although many of the approximately 30000 CGIs are located in the 5'-untranslated region, spanning the transcription start site (TSS) and the first exon of genes, certain CGIs may occasionally be found within the coding sequence or the 3' region of a gene (Ball, Li *et al.* 2009). CGIs in these "atypical" coding sequence locations are more prone to methylation; however, the RNA transcription machinery can pass over without any interference (Jones 1999; Nguyen, Liang *et al.* 2001). Furthermore, some publications revealed the presence of extensive DNA methylation at CGI 'shores', which are regions of relatively low CpG density located close to CGIs (Meissner, Mikkelsen *et al.* 2008; Doi, Park *et al.* 2009). Recently, the existence of 5-hydroxymethylcytosine (5-hmc) was described in embryonic stem cells and Purkinje neurons. 5-methylcytosine can be converted into 5-hmc by the oxoglutarate- and Fe (II)-dependent oxygenases TET1, TET2 and TET3. These enzymes are probably involved in the active demethylation associated with embryonic epigenetic reprogramming (Wossidlo, Nakamura *et al.* 2011). Nevertheless, the role of this cytosine modification in mature cells as well as its possible role in carcinogenesis has still to be elucidated (Rodriguez-Paredes and Esteller 2011).

Under physiological conditions, most CGIs are never methylated in eukaryotic cells (Schulz and Goering 2011). However, some CGIs become hypermethylated during aging, inflammation or preneoplasia, albeit not as dramatically as in cancer cells (Teschendorff, Menon *et al.* 2010). The main role of DNA methylation is to specialize groups of cells to perform specific functions during embryonic development and cell differentiation of multicellular systems. Furthermore, DNA methylation protects genomic stability through permanent suppression of transcription and homologous

recombination of ‘selfish’ repetitive sequences originated from ancient parasitical (e.g. human endogenous retrovirus HERV) or simple parasitical retroelements (e.g. short or long interspersed elements, SINEs or LINEs, respectively) (Smit and Riggs 1996; Bird 2002; Jones and Baylin 2007; Vaissiere, Sawan et al. 2008). In addition to repetitive elements, selective single copy genes, which are involved in cellular pluripotency, can be methylated in normal cells (Reik 2007). Indeed, DNA methylation is implicated in genomic imprinting, leading to a mono-allelic gene expression (e.g. H19 expression from the maternal chromosome) (Reik and Walter 2001). Moreover, DNA methylation is involved in gonosomal X-chromosome inactivation (Panning and Jaenisch 1996). Finally, DNA methylation can induce gene expression. Indeed, methylation of the IGF2 Silencer element region inhibits the binding of the repressor protein and thus activates IGF2 expression (Eden, Constanica et al. 2001; Murrell, Heeson et al. 2001).

Noteworthy, opinions differ about the mechanisms associated with DNA methylation-mediated gene silencing (Figure 3).

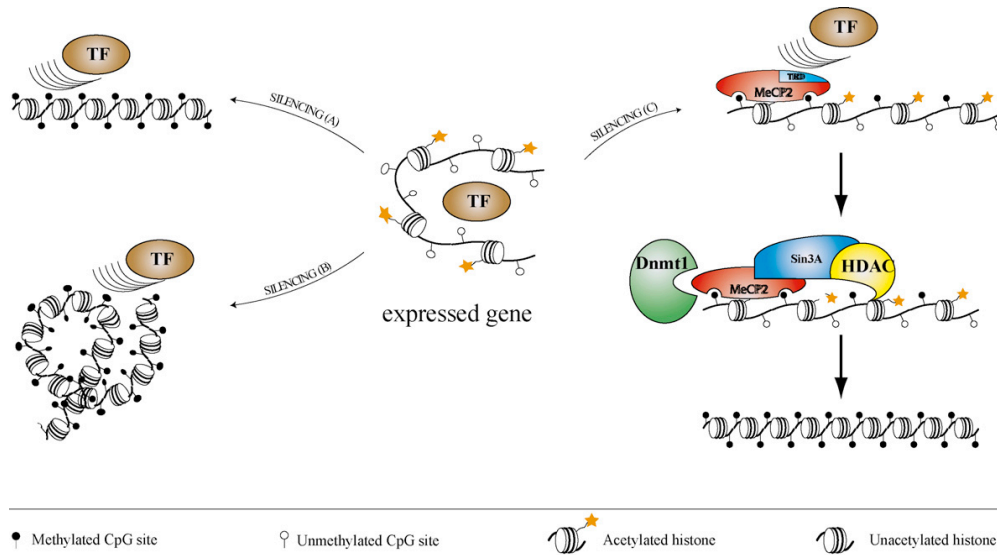


Figure 3: Possible mechanisms of DNA methylation-mediated gene silencing.

Several mechanisms can block transcription factor binding to the gene promoter region leading to gene silencing. (A) Direct inhibition by blocking the access of a transcription factor (TF) to its binding site. (B) Chromatin condensation by DNA methylation and histone deacetylation prevent the access for TFs. (C) Indirect silencing through the binding of methyl-binding proteins (e.g. MeCP2) and the formation of a repressor complex (e.g. HDACs, DNMTs), which prevents the binding of TFs (Vaissiere, Sawan et al. 2008).

DNA methylation can directly block binding of transcription factors to promoters, interfering with RNA polymerase II elongation or loading on DNA template to prevent transcription (Figure 3-A). Alternatively, the combination of DNA methylation and histone deacetylation leads to chromatin condensation. The resulting heterochromatin constricts the access to transcription factor binding sites inhibiting gene expression (Figure 3-B). Indirect repression may also involve proteins such as MBDs (*e.g.* MeCP2, MBD2) specifically bind to methylated DNA *via* their methyl CpG-binding domains. Subsequently, MBDs recruit HDAC activity to the methylated DNA region. This mechanism includes histone deacetylation and results in a condensed and repressive chromatin structure (Figure 3-C) (Vaissiere, Sawan et al. 2008).

Nevertheless, DNA methylation is not a static modification since it has to be modified during developmental and differentiation processes in order to adjust gene access rights (Haaf 2006). Indeed, remodeling of epigenetic marks happens first in primordial germ cells followed by a second wave during embryogenesis (Reik and Walter 2001). The final methylation signature should be maintained during lifetime; however, this pattern gets apparently altered in the course of life (Jones and Baylin 2007).

A family of DNMTs catalyzes the reaction of cytosine methylation (Chen, MacMillan et al. 1991) (Figure 4).

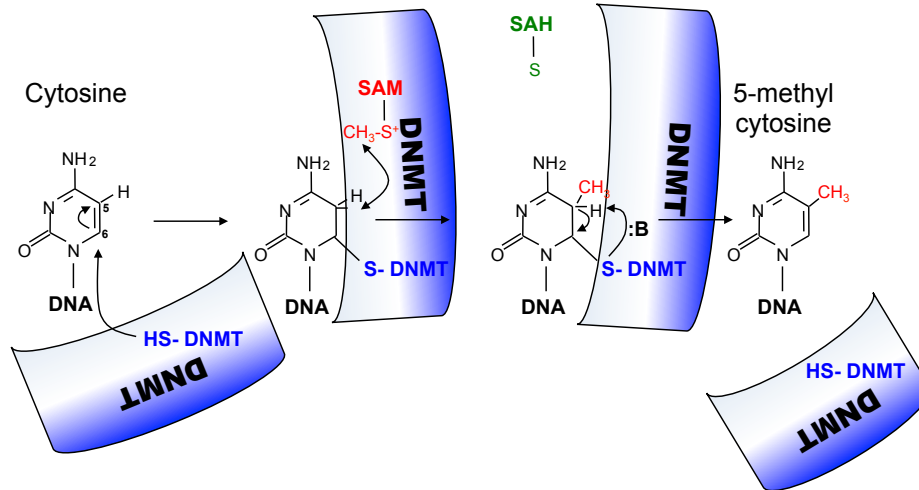


Figure 4: Schematic representation of the DNA methyltransferase-catalyzed endocyclic cytosine methylation.

DNA methyltransferases (DNMTs) catalyze the transfer of a methyl group from the methyl donor S-adenosylmethionine (SAM) on the fifth carbon atom of the cytosine pyrimidine ring. SAH: S-adenosylhomocysteine.

DNMT enzymes recognize specific sites on the DNA sequence and transfer a methyl group from the methyl group donor SAM to the cytosine within CpG dinucleotides. In a first step, base flipping fold out cytosine from the DNA helix. The subsequent nucleophilic attack of a cysteine HS-group from the DNMT's catalytic region on the carbon in position 6 of the cytosine leads to a covalent binding between the DNMT and target cytosine. This conformation activates the C5-position of the cytosine ring, which interacts with the methyl group of SAM. The complex is disrupted after the binding of the methyl group to the cytosine (Figure 4) (Wu and Santi 1987; Jeltsch 2002).

The *de novo* DNA methyltransferases DNMT3A and 3B are responsible for the establishment of the primary methylation pattern during embryogenesis, for the methylation of newly integrated retroviral elements and to respond to gene expression changes (Oswald, Engemann et al. 2000; Fatemi, Hermann et al. 2002). Enzymes of the DNMT3 class have no preference for un- or hemi-methylated CpG sites (Okano, Xie et al. 1998; Siedlecki and Zielenkiewicz 2006). However, knock out (KO) experiments showed that, in mammalian cells, DNMT3A and 3B were not redundant in their function but possess respective region specificities. DNMT3B

preferentially methylate repetitive elements (e.g. centromeric satellites or retroviral elements) (Okano, Bell et al. 1999). In contrast, DNMT3A plays an important role in methylation of differentially methylated regions (DMR), which are regulatory elements involved in the control of gene expression (e.g. DMR1 regulates H19 expression). Moreover, immunodeficiency syndrome, centromeric instability and facial abnormalities are linked to mutations in human DNMT3A gene (Hansen, Wijmenga et al. 1999; Okano, Bell et al. 1999). The third DNMT3 homolog DNMT3-L (DNMT3-like) has no methyltransferase activity but acts as a regulator for DNMT3A and 3B during *de novo* DNA methylation in germ cells (Bourc'his, Xu et al. 2001; Suetake, Shinozaki et al. 2004).

In contrast, DNMT1 methylates preferentially hemi-methylated CpGs 5- to 30-fold better than unmethylated sites. DNMT1 is associated with replication foci and is responsible for the post-replicative maintenance of genomic methylation patterns between cell generations. Thus, this enzyme is called the 'maintenance methyltransferase', which propagates the methylation pattern with an extreme fidelity from the mother cell to daughter cells (Siedlecki and Zielenkiewicz 2006; Vaissiere, Sawan et al. 2008). Lethality of DNMT1 KO mice underlines the importance of this enzyme during early embryogenesis (Li, Bestor et al. 1992; Jaenisch and Bird 2003).

1.2.3. RNA-mediated gene regulation

Britten and Davidson already postulated in 1969 that RNA is involved in gene regulation. However, the first ribo-regulator gene in animals was only described 24 years later in studies about the regulative potential of the small RNA *lin-4* on the target mRNA *lin-14* during the postembryonic development of *C.elegans* (Lee, Feinbaum et al. 1993; Wightman, Ha et al. 1993). Several years later, Reinhart *et al.* characterized another regulatory non-coding RNA *let-7* (Reinhart, Slack et al. 2000). Apart from tRNA and rRNA, most widely known non-protein-coding RNAs are the 19- to 24- nucleotides short microRNAs (miRNAs), which regulate mRNA function between the post-transcriptional and translational level (He and Hannon 2004; Bhagavathi and

Czader 2010). The highly conserved miRNAs are involved in many fine-tuned biological processes, such as development, tissue differentiation, cell metabolism, cell cycle, apoptosis, senescence, autophagy and metastasis (Sassen, Miska et al. 2008; Ruan, Fang et al. 2009).

Genes encoding for miRNAs are located either in intergenic regions or in defined transcription units. Around 50% of the miRNA genes are found in introns or exons of both protein-coding and long non-coding transcripts and are consequently co-transcribed with the gene in which they reside (Rodriguez, Griffiths-Jones et al. 2004; Weber 2005; Kim and Nam 2006).

MiRNA genes are usually transcribed by RNA polymerase (Pol) II into polycistronic primary transcripts (pri-miRNAs) with a length of about 1kb up to several kbs, except miRNAs located in Alu repeats that are transcribed by RNA pol III (Figure 5) (Lee, Jeon et al. 2002; Lee, Kim et al. 2004; Borchert, Lanier et al. 2006). Pri-miRNAs are further characterized by a 5' methyl cap structure, a 3'-end poly A-tail and at least one-hairpin structure of approximately 70 nucleotides. During the canonical miRNA pathway, a complex consisting of the double strand-specific endoribonuclease III Drosha, the binding protein Pasha and the DiGeorge syndrome critical region 8 protein (DGCR8), processes pri-miRNA into 70- to 100-nucleotide size range pre-miRNAs (Figure 5). Besides a stem-loop structure, pre-miRNAs bear a 3'-dinucleotide overhang (Kwak, Iwasaki et al. 2010). An alternative way of pri-miRNA processing consists in the mirtron pathway, whereby the nuclear splicing machinery takes over the tasks of Drosha and provides the pre-miRNA from introns, described as mirtrons (Figure 5) (Winter, Jung et al. 2009).

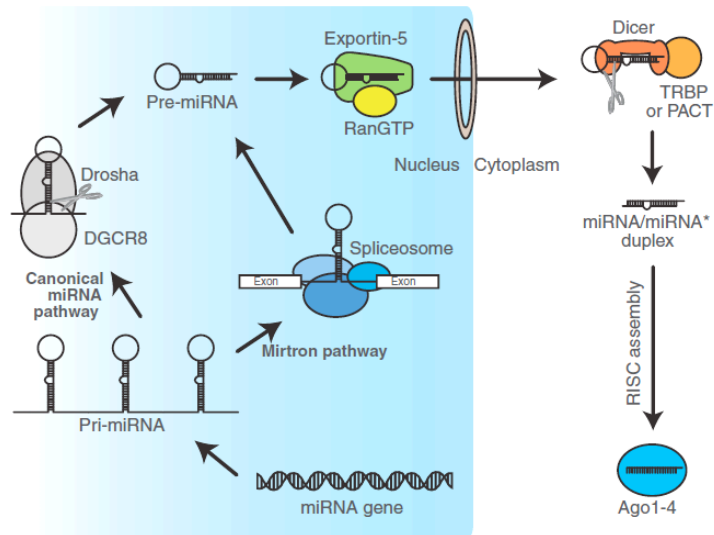


Figure 5: MicroRNA biogenesis.

MicroRNA (miRNA) biogenesis begins with the synthesis of a pri-miRNA. The following maturation of miRNA either happens by the canonical miRNA pathway or by the alternative mirtron pathway. In the first case, Drosha processes pri-miRNA in complex with DGCR8 into a pre-miRNA. As an alternative, pri-miRNA processing is undertaken by spliceosome. Nuclear export protein Exportin-5 together with Ran-GTPase carries pre-miRNA through nuclear pores. In cytoplasm, pre-miRNA is cleaved by the DICER/TRBP complex, resulting in the mature miRNA/miRNA* (* passenger strand) duplex. In the assembly process, miRNA is loaded into the RNA-induced silencing complex (RISC) complex where it is responsible for the sequence-specific targeting. DGCR8: DiGeorge critical region 8, TRBP: trans-activation-responsive RNA-binding protein, PACT: protein kinase R activating protein, RISC: RNA-induced silencing complex, Ago: Argonaute (Kwak, Iwasaki et al. 2010).

Exportin 5 / Ran-GTPase heterocomplex transports pre-miRNA from nucleus to cytoplasm where it undergoes further maturation (Figure 5). Indeed, the pre-miRNA is subsequently processed by Dicer III into a 19- to 24-nucleotide length double stranded miRNA/miRNA* (* passenger strand) duplex with 3' dinucleotide overhangs. Thus, Dicer is associated with the trans-activator RNA binding protein (TRBP) or the dsRNA-dependent serine/threonine protein kinase R (PKR) activating protein (PACT) (Kwak, Iwasaki et al. 2010) (Figure 5).

MiRNAs are on their own unable to induce silencing of targeted genes. Therefore, the mature miRNA require assembly into the multi-protein effector RNA-induced silencing complex (RISC). The essential core components of RISC are members of the Argonaute 1 to 4 (Ago 1-4) subfamily proteins. Noteworthy, the slicer protein Ago 2 is the only family member with an endonuclease activity (Liu, Carmell et al. 2004).

RISC assembly is initialized by the ATP-dependent incorporation of the miRNA/miRNA* duplex into the Ago complex (RISC loading) (Kawamata, Seitz et al. 2009; Yoda, Kawamata et al. 2010). Subsequently, the miRNA duplex get unwound and the miRNA passenger strand is discarded from the RISC complex either by a slicer Ago 2-dependent mechanism or a slicer-independent unwinding (Kwak, Iwasaki et al. 2010). The remaining mature miRNA strand determines the RISC complex specificity, interacting with the 3' untranslated region (UTR) of the target mRNA (Bhagavathi and Czader 2010). Noteworthy, RISC target recognition is primarily determined by base pairing of nucleotides in the 'seed' region and is enhanced by additional interactions in the middle of the 3' region (Parasramka, Ho et al. 2011).

How miRNAs induce translational repression is still an ongoing debate. It is known that perfect complementarity between miRNA and 3'UTR as well as the presence of Ago 2 in the RISC complex are prerequisites for targeted mRNA cleavage (Figure 5). Prevention of mRNA circularization by the RISC complex and thus translational inhibition or induction of mRNA degradation could possibly explain post-transcriptional gene silencing. Furthermore, RISC-mediated inhibition may occur at the stage of translational initiation or by blocking the late initiation step. It is postulated that RISC complex could also act on post-initiation steps by reducing the elongation rate of ribosomal machinery or inducing the proteolysis of the newly synthesized peptide. Finally, RISC complexes associated with their target mRNAs are found in processing or parking bodies (p-bodies) where mRNA undergoes degradation or becomes recycled after leaving the p-bodies (Kwak, Iwasaki et al. 2010).

In conclusion, interference of miRNAs with protein synthesis allows high flexibility in translational activity, fast response to changes, prevention of high levels of potentially harmful proteins (*i.e.* proteins involved in apoptosis), avoiding imbalances in gene expression. Thus, short non-coding RNAs provide "canalization" for the development of particular cell types *via* a strictly determined pathway (Cohen, Brennecke et al. 2006; Hornstein and Shomron 2006).

1.2.4. Cross talk of epigenetic modifications

The initiating event in epigenetic gene silencing remains unclear. DNA methylation may be the primary mark for gene silencing, triggering events that lead to non-permissive chromatin state. Another scenario proposes that the loss of histone acetylation may serve as the initial event for gene silencing, followed by DNMT targeting, leading to local hypermethylation (Tamaru and Selker 2001; Vaissiere, Sawan et al. 2008). Independently of this discussion, it is particularly important to stress that epigenetic modifications do not act independently, but are intimately interwoven and work together to establish, maintain, and modify global and local chromatin structures of a cell for life (Figure 6).

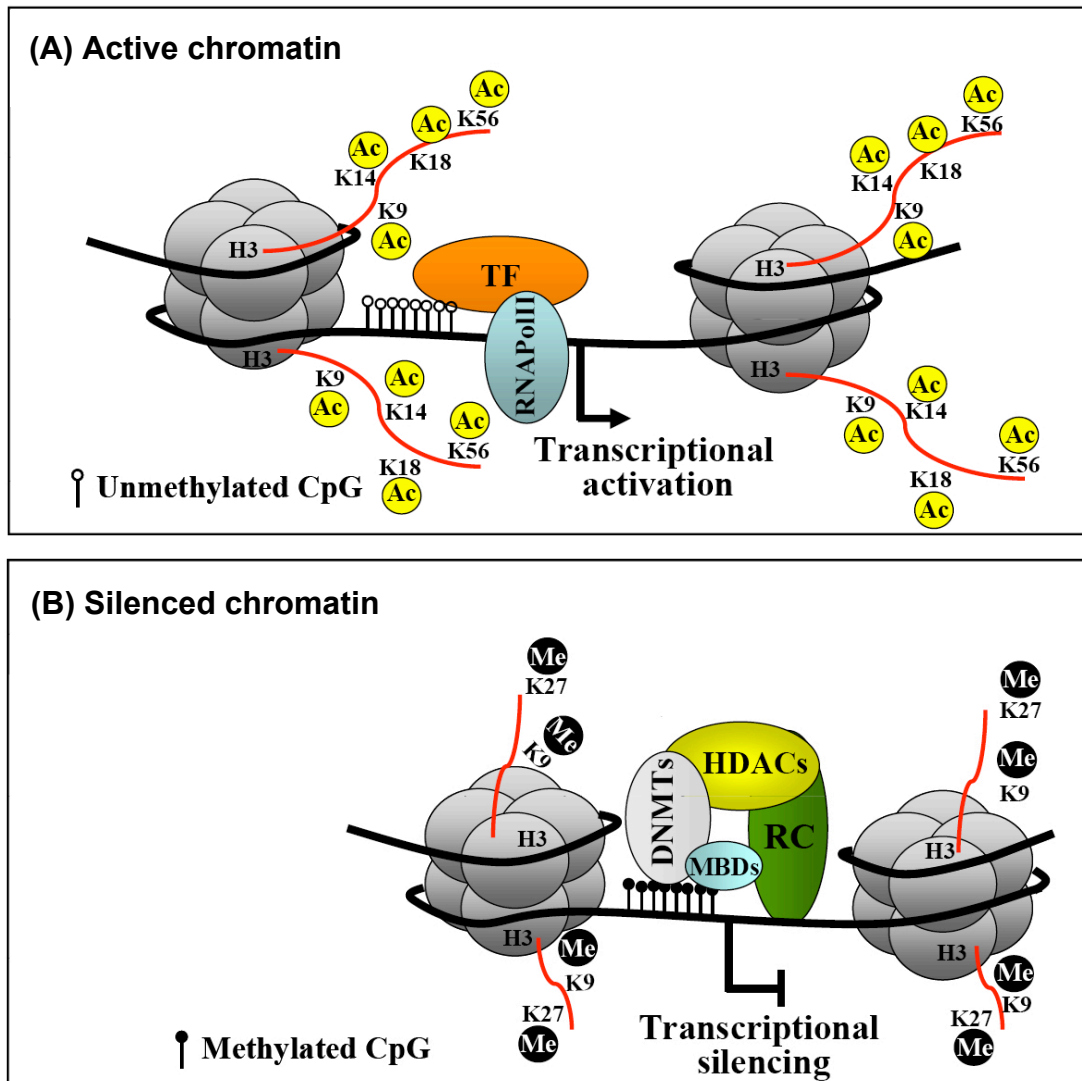


Figure 6: Schematic view of transcriptionally active and epigenetically silenced chromatin regions.

Epigenetic modifications and protein complexes modulate the formation of an active (A) and repressive (B) gene promoter state. Me: methylation. White circles: unmethylated CpG dinucleotides, black circles: methylated CpG dinucleotides, Ac: acetylation, TF: transcriptional factor, RNAPoIII: RNA polymerase II, DNMTs: DNA methyltransferases; HDACs: Histone deacetylases; MBDs: Methyl-CpG binding proteins; RC: transcriptional repressive complex (Leone, D'Alo et al. 2008).

For example, histone H3 acetylation on lysine 9, 14, 18 and 56 are associated with unmethylated CGs, representative for open chromatin configuration, allowing transcription factor recruitment and gene transcription by RNA polymerase II. In contrast, histone H3 methylation on lysine 9 and 27 and HDAC-induced depletion of H3 acetylation are associated with hypermethylated CGs, recruiting MBDs and DNMTs, leading to chromatin

condensation and transcriptional repression (Figure 6) (Leone, D'Alo et al. 2008).

1.3. Normal and malignant hematopoiesis

Since functional mature blood cells have a limited lifetime in peripheral blood, they need to be continuously replaced. The pluripotent self-renewable CD34⁺ and lin⁻ hematopoietic stem cells (HSCs) located in bone marrow can differentiate into different highly specialized mature blood cell types (Figure 7) (Okuno, Iwasaki et al. 2002). Mature hematopoietic cells are traditionally categorized into distinct lymphoid and myeloid lineages (Iwasaki and Akashi 2007). During differentiation process, the various lymphoid and myeloid lineages develop independently out of the common lymphoid and myeloid progenitors stem cells (CLP and CMP, respectively) raised from the HSCs (Kondo, Weissman et al. 1997; Akashi, Traver et al. 2000). During downstream hematopoietic differentiation, mature cells lose stepwise developmental potential and self-renewable capacities, resulting in fully differentiated and functional blood cells (Warner, Wang et al. 2004). The lymphoid lineage consists of T, B and natural killer cells, while the myeloid lineage includes a number of morphologically, phenotypically and functionally distinct cell types including granulocytes (*i.e.* neutrophils, eosinophils and basophils), monocytes-macrophages and erythrocytes (Figure 7) (Iwasaki and Akashi 2007). The hematopoiesis process is tightly regulated by extrinsic (*e.g.* growth factors and cytokines) and intrinsic factors (*e.g.* lineage-specific transcription factors and epigenetic markers) (Rice, Hormaeche et al. 2007).

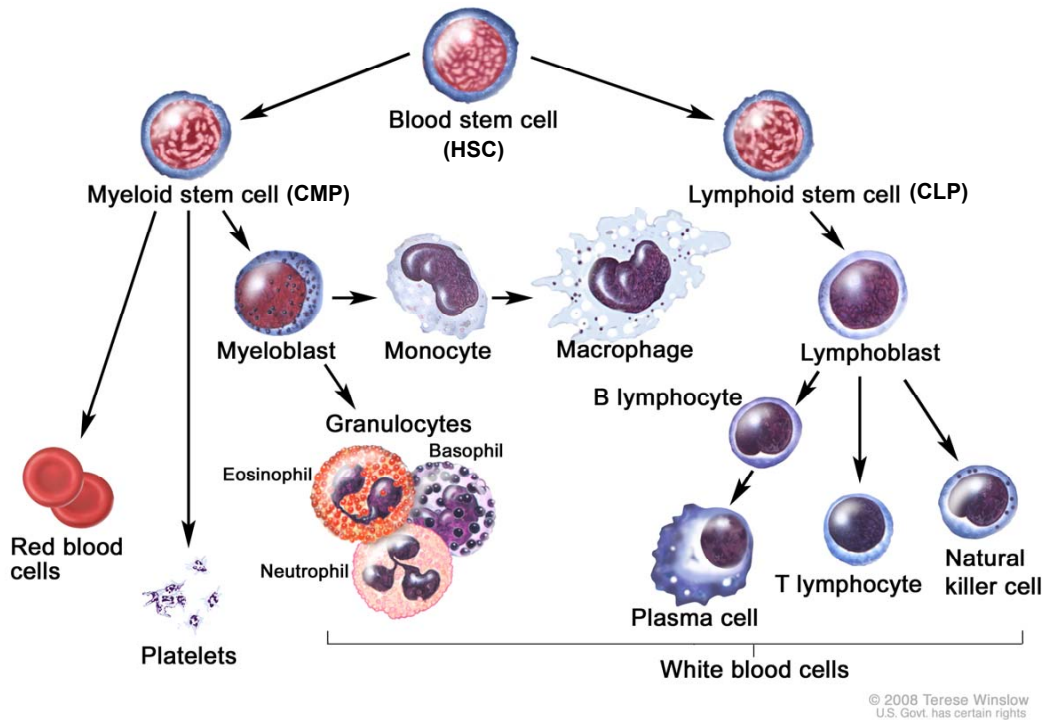


Figure 7: Hematopoiesis in adult mammalian organisms.

Hematopoietic stem cells (HSC) give rise to the myeloid (CMP) and the lymphoid progenitor cells (CLP). Mast cells, platelets, erythrocytes, eosinophils and neutrophils as well as monocytes emerge from the myeloid pathway. Cells of the immune system such as B and T-cells emerge from the lymphoid progenitor (modified from © 2008 Terese Winslow).

The German pathologist Rudolf Virchow introduced in 1856 the term “*leukemia*” (Greek for white blood) to describe excessive clonal proliferation of white blood cells in cancer patients. This symptom is caused by a malignant neoplasm of blood forming organs with the clinical manifestation of an inappropriate expansion of hematopoietic progenitor cells, often due to a blockage of cell maturation at early stages (Altucci, Clarke et al. 2005).

Hematological malignancies comprise all clinically, morphologically, immunophenotypically and pathologically heterogeneous neoplastic disorders of bone marrow and are first classified by the affected cell lineage (myeloid or lymphoid) and second by differentiation state or disease progression (acute or chronic). Abnormal white blood cells, consisting of primarily granulocytes or monocytes, are indicative for a myeloid disorder. In contrast, if abnormal blood cells arise from bone marrow lymphocytes, the cancer belongs to the class of lymphocytic disorders. The acute form of malignant hematopoiesis is characterized by very immature cells called blasts, which rapidly increase in

number in bone marrow and, in most cases, also in peripheral blood, leading to death within weeks without treatment. In contrast, the chronic form is characterized by an excessive accumulation of relatively mature but still abnormal and immunologically incompetent white blood cells. Without treatment, the relatively slow-growing chronic form is fatal within years after diagnosis (Figure 8).

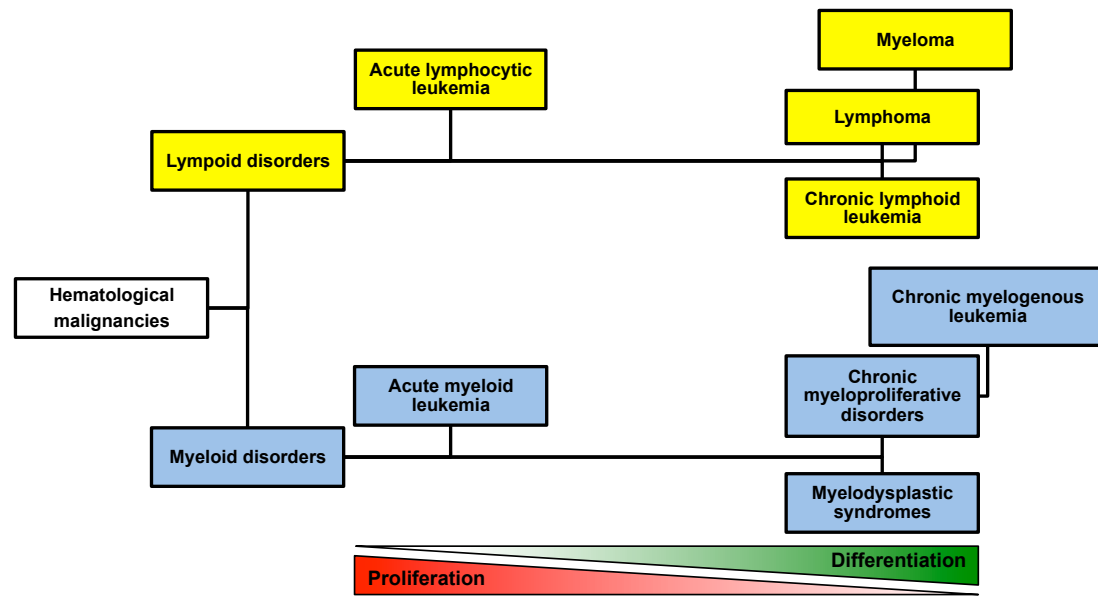


Figure 8: Classification of hematological malignancies.

Hematological malignancies (leukemia and lymphoma) are categorized by their lineage state (lymphoid (yellow) or myeloid (blue)) and functional differentiation state (acute or chronic). Highly proliferative acute myeloid and lymphoid leukemia cells are derived from cells in the early myeloid or lymphoid differentiation cascade, respectively. Chronic myeloid or lymphoid leukemia cells, myelodysplastic syndromes, myeloma and lymphoma are more differentiated but less proliferative and present therefore a reduced developmental potency compared to acute leukemia cells (modified from E. Attar; Leukemia Review: Types, Diagnostics, Treatments; www.calgb.org).

By considering whether they are acute or chronic, and whether they are myelogenous or lymphocytic, leukemia can be divided in four major types: acute myeloid leukemia (AML), acute lymphoid leukemia (ALL), chronic myeloid leukemia (CML) and chronic lymphoid leukemia (CLL). ALL is primarily a pediatric disease and occurs more commonly in children, whereas AML and chronic leukemia types mostly affect adults, but can appear theoretically in any age group. In leukemia, accumulation of leukemic immature and inoperable blood cells as well as suppression of the normal residual

hematopoiesis are responsible for crowding out other normal blood cells from bone marrow and bloodstream (Druker, Tamura et al. 1996; Deininger 2005). In consequence, normal blood cell features including immune defense or oxygen transport are disturbed, causing the characteristic blood cancer symptoms (e.g. anemia, thrombocytopenia and leukopenia). Noteworthy, lymphoma (i.e. Hodgkin's disease and Non-Hodgkin's lymphoma) and myeloma are further lymphoproliferative hematological malignancies, associated to a clonal proliferation of lymphoid cells. Myelodysplastic syndromes (MDS) are a clonal group of hematopoietic stem cell diseases characterized by hypercellular dysplasia and ineffective hematopoiesis by perturbed iron metabolism in one or more of the major myeloid cell lineages.

Leukemia appears to depend on a small population of leukemia stem cells (LSCs), characterized by their continuous growth and propagation. This assumption is supported by results showing that a highly proliferate clone of immature leukemic blast cells can lead to leukemogenesis (Kennedy and Barabe 2008). Nevertheless, the origin of LSC development is controversial (Passegue, Jamieson et al. 2003; Huntly and Gilliland 2005). Increased proliferation and differentiation capacities, telomere maintenance, uncoupling of self-renewal as well as decreased apoptosis rate lead to the development potential of blood cancer cells (Warner, Wang et al. 2004; Kennedy and Barabe 2008). Molecularly, leukemia are a heterogeneous disease entity with dysregulations of gene expression and pathways playing important functions in cellular growth, differentiation and cell death, resulting from different structural rearrangements or numerical chromosome aberrations. The presence of such specific genetic alterations allows the development of anti-cancer therapies. For example, the BCR/ABL1 chimeric protein, resulting from a translocation between chromosome 9 and 22 and leading to the Philadelphia chromosome, is now targeted with imatinib mesylate in CML patients (Druker, Tamura et al. 1996; Deininger 2005). Moreover, clinical tests analyze the use of fms-related tyrosine kinase (FLT) 3 inhibitors for AML patients (Fiedler, Serve et al. 2005; Stone, DeAngelo et al. 2005). The receptor tyrosine kinase, which is involved in regulation of multiple cytoplasmic effector molecules in pathways of apoptosis, proliferation and hematopoietic differentiation, is commonly altered and leads to a constitutive

activation in AML and ALL. Indeed, up to 264 different gene fusions were found in hematological malignancies. Finally, it is now well accepted that epigenetic alterations play a key role in the abnormal developmental program of blood cancer cells (Mitelman, Johansson et al. 2007; Kennedy and Barabe 2008).

1.4. Epigenetic alterations in hematological malignancies

In industrialized countries, cancer is ranked among the most prominent causes of death next to coronary heart disease and diabetes. Nutrition, environment, genetic background (predisposition) and previous anamnesis are important risk factors for cancer development. Malignant cells possess six characteristic hallmarks: (i) unlimited potential for cell division, (ii) invasion and metastasis potential, (iii) resistance to anti-growth signaling, (iv) self-sufficient growth, (v) evasion of apoptosis, and (vi) sustained angiogenesis (Balch, Montgomery et al. 2005). Astonishingly, ubiquitous alterations in the elaborated DNA methylation pattern may be a causative factor as significant as genetic alterations for progression of a normal to a cancerous cell (Baylin and Bestor 2002; Hopkins, Burns et al. 2007). Genome-wide DNA hypomethylation was the first epigenetic abnormality that was identified in human tumors (Feinberg and Vogelstein 1983; Feinberg and Vogelstein 1983). Several years later, opposite results claimed increased CGI methylation in human tumors (Baylin, Hoppener et al. 1986). The promoter region of the tumor suppressor gene (TSG) Retinoblastoma (Rb) was identified as the first hypermethylation hotspot that is unmethylated in normal cells (Greger, Passarge et al. 1989). Nowadays, it is well accepted that cancer cells are subjected to genome-wide loss of methylation and gene-specific hypermethylation (Figure 9) (Sincic and Herceg 2011). Indeed, benign neoplasia or cancer cells in early developmental stages already possess the typical cancer-specific features of global hypomethylation and local hypermethylation, leading to the hypothesis that early epigenetic deregulation may precede genetic aberrations (Feinberg 2005).

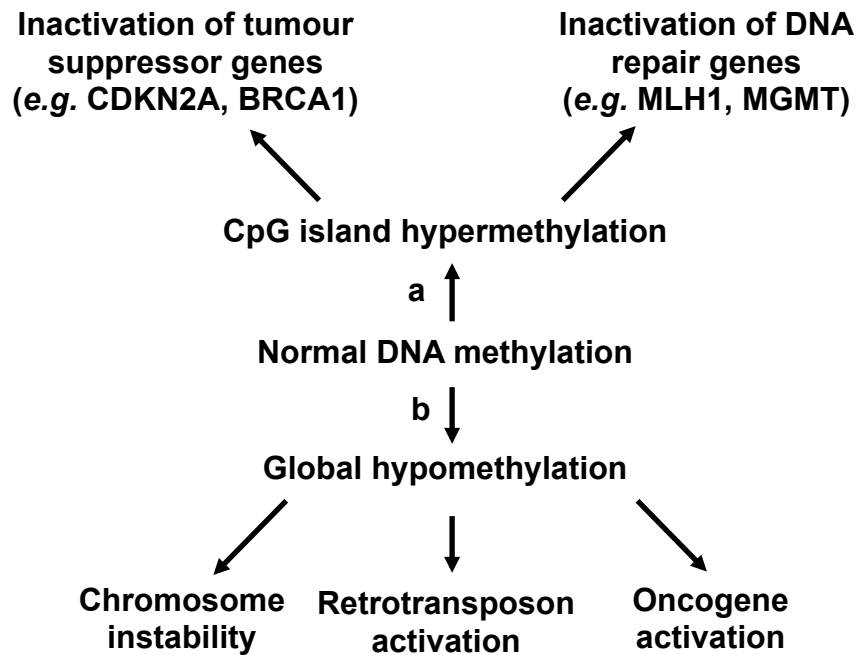


Figure 9: Consequences of cancer-specific methylation alterations in tumor development.

(a) Increase of CpG island promoter methylation can inactivate tumor suppressor genes and DNA repair genes. (b) Reduced global methylation might lead to chromosome instability, reactivation of transposons and activation of oncogenes (Strathdee and Brown 2002).

The overall genomic methylcytosine content of approximately 4% (compared to total cytosines) in normal cells is decreased to 2-3% in cancer tissues. Even if loss of genome-wide methylation is a common feature of cancer cells, the degree of global hypomethylation varies among cancer subtypes. For example, undifferentiated germ cell tumors are hypomethylated, whereas their more differentiated counterparts show higher levels of global methylation. Testicular germ cells seminoma exhibit particularly high degrees of global hypomethylation (Wild and Flanagan 2010; Sincic and Herceg 2011). These observations emphasize that overall DNA hypomethylation may differentially play an essential role in disease onset or progression, and increased tumor frequency and malignancy (Wilson, Power et al. 2007).

Hypomethylation mostly affects both intra- and extra-genic repetitive sequences, *i.e.* centromeric and pericentromeric regions (Figure 9). Indeed, failure of transcriptional repression of these satellite repeats may provoke DNA double-strand breaks, promoting aneuploidy formation. In the same way, global loss of methylation induces the reactivation of retrotransposons,

increasing the probability of translocations to other genomic regions and favoring chromosome instability (Strathdee and Brown 2002). Remarkably, transcriptional activation of LINE1 by promoter hypomethylation is an important feature of CML (Roman-Gomez, Jimenez-Velasco et al. 2005). In contrast, the SINE Alu appears to be resistant to demethylation and is rarely reported to be hypomethylated in cancer (Wild and Flanagan 2010). Moreover, single gene-specific DNA hypomethylation can achieve aberrant gene expression of proto-oncogenes, which mainly promote cell proliferation (Figure 9) (Strathdee and Brown 2002; Galm, Herman et al. 2006). Indeed, DNA hypomethylation and derepression of the oncogenes Harvey rat sarcoma viral oncogene homolog (H-RAS) and T-cell leukemia/lymphoma 1 (TCL-1) were reported in CLL patients (Melki and Clark 2002). Furthermore, *in vitro* and *in vivo* studies described the activation of genes associated with tumor invasion and metastasis by the loss of DNA methylation (Ateeq, Unterberger et al. 2008). Finally, cancer-induced loss of imprinting leads to the biallelic expression of IGF-2 and thus stimulation of cancer cell proliferation (e.g. Wilms' tumor) (Jirtle 1999).

Partial or complete abrogation of DNMT expression and function might lead to the passive loss of DNA methylation in malignant cells. However, this is unlikely since it was shown that DNMT1, DNMT3A and DNMT3B were overexpressed in AML and CML patients (Mizuno, Chijiwa et al. 2001). Moreover, latest results reported that abnormal methylcytosine content in AML cells was independent of somatic mutations in DNMT3A gene (Ley, Ding et al. 2010). Furthermore, cancer cell-specific deficiency of the DNMT cofactor SAM could initiate similar effects. DNMTs have the property to bind with high affinity to DNA damages, leading to site-directed neglect of DNA methylation maintenance and subsequent DNA demethylation. Likewise, alterations in DNA repair mechanisms are probably responsible for active DNA demethylation of cancer methylomes (Wild and Flanagan 2010).

Mainly '*bona fide*' TSGs, implicated in all six aforementioned hallmarks of cancer, are repressed through hypermethylation of their promoter CGIs (Jones and Baylin 2002; Herman and Baylin 2003; Hopkins, Burns et al. 2007). Target genes of aberrant DNA hypermethylation play major roles for the physiological cell existence including DNA repair, cell cycle regulation, cell

invasion and adhesion, apoptosis, detoxification and hormonal response (Figure 9) (Esteller and Herman 2002; Galm, Herman et al. 2006). DNA hypermethylation-associated silencing of TSGs occurs in various hematological neoplasia and thereby may contribute to early carcinogenesis. Table 1 gives an overview of genes that are found frequently hypermethylated in hematological malignancies.

Table 1: Genes found frequently hypermethylated in hematopoietic malignancies.

<i>Function</i>	<i>Gene</i>	<i>Hematological malignancy</i>	<i>Literature</i>
Cell cycle control	CDKN2B (p15 ^{INK5B})	NHL, AML, ALL, CML, CLL, MDS	(Herman, Jen et al. 1996; Herman, Civin et al. 1997; Drexler 1998; Baur, Shaw et al. 1999; Rush and Plass 2002; Esteller 2003; Galm, Wilop et al. 2005; Galm, Herman et al. 2006)
	CDKN2A (p16 ^{INK4A})	ML, MM, AML, ALL, CLL	(Melki and Clark 2002; Boultonwood and Wainscoat 2007; Esteller 2008)
	CDKN1C (p57 ^{KIP2})	ML, MM, ALL, CLL	(Li, Nagai et al. 2002)
	TP73	ML, MM, ALL, AML	(Kawano, Miller et al. 1999; Ekmekci, Gutierrez et al. 2004; Ropero, Setien et al. 2004)
Biosynthesis enzyme	EXT1	ALL	(Ropero, Setien et al. 2004)
DNA damage repair	MGMT	NHL, ALL, AML	(Esteller, Hamilton et al. 1999; Esteller, Gaidano et al. 2002; Margison, Povey et al. 2003)
Apoptosis	DAPK1	ML, MM, ALL, AML, CLL	(Ekmekci, Gutierrez et al. 2004; Rossi, Capello et al. 2004; Raval, Lucas et al. 2005)
	RASSF1A	Hodgkin's lymphoma	(Murray, Qiu et al. 2004)
Cell adhesion	CDH1	MM, ALL, AML, CLL, MDS	(Melki and Clark 2002; Aggerholm, Holm et al. 2006; Garcia-Manero, Yang et al. 2009)
Growth regulation	HIC1	NHL, ALL, AML, CML, MDS	(Issa, Zehnbauser et al. 1997; Melki, Vincent et al. 1999; Aggerholm, Holm et al. 2006; Deneberg, Grovdal et al. 2010)
Cytokine signaling	SOCS1	MM, AML	(Ekmekci, Gutierrez et al. 2004; Galm, Wilop et al. 2005)
Nuclear matrix	LMNA	NHL, ALL	(Agrelo, Setien et al. 2005)
Hormone receptor	RARB2	NHL, AML	(Esteller, Guo et al. 2002; Ekmekci, Gutierrez et al. 2004; Galm, Wilop et al. 2005; Rethmeier, Aggerholm et al. 2006)
	ESR1	ALL, AML, CML, MDS	(Issa, Baylin et al. 1997; Melki, Vincent et al. 1999; Galm, Wilop et al. 2005; Aggerholm, Holm et al. 2006; Yao, Huang et al. 2009)
	AR	NHL	(McDonald, Gascoyne et al. 2000)
Transporter (Importer)	CRBP1	NHL, AML	(Esteller, Guo et al. 2002; Takahashi, Shivapurkar et al. 2004)
Transporter (Exporter)	ABCB1	AML, ALL	(Toyota, Kopecky et al. 2001; Garcia-Manero, Daniel et al. 2002; Taylor, Pena-Hernandez et al. 2007)
Tyrosine kinase	EPHA7	NHL	(Dawson, Hong et al. 2007)
	ABL1	ALL, CML	(Asimakopoulos, Shteper et al. 1999; Asimakopoulos, Shteper et al. 1999; Shteper, Siegfried et al. 2001)
Tyrosine	SHP1	ML	(Koyama, Oka et al. 2003)

Function	Gene	Hematological malignancy	Literature
phosphatase			
Differentiation	MYOD1	AML, ALL	(Toyota, Kopecky et al. 2001; Garcia-Manero, Yang et al. 2009)
	PITX2	AML	(Toyota, Kopecky et al. 2001)
	ID4	ML, AML	(Hagiwara, Nagai et al. 2007; Uhm, Lee et al. 2009)
Receptor	SDC4	AML	(Toyota, Kopecky et al. 2001)
Homeostasis	CEBP	AML	(Agrawal, Hofmann et al. 2007)
Calcium metabolism	CALCA	AML, ALL, CLL	(Nelkin, Przepiorka et al. 1991; Melki and Clark 2002; Paixao, Vidal et al. 2006; Ismail, El-Mogy et al. 2011)
Purine metabolism	FHIT	AML, MDS	(Iwai, Kiyoi et al. 2005)
Detoxification	AHR	ALL	(Mulero-Navarro, Carvajal-Gonzalez et al. 2006)
Cell adhesion	THBS1	AML; ALL	(Toyota, Kopecky et al. 2001; Garcia-Manero, Daniel et al. 2002)

ABCB1: ATP-binding cassette, sub-family B (MDR/TAP), ABL1: c-Abelson oncogene 1 non-receptor tyrosine kinase, AHR: aryl hydrocarbon receptor, ALL: acute lymphoid leukemia, AML: acute myeloid leukemia, AR: androgen receptor, CALCA: calcitonin A, CDH1: E-cadherin, CDKN2A: cyclin-dependent kinase (CDK) inhibitor 2A, CDKN2B: CDK inhibitor 2B, CDKN1C: CDK inhibitor 1C, CEBP: CCAAT/enhancer binding protein, CLL: chronic lymphoid leukemia, CML: chronic myeloid leukemia, CRBP1: cellular retinol-binding protein 1, DAPK1: death-associated protein kinase 1, ER: estrogen receptor, EPHA7: EPH receptor A7, EXT: exostosin 1, FHIT: fragile histidine triad gene, HIC1: hypermethylated in cancer 1, ID4: inhibitor of DNA binding 4, INK: kinase inhibitor, KIP: kinase inhibitor protein, LMNA: lamin A/C, MGMT: O-6-methylguanine-DNA methyltransferase, ML: multiple lymphoma, MM: multiple myeloma, MDS: myelodysplastic syndrome, MYOD1: myogenic differentiation 1, NHL: Non Hodgkin's lymphoma, PITX2: paired-like homeodomain 2, RARB2: retinoic acid receptor beta 2, RASSF1: Ras association domain family protein 1, SDC4: syndecan 4, SHP1: Protein-tyrosine phosphatase SHP-1, SOCS1: suppressor of cytokine signaling 1, THBS1: thrombospondin 1, TP73: tumor protein p73.

Noteworthy, late stage AML patients who relapsed after a chemotherapy-induced remission showed abnormal methylation of hypermethylated in cancer 1 (HIC1) gene (Issa, Zehnbaauer et al. 1997; Deneberg, Grovdal et al. 2010). The transcriptional repressor HIC1 is involved in regulation of genes involved in proliferation, tumor growth and angiogenesis. Validated transcriptionally repressed targets of HIC1 are silent mating type information regulation 2 homolog 1 (SIRT1) HDAC, fibroblast growth factor binding protein (FGFBP1), patched (ptch) 1 tumor suppressor, scavenger chemokine receptor 7 (CXCR7), ephrin-A1 (EFNA1), E2F1 and T-cell-specific transcription factor 4 (TCF4) (Jenal, Britschgi et al. 2010). As shown in xenograft tumor assays, constitutive expression of FGFBP1 results in highly angiogenic tumors (Jenal, Britschgi et al. 2010). Moreover, bidirectional ephrin/eph-signaling has been implicated in many aspects of malignancy, such as tumor growth, invasion, metastasis and angiogenesis (Pasquale 2010). In consequence, epigenetic inactivation of the transcriptional repressor HIC1 plays an important role in leukemogenesis. Furthermore, simultaneous cyclin-

dependent kinase (CDK) inhibitor 2B and CDK inhibitor 1C hypermethylation, which leads to dysregulation of the cell cycle, has been reported in ALL cells (Garcia-Manero, Yang et al. 2009). Moreover, hypermethylation of the c-Abelson oncogene 1 (ABL1) promoter region repressing the expression of the oncogenic fusion gene BCR/ABL is found in CML samples (Asimakopoulos, Shteper et al. 1999). Since intragenic hypermethylation of the enhancer-blocking transcription factor CTCF binding region prevents silencing of the oncogene B-cell CLL/lymphoma (BCL) 6 in B-cell lymphoma, consequences of DNA hypermethylation appears to be region-specific (Lai, Fatemi et al. 2010). Noteworthy, a recent study on colon cancer cells showed that aberrant methylation is not only limited to CGIs, but also appears in highly conserved CpG island shores (Irizarry, Ladd-Acosta et al. 2009). Recently, methylation along the CGI borders was also described in human B-cells in transition to lymphoma (Conerly, Teves et al. 2010). However, the importance of differential methylation in these regions requires further studies.

Cancer-associated TSG hypermethylation is probably established progressively in several waves of aberrant methylation. As previously mentioned, methylation pattern is not stable and changes arise in normal cellular processes such as aging, which is one of the strongest risk factors for cancer (Teschendorff, Menon et al. 2010). In addition, recent publications linked environmental and lifestyle factors to the acquisition of inappropriate DNA methylation of various genes (Marsit, Houseman et al. 2007; Christensen, Houseman et al. 2009). In both cases, initial abnormal DNA methylation acts as a seed and promotes further methylation (Song, Stirzaker et al. 2002). Another theory postulates that hypermethylation may spread from normally methylated genomic element (e.g. transposons) over to usually unmethylated genes (Graff, Herman et al. 1997). In addition, disruptions of the epigenetic machinery, for instance by genetic mutations, could lead to increase transcription rate and aberrant enzymatic activity of any of its component. Hence this could be attributed to abnormal epigenetic events in hematological cancers (Robertson, Uzvolgyi et al. 1999; Baylin, Esteller et al. 2001; Mizuno, Chijiwa et al. 2001). For example, the AML-associated translocation t(15:17) leads to the expression of the oncogenic promyelocytic leukemia (PML) / retinoic acid receptor beta (RARβ) fusion protein. The

chimeric transcription factor recruits DNMTs to target promoters and induce abnormal methylation (e.g. RARB2) (Di Croce, Raker et al. 2002). Moreover, substantial alterations were detected in apparently normal cells of individuals with infections. Indeed, virus-encoded proteins could affect DNMT activity. For example, DNMT expression gets upregulated by the hepatitis B virus specific protein X (Herceg and Paliwal 2011). Alternatively, a recent publication reported that *Helicobacter pylori* infection is associated with aberrant methylation (Niwa, Tsukamoto et al. 2010).

Taking together, these data lead to the following question: why CGIs of certain genes become hypermethylated and others remain unmethylated in cancer cells? Manuel Esteller is in favor of the Darwinian idea (natural selection) that a certain pattern of hypermethylated genes confers a selective survival or growth advantage of a particular cell and may play a pivotal role in the stepwise progression towards carcinogenesis (Esteller 2002). On average, 5% of genes of an individual tumor exhibit a hypermethylated promoter region. These alterations appear to be a far more drastic change in the cellular metabolism than genomic point mutations (Jones and Baylin 2002; Hirst and Marra 2009). However, since these epimutations can silence the remaining active allele of a previously mutated TSG, accordingly to Knudson's two-hits hypothesis, they may provide the second hit for cancer initiation (Knudson 1971; Rodriguez-Paredes and Esteller 2011). Alternatively, the "Barker hypothesis" states that placental exposure or early life energy restriction cause errors in fetal reprogramming that persist into adulthood and may contribute to enhance risk for cancer development (Barker, Eriksson et al. 2002; Hughes, van den Brandt et al. 2009).

Another layer of epigenetic modifications was added with the discovery of 5-hmc. Even if the knowledge about the relationship between 5-hmc and cancer is still at the beginning, it is already well known that TET genes, involved in methylcytosine metabolization, are often subject to somatic mutations such as fusion genes, homozygous null mutations or deletions in hematological malignancies (Burmeister, Meyer et al. 2009; Delhommeau, Dupont et al. 2009; Meyer, Kowarz et al. 2009; Ko, Huang et al. 2010). These observations lead to the assumption that 5-hmc may play a role in carcinogenesis.

Besides alterations in DNA methylation patterns, disruptions of covalent histone modifications are further hallmark of cancer. For example, repressive marks, *i.e.* loss of acetylation of H4K16 and increased methylation of H4K20, were found at hypomethylated repetitive sequences (*e.g.* pericentromeric repeats) in many primary tumors compared with normal tissues (Fraga, Ballestar et al. 2005). Alterations in histone modification patterns are the results of abnormal expression, activity or recruitment of histone-modifying enzymes and histone code-reading proteins, induced by genetic or epigenetic alterations (Cress and Seto 2000; Mahlknecht and Hoelzer 2000; Ellis, Atadja et al. 2009). Thus, H4K20 was correlated to hematological malignancy by a recent report about MMSET, a gene coding for a H4K20 histone trimethylase, which is overexpressed in an aggressive subset of multiple myeloma carrying the t(4;14) translocation (Schotta, Lachner et al. 2004). Moreover, AML is associated with the t(8;21) chromosomal translocation that is responsible for the AML1-ETO fusion protein. This chimeric protein is a potent dominant transcriptional repressor that recruits HDAC activity, inducing alterations in histone modification landscape and gene expression profiles (Wang, Hoshino et al. 1998; Wang, Sauntharajah et al. 1999). Other leukemia fusion proteins, such as PML-RAR or PLZF-RAR, have similar HDAC recruiting features (Minucci, Nervi et al. 2001).

Finally, alterations in miRNA processing and expression profiles play a major role in carcinogenesis. The link between miRNAs and cancer pathogenesis has emerged from the discovery that miRNA expressing genes are frequently located in cancer-associated genomic regions (CAGR). Indeed, about 50% of all annotated human miRNA genes are located in minimal regions of amplifications, common breakpoint regions in or near oncogenes, TSGs and chromosomal fragile sites (Calin, Sevignani et al. 2004; Sevignani, Calin et al. 2007; Melo and Esteller 2010). Since miRNAs are frequently expressed as polycistronic transcripts, deregulation of one member of the cluster is accompanied by a deregulation of other cluster members.

Obviously, the miRNome varies between normal and pathological tissue as well as between different cancer types. Expression of miRNAs seems to be generally downregulated in cancer cells excepting a few cancer type-specific miRNA genes, whose increased expression is associated with carcinogenesis

(Deng, Calin et al. 2008; Zhang, Li et al. 2010). Rather than a change of a single miRNA gene that regulates one oncogene or TSG, miRNome-wide alterations contribute to carcinogenesis. Thus, miRNAs with a protective or tumor suppressive role, called anti-oncomirs, are commonly silenced in cancer cells. Calin *et al.* reported for the first time abnormal expression of miR-15a and miR-16-1, a cluster often downregulated in CLL, which is involved in the regulation of human genes such as BCL-2 (Melo and Esteller 2010; Zheng, Wang et al. 2010). Both miRNA genes are located at chromosomal position 13q14.3, which is frequently deleted in CLL and lymphoma (Chiorazzi, Rai et al. 2005). In contrast, the oncomir subclass regroups miRNAs that are mostly overexpressed in cancer cells and responsible for TSG silencing. Hence, the polycistron miR-17~92, which is often upregulated in lymphoma and CLL samples, suppresses the expression of both the pro-apoptotic gene Bim and the TSG PTEN, leading to enhanced cell survival and proliferation rate (Ota, Tagawa et al. 2004; Xiao, Srinivasan et al. 2008). In addition, some miRNAs such as miR-328 may even have a dual oncogenic and tumor-suppressive role in cancer, depending on cell type and gene expression pattern (Eiring, Harb et al. 2010; Melo and Esteller 2010).

In analogy with protein-coding genes, miRNA functions are also influenced by point mutations. Nevertheless, site restricted errors in the sequence of mature miRNA seed region seem to be rare (He, Jazdzewski et al. 2005; Diederichs and Haber 2006; Yang, Zhou et al. 2008). Nevertheless, point mutations in the 3' UTR of the miRNA target mRNA can reduce or induce the loss of miRNA target sensitivity, specificity, and response to miRNA target recognition (Visone and Croce 2009). Genetic aberrations can also affect RISC complex assembly and compromise miRNA-mediated silencing (Kwak, Iwasaki et al. 2010). Furthermore, tumor-specific mutations in miRNA sequences influence the stability of precursor as well as mature miRNA, and play on miRNA expression level (Diederichs and Haber 2006). Moreover, alterations in the expression of miRNA regulating transcription factors induce aberrant transcription of pri-miRNAs. Finally, impairments in the miRNA processing step can change miRNA expression pattern in cancer

cells (Kwak, Iwasaki et al. 2010). Remarkably, since approximately half of all miRNA genes contain CGIs, aberrant DNA hypermethylation-mediated silencing can also affect miRNA network (Calin and Croce 2006; Esquela-Kerscher and Slack 2006; Deng, Calin et al. 2008). Thus, the miR-203 locus frequently undergoes DNA methylation in T-cell lymphoma compared to normal T-lymphocytes (Bueno, Perez de Castro et al. 2008). Additional miRNAs are targets for DNA hypermethylation, such as miR-9-1, miR124a, miR-127 and let-7 family in breast, colorectal, bladder or epithelial ovarian cancer, respectively (Lujambio, Ropero et al. 2007; Lehmann, Hasemeier et al. 2008; Guil and Esteller 2009).

These observations clearly demonstrate that miRNA expression is often deregulated in cancer cells, with numerous miRNAs being overexpressed in one type of cancer and downregulated in another. Therefore, cancer-specific miRNA expression signature could be used as a cancer diagnosis or therapeutic tool.

1.5. DNA methylation in the management of blood cancer

Current knowledge indicates that the development of malignancies is based on a mixture of genetic and epigenetic defects (Issa and Kantarjian 2009). Cytogenetic alterations in AML and multiple myeloma at diagnosis are considered to be valuable prognostic determinants (Grimwade, Walker et al. 1998; Hideshima, Bergsagel et al. 2004). Nevertheless, genomic aberrations, leading to misexpression or appearance of a truncated gene form can occur in multiple sites of a gene such as the promoter or the gene body. This feature limits the effective use of somatic mutations as cancer biomarker. In contrast, hypermethylation occurs mainly in the regulatory gene promoter region. Moreover, aberrant hypermethylation of cancer cells is detectable in the background of hypomethylated normal cells, whereas tumor-associated loss of heterozygosity and homozygous deletions disappear in a healthy heterozygote background. Furthermore, DNA molecules *per se* as well as methylation at the 5' position of cytosine are chemically stable and can only be modified by specific enzymes. Under most conditions turnover of

methylcytosine in slow. In consequence, DNA methylation changes can be robustly and specifically analyzed in a large variety of fresh or archived biological samples (e.g. biopsies or body fluids). The development of new highly sensitive analysis techniques (e.g. high throughput deep sequencing) allows the specific detection of hypermethylation signatures in small DNA amounts (Schulz and Goering 2011). Accordingly, four major clinical oncology areas could potentially benefit from the identification of methylation signatures. Powerful epigenetic biomarkers can be applied for cancer diagnosis (early detection and prevention), prognosis (tumor behavior), pharmacogenetics (drug response to follow efficacy of treatment) and as target for epigenetic drugs (Figure 10) (Esteller 2011).

Analysis of the methylation signatures allow to distinguish normal surrounding tissues from cancer cells. Moreover, stratification of the different cancer types and stages by mapping of the CGi methylation pattern could improve early detection of tumor cells (Figure 10). For example, hypermethylation of O-6-methylguanine-DNA methyltransferase (MGMT) or CDKN2A can be observed up to three years prior to classical cancer diagnosis by medical check-up in squamous cell lung carcinoma. Moreover, hypermethylation of HIC1 is a poor prognosis marker in lung cancer (Hayashi, Tokuchi et al. 2001). Thus, the early presence of hypermethylated TSGs does not necessarily indicate an invasive cancer, as premalignant or cancer precursor lesions can also carry these epigenetic signatures. Hence, these signatures could be used for early cancer detection in individuals with genetic predispositions or exposed to carcinogens. Moreover, many tumors 'shed' DNA into the serum or other easily accessible body fluids (e.g. blood, bronchoalveolar lavage, lymph nodes, sputum, urine, semen, ductal lavage or saliva) simplifying epimutation detection in an early tumorigenesis stage (Ahrendt, Chow et al. 1999; Sanchez-Cespedes, Esteller et al. 1999; Goessl, Krause et al. 2000; Palmisano, Divine et al. 2000; Cairns, Esteller et al. 2001; Evron, Dooley et al. 2001; Rosas, Koch et al. 2001). Noteworthy, the gold standard epigenetic biomarker for prostate cancer is the hypermethylated status of the detoxification enzyme GSTP1, since neoplastic prostate cancer cells are hypermethylated in up to 90% of patients (Lee, Morton et al. 1994; Esteller, Corn et al. 1998).

As previously mentioned, these epigenetic markers could be used in cancer risk assessment, 'cancer prevention' and identification of predispositions that act epigenetically as a cause of cancer (Sincic and Herceg 2011). However, a clear definition about minimal genetic, epigenetic and phenotypic characteristics associated with tumor initiation and progression (*i.e.* from a benign to a malignant cell) of cancer cells is still pending.

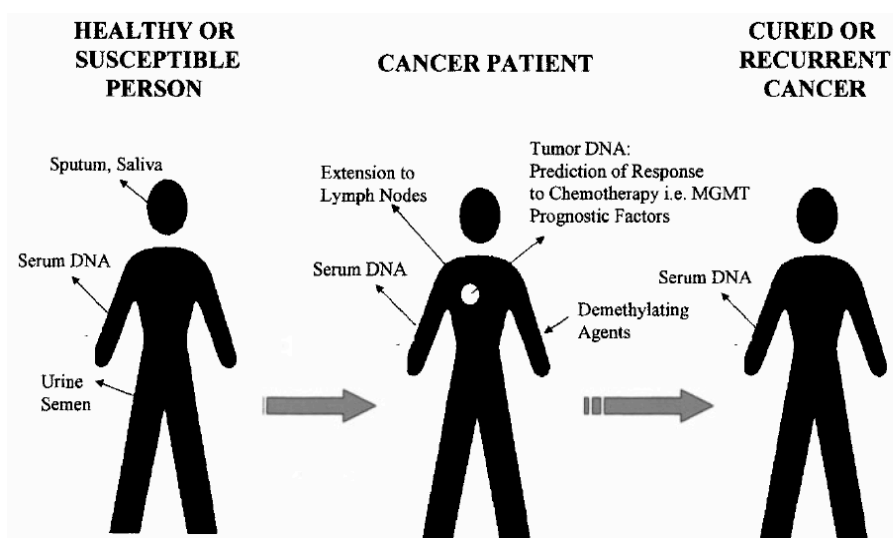


Figure 10: Application range for CpG island hypermethylation in cancer diagnostic and treatment routine.

Possible biological samples used for the detection of hypermethylation as well as the possible application fields (prognosis, diagnosis, treatment). MGMT: O-6-methylguanine-DNA methyltransferase (Esteller 2002).

In addition, screening of the unique DNA methylation signature may reveal biomarkers with clinical potential, providing information about tumor behavior (Rodriguez-Paredes and Esteller 2011, Esteller, 2002 #145). For example, hypermethylation of CDKN2B and HOXA4 genes was considered to be a negative prognostic marker for AML (Wong, Ng et al. 2000; Chim, Liang et al. 2001; Strathdee, Holyoake et al. 2007). Furthermore, calcitonin A (CALCA) gene is frequently hypermethylated in ALL and is associated with enhanced risk of relapse (Roman, Castillejo et al. 2001).

Mapping of DNA hypermethylation could further provide information about drug pharmacodynamics. Common chemotherapeutic agents target uncontrolled rapidly dividing cancer cells and induce DNA damages.

Consequently, genes involved in DNA repair (e.g. MGMT, mutL homolog (MLH) 1 or breast cancer (BRCA) 1) are promising epigenetic candidates to predict pharmacoepigenetic response. The methylation status of MGMT gene, which repairs alkylated guanines, is used to predict glioma tumor response to the alkylating drugs carmustine and temozolomide (Hegi, Liu et al. 2008). The MGMT gene was one of the first genes, where functionality and methylation status were commercially analyzed for the prediction of progression-free and overall cancer survival (www.oncomethylome.com) (Costa 2010). Hypermethylation-associated silencing of MGMT prevents repair of chemotherapy-induced DNA lesions, finally resulting in programmed cell death. Moreover, MGMT hypermethylation, in tumor samples from diffuse large B-cell lymphoma (DLBCL) patients receiving cyclophosphamide-based chemotherapy, was associated with a significant increase of overall survival (Esteller, Gaidano et al. 2002). Likewise, methylation status of genes involved in cell cycle regulation, drug transport and metabolism may have a predictive potential value for drug response or chemoresistance (Rodriguez-Paredes and Esteller 2011). Accordingly, epigenetic silencing of organic solute carrier partner 1 (OSCP1), which is involved in drug transport, is associated with CML resistance to imatinib (Jelinek, Gharibyan et al. 2011). Since the aim of most cancer treatments is to induce cell death, chemotherapy sensitivity may also depend on the apoptotic potential of the targeted cancer cells. In accordance, cells with hypomethylated prosurvival genes (e.g. XIAP, BCL-2) as well as hypermethylated and repressed proapoptotic genes (e.g. PTEN, APAF-1) are highly resistant to cell death induction (Balch, Montgomery et al. 2005).

In addition to classical epigenetic cancer markers, current research is dedicated to detect new candidate genes with abnormal methylation pattern for their translation into biomarkers. First indications for an epigenetically silenced gene are the loss of expression in tumors, the absence of genomic mutations in the gene of interest as well as the presence of a promoter CGi. The next step consists in the analysis of the CGi methylation status by bisulfite conversion and non-bisulfite methods in cancer cell lines and patient samples. To compare hypermethylation and transcriptional silencing, treatment with a demethylating agent should restore gene functionality.

Finally, it should be demonstrated that the epigenetic silencing of the gene of interest contributes to human tumorigenesis (Esteller 2002).

Since every cancer type has its unique and complex epigenetic signature, it is unlikely that a single biomarker will be enough to predict the outcome of a cancer. For example, CDKN2A, CDKN1C and TP73 genes are found commonly methylated in cancer. When analyzed individually, none of these genes showed clear prognostic value. Nonetheless, patients with concomitant methylation of at least two of this triad had a lower median survival than patients either with methylation of only one these 3 genes or without methylation (Garcia-Manero, Yang et al. 2009). Assaying multiple methylation markers is mandatory in cancer management in order to cover the biological heterogeneity, arising during cancer progression and histological subtypes, to increase sensitivity and to discriminate age-related background noise (Schulz and Goering 2011).

Similarly to DNA hypermethylation, global DNA hypomethylation may also be used in the future as an epigenetic marker for cancer diagnosis. In accordance, loss of LINE hypermethylation occurs with the progression of the hematological malignancy and could be used for cancer detection and prognosis (Roman-Gomez, Jimenez-Velasco et al. 2005). In addition, genome-wide analysis showed that AML cells are hypomethylated compared to isolated normal B- and T-lymphocytes. However, comparison of the global methylation level between malignant AML and benign bone marrow cells showed no significant differences (Giotopoulos, McCormick et al. 2006). Thus, the application of hypomethylation pattern for cancer management is still at its beginning. Establishment of appropriate control samples will help to get a clear view of leukemogenesis-associated global hypomethylation signatures and evaluate their prevalence and clinical relevance.

1.6. DNA methylation as a therapeutic target

During early embryogenesis as well as gametogenesis, cells are reprogrammed by undergoing a massive genome-wide DNA demethylation. This epigenetic remodeling also arises in adult cells after nuclear

transplantation (Rideout, Eggan et al. 2001). In the same way, this approach seems to reverse the malignant phenotype of cancer cells, even in a background of somatic mutations (Hochedlinger, Blelloch et al. 2004). DNA methylation is reversible, thus representing an attractive target for anticancer therapeutic intervention.

In the early 1960s, Sorm *et al.* first synthesized the common cytosine analogue azacytidine (AZA) (Piimi 1964; Pískala 1965). The nucleoside analogue AZA is an S phase-specific prodrug, which is incorporated into RNA and during replication into DNA. In contrast, its derivate 5-aza-2'-deoxycytidine (DAC, decitabine) is only incorporated into DNA (Figure 11). Initially designed as cytotoxic agents, their DNMT inhibiting and DNA demethylating activities were discovered by pure chance (Issa and Kantarjian 2009).

After its cellular uptake, DAC is successively phosphorylated to mono, di and triphosphate forms. The latter is incorporated into nascent daughter strands of replicating DNA (Figure 11-A) (Momparler and Derse 1979; Glover, Leyland-Jones et al. 1987). The azacytidine ring, which protrudes out from the DNA double strand, subsequently catches and covalently binds DNMTs. The following polyubiquitylation targets DNMTs for their subsequent proteasomic degradation (Figure 11-B) (Ghoshal, Datta et al. 2005). The resulting cellular depletion of DNMTs makes it impossible to maintain the methylation during replication and thus provokes a passive loss of DNA methylation (Figure 11-B). Paradoxically, trapping of DNMTs onto DNA creates bulky adducts that can inhibit DNA synthesis and eventually result in cell death by cytotoxicity (Juttermann, Li et al. 1994). Dose-response analysis showed that optimal biological effects on DNA demethylation and gene expression induction are obtained at relatively low DAC concentrations ($<5\mu\text{M}$), whereas DNA synthesis and replication are blocked at higher doses ($>50\mu\text{M}$) impairing the DNA demethylation effect (Qin, Jelinek et al. 2009). Once a hypomethylation pattern has been induced, it can be carried over through subsequent cell divisions, resulting in prolonged alterations of gene expression. Unfortunately, cells show a tendency to remethylate DNA sequences that have been

demethylated by drug treatment, resulting in a gradual blunting of the cellular response (Bender, Gonzalzo et al. 1999).

As previously described, nucleoside analog DNA methylation inhibitors (DNMTi) require incorporation into DNA to be effective. In consequence, they have no measurable effects on non-cycling cells, which constitute the vast majority of the human body cells. Since cancer cells tend to scavenge more effectively nucleosides than normal cells, they integrate more drugs into their DNA (Cheng, Yoo et al. 2004).

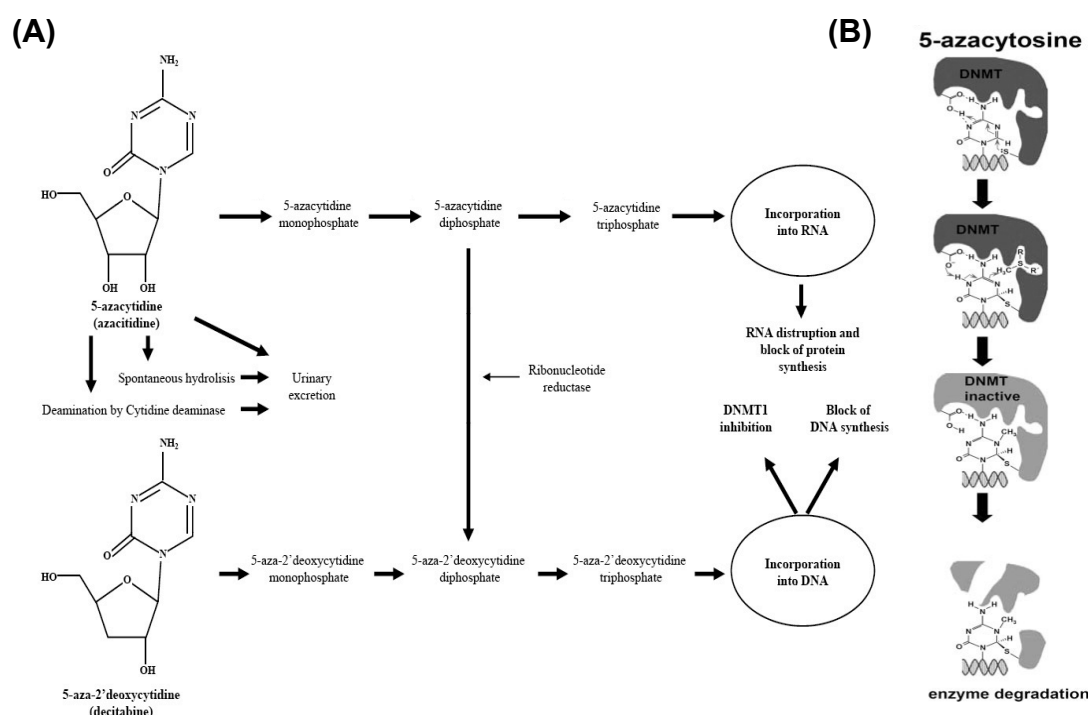


Figure 11: Intracellular metabolic pathways of azacytidine and 5-aza-2'-deoxycytidine.

(A) After cellular uptake, both drugs require phosphorylation to triphosphate derivatives to be incorporated into newly synthesized RNA and DNA. 5-azacytidine diphosphate is also reduced by ribonucleotide reductase to 5-aza-2'-deoxycytidine diphosphate, which is furthermore phosphorylated and incorporated into DNA. Elevated expression of the cytidine deaminase can mediate a 5-azacytidine resistance. (B) The incorporated 5-azacytosine ring bind covalently DNA methyltransferase (DNMT) 1. Resulting adducts induce loss of DNA methylation through DNMT1 depletion by ubiquitylation-mediated proteasomal degradation. Adapted from (Leone, D'Alo et al. 2008; Stresemann and Lyko 2008).

At the beginning, DNMTi were exclusively used in cell culture as tools to induce genomic demethylation, restore gene expression and trigger cell differentiation (Jones, Taylor et al. 1982; Jones 1985). Even though DAC is

one of the most effective DNA demethylating drugs, downstream effects of DNMTi-mediated DNA demethylation are quite unspecific and thereby complicate clinical application (Villar-Garea and Esteller 2003; Issa and Kantarjian 2009). Indeed, it must be taken into account that DAC-mediated demethylation, even at low doses, will affect a broad range of usually silenced pathways implicated in cell proliferation, differentiation, apoptosis, invasion (upregulation of motility genes) and angiogenesis (through angiogenesis inhibitors). Furthermore, DAC-induced demethylation can achieve detrimental effects such as the restoration of epigenetically silenced oncogenes, awakening of transposable elements, and activation of the deleterious expression of the X-chromosome or imprinted genes (Issa and Kantarjian 2009). Similarly, non-coding RNAs such as miRNAs (*i.e.* oncomirs) that are often repressed by DNA methylation are inducible by DNA demethylating drugs (Saito, Liang et al. 2006). In consequence, effects of DNA methylation inhibition are probably cell-specific and it is likely that a mixture of effects reflecting the total sum of pathways activated is the reality in most cases.

Early clinical trials have tested high doses of DAC for its cytotoxicity on cancer cells. DAC at 1500 to 2500 mg/m² were administered for relatively short exposure time. However, disappointing results concerning efficacy and toxicity were largely unfavorable and the use of nucleoside analogs was abandoned by the U.S. Food and Drug administration (FDA) (Rivard, Momparler et al. 1981; Momparler, Rivard et al. 1985). Hypomethylating nucleoside analogs came back to life over the past decade through the persistence of a few investigators (Wijermans, Lubbert et al. 2000). Zagonel *et al.* explored low dose schedules of DAC (*i.e.* 45mg/m²/day over 4h for 3 days and 50mg/m²/day by continuous daily infusion for 3 days) in 10 MDS patients. An overall response rate of 50% was obtained in these studies. Accordingly, a European clinical phase II trial was initiated in the early 90s, exploring this low-dose DAC schedule delivery. The overall response rate was around 50% in MDS and AML patients (Schwartzmann, Fernandes et al. 1997; Wijermans, Krulder et al. 1997). Final phase III studies further confirmed DAC-mediated responses but failed to demonstrate substantial effects on survival, probably due to the limited numbers of treatment cycles (Kantarjian, Issa et al. 2006). In contrast, the use of an open-end approach for

DAC treatment resulted in a very high response and survival rate superior to what was observed with cytotoxic chemotherapy. Furthermore, treatments with hypomethylating agents improve disease burden and quality of life as well as the side effect profile, which is more favorable as compared with classical anti-cancer therapy (e.g. no hair loss or renal failure) (Issa and Kantarjian 2009). DAC is the first epigenetic drug specifically approved by the FDA in 2006 for MDS treatment. The fact that no standard of care exists for MDS was probably in favor for DAC application. Nevertheless, there is no special reason why MDS should be the only epigenetically responsive disease. Today, DAC is also tested in clinical trials for CML treatment (Altucci, Clarke et al. 2005). These interesting and promising results encourage research to further develop more effective and selective DNA demethylating agents.

As mentioned above, demethylating drugs can restore apoptotic potential and thereby chemosensitized tumor cells. Therefore, successive first-line therapy with DNA demethylating agents followed by a conventional second-line therapy could resensitize tumor cells and induce cancer regression (Balch, Montgomery et al. 2005). Accordingly, combination of DNMTis with other epigenetic drugs such as HDAC inhibitors (HDACi) can improve cancer therapy (Altucci, Clarke et al. 2005). HDACi are inducing hyperacetylation of lysine residues in the histone tails, leading to chromatin decondensation and transcriptional activation. HDACi are categorized according to their structure into five categories: short fatty acids (sodium butyrate, valproic acid), hydroxamin acid derivate (trichostatin A (TSA), suberoylanilide hydroxamic acid (SAHA)), benzamides or cyclic peptides (Miller, Witter et al. 2003). In addition, many molecules with a potential inhibitory activity against HDACs but a chemical structure different than the first five were identified. HDAC inhibition induces diverse cell- and compound-specific outcomes including inhibition of cell cycle and cell growth, induction of differentiation and apoptosis. Due to aberrant histone acetylation patterns in cancer, HDACs are novel targets for cancer therapy (Glaser, Staver et al. 2003; Mitsiades, Mitsiades et al. 2004; Peart, Smyth et al. 2005). For example, combination of DAC and TSA acts synergistically in activation of PTGS2, hMLH1, TIMP3, CDKN2B and CDKN1C expression in colorectal

cancer cell lines (Cameron, Bachman et al. 1999; Suzuki, Gabrielson et al. 2002). Similarly, the combined treatment led to the activation of ESR1 gene in breast cancer cell lines (Yang, Phillips et al. 2001).

1.7. Glutathione S-transferase P1

As previously described, analysis of the cancer epigenome revealed useful diagnostic, prognostic and treatment response biomarkers. DNA methylation-mediated epigenetic silencing of the glutathione S-transferase (GST) P1 is considered to be a molecular hallmark and diagnostic marker for human prostate cancers (Lee, Morton et al. 1994; Lee, Isaacs et al. 1997).

GST multi-gene superfamily is coding for homo- or heterodimeric metabolic enzymes, which represent the major group of multifunctional phase II detoxification enzymes. GSTs catalyze the conjugation of the tripeptide gamma-glutamyl-cysteinyl-glycine (glutathione, GSH) to genotoxic xenobiotics occurring from extracellular environment or intracellular phase I metabolism (Figure 12). In consequence, neutralization of the electrophilic site reduces genotoxic activity, improves water solubility and favors the cellular export of GS-X through ATP-dependent pumps (Eaton and Bammler 1999). This biotransformation-mediated detoxification of exogenic and endogenic molecules protects cellular macromolecules from damage and guarantees cell integrity.

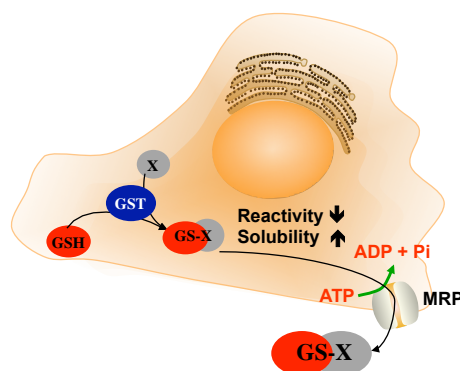


Figure 12: Schematic representation of GST-mediated cellular detoxification.

GSTs catalyze the neutralization of the electrophilic compound (X) by conjugation with glutathione (GSH), reducing the reactivity, improving water solubility and promoting compound export by MRP/GS-X pumps in an ATP-dependent manner. GST: glutathione S-transferase, ATP: adenosine triphosphate, ADP: adenosine diphosphate, Pi: phosphate, MRP: multidrug resistance protein.

GSTP1 is the major isoform of the GST multi-gene superfamily and is implicated in oxidative stress response, proliferation and chemotoxic resistance. In accordance, GSTP1 interacts with c-Jun NH₂-terminal kinase (JNK) and tumor necrosis factor receptor-associated factor 2 (TRAF2), and suppresses the induction of apoptosis (Ruscoe, Rosario et al. 2001; Wu, Fan et al. 2006). GSTP1 gene is located on chromosome 11 from position 67,351,066 to 67,354,123 and is preceded by a high density of CGIs. The largest CGI, upstream of the transcription start site, is divided by a long ATAAA repetitive stretch (Figure 13). It is assumed that this repetitive element acts as an insulator to separate different epigenetic states (Millar, Paul et al. 2000). GSTP1 transcription is controlled by the transcription factors AP-1, SP-1 and NF-κB (Figure 13) (Duvoix, Schnekenburger et al. 2004; Morceau, Duvoix et al. 2004). Moreover, GSTP1 is a downstream transcriptional target of the tumor suppressor p53 (Lo, Stephenson et al. 2008).

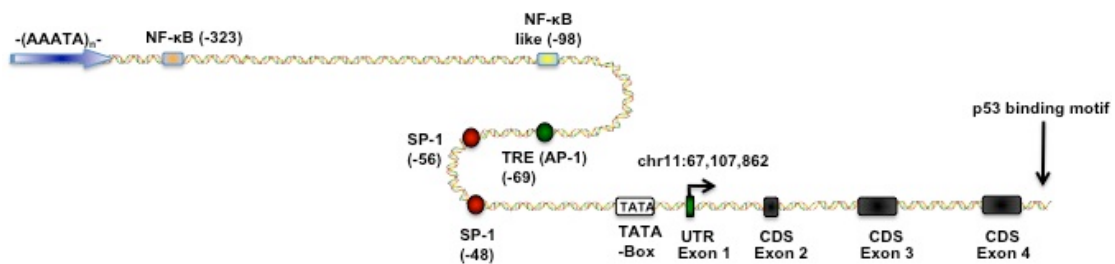


Figure 13: Organization of GSTP1 gene promoter in human.

Map of GSTP1 promoter region that is located on chromosome 11. Transcription factors and their binding sites as well as untranslated region (UTR) and coding sequences (CDS) are indicated related to the transcription start site. NF-κB: nuclear factor-κB, SP-1: specificity protein 1, TRE: TPA response element.

GSTP1 is expressed in normal epithelial tissues and cells of the urinary, digestive and respiratory tracts, and is increased after exposure to carcinogens (Sawaki, Enomoto et al. 1990; Terrier, Townsend et al. 1990; Zhang, Sun et al. 2011). In addition, GSTP1 null allele mice have a higher mutation risk after carcinogen exposure. This result suggests that even the lack of one single GST isoform could increase susceptibility to cancer (Ketterer 1998).

Overexpression of GSTP1 gene may lead to an enhance detoxification activity and may protect human cells against cytotoxic drugs. Increased

expression of GSTP1 was detected in multiple cancers (e.g. ovary, bladder, pancreas, head and neck cancers) (Green, Robertson et al. 1993; Bentz, Haines et al. 2000; Trachte, Suthers et al. 2002; Simic, Mimic-Oka et al. 2005). Consequently, electrophilic cytostatics are inactivated through conjugation with GSH or reduction of toxicity by GSH-dependent denitrosation (e.g. nitrosocaramide). Moreover, upregulation of GSTP1 peroxidase activity leads to enhanced elimination of DNA adducts (e.g. cisplatin) (Goto, Iida et al. 1999). In contrast, genetic (e.g. deletions, polymorphism) or epigenetic alterations (e.g. DNA methylation-mediated silencing) may reduce the occurrence, function or activity of GSTP1. Accordingly, detoxification efficiency is attenuated leading to an increased sensitivity to environmental toxins and to subsequent higher risk for mutations and cancer development (Coughlin and Hall 2002; Coughlin and Hall 2002).

Hypermethylation of the regulatory promoter region near the GSTP1 gene has been associated with gene silencing in prostate, breast and kidney cancers (Dulaimi, Ibanez de Caceres et al. 2004; Hopkins, Burns et al. 2007; Lasabova, Tilandyova et al. 2010). GSTP1 hypermethylation is best investigated in prostate cancer, including prostatic intraepithelial neoplasia (PIN), adenocarcinoma biopsies and body fluids (*i.e.* plasma, serum, ejaculate and urine) of patients, whereas GSTP1 promoter is unmethylated in benign prostatic epithelium (Lee, Isaacs et al. 1997; Jeronimo, Usadel et al. 2002; Gonzalzo, Nakayama et al. 2004; Hopkins, Burns et al. 2007; Cao and Yao 2010). GSTP1 silencing by DNA hypermethylation was detected in 90% of all prostate tumors and in 70% of the high-grade PIN (Nakayama, Bennett et al. 2003; Henrique and Jeronimo 2004). Moreover, comparative analysis showed lower GSTP1 expression in correlation with hypermethylated promoter region in invasive than in non-invasive pituitary tumors, providing predictive information about pituitary tumor aggressiveness (Yuan, Qian et al. 2008). Interestingly, Lin *et al.* linked GSTP1 silencing in MCF-7 cells to promoter hypermethylation and enrichment of MBDs and DNMT1 in this region (Lin and Nelson 2003). Similar analysis of prostate cancer cell lines revealed that GSTP1 gene is hypermethylated in expressing LNCaP but hypomethylated in non-expressing DU145 cells (Song, Stirzaker et al. 2002). As previously shown, DAC treatment of LNCaP cells is associated with GSTP1

demethylation and induction of GSTP1 expression (Chiam, Centenera et al. 2011). In addition, GSTP1 promoter hypermethylation was associated with a repressive histone modification pattern in LNCaP cells. The HDAC inhibitor depsipeptide reversed GSTP1 epigenetic silencing and induced its expression (Stirzaker, Song et al. 2004; Hauptstock, Kuriakose et al. 2011). Studies performed with a xenograft model and human prostate cancer LNCaP cells showed that hypermethylation and repression of GSTP1 was reversed *in vivo* after treatment with the nucleoside analog procainamide (Cairns, Esteller et al. 2001). Alternatively, recent results showed that natural products such as green tea polyphenols reactivate GSTP1 expression in prostate cancer cell lines (Pandey, Shukla et al. 2010).

The significance of GSTP1 silencing in prostate cancer is still unclear. Nevertheless, heterogeneous distribution of methylation-mediated GSTP1 repression leads to the assumption that this could be one of the initiating events in prostate carcinogenesis. Indeed, since GSTP1 acts as a 'caretaker' gene, its inactivation reduces cellular detoxification ability and therefore cells get more vulnerable to somatic alterations upon exposure to mutagens (Meiers, Shanks et al. 2007).

In conclusion, these data reveal that a balanced and tightly regulated expression of GSTP1 is of major importance for cell integrity in order to avoid on the one hand drug resistance and on the other hand genetic damages.

A previous work of the laboratory on the regulation of GSTP1 expression in blood cancer cell lines identified GSTP1 positive (*e.g.* K-562, U-937 and JURKAT) and the GSTP1 non-expressing RAJI lymphoma cell line. In addition, *in vitro* methylation of the GSTP1 minimal promoter had a transcriptional inhibitory effect. However, *in vivo* methylation analysis failed to correlate GSTP1 promoter methylation and expression (Borde-Chiche, Diederich et al. 2001).

1.8. Prostaglandin-endoperoxide synthase 2

In analogy to GSTP1 promoter aberrant methylation, prostaglandin-endoperoxide synthase (PTGS) 2 represent another hotspot for epimutations

in various cancer types (Toyota, Shen et al. 2000; Wang, Guo et al. 2005; Meng, Zhu et al. 2010).

The pro-inflammatory PTGS, also known as cyclooxygenase, genes are rate-limiting enzymes, which catalyze the conversion of arachidonic acid into the intermediate prostaglandins (PG) H₂, from which prostaglandins, prostacyclines and thromboxanes are derived. PTGS1 is constitutively expressed in many tissues and is responsible for the maintenance of various cell physiological functions. In contrast, PTGS2 isoform is an immediate early response gene, which is induced by inflammation-related factors, proinflammatory cytokines, growth factors as well as mitogenic and tumor promoting agents (Toyota, Shen et al. 2000; Ma, Yang et al. 2004; Wun, McKnight et al. 2004).

PTGS2 gene is located on chromosome 1 from position 186,640,945 to 186,649,559 and its expression is regulated by a number of regulatory elements presented in Figure 14.

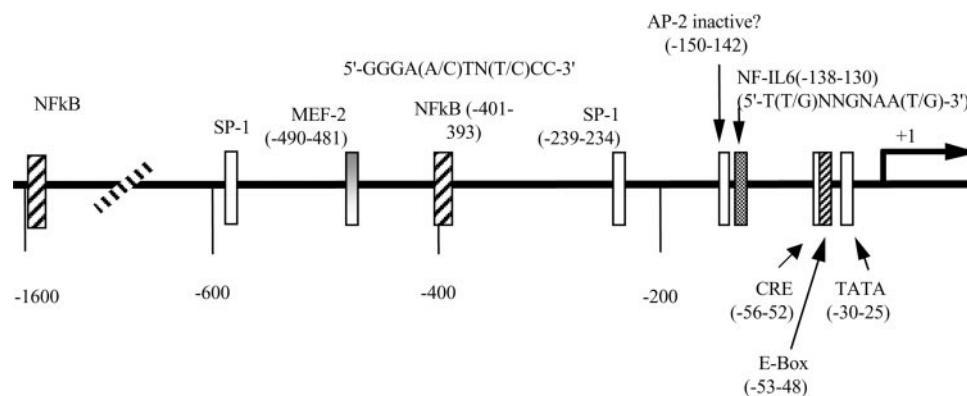


Figure 14: Configuration of PTGS2 promoter.

Multiple response elements are involved in the transcriptional regulation of PTGS2 expression. AP-2: activator protein-2, CRE: cAMP-responsive element, IL-6: interleukin-6, MEF-2: myocyte-enhancer factor, NF-κB: nuclear factor-κB, SP1: specificity protein 1 (Harris and Breyer 2001).

PTGS2 promoter include basal elements such as a TATA-box as well as binding domains for specific transcription factors including cAMP response element binding (CREB), NF-κB and SP1 (Harris and Breyer 2001). The precise mechanism of PTGS2 regulation remains unclear. Nevertheless, it is known that PTGS2 is a K-RAS target gene, which can induce PTGS2

transcription or mRNA stabilization by mitogen-activated protein kinase pathways (*i.e.* MEKK/SEK/JNK, Raf/MEK/ERK or PI3-K/Akt/PKB) (Sheng, Shao et al. 2001). Moreover, PTGS2 expression is upregulated by the transcription factor encoding the proto-oncogene c-MYB, whereas p53 acts as a PTGS2 repressor (Subbaramaiah, Altorki et al. 1999; Ramsay, Friend et al. 2000).

It is generally accepted that PTGS2 is often overexpressed in breast, gastric, colorectal, lung, liver and prostate cancer cells (Eberhart, Coffey et al. 1994; Liu and Rose 1996; Ristimaki, Honkanen et al. 1997; Liu, Yao et al. 1998; Wolff, Saukkonen et al. 1998). Apparently, PTGS2 overexpression progresses with gastric and urinary bladder carcinogenesis, inducing the constitutive synthesis of PGE₂ and activation of APC/β-catenin/Wnt signaling pathway (Wadhwa, Goswami et al. 2005). β-catenin in complex with transcription factors leads to the expression of metalloproteinases (MMPs) and vascular growth factors (VEGFs) (Figure 15) (Ben-Av, Crofford et al. 1995; Cheng, Cao et al. 1998).

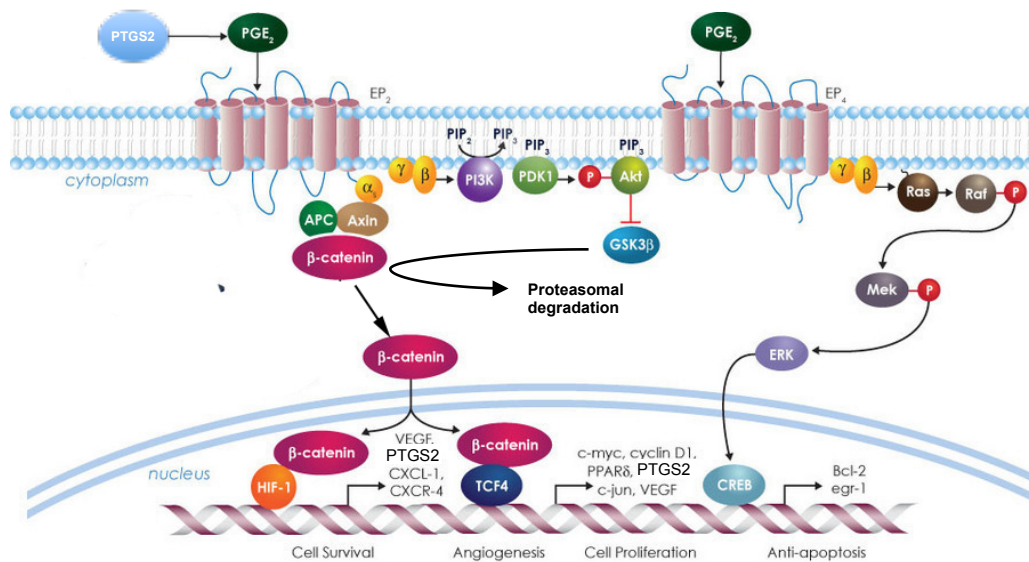


Figure 15: Implication of PTGS2/PGE₂ signaling in the hallmarks of cancer.

Overexpression of PTGS2 leads to PGE₂ oversynthesis inducing the expression of genes regulating cell survival, angiogenesis, cell proliferation and apoptosis through activation of Wnt and Ras/Raf signaling pathways (modified from May, O (<http://www.caymanchem.com/app/template/Article.vm/article/2136>)).

Activation of these genes induces proteolysis of extracellular matrix and promotes angiogenesis, which in turn favors the transition from limited tumor growth to invasion and metastasis (Price, Bonovich et al. 1997; John and Tuszynski 2001). Furthermore, high intrinsic PTGS2 expression constitutively activates the survival gene BCL2 through the Ras/Raf signaling pathway and inhibits apoptosis (Tsujii and DuBois 1995; Tsujii, Kawano et al. 1997; Murata, Tsuji et al. 2004) (Figure 15). Moreover, PTGS2 overexpression and enhanced prostaglandin production are associated with aggressive breast cancer subtypes (Rolland, Martin et al. 1980; Parrett, Harris et al. 1997; Ristimaki, Sivula et al. 2002). Accordingly, inhibition of PTGS2 by nonsteroidal anti-inflammatory drugs or specific inhibitors causes cell death in cancer cells (Sheng, Shao et al. 1998; Elder, Halton et al. 2000). These results suggest that PTGS2 overexpression attenuates the apoptosis potential of premalignant cells and leads to their protection against cell death. In consequence, prolonged cell survival will lead to the accumulation of multiple genetic mutations, resulting ultimately in a transformed phenotype with continuous cell growth.

Paradoxically, ectopic PTGS2 overexpression seems to avoid chemically induced skin cancer in a transgenic mouse model, confirming a preventive role of PTGS2 in carcinogenesis (Bol, Rowley et al. 2002). Moreover, PTGS2 overexpression was reported to induce cell cycle arrest and cell growth inhibition in various cancer and vascular epithelial cells (DuBois, Shao et al. 1996; Trifan, Smith et al. 1999). Finally, in adenomatous polyposis coli (APC) knockout mice, lack of PTGS2 expression resulted in the decrease of neoplastic growth and number of tumors (Oshima, Dinchuk et al. 1996). Nevertheless, loss of PTGS2 expression blocks inflammatory response and thus compromise cellular integrity.

In analogy to GSTP1 gene, a tightly regulated expression of PTGS2 is of major importance to avoid cancer development. Surprisingly, a short-term PTGS2 overexpression may suppress cell progression, whereas a long-term overexpression contributes to tumor growth, invasion and metastasis (Fosslie 2001; Murata, Tsuji et al. 2004). Accordingly, regulation of PTGS2 expression as well as the consequences of abnormal expression should be

explored deeper in order to better understand the mechanisms of cancer development.

Toyota *et al.* first proposed that dense PTGS2 promoter methylation is associated with transcriptional silencing in colorectal cancer (Toyota, Shen *et al.* 2000). Publications about human tumors of esophageal and gastric origin further evinced a strong correlation between PTGS2 inactivation and promoter hypermethylation. Moreover, treatments with demethylating agents such as DAC restored PTGS2 expression in various cancer cell lines (Toyota, Shen *et al.* 2000; Wang, Guo *et al.* 2005; Meng, Zhu *et al.* 2010). Taking together, these data suggest that PTGS2 promoter region is a target for DNA hypermethylation-mediated transcriptional silencing in cancer cells.

Regarding hematological malignancies, it was shown that CML and CLL as well as lymphoma were shown to be constitutively overexpressed PTGS2 (Ladetto, Vallet *et al.* 2005; Ohsawa, Fukushima *et al.* 2006; Ryan, Pollock *et al.* 2006). Nevertheless, Hazar *et al.* reported in 2004 that only 24 out of 42 non-Hodgkin lymphoma patients as well as 7 out of 10 Hodgkin lymphoma patients expressed PTGS2 (Hazar, Ergin *et al.* 2004). However, the possibility that aberrant cancer-related DNA hypermethylation may be involved in PTGS2 repression in hematological malignant cells was never evaluated.

2. Hypothesis and aim of this thesis

Epigenetic alterations such as DNA methylation of CpG islands, which leads to gene silencing, play important roles in carcinogenesis. It is now established that methylation of genes or methylation patterns of groups of genes are tumor-specific. Therefore, DNA methylation signatures can be used as diagnosis biomarkers to detect cancer cells, and was found to be associated with responses to chemotherapeutics and prognosis. In contrast to DNA mutations, which are passively inherited through DNA replication, epimutations must be actively maintained because they are reversible, allowing therapeutic intervention with DNA demethylating/hypomethylating agents.

In the past years, it clearly appeared that during the development of hematological malignancies, genes that suppress growth and induce differentiation could be silenced by aberrant DNA methylation. Significant advances have been made in the elucidation of these processes as well as in translating this knowledge to the clinic, as in the development of new prognostic biomarkers or targeted therapies. Among drugs inducing DNA demethylation, the cytosine nucleoside analogue 5-aza-2'-deoxycytidine is commonly used in clinical trials for various leukemia and promotes tumor cell death.

Nevertheless, the potential of DNA methylomic regarding either disease-specific biomarker discovery or for DNA demethylation-based therapeutic intervention in hematological malignancies still require attention. Hence, our general working hypothesis is that before we are able to properly target DNA methylation in cancer therapy against hematological malignancies, a better understanding of DNA methylation patterns tightly correlated with chromatin structure as well as of the effect of 5-aza-2'-deoxycytidine are required to improve targeted therapy.

Despite clinical observations involving GSTP1 and PTGS2 in carcinogenesis, mechanisms regulating their expression are not completely elucidated. Although both genes are commonly silenced by promoter hypermethylation in various cancers, molecular mechanisms leading to their

silencing by DNA hypermethylation in hematopoietic malignancies and its relationship with pathological alterations of the chromatin structure (*i.e.* histone modifications and co-repressor/co-activator complexes) remain poorly understood. Furthermore, it remains to evaluate, if the aberrant methylation of GSTP1 and PTGS2 gene promoters is characteristic for blood cancer patients.

Thus, the aim of our work is to gain further insight into GSTP1 and PTGS2 epigenetic regulation in hematological malignancies and to compare their implication to other already identified DNA methylation cancer biomarkers as well as the impact of 5-aza-2'-deoxycytidine at gene-specific, genome-wide and cellular levels.

In our attempt to reach these aims we will investigate the following points:

1. First, we will investigate the epigenetic regulation of the expression of GSTP1 and PTGS2 genes in blood cancer cells presenting various gene expression levels, and evaluate the involvement of GSTP1 and PTGS2 promoter hypermethylation in patients with malignant hemopathies.

2. In a next step, we propose to extend our study regarding DNA methylation biomarkers in hematological malignancies by comparing the results obtained regarding PTGS2 and GSTP1 genes to other tumor suppressor genes found frequently methylated in cancer.

3. Finally, we will investigate the effects induced by the DNA demethylating agent 5-aza-2'-deoxycytidine in leukemia and lymphoma cell lines on (i) cell proliferation and survival, (ii) local and global DNA demethylation, and (iii) the relationship between 5-aza-2'-deoxycytidine-induced DNA demethylation and cell proliferation.

3. Material

3.1. Chemicals

Table 2: List of chemical products and their suppliers.

Chemical	Supplier
Acetone	Merck, Darmstadt, Germany
30% Acrylamide Mix/Bis solution (37.5:1)	Bio Rad, Nazareth Eke, Belgium
Agar	MP biomedicals LLC, Illkirch, France
Agarose	Promega, Madison, USA
A/G agarose bead (50% slurry)	Upstate, Millipore, Brussels, Belgium
Ampicillin	Sigma, St Louis, USA
Ammonium persulfate (APS)	MP biomedicals LLC
Ultradistilled water (ddH ₂ O)	Millipore, Brussels, Belgium
Distilled water (dH ₂ O)	Millipore
Bovine serum albumin (BSA)	MP biomedicals LLC
Boric acid (H ₃ BO ₃)	MP biomedicals LLC
5-Brom-4-Chloro-3-indoyl-beta-D-galactopyranosid (X-Gal)	Sigma
Bromphenol blue	LKB, Bromma, Sweden
Protease inhibitor cocktail (Complete+/- EDTA)	Roche, Prophac, Howald, Luxembourg
Carboxyfluorescein diacetate (CFSE)	Invitrogen, Carlsbad, USA
Chloroform	Sigma
5-aza-2'-deoxycytidine (DAC)	Sigma
Deoxycholic acid	Sigma-Aldrich, Bornem, Belgium
Deoxyribonucleoside triphosphate (dNTP)	Invitrogen
Diethylpyrocarbonate (DEPC)	Acros, Geel, Belgium
Dimethyl sulfoxide (DMSO)	Sigma
Di-sodium hydrogen orthophosphate (Na ₂ HPO ₄)	MP biomedicals LLC
Dithiothreitol (DTT)	Roche
Ethanol (EtOH)	VWR, Darmstadt, Germany
Ethidium bromide (EtBr)	Promega
Ethylene diamine tetra acetic acid (EDTA)	MP biomedicals LLC
Ethylene glycol tetra acetic acid (EGTA)	MP biomedicals LLC
Ficoll-Paque PREMIUM	GE Healthcare, Fischer Scientific, Tournai, Belgium
Formaldehyde	MP biomedicals LLC
Glycerol (C ₃ H ₅ (OH) ₃)	VWR

Chemical	Supplier
Glycine (C ₂ H ₅ NO ₂)	MP biomedicals LLC
HEPES (4-(2-hydroxyethyl)-1-piperazineethanesulfonic acid)	MP biomedicals LLC
Hydrogen chloride (HCl)	VWR
(±)-6-Hydroxy-2,5,7,8-tetramethylchromane-2-carboxylic acid	Sigma-Aldrich
Hoechst 33342	Calbiochem, Darmstadt, Germany
IGEPAL	MP biomedicals LLC
Isopropanol (2-propanol, C ₃ H ₇ OH)	VWR
Isopropyl-beta-D-thio-galacto-pyranosid (IPTG)	Invitrogen
Lithium chloride (LiCl)	Sigma-Aldrich
Magnesium chloride (MgCl ₂)	MP biomedicals LLC
Magnesium sulfate (MgSO ₄)	MP biomedicals LLC
β-Mercaptoethanol (C ₂ H ₆ OS)	Merck, Darmstadt, Germany
Methanol (MeOH)	VWR
Monopotassium phosphate (KH ₂ PO ₄)	VWR
Paraformaldehyde	Merck
Phenylmethylsulfonylfluorid (PMSF)	Roche
Piperazine-1,4-bis(2-ethanesulfonic acid) (PIPES)	Sigma-Aldrich
Potassium chloride (KCl)	MP biomedicals LLC
Potassium diphosphate (K ₄ O ₇ P ₂)	VWR
Potassium hydroxide (KOH)	Merck
Protein Assay Bradford solution	Bio Rad
Propidium iodide (PI)	Sigma-Aldrich
Salmon sperm DNA	Upstate
Suberoylanilide hydroxamic acid (SAHA)	Cayman, Michigan, USA
Sodium acetate (C ₂ H ₃ NaO ₂)	VWR
Sodium bicarbonate (NaHCO ₃)	Sigma-Aldrich
Sodium butyrate	Sigma-Aldrich
Sodium chloride (NaCl)	VWR
Sodium dihydrogen orthophosphate (NaH ₂ PO ₄)	ICN, Eschwege, Germany
Sodium disulfite	Merck
Sodium dodecyl sulfate (SDS)	MP biomedicals LLC
Sodium hydroxide (NaOH)	MP biomedicals LLC
Sodium phosphate monobasic anhydrous (NaH ₂ PO ₄)	ICN
Sulfuric Acid (H ₂ SO ₄)	Merck
N,N,N',N'-Tetramethylethyldiamin (TEMED)	MP biomedicals LLC

Chemical	Supplier
Tris	MP biomedicals LLC
Triton-X100	Merck
Trypan blue	Lonza, Basel, Switzerland
Tween [®] 20	Sigma
Valproic acid (VPA)	Sigma-Aldrich
Xylene cyanol	ICN

3.2. Buffers and solutions

3.2.1. General buffers

Table 3: Common buffers and solutions.

Name	Composition
10X Phosphate buffered saline buffer (PBS)	80mM Na ₂ HPO ₄ , 20mM NaH ₂ PO ₄ , 100mM NaCl adjust pH at 5.7 Autoclaved for cell culture use
1X Phosphate buffered saline / Tween buffer (PBS-T)	1X PBS, 0.1% (v/v) Tween [®] 20
Tris/EDTA buffer (TE)	10mM Tris-HCl (pH 7.5), 1mM EDTA
MACS buffer	1X PBS (pH 7.2), 0.5% BSA, 2mM EDTA

3.2.2. Gel electrophoresis

Table 4: Gel electrophoretic migration of DNA molecules.

Name	Composition
10X Tris/Borate/EDTA Buffer (TBE)	89mM Tris, 89mM Boric acid and 2mM EDTA
6X Blue/Orange Loading Dye	0.4% Orange G, 0.03% Bromophenol blue, 0.03% Xylene cyanol FF, 15% Ficoll [®] 400, 10mM Tris-HCl and 50mM EDTA
0.8 to 1.2% TBE-agarose gel	0.8 to 1.2% agarose, 1X TBE buffer
12% Polyacrylamide gel	12% Acryl/Bisacryl (37.5:1), 1X TBE buffer, 0.1% APS, 0.05% TEMED

3.2.3. Western Blot

Table 5: Buffers and solutions used for the Western Blot.

Name	Composition
8 to 12% Separation gel	8 to 12% Acryl/Bisacryl (37.5:1), 0.373M Tris-HCL (pH8.8), 0.1% SDS, 0.1% APS, 0.05% TEMED

Name	Composition
4% Stacking gel	4% Acryl/Bisacryl (37.5:1), 0.125M Tris-HCL (pH6.8), 0.1% SDS, 0.1% APS, 0.05%TEMED
Electrophoresis buffer	25mM Tris, 2M Glycine, 35mM SDS
Transfer buffer I	25mM Tris, 0.2M Glycine, 5% (v/v) Methanol
Transfer buffer II	25mM Tris, 0.2M Glycine, 5% (v/v) Methanol, 0.1% SDS
2X Loading buffer	0.125M Tris-HCL (pH 6.8), 20% (v/v) Glycerol 100%, 4% (v/v) SDS 10%, 0.005%(p/v) Bromphenol blue, 5% (v/v) β -Mercaptoethanol

3.2.4. Nuclear extraction

Table 6: Buffers used for the extraction of nuclear factors.

Name	Composition
Buffer A	10mM Hepes (pH 7.9), 10mM KCl, 0.1mM EDTA (pH 8.0), 0.1mM EGTA, 1mM DTT, 0.5mM PMSF, 1X protease inhibitor cocktail (Complete [®] plus EDTA)
Buffer C	10mM Hepes (pH 7.9), 10mM NaCl, 0.1mM EDTA (pH 8.0), 0.1mM EGTA, 1mM DTT, 0.5mM PMSF, 20% Glycerol, 1X protease inhibitor cocktail (Complete [®] plus EDTA)

3.2.5. Acid extraction

Table 7: Buffer used for histone isolation.

Name	Composition
Hypotonic lysis buffer	10mM Tris-HCl (pH 8.0), 1mM KCl, 1.5mM MgCl ₂ , 1mM DTT, 10mM Sodium butyrate, 1X protease inhibitor cocktail

3.2.6. Cross-linking chromatin immunoprecipitation

Table 8: Buffers used for cross-linking chromatin immunoprecipitation (X-ChIP).

Name	Composition
Cell lysis buffer	5 mM PIPES (pH 8.0), 85 mM KCl, 0.5% IGEPAL
Nuclei lysis buffer	50 mM Tris-HCl (pH 8.1), 10 mM EDTA, 1% SDS, 1X protease inhibitor cocktail
IP dilution buffer	0.01% SDS, 0.5% Triton X-100, 2 mM EDTA, 16.7 mM Tris-HCl (pH 8.1), 100 mM NaCl, 1 X protease inhibitor cocktail
Low salt buffer	0.1% SDS, 1% Triton X-100, 2 mM EDTA, 20 mM Tris-HCl (pH 8.1), 150 mM NaCl and 1X protease inhibitor cocktail

Name	Composition
High salt buffer	0.1% SDS, 1% Triton X-100, 2 mM EDTA, 20 mM Tris-HCl (pH 8.1), 500 mM NaCl and 1X protease inhibitor cocktail
LiCl buffer	1 mM EDTA, 10 mM Tris-HCl (pH 8.1), 250 mM LiCl, 1 % Igepal, 1% deoxycholic acid and 1X protease inhibitor cocktail
Tris-EDTA buffer	1 mM EDTA (pH 8.0) and 20 mM Tris-HCl (pH 8.1)
Elution buffer	100 mM NaHCO ₃ and 1% SDS

3.3. Kits

3.3.1. Extraction/Purification

Table 9: Kits for the extraction and purification of PCR products, DNA, RNA and proteins.

Designation	Supplier	Application
DNeasy Blood and Tissue Kit	Qiagen, Venlo, Netherlands	Genomic DNA extraction
QIAamp DNA Micro Kit	Qiagen	Genomic DNA extraction
AllPrep DNA/RNA Micro Kit	Qiagen	DNA/RNA extraction
AllPrep DNA/RNA Mini Kit	Qiagen	DNA/RNA extraction
NucleoSpin RNAII Kit	Macherey-Nagel	mRNA extraction
miRNeasy Mini Kit	Qiagen	Total RNA extraction
M-Per [®] Mammalian protein extraction reagent	Thermo scientific, Waltham, USA	Protein extraction reagent
QIAquick PCR purification Kit, QIAEX II gel extraction Kit	Qiagen	PCR product and DNA purification
AveGene Gel PCR DNA fragments Extraction Kit	AveGene, Taipei, Taiwan	PCR product purification and Gel extraction

3.3.2. Bisulfite conversion

Epitect[®] Bisulfite Kit (Qiagen) was used for bisulfite conversion of genomic DNA. Alternatively, for deep sequencing analyses, genomic DNA was converted by the bisulfite conversion protocol 4.6.14 with the following solutions (Table 10).

Table 10: Solutions used for bisulfite conversion of genomic DNA for deep sequencing analysis on the GS FLX-platform.

Name	Composition
Conversion solution	2M NaOH

Name	Composition
Scavenger solution	0.39mM (\pm)-6-Hydroxy-2,5,7,8-tetramethylchromane-2-carboxylic acid in 1,4-dioxane
Desulphonation solution	0.3M NaOH

3.3.3. Microfluidic Lab-on-a-Chip application

Table 11: DNA and RNA capillary electrophoresis

Name	Supplier	Application
Agilent RNA 6000 Kit	Agilent Technologies, Santa Clara, USA	RNA Quality control
Agilent DNA 1000 Kit	Agilent Technologies	CoBRA analysis

Bio-CoBRA: Combined bisulfite restriction assay.

3.3.4. DNA quantification

Double-stranded PCR products were quantified with the Qubit[®] dsDNA HS assay Kit (Invitrogen).

3.3.5. Western Blot

Table 12: Immunodetection of blotted proteins.

Designation	Supplier	Application
ECL Plus Western Blotting Detection System	Amersham Bioscience, Vienna, Austria	Horse radish peroxidase immunodetection (Western Blot)

3.3.6. Purification and separation of blood cells

Separation of peripheral blood mononuclear cells by density gradient centrifugation was done on Ficoll-paque premium (GE Healthcare, Fisher Scientific, Illkirch Cedex, France). CD34 Microbead Kit (Miltenyi Biotec, Auburn, USA) was used for the separation of CD34⁺ cells from umbilical cord blood.

3.3.7. Analysis of GST activity

GST activity was detected by the GST Fluorometric Activity Assay Kit (Biovision, Mountain View, USA).

3.3.8. Analysis of cell proliferation

Cell proliferation was assessed with the CellTrace™ CFSE Cell Proliferation Kit (Invitrogen).

3.4. Media

3.4.1. Mammalian cell culture

Table 13: Medium and additives to culture mammalian suspension cells.

Component	Supplier
Roswell Park Memorial Institute (RPMI-1640)	Lonza
Iscove's Modified Dulbecco's Medium (IMDM)	Lonza
Fetal bovine serum (FBS)	Lonza
Penicillin, Streptomycin, Amphotericin B	Lonza
Granulocyte macrophage colony-stimulating factor (GM-CSF)	Relia Tech, Wolfenbüttel, Germany

3.4.2. Bacterial culture

Table 14: Medium and their additives used in bacterial culture.

Component	Supplier
Luria-Beltani (LB) broth, Miller	MP Biomedicals LLC
Super optimal broth medium with catabolite repression (SOC)	Invitrogen
LB-Agar Miller	MP Biomedicals LLC

3.5. Cells

3.5.1. Mammalian cell lines

Table 15: Mammalian cell lines used in cell culture

All cell lines were provided by the Deutsche Sammlung für Mikroorganismen und Zelllinien (DSMZ, Braunschweig, Germany).

Name	Morphology	Disease (Diagnosis)
HEL	Erythroblast	AML
HL-60	Lymphoblast-like	AML
JURKAT	T-lymphoblast	ALL
JVM-2	Lymphoblast	CLL
K-562	Lymphoblast	CML
KBM-5	Blast-like	CML
KG-1	Myeloblast	AML
KG-1A	Myeloblast	AML
MEG-01	Megakaryoblast	CML
MOLT-3	T-lymphoblast	ALL
RAJI	B-lymphoblast	Burkitt's lymphoma
TF-1	Lymphoblast	AML
THP-1	Monocyte	AML
U-937	Lymphoblast	Histiocytic lymphoma

AML: acute myeloid leukemia, ALL: acute lymphoblastic leukemia, CML: chronic myelogenous leukemia, CLL: chronic lymphocytic leukemia.

3.5.2. Prokaryotic cells

Table 16: Bacterial cell clones and their suppliers.

Name	Supplier
<i>Escherichia coli</i> JM109	Promega
<i>Escherichia coli</i> TOP10	Invitrogen

3.5.3. Patient samples

Diffuse large B-cell, mantle cell, follicular and Burkitt's lymphoma patient samples as well as chronic lymphocytic and myeloid leukemia, acute lymphoblastic and myeloid leukemia and myelodysplastic syndrome patient samples were provided in an anonymized form by the "Bibliothèque de l'Université de Liège" (Belgium), "Centre Hospitalier Universitaire de Nancy" (France), "Institut Paoli-Calmettes" (Marseille, France) and "Centre Hospitalier Luxembourg". Blood cells from supposed healthy donors were provided by the

Red Cross Luxembourg. Cord blood was obtained from the “Clinique privée Dr. E. Bohler” (Luxembourg). Informed consent was obtained from patients. Detailed patient information is annexed.

3.6. Enzymes

3.6.1. Endonucleases

Table 17: Endonucleases used for restriction assays.

Name	Buffer	Supplier	^m CpG sensitivity
<i>Bgl</i> II	10X Buffer D 100X BSA	Promega	No
<i>Hpa</i> II	10X NEBuffer 1	NEB, Ipswich, USA	Yes
<i>Msp</i> I	10X NEBuffer 4	NEB	No
<i>Rsa</i> I	10X Buffer C 100X BSA	Promega	No

temp.: temperature, ^mCpG: methylated CpG.

3.6.2. Polymerases

3.6.2.1 DNA-specific DNA polymerases

Table 18: DNA-specific DNA polymerases used for various PCR applications.

Name	Buffer	Supplier	Application
GoTaq polymerase	5X Colorless GoTaq [®] Flexi Buffer	Promega	Colony PCR
Hot Fire Pol	10X Buffer B	Solis BioDyne, Tartu, Estonia	Bisulfite deep sequencing
Hot Start Taq	10X PCR Buffer	Qiagen	BSP, Bio-CoBRA, MSP, Bisulfite deep sequencing
Platinum Taq	10X PCR Buffer	Invitrogen	Bisulfite deep sequencing
Platinum Taq high fidelity	10X High Fidelity PCR Buffer	Invitrogen	MSP
Power SYBR [®] Green PCR Master Mix	n.a.	ABI, Foster City, USA	Real-time PCR

n.a.: information not available

3.6.2.2 RNA-specific DNA polymerases

Table 19: RNA-specific DNA polymerases used for expression analysis.

Name	Buffer	Supplier	Application
Superscript RT	5X RT buffer	Invitrogen	Reverse transcription of mRNA
miScript Reverse Transcriptase mix	5X miScript RT Buffer	Qiagen	Polyadenylation and reverse transcription of total RNA

3.6.3. Other enzymes and proteins

Table 20: Nucleases, proteases and proteins.

Name	Supplier	Application
DNase	Machery-Nagel ¹ , Düren, Germany, Qiagen ²	Nucleospin ¹ , miRNeasy ²
Hot Start binding protein	USB, Affimetrix, Santa Clara, USA	BSP for deep sequencing
Proteinase K	Qiagen ³ , Roche ⁴	DNeasy blood and tissue Kit ³ , X-ChIP ⁴
RNase	Roche	DNeasy blood and tissue Kit

3.7. Oligonucleotides

Table 21: Oligonucleotides used for BSP and Bio-CoBRA analysis.

All primers were synthesized by Eurogentec (Seraine, Belgium). * PCR was done with 35 repetitive cycles.

Target	Sequence (5' to 3')	Annealing temp. (°C)	Amplicon length (bp)
GSTP1	F: GGAAAGAGGGAAAGGTTTTTT R: ACTCTAAACCCCATCCCC	55 *	292
LacZ	F: GGCTCGTATGTTGTGTGGAAT R: GTGCTGCAAGGCCGATTAAGT	65	592

temp.: temperature.

Table 22: Oligonucleotides used for MSP assays.

All primers were synthesized by Eurogentec. Unless otherwise indicated, PCRs were done with Platinum *Taq* HIFI. Alternatively, # Hot Start *Taq* was used for MSP analysis. Unless otherwise indicated, MSPs were done with 36 repetitive cycles. Alternatively, * 32, **40, ***42 or **** 43 repetitive cycles were done for MSP analysis. Unmethylated (UM) and methylated (M) behind the gene name indicate the primer specificity. Sequences of MGMT, CASP8, TP73 and CDKN2A (p16), RASSF1A MSP primers were described by (Esteller, Hamilton et al. 1999), (Hopkins-Donaldson, Ziegler et al. 2003), (Siu, Chan et al. 2002), (Siu, Chan et al. 2002) and (Schagdarsurengin, Gimm et al. 2002), respectively.

Target	Sequence (5' to 3')	Annealing temp. (°C)	Amplicon length (bp)
AHR-UM	F: GGGGATTTGGTTGTTAGTGTTT R: ACATTTTCTACACCAACTTCCA	63	116
AHR-M	F: GGATTCGGTCGTTAGTGTTT R: GTTTTCTACACCGACTTCCG	63	116
APAF-1-UM	F: GGTGGGATTTGATTGTTTT R: CTACAACACCTCAAATCTTCA	57	143
APAF-1-M	F: GCGGGATTTGATTGTTTC R: TACGACACCTCAAATCTTCG	57	143
APC-UM	F: TTTTGTGTTTTATTGTGGAGTGT R: ACAAACTCCCAACAAAAATAAA	63	101
APC-M	F: TGTGTTTTATTGCGGAGTGC R: CGAACTCCCGACGAAAATA	63	101
BCL2-UM	F: TTTTAAATTCGGGTTAGGGAGC R: CTCTACACAACCCGACCGAT	64.5 *	129
BCL2-M	F: GTTTTAATTTGGGTTAGGGAGT R: TCTCTACACAACCCAACCAAT	64.5 *	129
BCL-XL-UM	F: TGTTGATTTTTGTGTTTTTT R: ACTCAATCACTTCCAATACCA	60	138
BCL-XL-M	F: TGATTTTTTGCCTTTTTTC R: CAATCACTTCCGATACCG	56.5 **	138
CALCA-UM	F: GGGAATAAGAGTAGTTGTTGGT R: CTCAAAACCTCACCTAACAAAA	63	149
CALCA-M	F: GGAATAAGAGTAGTCGTTGGC R: TCGAAAACCTCACCTAACGAAA	64	149
CASP7-UM	F: GTTTTTTAGGGATTATGTGTGT R: AAAATCTCAACACTACAAAAAA	60	142
CASP7-M	F: TTTTLAGGGATTATGCGTGC R: AAAATCTCGACGCTACGAAA	63	142
CASP8-UM	F: TAGGGGATTTGGAGATTGTGA R: CCATATATCTACATTCAAACAA	59	322
CASP8-M	F: TAGGGGATTCGGAGATTGCGA R: CGTATATCTACATTCGAAACGA	64	322
CDH1-UM	F: TTTAGGTTTTAGTGAGTTATTGGT R: TAAACACAATAACCCTCTAACC	62	117
CDH1-M	F: TAGGTTTTAGTGAGTTATCGGC R: TAAACGCGATAACCCTCTAA	64	117
CDKN2A (p14)-UM	F: AGGTAGATTGTAGGTTTTGGGTT R: AAACAAAACCTCAACTCTCATCCA	62	133
CDKN2A (p14)-M	F: TAGATCGTAGGTTTTCGGGTC R: AAACGAAAACCTCGACTCTCGT	62	133

Target	Sequence (5' to 3')	Annealing temp. (°C)	Amplicon length (bp)
CDKN2A(p16)-UM	F: TTATTAGAGGGTGGGGTGGATTGT R: CAACCCCAAACCACAACCATAA	58	111
CDKN2A (p16)-M	F: TTATTAGAGGGTGGGGCGGATCGC R: GACCCCGAACCGCGACCGTAA	63	111
CDKN2B (p15)-UM	F: GGGGTAGTGAGGATTTTGTGAT R: AATCATTAACTCCAAACTTTTCC	62	143
CDKN2B (p15)-M	F: GTAGTGAGGATTTTCGCGAC R: CGTAACTCCGAACTTTTCC	62	143
DAPK1-UM	F: TAAGGAGTTGAGAGGTTGTTTT R: AAACCCTACCACTACAAATTA	62	110
DAPK1-M	F: AAGGAGTCGAGAGGTTGTTTC R: AACCCCTACCGCTACGAATTA	62	110
ESR1-UM	F: TTGTGGTTGGTTGTGTATGTAATT R: TACCCCATACCAAACCTCCAATAT	65	169
ESR1-M	F: TGGTTGGTTGCGTATGTAATC R: CCCGTACCAAACCTCCGATAT	64	169
GSTP1 MGD-U	F: GTGAAGTGGGTGTGTAAGTTTT R: AAAAAAAAAAAACCACAACAAA	60	106
GSTP1 MGD-M	F: AAGCGGGTGTGTAAGTTTC R: CAAAAAAAAAAACCGCAACG	62	106
GSTP1 MGP-U	F: GTGGGATTTTTTAGAAGAGT R: CACATACTCACTAATACCAAAA	58.9	140
GSTP1 MGP-M	F: CGGGATTTTTTAGAAGAGC R: CGCGTACTCACTAATAACGA	63	140
HIC-UM	F: GGGATAGTTTTGGTTTTTGTGT R: AAATCCAAAAAAAAACAACACC	58 # **	111
HIC-M	F: GGATAGTTCGGTTTTTCGTGC R: AATCCGAAAAAAAAACGACACC	60 #	111
LINE1-UM	F: GTGATGGATGTATTTGGAAAATT R: TCCATAAACATAAAAACCCTCTAA	62.8	123
LINE1-M	F: ACGGACGTATTTGGAAAATC R: TCCGTAAACGTAAAACCCTC	64.5	123
MGMT-UM	F: TTTGTGTTTTGATGTTTGTAGGTTTTGT R: AACTCCACACTCTTCCAAAAACAAAACA	61 **	93
MGMT-M	F: TTTTCGACGTTTCGTAGGTTTTCGC R: GCACTCTTCCGAAAACGAAACG	61 **	81
MLH1-UM	F: GTAGTTGTTTTAGGGAGGGAT R: CCTCAATACCTCATACTCACATTCT	64	151
MLH1-M	F: GTCGTTTTAGGGAGGGAC R: CAATACCTCGTACTCACGTTCT	67	151
PTGS2-UM	F: GTTTTTGGATTTTAGGGTT R: TCTTCACAATCTTTACCCA	60 ****	130
PTGS2-M	F: TTTTCGGATTTTAGGGTC R: CTTTCGCAATCTTTACCCG	58	130
RARB-UM	F: TTAAGTTGTTGTAATAAAAAAGGT R: AACCAACATTTTCTTTCTATTT	60	144
RARB-M	F: AGTCGTCGTAAATAAAAAAGGC R: ACCGACGTTTTCTTTCTAT	64	144
RASSF1A-UM	F: TTTGGTTGGAGTGTGTTAATGTG R: CAAACCCACAAACTAAAAACAA	62 **	93

Target	Sequence (5' to 3')	Annealing temp. (°C)	Amplicon length (bp)
RASSF1A-M	F: GTGTTAACGCGTTGCGTATC R: AACCCCGCGAACTAAAAACGA	62 **	105
Rb-UM	F: TTAGATATTTTTGTGGGGTTT R: ACCCAAACATACTTCTACCCAA	63.5	145
Rb-M	F: GATATTTTTTGC GG GGTTC R: CCCGAACGTACTTCTACCC	65	145
SOCS-UM	F: GAGAGGGAAATAGGGTTGAAGT R: TAAACCAACTCAAAAACAAAAC	63	130
SOCS-M	F: AGGGAAATAGGGTCTGAAGC R: TAAACCGACTCGAAAACGAA	68 ***	130
TIMP3-UM	F: GTTTAGGTAGTGGTGTAGAGT R: AAAACTACCTCAACACTAACAC	64 *	137
TIMP3-M	F: TTAGGTAGCGGCGTAGAGC R: AA ACTACCTCGACGCTAACG	70 *	137
TMS1-UM	F: AGGATTTTAAGGTTTGGGGAATT R: CTTACACCAACAAATACAAACCA	63 #	123
TMS1-M	F: GATTTTAAGGTTCTGGGGAATC R: TACACCAACGAATACAAACCG	62 #	123
TP73-UM	F: TTAGGTTAGTTGGGATGGAT R: CCCAACTTCAAACTACAAACCC	63 **	141
TP73-M	F: AGGTTAGTCGGGACGGAC R: CAACTTCGAAACTACGAACCC	58 **	141

temp.: temperature, primer specificity: UM: unmethylated, M methylated. AHR: aryl hydrocarbon receptor, APAF-1: apoptotic peptidase activating factor 1, APC: adenomatous polyposis coli, BCL-2: B-cell CLL/lymphoma 2, BCL-XL: apoptosis regulator Bcl-X, CALCA: calcitonin-related polypeptide alpha, CASP: caspase, CDH1: epithelial cadherin, CDKN cyclin-dependent kinase inhibitor, DAPK1: death-associated protein kinase 1, ESR: estrogen receptor, GSTP1: glutathione S-transferase P1, HIC1: hypermethylated in cancer 1, LINE1: long interspersed nuclear element, MGMT: O-6-methylguanine-DNA methyltransferase, MLH1: human MutL protein homolog 1, PTGS2: prostaglandin-endoperoxide synthase 2, RARB: retinoic acid receptor beta, RASSF1A: Ras association domain family protein 1A, RB1: retinoblastoma 1, SOCS: suppressor of cytokine signaling, TIMP3: tissue inhibitor of metalloproteinase, TMS1: target of methylation-induced silencing 1, TP73: tumor protein p73.

Table 23: Oligonucleotides used for bisulfite deep sequencing analysis.

Oligonucleotide primers were synthesized by Metabion (Martinsried, Germany). Every forward and reverse primers were supplemented by 5' adaptors with the following sequences 5'-CGTATCGCCTCCCTCGCGCCATCAGTCTCTATGCG-3' and 5'-CTATGCGCCTTGCCAGCCCGCTCAGTCTCTATGCG-3', respectively. PCRs were done with 2.5 units of Hot Fire Pol and 42 cycles. Otherwise, + 5 units of Hot Fire Pol (42 cycles), ++ 3.125 units of Hot Start *Taq* (42 cycles), +++ 1.5 units Platinum *Taq* (41 cycles) were used for PCR amplification.

Target	Sequence (5' to 3')	Anneal. temp. (°C)	Amplicon length (bp)
BCL2L11	F: GGGTGTAGATTTAGAGGATTGGAGAG R: CACTACATTTAACTAAAACCCCAAAA	55	336
CALCA	F: GATTTTTTAGGTTTTGGAAGTATG R: AAAAAAAAAACATATACCTAAACCAA	54	355
CHFR	F: TGGTTTGTTTTATATAAATGGATGTTT R: AACTTTTACCTCAATATCTCACTTCTTAAA	55	466

Target	Sequence (5' to 3')	Anneal. temp. (°C)	Amplicon length (bp)
DAB2IPA	F: AAGGTGGTTGTTTTGTTGGGGTA R: CCACACCCACCTAAAAAATCCA	58	347
DAPK1	F: TTTTAGAATTTAGTTAGAGGGTAGT R: ACCAATAAAAACCTACAAAC	54	337
DCR1	F: GGAGGTGTTAGGGGAGGTTATGTTTT R: CCCTTACATCTCTAATCAAACCTCCAAA	55	280
DLC1	F: TTTTGGAGGAGTGATTTTTGATTATTTT R: AATCTAAAATATTCCCAAACAATAAACTCTCC	55	357
ESR1	F: TTTTATATGTTTGTGTTAGATTTTAAAGT R: TTATCACTCAAAAACCTATCTTCTTATA	54 *	493
EYA4	F: GTAAATTATGATAATAGGTAGTTATT R: CAACTCTTCCCTCTCTAAAACAAC	54 *	349
GSTP1	F: GGAAAGAGGGAAAGGTTTTTTT R: ACTCTAAACCCCATCCCC	56	368
H19 CTCF6	F: GATATTAGGGGAATAATGAGGTGTT R: ATAAATATCCTATTCCCAAATAACCC	54	407
HIC1	F: GGGTTGTGTGGGTAATTTTTGTTT R: CCTCCCACCTATACCCACCTAAA	54 *	526
IGSF4	F: GTATGTTATTAGTATTTTATTAGTTGTT R: CTCTATAACCAAACTACTAAAATA	56	342
KLF4	F: TTTTTTTGGTTTTTTTTGAGGTTT R: TAACTCATCCAACCCTCCATCT	54	294
LINE1	F: TTATTAGGGAGTGTTAGATAGTGGG R: CCTCTAAACCAATATAAAATATAATCT	54	247
MGMT	F: TTATTATAGGTTTTGGAGGTTGTT R: TACCTTTTCTATCACAAAAATAAT	54	322
RASSF5/ NORE1A	F: GAAGGAAGGGGAAATTTAATTAGAG R: TAAACCTTCAACCCTACCTCTTTC	54	468
OSMR	F: GGGATGATAAGTGTTTTTGTGGGAT R: ACACTCCTAAAACCCACAAAAATTCC	54 #	376
PROX1	F: AGTTGTATTTGGGAAATGAAAAA R: CCCACCCTACCACAACCTTC	54	249
PTGS2	F: GTTATATGGGTTTGGTTTTTAGTT R: AAATACTAAAATAAACCCAAAAAATC	54 *	402
RARB	F: TGTTAGATTAGTTGGGTTATTTGAAGGT R: CAAATAATCATTACCATTTCCTCAAAC	54	450
THBS1	F: GGAGAGAGGAGTTTAGATTGGTT R: CACCAAAAAACTAAAACCTCAA	54	423
TIMP3	F: TGGGTTAGAGATTTTAGTGTTTT R: TTCAAATCCTTATAAAAAATAATACC	54	237
TP73	F: AAATAGTGGGTGAGTTATGAAGATGT R: TACACCAAACCTAACTAAAAAACC	54	354

temp.: temperature. BCL2L11: B-cell CLL/lymphoma 2-like 11, CALCA: calcitonin A, CHFR: checkpoint with forkhead and ring finger domains, DAB2IBA: DAB2 interacting protein, DAPK1: death-associated protein kinase 1, DCR1: decoy receptor 1, DLC1: deleted in liver cancer 1, ESR1: estrogen receptor 1, EYA4: eyes absent homolog 4, GSTP1: glutathione S-transferase P1, H19-CTCF: imprinted gene, HIC1: hypermethylated in cancer 1, IGSF4: cell adhesion molecule 1, KLF4: krueppel-like factor 4, LINE1: long interspersed nuclear element 1, MGMT: O-6-methylguanine-DNA methyltransferase, RASSF5/NORE1A: Ras association (RalGDS/AF-6) domain family 5, OSMR: oncostatin M receptor, TP73: tumor protein P73, PROX1: prospero homeobox 1, PTGS2: prostaglandin-endoperoxide synthase 2, RARB2: retinoic acid receptor

beta, THBS1: thrombospondin 1, TIMP3: tissue inhibitor of metalloproteinase, TP73: tumor protein p73.

Table 24: Oligonucleotides used for expression analysis.

Primers were obtained from Eurogentec and have an annealing temperature of 60°C.

Target	Sequence (5' to 3')	Amplicon length (bp)
β-actin	F: CTCTTCCAGCCTTCCTTCCT	116
	R: AGCACTGTGTTGGCGTACAG	
DNMT1	F: TCAGCAAGATTGTGGTGGAG	104
	R: CAAGTTGAGGCCAGAAGGAG	
DNMT3a	F: TGCCAAAAGTCAAGAAGTCA	83
	R: CAGCAGATGGTGCAGTAGGA	
DNMT3b	F: TTTGGCCACCTTCAATAAGC	119
	R: GGTCCCTCAATGAGTCTCCA	
GSTP1	F: GGCAACTGAAGCCTTTTGAG	128
	R: GGCTAGGACCTCATGGATAC	

Table 25: Oligonucleotides used for X-ChIP analysis.

Primers were obtained by Eurogentec and have an annealing temperature of 60°C.

Target	Sequence (5' to 3')	Amplicon length (bp)
CG1	F: CTCTATGGGAAGGACCAGCA	81
	R: GATGTATTTGCAGCGGAGGT	
CG2	F: CCAGTTCGAGGTAGGAGCAT	103
	R: GATAAGGGGGTTCGGATCTC	
CG3	F: GCAGCGGTCTTAGGGAATTT	131
	R: CTTTCCCTCTTCCAGGTC	
CG4	F: AAGTAGGCAGCAAAGCCAAA	77
	R: GTCCCTGCAAAGGACATGAT	
CG5	F: AAGCCAGGAACCTCAAGAT	86
	R: TGATCAGCCTGTGCCTGTAG	

Table 26: Oligonucleotides used for miRNA expression profile analysis.

Primers were synthesized by Qiagen and have an annealing temperature of 55°C.

Assay name	Entrez Gene Symbol
Hs_let-7f_1	MIRLET7F1, MIRLET7F2
Hs_miR-124a_1	MIR124-1, MIR124-2, MIR124
Hs_miR-125a_1	MIR125A
Hs_miR-125a-3p_1	MIR125A
Hs_miR-133a_1	MIR133A1, MIR133A2
Hs_miR-142-5p_1	MIR142
Hs_miR-148b_1	MIR148B
Hs_miR-149_1	MIR149
Hs_miR-150_1	MIR150
Hs_miR-185_1	MIR185

Assay name	Entrez Gene Symbol
Hs_miR-193_2	MIR193B
Hs_miR-198_2	MIR198
Hs_miR-296-3p_1	MIR296
Hs_miR-296-5p_1	MIR296
Hs_miR-324-3p_2	MIR324
Hs_miR-339_1	MIR339
Hs_miR-339-3p_1	MIR339
Hs_miR-345_2	MIR345
Hs_miR-346_2	MIR346
Hs_miR-422b_1	MIR378
Hs_miR-432_1	MIR432
Hs_miR-484_1	MIR484
Hs_miR-486_1	MIR486
Hs_miR-486-3p_1	MIR486
Hs_miR-506_2	MIR506
Hs_miR-512-3p_1	MIR512-1
Hs_miR-512-5p_1	MIR512-1
Hs_miR-516a-3p_1	MIR516A1, MIR516A2
Hs_miR-516a-5p_1	MIR516A1, MIR516A2
Hs_miR-516b_1	MIR516B1, MIR516B2
Hs_miR-518c_1	MIR518C
Hs_miR-519e_3	MIR519E
Hs_miR-526b_1	MIR526B
Hs_miR-539_1	MIR539
Hs_miR-572_2	MIR572
Hs_miR-574_1	MIR574
Hs_miR-590-3p_1	MIR590
Hs_miR-618_1	MIR618
Hs_miR-637_1	MIR637
Hs_miR-650_1	MIR650
Hs_miR-657_2	MIR657
Hs_miR-659_2	MIR659
Hs_miR-767-3p_1	MIR767
Hs_RNU1A_1	n.a.

n.a.: not available.

3.8. Antibodies

Table 27: Primary antibodies used for Western Blot analysis.

Antibody working solutions were prepared at the appropriated dilution in 1X PBS-T with 5% milk.

Target specificity	Membrane saturation	Dilution	Supplier
Ach4	5% BSA, 1X PBS-T	1:50000	Upstate
CBP	5% milk, 1X PBS-T	1:1000	Santa Cruz, Tebu Bio, Boechout, Belgium
DNMT1	5% milk, 1XPBS-T	1:250	Active motif, Rixensart, Belgium
DNMT1	5% milk, 1X PBS-T	1:250	Active motif
DNMT3A	5% milk, 1X PBS-T	1:200	Santa Cruz
DNMT3B	5% milk, 1X PBS-T	1:500	Abcam, Cambridge, UK
GSTP1	5% milk, 1X PBS-T	1:10000	BD bioscience, Franklin Lakes, USA
H4	5% BSA, 1X PBS-T	1:10000	Upstate
HDAC1	5% milk, 1X PBS-T	1:10000	Upstate
HDAC2	5% milk, 1X PBS-T	1:10000	Abcam
MBD1	5% milk, 1X PBS-T	1:1000	Abcam
MBD2	5% milk, 1X PBS-T	1:250	Santa Cruz
MBD3	5% milk, 1X PBS-T	1:250	Santa Cruz
MeCP2	5% milk, 1X PBS-T	1:2500	Upstate
p300	5% BSA, 1X PBS-T	1:500	Upstate
Sp1	5% milk, 1X PBS-T	1:10000	Active motif
Sp3	5% milk, 1X PBS-T	1:2500	Santa Cruz
β -actin	5% milk, 1X PBS-T	1:5000	Sigma

Ac: acetylation, CBP: cAMP-response element binding protein (CREB) binding protein, DNMT: DNA methyltransferase, GSTP1: glutathione S-transferase P1, H4: Histone 4, HDAC: histone deacetylase, MBD: methyl binding protein, MeCP2: methyl CpG binding protein 2, p300: histone acetyltransferase, SP: specificity protein.

Table 28: Antibodies used for X-Chip.

Target specificity	Supplier
Ach3	Upstate
Ach4	Upstate
CBP	Abcam
DNMT1	Active motif
DNMT3A	Active motif
DNMT3B	Active motif
H3K4Me2	Abcam
H3K4Me3	Abcam
H3K9Me3	Upstate

Target specificity	Supplier
H3K27Me3	Upstate
HDAC1	Upstate
HDAC2	Abcam
MBD1	Abcam
MBD2	Upstate
MBD3	Abcam
MeCP2	Upstate
p300	Upstate
RNA pol II	Upstate
Sp1	Active motif
Sp3	Santa Cruz

Ac: acetylation, CBP: cAMP-response element binding protein (CREB) binding protein, DNMT: DNA methyltransferase, H: Histone, HDAC: histone deacetylase, K: lysine, MBD: methyl binding protein, Me: methylation, MeCP2: methyl CpG binding protein 2, p300: histone acetyltransferase, RNA pol II: RNA polymerase II, SP: specificity protein.

Table 29: Horseradish peroxidase-conjugated secondary antibodies used for Western Blot analysis.

Secondary antibodies were obtained from Tebu Bio (Boechout, Belgium). Antibody dilutions were prepared with 5% milk in 1X PBS-T.

1 st antibody specificity	Target specificity	Dilution
AcH4	Anti-rabbit IgG	1:5000
CBP	Anti-rabbit IgG	1:2500
DNMT1	Anti-mouse IgG	1:2500
DNMT3A	Anti-rabbit IgG	1:500
DNMT3B	Anti-rabbit IgG	1:500
GSTP1	Anti-mouse IgG	1:10000
H4	Anti-rabbit IgG	1:5000
HDAC1	Anti-mouse IgG	1:5000
HDAC2	Anti-rabbit IgG	1:5000
MBD1	Anti-rabbit IgG	1:2500
MBD2	Anti-goat IgG	1:1000
MBD3	Anti-goat IgG	1:2500
MeCP2	Anti-rabbit IgG	1:2500
p300	Anti-mouse IgG	1:2500
Sp1	Anti-goat IgG	1:5000
Sp3	Anti-goat IgG	1:2500
β -actin	Anti-mouse IgG	1:10000

For indirect immunofluorescence detection, GSTP1 antibody (BD bioscience) was used at a dilution of 1:15 in 0.5% BSA, 1X PBS.

Table 30: Secondary antibodies used for immunodetection by cytometry or microscopy analyses.

Secondary antibodies were diluted 1:50 in 0.5% BSA, 1X PBS.

1 st antibody specificity	Target specificity	Label	Supplier
GSTP1	Anti-mouse IgG	Alexa Fluor [®] 488	Molecular probes, Carlsbad, USA
GSTP1	Anti-mouse IgG	Alexa Fluor [®] 647	Molecular probes

3.9. Markers

Table 31: DNA markers used in electrophoretic migrations.

All DNA markers were obtained from Promega.

Name	Fragment length (bp)
1kb DNA Ladder	250, 253, 500, 750, 1000, 1500, 2000, 2500, 3000, 4000, 5000, 6000, 8000, 10000
Bench TOP 100bp Ladder	100, 200, 300, 400, 500, 600, 700, 800, 900, 1000, 1500
25bp DNA Step Ladder	25, 50, 75, 100, 125, 150, 175, 200, 225, 250, 275, 300

bp: base pairs.

Table 32: Protein marker used in Western Blot.

As a protein size marker, Precision Plus protein standards, Kaleidoscope marker from Biorad was used.

3.10. Plasmid/control DNA

Table 33: Plasmid vectors and modified DNA.

Name	Supplier
pGEM [®] -T Easy Vector	Promega
Epitect [®] PCR Control DNA	Qiagen

3.11. Devices and instruments

Table 34: Devices and instruments

Description	Name	Supplier
Autoradiography cassettes	Hypercassette [™]	Amersham Bioscience, Vienna, Austria

Description	Name	Supplier
Autoradiography films	Hyperfilm ECL	Amersham Bioscience
Balances	Explorer Pro	Ohaus, Pine Brook, USA
Biological safety cabinets	Clean Air	Clean Air, Minneapolis, USA
Gel electrophoresis chamber	Horizon 11-14, Horizon 20-25	Gibco, Carlsbad, USA
Cell counter	Cedex XS	Innovatis, Roche, Howald, Luxembourg
Centrifuge	5415R ¹ , 5415D ¹ , 5810R ¹ , 5424 ¹ , KR25i ² , RC1010 ² , Cytofuge 2 ³	Eppendorf ¹ , Hamburg Germany; Jouan ² , St-Herblain, France; Stat spin ³ , Westwood, USA
Cytometer	Facscalibur	BD bioscience
Film processor	Curix 60	AGFA, Mortsels, Belgium
Fluorometer	Qubit [®] Fluorometer	Invitrogen
Fume cupboard	Astec	Monair, Hants, England
Homogenizer	Qiashredder	Qiagen
Incubator	IGO 159	Memmert, Jouan, Binder
Incubator with shaker function	Thermoshake	Gerhardt analytical systems, Königswinter, Germany
Magnetic stirrer	EM-1100-T	Retsch, Haan, Germany
Microplate spectrofluorometer	SpectraMax Gemini EM	Molecular Devices, Sunnyvale, USA
Microscope	DM2000 ¹ , DMIRB ¹ , IX81 ² (MT10), Eclipse E200 ³	Leica ¹ , Zaventem, Belgium; Olympus ² , Aartselaar, Belgium; Nikon ³ , Amstelveen, Netherland
Microscopy slide for cell counting	Malassez slide	Marienfild, Lauda-Königshofen, Germany
PCR plates	Real-time PCR plates	Thermo, Waltham, USA
PCR workstation	Captair bio	Erlab, Val de Reuil, France
pH meter	Cyberscan 500	Eutech instruments, Nijkerk, Netherland
Pipet	Pipetman	Gilson, Middleton, USA
Pipet-Aid	Express	Falcon, VWR, Leicestershire, England
Power supply	Power Pac HC, Power Pac Basic	Bio-Rad Laboratories
Protein blotting cells	Mini Protean Tetra cells, Mini Protean 3-cells	Bio-Rad Laboratories
Pipetting robot	Qiacube	Qiagen
Real-time PCR	7300 Real-Time PCR System	Applied biosystems

Description	Name	Supplier
Refrigerated cold traps	RCT60	Jouan, St-Herblain, France
Sequencer	GS-FLX titanium system	Roche
Separator	Midi MACS separation unit, MACS multi stand	Miltenyi
Shaker	3015	GFL, Burgwedel, Germany
Sonicator	Bioruptor™	Diagenode, Liège, Belgium
Spectral photometer	SpectraCount ¹ , ND-1000 ²	Packard ¹ , Schwadorf, Austria; Nanodrop ² , Wilmington, USA
Storage (4°C ¹ , -20°C ² , -80°C ³ , -196°C ⁴)	VX490 E ¹ , Comfort ² , VWR ³ , LS750 ⁴	Jouan ¹ , St-Herblain, France; Liebherr ² , Biberach an der Riss, Germany ; VWR ³ , Leicestershire, England ; Taylor Wharton ⁴ , Husum, Germany
Thermocycler	Mastercycler Gradient	Eppendorf, Hamburg Germany
Tips, tubes, etc.	Plastic ware	Greiner, Wemmel, Belgium
Tube roller-mixer	SRT2 Rollomatic	Stuart scientific
UV Gel documentation	UV illumination in a Molecular Imager® Gel Doc XR™ System,	Bio-Rad Laboratories
Vortexer	Vortex Genie 2	Scientific Industries, Bohemia, USA
Water bath	1002	GFL, Burgwedel, Germany
Water purification	Elix3, Simplicity	Millipore, Billerica, USA
Western Blot densitometry	Image station 440 CF	Kodak, Stuttgart, Germany

4. Methods

4.1. Bioinformation

4.1.1. Oligonucleotide design

Oligonucleotides (Primers) for semi-quantitative real-time or conventional non-quantitative PCRs were designed with the online tool Primer3 (Rozen and Skaletsky 2000). The Methyl Primer express software (Applied biosystems) was used to design primers for bisulfite sequencing and methylation-specific PCR (MSP) (Li and Dahiya 2002).

4.1.2. CpG island identification

CpG-rich regions were identified and plotted with the Methyl Primer express software applying the following conditions: GC%=50%, CpG O/E=0.6, min. length=200bp. Further analysis were realized with the online tool EMBOSS CpGPlot/CpGReport/Isochore (<http://www.ebi.ac.uk/Tools/emboss/cpgplot/index.html>) applying the following conditions: calculation window size=100, migration step=1, CpG O/E=0.6, GC%=50%, CGi length=200bp) (Gardiner-Garden and Frommer 1987; Rice, Longden et al. 2000).

4.1.3. Bisulfite sequencing data analysis

Chromatogram accuracy of sequencing data was checked with the Codon Code aligner software (CodonCode Corporation, Dedham, USA). Qualitatively acceptable sequences were then imported into the CLC Sequence viewer software (CLC bio, Aarhus, Denmark) and reoriented with the reverse complement tool. To identify eventual sequencing errors, resulting sequences were aligned against an *in silico* converted “ensembl”-based DNA sequence (Ensembl release 50 - Jul 2008, <http://www.ensembl.org/>). The BIQ conversion software (<http://biq-analyzer.bioinf.mpi-sb.mpg.de/>) was used for *in silico* conversions (Bock, Reither et al. 2005). Methylation percentages of bisulfite sequencing results were finally determined with the methylation quantification analysis tool (QUMA) (<http://quma.cdb.riken.jp/>) as well as with

the BIQanalyzer software (Bock, Reither et al. 2005; Kumaki, Oda et al. 2008). Deep sequencing analyses were processed with the BIQanalyzer HT software (Lutsik, Feuerbach et al. 2011).

4.1.4. Image analysis

Bright-field microscopy images were recorded with the Leica Firecam software and processed with the ImageJ (rsbweb.nih.gov/ij/) or the Leica Firecam softwares (Leica Microsystems) (Rasband 1997-2008). Cell[^]R software (Olympus) was used to acquire and process fluorescence microscopy pictures. Kodak 1D image analysis (Kodak) and Image J softwares were used for densitometry analysis. DNA gels were documented with the Quantity One software (Bio-Rad Laboratories).

4.1.5. Heat map analysis

MSP methylation data and real-time PCR miRNA expression results were analyzed by the R software environment for statistical computing and graphics. Data were represented on a heat map (Team 2010). Correlation coefficient was used to determine cluster similarity.

4.1.6. Prediction of putative miRNAs targeting GSTP1 expression

A long list of approaches, based on different algorithms, has been developed for putative computational miRNA target prediction. In this study, 9 different public online tools were used to analyze the 3'UTR of GSTP1 gene and predict possible miRNAs targeting GSTP1 mRNA (Table 35).

Table 35: Tools and resources for GSTP1 miRNA target prediction.

Tool	Resource	References
Human miRNA target	http://diana.pcbi.upenn.edu/CGI-bin/TargetCombo.cgi	(Sethupathy, Corda et al. 2006)
Target Scan	http://www.targetscan.org/	(Lewis, Burge et al. 2005; Grimson, Farh et al. 2007; Friedman, Farh et al. 2009)

Tool	Resource	References
Target Gene Prediction at EMBL	http://www.russell.embl-heidelberg.de/miRNAs/	(Stark, Brennecke et al. 2003; Brennecke, Stark et al. 2005; Stark, Brennecke et al. 2005)
miRNA map	http://mirnamap.mbc.nctu.edu.tw/	(Hsu, Chu et al. 2008)
Mirtar	http://mirtar.mbc.nctu.edu.tw/human/	
RefGene	http://refgene.com/	
miRwalk	http://www.ma.uni-heidelberg.de/apps/zmf/mirwalk/	
EiMMO	http://www.mirz.unibas.ch/EiMMo3/	
mimiRNA	http://mimirna.centenary.org.au/mep/formulaire.html	(Ritchie, Flamant et al. 2010)

4.2. Microbiology

4.2.1. Bacterial cell culture

Culture in liquid growth medium

A preculture of 5ml lysogeny broth miller medium (LB, Luria Bertani broth) supplemented with 100µg/ml ampicillin was inoculated with a bacterial clone and incubated under agitation (200rpm) for eight hours at 37°C. The main culture of 150ml LB with ampicillin (100µg/ml) was afterwards inoculated with 1ml preculture and incubated under agitation overnight at 37°C.

Culture on solid growth medium

Autoclaved LB-agar miller medium was melted at 400W in a microwave, cooled down under agitation, supplemented with 100µg/ml ampicillin, and poured into sterile Petri dishes. The antibiotic agent ampicillin interacts with bacterial wall synthesis and thereby inhibits bacterial growth. Only bacterial cells expressing the ampicillin resistance gene survive to the selective pressure.

LB-agar-Ampicillin-IPTG-X-Gal plates with 100µg/ml ampicillin, 0.05M IPTG and 0.004% X-Gal were used for Blue/White colony screening. IPTG induces the expression of the *LacZ* gene encoding β-galactosidase, which metabolizes the lactose analogue X-Gal into a blue reaction product.

4.2.2. Transformation

The procedure that induces the introduction of a foreign DNA molecule into any bacterial cell type is called transformation.

For the transformation of pGEM-T easy vector into *E.coli* strain JM109 high efficiency competent cells, 2 μ l of the ligation reaction were added to 50 μ l of chemocompetent cells. This mixture was incubated 20 minutes on ice, then heat shocked for 45 seconds at 42°C and stored for 2 minute on ice. During this process, the short-term increase of temperature to 42°C reduces the rigidity of the cell wall and induce DNA migration through the phospholipid bilayer. Cells were regenerated by adding 950 μ l SOC medium to the transformation mixture and incubated 1 hour at 37°C. SOC is a medium without antibiotics that allows cells to recover as well as to initiate plasmid replication and gene expression. Finally, cells were plated on solid growth medium and incubated overnight at 37°C.

4.3. Cell culture

All manipulations for cell culture were done under sterile conditions.

4.3.1. Storage of eukaryotic cells

Cell stock aliquots were prepared in regular cell culture medium supplemented with 10% DMSO and 10% FBS. Aliquots were slowly frozen until -80°C and stored in liquid nitrogen. Cells revitalized by quick thawing at 37°C were then placed under their usual culture conditions. Cells were used during a limited number of passages (+/- 30) before thawing a new stock.

4.3.2. Culturing of eukaryotic cells

Cell lines were routinely maintained in RPMI 1640 medium supplemented with 10% FBS except KG-1a cells that require 20% FBS. Furthermore, growth medium for TF-1 was supplemented with 5ng/ml of GM-CSF. KBM-5 cell lines were maintained in IMDM medium supplemented with 15% FBS. All medium were supplemented with 1% of a mixture of antibiotic

and antifungal agents (Pen/Strep Amphotericin B). Cells were cultured under an atmosphere of 5% CO₂ with 95% humidity at 37°C. Medium exchange and cell concentration adjustment were done regularly. Therefore, cells were counted and a defined volume of cells transferred into a falcon. To eliminate the old medium, cells were centrifuged at 350 *g* for 7 minutes at room temperature. The supernatant was discarded and cells resuspended in an appropriated volume of new medium at a concentration of 2.0 - 2.5 x 10⁵ cells per ml.

4.3.3. Trypan blue exclusion test

Trypan blue staining is used to determine the number of viable cells. Live cells possess intact cell membranes that actively exclude the trypan blue dye. In contrast, dead cells do not exclude the dye and show a distinctively blue stain under the microscope.

Cells in medium were mixed at an equal volume with trypan blue. Then 20µl of this mix was directly transferred onto a Malassez cell counting chamber and stained (unviable) as well as unstained (viable) cells were counted separately.

4.3.4. Cell line treatments

The stock solution of 10mM 5-aza-2'-deoxycytidine (DAC) was prepared in DMSO, aliquoted and stored at -20°C. The stock solution of 2.3M valproic acid (VPA) was diluted in water, trichostatin A (TSA) (1mg/ml) and SAHA (10mM) were prepared in DMSO. All solutions were aliquoted and stored at -20°C. Cells were treated in the beginning of exponential growth phase. Due to the reduced stability of DAC, cells were treated every day.

4.3.5. Purification of peripheral blood mononuclear cells

Peripheral blood mononuclear cells (PBMCs) were purified from whole blood by density gradient centrifugation on Ficoll-Paque, taking in advantage the different densities of blood components (Boyum 1976). Anticoagulant-

treated whole blood is diluted with a balanced salt solution and then slowly layered above Ficoll-Paque. The differential sedimentation of blood cells in the density gradient during the following centrifugation leads to a separation into distinct phases (Figure 16).

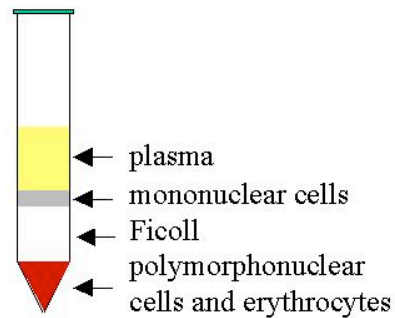


Figure 16: Sedimentation profile of whole blood cells separated by Ficoll.

Ficoll is overlaid in a conical tube by diluted whole blood. After centrifugation, the following layers are visible from top to the bottom: plasma, mononuclear cells, Ficoll, polymorphonuclear cells and erythrocytes (www.life.umd.edu).

The pellet on the bottom of the tube consists of the high-density erythrocytes and polymorphonuclear granulocytes that are overlaid by the Ficoll-Paque. With a similar density as the Ficoll, lymphocytes (mononuclear cells) stay in the interphase between Ficoll and the upper fraction containing blood plasma, monocytes and platelets (Figure 16).

One volume of Ficoll-Paque PREMIUM (density: 1.077g/ml) was gently overlaid with 2 volumes of diluted blood (1:3 dilution with 1X PBS) in a 50ml falcon-type tube. Tube was centrifuged at 600 g without break for 30 minutes at room temperature. PBMCs were collected by transferring into a new tube the lymphocyte ring located in the interphase of Ficoll/Plasma. Collected cells were washed twice with 1X PBS and stored at -80°C.

4.3.6. Separation of CD34+ cells from umbilical cord blood

Umbilical cord blood is the fraction of blood that remains in placenta and in the attached umbilical cord after childbirth. Cord blood contains all the basic elements of blood such as red blood cells, white blood cells, blood platelets and plasma. In addition, it contains blood-forming stem cells, positive for the

transmembrane glycoprotein CD34 antigen. These human hematopoietic progenitor cells have the potential to develop into any blood cell types.

CD34⁺ cells were separated from umbilical cord blood as described by Miltenyi Biotec's protocol. Cord blood was collected in tubes containing Heparin as anticoagulant. PBMCs were purified by density gradient centrifugation on Ficoll-Paque (see 4.3.5). Purified PBMCs (10^8) were resuspended in 300 μ l MACS buffer (Table 3). Then, 100 μ l of FcR blocking reagent and 100 μ l of CD34 MicroBeads (anti-CD34 antibody-coupled magnetic beads) were added to the cell suspension. Fc fragments of antibodies in the blocking reagent bind to the Fc receptors of nucleated cells and block any non-specific binding of CD34 MicroBeads. After 30 minutes incubation on ice, cells were washed with 10ml of MACS buffer and gently resuspended in 500 μ l of the same buffer. Cells were passed successively through a pre-separation filter and a MACS LS separation column positioned in a MidiMACS Separation Unit on a MACS multi stand. The magnetic field, created by the interaction between the separation unit and the column allows unlabeled CD34⁻ cells to elute through the column while positively labeled cells (CD34⁺ cells) remain in the column's magnetic shaft. After the negative elution containing CD34⁻ cells, the column was washed with 9ml of MACS buffer, removed from the separation unit and eluted with 5ml MACS buffer. The eluate containing CD34⁺ cells was purified an additional time on a MACS LS separation column to improve fraction purity.

4.4. Biological chemistry

Cells were collected and washed two times with ice-cold 1X PBS. All centrifugation steps were done at 4°C.

4.4.1. Whole cell extracts

A pellet of 10×10^6 cells was resuspended at a ratio of 1:10 (v/v) with lysis mix (25:1 M-PER / proteinase inhibitor cocktail) for 10 minutes at room temperature. The sample was vortexed for 10 minutes and subsequently

centrifuged at 15000 *g* for 15 minutes. The supernatant containing proteins was transferred into a new tube and stored at -80°C.

4.4.2. Nuclear protein extraction

A pellet of 10^7 cells was resuspended in 400µl buffer A (Table 6) and incubated for 15 minutes on ice. The cell lysate was supplemented with 25µl of 10% IGEPAL, vortexed for 10 seconds and centrifuged at 15000 *g* for 15 minutes. The cytoplasmic protein fraction was transferred into a new tube and stored at -80°C. Nuclei were dissolved in 50µl buffer C (Table 6), vigorously vortexed at 4°C for 15 minutes and centrifuged at 10000 *g* for 5 minutes. The supernatant, containing nuclear proteins, was transferred into a new tube and stored at -80°C.

4.4.3. Histone acid extraction

A pellet of 5×10^6 cells was resuspended in ice-cold hypotonic lysis buffer (Table 7) and incubated for 30 minutes at 4°C. Nuclei were collected by centrifugation at 10000 *g* for 10 minutes, resuspended in 0.4N H₂SO₄, and incubated for 30 minutes at 4°C. Histones were collected by precipitation with 25% trichloroacetic acid, incubated 30 minutes on ice, centrifuged at 15000 *g* for 10 min, washed with ice-cold 100% acetone, dissolved in water and stored at -80°C.

4.4.4. Protein quantification

The Bradford Dye assay is the most common colorimetric method to determine the concentration of a protein solution. The maximum absorbance for an acidic solution of Coomassie Brilliant Blue G-250 shifts from 465 nm to 595 nm when binding to protein occurs. Under strong acidic conditions, the dye is most stable as a doubly-protonated, red form. However, binding to protein leads to a deprotonated, blue form. The reaction depends on the content of aromatic and basic amino acids (Bradford 1976).

The determination of protein concentration is based on the comparison of BSA calibration curve and sample extinction spectrum. Therefore, a dilution series with BSA and water was prepared with the following concentrations:

BSA concentration ($\mu\text{g/ml}$)	0	1	2	2.5	5	7.5	10	12.5	15	20
---	---	---	---	-----	---	-----	----	------	----	----

A volume of 40 μl of Bio-Rad Protein assay solution was added to 160 μl of either samples or BSA dilution series. The extinction coefficients of the calibration curve and samples were measured by a spectral photometer at a wavelength of 595nm. Data were plotted and the equation of the standard curve was used to calculate sample concentration.

4.4.5. SDS-Page

Sodium dodecyl sulfate polyacrylamide gel electrophoresis (SDS-Page) is a variant of the polyacrylamide gel electrophoresis to separate proteins in an electric field. The separation medium is a polyacrylamide gel consisting of acrylamide, bisacrylamide, APS, TEMED and SDS. Polymerization of acryl monomers with the cross-linking agent bisacrylamide is catalyzed and initiated by TEMED and APS, respectively. SDS is an anionic detergent and coats the proteins with its negative charge. Discontinuous gel electrophoresis consists of a large-pore stacking gel that concentrates proteins on one same starting point. The following separation gel has small pores, allowing the separation of proteins according to their size.

The resolving gel (Table 5) was poured between two glass plates and covered by 100% ethanol. After polymerization, ethanol was removed, the resolving gel covered with stacking gel (Table 5) and a comb introduced to form wells. The electrophoresis apparatus was set up with electrophoresis buffer (Table 5), covering the gel in the anode and cathode chamber. Protein samples were diluted with 2X loading buffer (Table 5) and subsequently denatured for 5 minutes at 100°C. To avoid protein renaturation, samples were placed for 2 minutes on ice. Samples were loaded onto a gel and then the electrophoresis chamber was connected to a power supply under appropriate running conditions (migration in stacking gel: 80 Volts, migration in resolving gel: 160 Volts).

4.4.6. Western Blot

Western blot is an analytical technique used to detect specific proteins in a given sample of tissue homogenate or extract. Proteins are separated on a SDS-page according to their molecular weight. A vertical electric field is applied on the SDS-page to transfer proteins from the polyacrylamide gel onto a high hydrophobic polyvinylidene fluoride (PVDF) membrane. Target proteins are analyzed by immunodetection.

The PVDF membrane was activated by methanol and together with the SDS-PAGE gel pre-incubated in transfer buffer I (Table 5) for 15 minutes under agitation. The blotting unit was setup up, starting with a transfer buffer I-soaked sponge on which three layers of filter paper are disposed. Next, the protein containing gel was added and overlaid by the PVDF membrane. This assembly was completed with another three filter papers and a sponge. The blotting unit was then introduced into the transfer chamber, which was filled up with transfer buffer I and blotted for 1 hour at 200mA.

For the transfer of large proteins (>80kDa) onto the PVDF membrane, transfer buffer I was replaced by transfer buffer II (Table 5) and proteins transferred at 4°C for 15 hours at 40mA.

After transfer, the blotting unit was disassembled and the PVDF membrane blocked overnight at 4°C or 30 minutes at 37°C either in a 5% milk or in a 5% BSA, 1X PBS solution, depending on the antibody. Afterwards, the membrane was incubated overnight at 4°C or 1h at room temperature with an appropriate dilution of primary antibody directed against the protein of interest. After 3 washing steps with 1X PBS-T 0.1%, the membrane was incubated with the secondary horseradish peroxidase-conjugated antibody for 1h at room temperature. Following 3 washing steps with 1X PBS-T 0.1%, the membrane was incubated in a mix of 4ml buffer A and 100µl buffer B of ECL plus Western blot reagents for 5 minutes at room temperature. The peroxidase coupled to the secondary antibody reacts with the luminol from the ECL plus reagents producing a light signal that is detected by an Amersham Hyperfilm. The autoradiography film was developed in a Curix 60 film processor.

4.4.7. GST activity assay

GST Fluorometric Activity Assay Kit using monochlorobimane (MCB) as substrate was used to measure cellular GST activity. The free form of MCB is almost non-fluorescent, whereas the conjugated form with glutathione fluoresces in blue (ex.380/em.461nm). This reaction of MCB-glutathione conjugation is catalyzed by GSTs, whereby the MCB fluorescence level is proportional to the total amount of GST activities, present in the reaction.

Briefly, 1×10^6 cells were collected in duplicates and subsequently homogenized by sonication (Diagenode Bioruptor, settings: mode high, 2 cycles of 30sec on/30sec off) in 100 μ l of GST sample buffer. After centrifugation at 10000 g for 15min at 4°C, supernatants were collected and stored at -80°C. A mix constituted of 2 μ l of MCB solution, 98 μ l of GST assay buffer and 10 μ l of glutathione was incubated with supernatants. Fluorescence was read at ex.380/em.460nm after 1 hour of incubation at room temperature using a SPECTRA MAX Gemini EM. Standard calibration curve of GST activity was set with the GST standard. GST activity was expressed as mU of GST per million of cells.

4.5. Cell biology

4.5.1. Indirect immunofluorescence labeling

Immunofluorescence is used to detect the clonal expression or the presence of a specific antigen in a cellular system. Indirect immunofluorescence labeling requires the use of two antibodies. The primary recognizes and binds to the antigen of interest. The fluorescence-tagged secondary antibody recognizes the constant fragment of the primary antibody allowing the localization of the antigen.

Localization and quantification of GSTP1 expression was performed on paraformaldehyde-fixed cells. A pellet of 8×10^6 cells was resuspended in 200 μ l of a 2% paraformaldehyde solution (in 1X PBS) (v/v) and incubated for 15 minutes at room temperature in the dark. The reaction was diluted by adding 800 μ l of 1X PBS and then washed once with 1X PBS to remove the remaining paraformaldehyde. Fixed cells were subsequently permeabilized

with 100 μ l 0.1% Triton-X (in 1X PBS) (v/v) for 8 minutes at room temperature. This step allows antibodies to diffuse into cells and to label proteins in the cyto- and nucleo-plasma. This permeabilization reaction was stopped with 900 μ l 1X PBS and the cells were additionally washed once with cold 1X PBS. The primary GSTP1 antibody was diluted with 0.5% BSA in 1X PBS. After 1h of incubation at room temperature, cells were washed twice with 1X PBS and incubated with a dilution of a fluorochrome-linked secondary antibody (Table 30) for one hour at room temperature in the dark. After washing twice with 1X PBS, cells were preserved in a solution of 0.2% paraformaldehyde in 1X PBS. Alexa Fluor 488 and Alexa Fluor 647 fluorescences were read at ex.495/em.519nm and ex.650/em.668nm, respectively.

4.5.2. Fluorescent nucleic acid staining

The blue fluorescent Hoechst 33342 is a cell permeable nucleic acid dye, used for DNA labeling in viable cell. This bisbenzimidazole derivative is a supravital minor groove-binding DNA dye that binds preferentially to A-T base pairs. AT-rich double stranded DNA enhance the Hoechst fluorescence ~2-fold greater than GC-rich strands (Portugal and Waring 1988). Because of the lipophilic property of Hoechst 33342, cells do not require any permeabilization for labeling, but do require physiologic conditions since the dye internalization is an active transport process. Hoechst staining is analyzed at ex.350/em.461nm.

The red-fluorescence dye (ex.536/em.617nm) propidium iodide (PI) is a DNA/RNA intercalating agent, is membrane impermeant and is excluded from living cells. This characteristic is taken in advantage to detect necrotic cells in a cell population (Moore, Donahue et al. 1998).

Cells were incubated with Hoechst 33342 (1 μ g/ml) for 15 minutes at 37°C in the dark. Then, PI was added at a final concentration of 1 μ g/ml and DNA staining was analyzed by fluorescence microscopy.

4.5.3. Cell trace proliferation assay

The colorless and non-fluorescent carboxyfluorescein diacetate succinimidyl ester (CFSE) diffuses passively into cells where it is metabolized by intracellular esterases to fluorescent carboxyfluorescein succinimidyl ester. This degradation product reacts with intracellular amines, forming fluorescent conjugates that are evenly distributed between two daughter cells during division. This property can be used to label cells and to trace cell proliferation.

To analyze population-based proliferation, cells were CFSE-stained using CellTrace™ CFSE Cell Proliferation Kit. Cells in exponential growth phase were resuspended in pre-warmed 1X PBS/0.1% BSA in a final concentration of 1×10^6 cells/ml and stained with 0.2 μ M CFSE for 10 minutes at 37°C. Dye was quenched by the addition of 5 volumes of ice-cold culture media. After 5 minutes of incubation on ice, cells were centrifuged and the pellet washed twice with fresh media. CFSE staining was analyzed using FACSCalibur flow cytometer with 488 nm excitation and emission filter.

4.5.4. Flow cytometry

Flow cytometry uses the principles of light scattering, light excitation and fluorescence emission from molecules to simultaneously analyze multi-parameters of single cells or particles in the size range between 0.2 μ m to 150 μ m. This technique is applied to determine the expression profile of cell surface and intracellular molecules, to characterize and define different cell types in heterogeneous cell populations, to assess the purity of isolated subpopulations as well as to analyze cell size, granularity and cell volume. The flow cytometer is composed of three main systems: fluidics, optics and electronics. The sample is first transported through the fluidic system where it is hydrodynamically focused using sheath fluid and a very small nozzle (Figure 17).

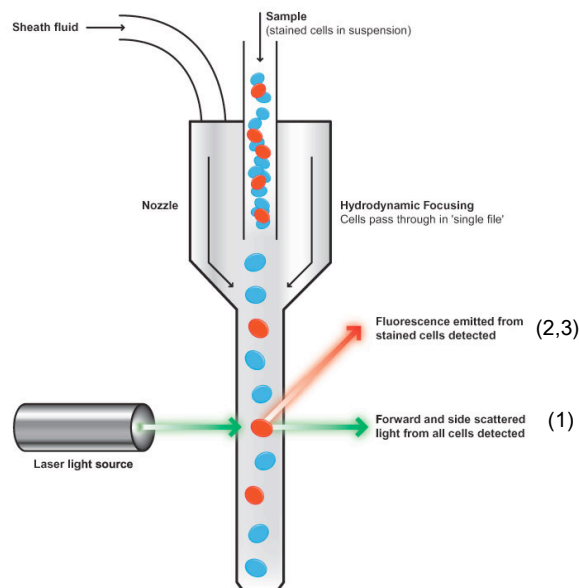


Figure 17: Schematic representation of flow cytometry principle.

Flow cytometer uses the technique of hydrodynamic focusing for presenting cells to a laser. The sample composed of unstained cells (blue bubbles) and fluorochrome-stained cells (red bubbles) is injected into the center of a sheath flow. The combined flows are reduced into diameter, forcing cells into the center of the stream to pass through the laser beam. In line (1) and perpendicular (2) detectors with the light beam as well as fluorescence (3) detectors pick up the combination of scattered and fluorescence signals. Analyses of fluctuations in brightness and fluorescence allow to obtain various types of information about the physical and chemical structure of each individual particle (www.abcam.com/technical).

In the stream of fluid, cells pass like a string of pearls, only one cell at the time, the laser light. Since cells intercept the light source, they scatter light and fluorochromes are excited. The optical part of the cytometer is constituted of a laser to illuminate samples in the stream as well as optical filters to direct the resulting light to different detectors (Figure 17). The electronic part collects the laser light scattered from cells and converts this information into a signal, processed by a computer. A detector in front of the laser light beam (Forward scatter, FSC) recognizes the cell size and a second perpendicular (Side scatter, SSC) is responsible for the density measurement that means the relative granularity and the internal complexity of the cell (Figure 17). Fluorescence detector, in the same position as the SSC detector, is used to measure the fluorescence intensity of cells (Figure 17).

Based on the specific light scattering and fluorescent characteristic, it is possible to sort a heterogeneous mixture of cells. The FACSCalibur cytometer possess a mechanical device “catcher tube” to collect cells of interest. Cells

pass through the detector system, the computer determines if cells fulfill the selected criteria and separate them mechanically from the remaining population.

Immunostained samples were quantitatively processed by flow cytometry using BD FACSCalibur™ with the CellQuest Pro (BD bioscience) software and analyzed with FlowJo (Treestar, Ashland, USA). Results were expressed both as percentage of positive cells and as mean fluorescence intensity (MFI). Isotopic control labeling was performed in order to determine non-specific fluorescence and to calculate MFI ratios. To separate and collect cells of interest from a heterogeneous cell population, immunostained samples were sorted using BD FACSCalibur™ with CellQuest Pro software.

4.5.5. Fluorescence microscopy

For the analysis of fluorescence- or immunofluorescence-labeled samples by microscopy, 100µl of cell suspension was precipitated on a glass slide with a cytofuge centrifuge system at 20 *g* for 4 minutes. A coverglass was mounted on the glass slide and cells were observed under the microscope. Observation and image acquisition were done with the IX81 Olympus microscope under an UPlanFL 40X/0.75 objective.

4.6. Molecular biology

4.6.1. Electrophoretic migration

Gel electrophoresis is a useful method to analyze DNA molecules. The naturally present negative charge of the DNA sugar phosphate backbone induces, in a direct current field, a migration of the molecule from the cathode (-) to the anode (+). Linear double-stranded DNA molecules migrate through the agarose matrix with a speed that is inversely proportional to the logarithm of its size. A lot of variables, such as size and form of DNA as well as current intensity, buffer conditions and gel concentration influence DNA migration speed into a gel.

Samples were diluted with 6X loading buffer, loaded into a gel and migration was done in 1X TBE running buffer and 10 Volts per centimeter. A

DNA marker with known fragments length was simultaneously migrated to determine DNA sample length. The separation of short DNA fragments below 300bp was realized in 12% TBE-polyacrylamide gels. Larger DNA fragments were separated in 0.8% TBE-agarose gels (Table 4).

4.6.2. Ethidium bromide staining

Ethidium bromide is a DNA/RNA intercalating agent with a detection limit of up to 20ng of DNA.

TBE-polyacrylamide gels were stained in a solution of 0.5µg/ml ethidium bromide for 30 minutes at room temperature. Ethidium bromide was directly added to agarose gels in a final concentration of 0.5µg/ml. Results of electrophoretic migrations were documented on a UV illumination desk in a Molecular Imager® Gel Doc XR™ System with the Quantity One® software.

4.6.3. DNA extraction

Genomic DNA extraction was performed using the DNeasy® Blood and Tissue Kit as proposed by the manufacturer. An additional step of RNase treatment was added in order to eliminate RNA in the extracted DNA. Thus, 200µg of RNase A was added and incubated for 2 minutes at room temperature. Genomic DNA extraction from low number of cells (<5 X 10⁵) was performed using the QIAamp® DNA micro Kit as proposed by the manufacturer. All genomic DNA samples were stored at 4°C.

4.6.4. DNA quantification

DNA concentration was measured using a NanoDrop ND-1000 Spectral photometer. The UV absorption of DNA solutions is measured at a wavelength of 260nm. The amount of absorbed UV-light is proportional to the quantity of DNA. A DNA solution with an OD of 1 at a wavelength of 260nm has a DNA concentration of 50µg/ml.

Double-stranded PCR products were quantified with the Qubit[®] fluorometer by using the Qubit[®] dsDNA HS assay according to the user manual.

4.6.5. DNA precipitation

Purification of colony PCR products by sodium acetate/ethanol precipitation allows optimal conditions for the following reactions. The addition of ethanol to the PCR batch causes a lowering of the dielectric constant (ϵ), which induces the formation of ion pairs between the polyanion DNA and sodium cations. The neutralization of the negative charge on DNA backbone provokes its precipitation.

To one volume of PCR mix, 0.1 volume of 3M Na acetate (pH 5.2) and 3 volumes of 100% ice-cold ethanol were added. The mixture was incubated one hour at -80°C and DNA was precipitated by centrifugation at 15000 g for 20 minutes at 4°C . The pellucid pellet was washed once with 70% ethanol, air-dried and dissolved in an adequate volume of ddH₂O.

Avegene Gel PCR/DNA fragments extraction kit solutions and the corresponding protocol in combination with the econospin DNA columns (Epoch life science, Sugarland, Texas, USA) were used to purify PCR products for deep sequencing analysis.

4.6.6. Gel extraction

PCR products for sequencing were purified with the QIAquick[®] PCR purification Kit. PCR products for Bio-CoBRA assays were purified with the QIAEX[®] II Gel extraction Kit. Both kits were used as proposed by the manufacturer Qiagen.

4.6.7. RNA extraction

For mRNA expression analysis, total RNA was extracted following the protocol of the NucleoSpin[®] RNA II Kit. For miRNA expression analysis, total

RNA was extracted following the protocol of the miRNeasy[®] extraction Kit. All RNA samples were stored at -80°C.

4.6.8. RNA quantification

RNA concentration was measured using a NanoDrop ND-1000 Spectral photometer. The amount of absorbed UV-light is proportional to the amount of RNA; a solution with an OD of 1 at a wavelength of 260nm has an RNA concentration of 40µg/ml.

4.6.9. Determination of RNA quality

RNA quality was verified using the Agilent chip technology (RNA 6000 Nano Labchip[®]) on a Bioanalyzer 2100 following manufacturer's protocol.

4.6.10. Simultaneous RNA and DNA purification

ALLprep[®] DNA/RNA Micro/Mini Kit was used to isolate both DNA and RNA from the same biological sample.

Patient tissue samples fixed in OCT Tissue TEK were disrupted in 350µl RLT buffer supplemented with 1% β-mercapthoethanol and homogenized into Qiashredder spin columns. DNA and RNA were extracted from the lysate by following the protocol proposed by the manufacturer.

Frozen patient samples in DMSO solution were quickly thawed at 37°C, transferred in 50ml of 1X PBS containing 10% FBS and centrifuge at 300 g at 4°C for 7 minutes. Resulting pellets were disrupted as described above.

4.6.11. DNA digestion

Restriction enzymes were used to cut DNA into small and defined pieces. The recognition motives consist mostly in palindromic sequences of four to eight base pairs. Endonucleases may generate either blunt or sticky (overhangs) ends, where sticky ends are more suitable for a later directional ligation. Several enzymes are methylation sensitive and cut only

unmethylated sequences, a characteristic used to determine the methylation status of a restriction site.

Restriction enzymes work only under defined buffer, cofactor and temperature conditions. Up to 1 μ g of genomic DNA was digested with 10 units of endonuclease in 1X of the corresponding buffer and 1X BSA for 3 hours at 37°C. DNA digestion products were analyzed by gel electrophoresis.

For methylation sensitive restriction assay (MSRA), 1 μ g of genomic DNA was incubated with 20 units of *Hpa*II or *Msp*I for 15 hours at 37°C. Then, 10 additional units of each enzyme were added and incubated for 2 hours at 37°C. Digestion products were analyzed by electrophoretic migration on a 0.8% agarose gel.

4.6.12. Cloning, ligation and Blue/White colony screening

Cloning is a standard procedure to introduce a DNA insert into a vector. Both ends of the host vector possess T-overhangs, which prevent recircularization and allow fixation of inserts with the A-overhangs, produced by *Taq* polymerases during PCR. A T4-ligase covalently ligates PCR products into the pGEM[®]-T vector.

The Blue/White selection allows the detection of successful ligation between a vector and an insert after transformation. The *lacZ* gene in the multiple cloning site of pGEM[®]-T Easy vector encodes the β -galactosidase enzyme, which can metabolize the X-Gal, present in the medium, into a blue dye. The ligation of an insert into the multiple cloning site disrupts the *lacZ* gene leaving cells unstained, whereas vector religation without insert leads to β -galactosidase expression and blue-stained cells.

The pGEM[®]-T Easy vector cloning system from Promega and the enclosed protocol was used to clone PCR products into the pGEM[®]-T Easy vector.

4.6.13. PCRs

PCR (polymerase chain reaction) is an *in vitro* process for the selective isolation and amplification of a specific DNA region (Mullis, Faloona et al. 1986; Mullis and Faloona 1987).

The multi stages PCR reaction relies on thermal cycling, consisting of cycles of repeated heating and cooling of the reaction for DNA melting and enzymatic replication of the DNA.

- *Initialization step*: this first heating step (94-98°C) is required for activation of chemically- or immunologically-inactivated polymerases.

- *Denaturation step*: this step is the first regular cycling event and consists of heating the reaction to 93°-97°C, causing DNA melting and the separation of double-stranded DNA.

- *Annealing step*: the annealing temperature is depending on oligonucleotides (size and composition) and buffer conditions. Single strand oligonucleotides hybridize on heat-denatured single strand DNA template.

- *Extension/elongation step*: the temperature of this step is depending on the DNA polymerase (60-72°C). Polymerase catalyzes the synthesis of a DNA strand in direction 5' to 3', complementary to the DNA template strand by adding dNTPs to the 3'-OH oligonucleotide end. Typically, the last three steps are repeated in this order up to 40 times.

Final elongation: this single step is responsible for the A-tailing of PCR products.

To check whether the PCR generated the desired DNA fragment (amplicon), PCR products were resolved using gel electrophoretic migration.

Bisulfite sequencing PCR

Bisulfite sequencing PCR was used to amplify a specific region of bisulfite converted DNA (3.3.2). Depending on the gene, an appropriated PCR master mix was prepared as described in Table 36 in a final volume of 50µl. Reactions were incubated under polymerase- and primer-specific conditions in a thermocycler (Table 37, Table 38, Table 39).

Table 36: Composition of the bisulfite sequencing and bisulfite deep sequencing PCR master mixture.

Component	Final concentration		
	Hot Star <i>Taq</i>	Hot Fire Pol	Platinum <i>Taq</i>
10X PCR Buffer	1X	1X	1X
MgCl ₂	/	2.5mM	1.5mM
dNTPs	0.2mM each	0.2mM each	0.2mM each
Hot Start binding protein	/	2µg	2µg
Reverse primer	0.40mM	0.16mM	0.20mM each
Forward primer	0.40mM	0.16mM	0.20mM each
Template	40ng	20ng	20ng
Hot Start <i>Taq</i>	2.5U	2.5U	1.5U

Table 37: Cycling conditions for the bisulfite sequencing PCR with the Hot Start *Taq* polymerase.

Phase	Temperature (°C)	Time (minutes)	
Initialization	95	15	
Denaturation	94	1	} Number of cycles (see Table 21 and Table 23)
Annealing	Table 21 and Table 23	1	
Extension	72	1	
Final extension	72	10	

Table 38: Cycling conditions for the bisulfite PCR with the Hot Fire Pol polymerase.

Phase	Temperature (°C)	Time (minutes)	
Initialization	95	15	
Denaturation	95	1	} 42 cycles
Annealing	Table 23	1	
Extension	72	1.5	
Final extension	72	10	

Table 39: Cycling conditions for the bisulfite PCR with the Platinum *Taq* polymerase.

Phase	Temperature (°C)	Time (minutes)	
Initialization	94	2	
Denaturation	94	0.5	} 42 cycles
Annealing	Table 23	0.5	
Extension	72	1	

Resulting amplicons were resolved on a 1.2% agarose gel. Acquisition of the ethidium bromide-stained gels was realized in the Molecular Imager[®]

Gel Doc XR™ System. Selected amplicons were subsequently extracted from the gel and used for combined bisulfite restriction assay, cloned into an amplification vector for sequencing or directly used for deep sequencing.

Colony PCR

Colony PCR is an additional method to both identify clones with insert-containing plasmids and amplify simultaneously regions of interest for subsequent processes. Instead of purified DNA, a whole bacterial clone is used as template in the PCR step. The high denaturation temperature, at the beginning of the PCR, lyses cells and denatures proteins responsible for DNA degradation. Plasmid DNA molecules enclosed in cells are liberated and used as template for amplification.

A PCR master mix with a final volume of 40µl was prepared and inoculated with a bacterial clone. The reaction was then incubated under specific conditions in a thermocycler (Table 40 and Table 41).

Table 40: Composition of colony PCR master mix.

Component	Final concentration
5X GoTaq Buffer	1X
MgCl ₂	1.5mM
dNTPs	0.25mM each
LacZ reverse primer	0.2mM
LacZ forward Primer	0.2mM
Platinum <i>Taq</i> DNA polymerase HIFI	1.5U

Table 41: Cycling program for colony PCR.

Phase	Temperature (°C)	Time (minutes)	
Initialization	95	3	
Denaturation	95	0.5	} 30 cycles
Annealing	65	0.5	
Extension	72	1	
Final extension	72	5	

PCR products were analyzed on a 1% agarose gel. Colony PCR products were additionally precipitated and sequenced.

Methylation-specific PCR

MSP is a bisulfite conversion-based PCR technique that can rapidly assess the methylation status of almost any group of CpG sites within a CpG island, even in regions with high CpG density (Figure 18).

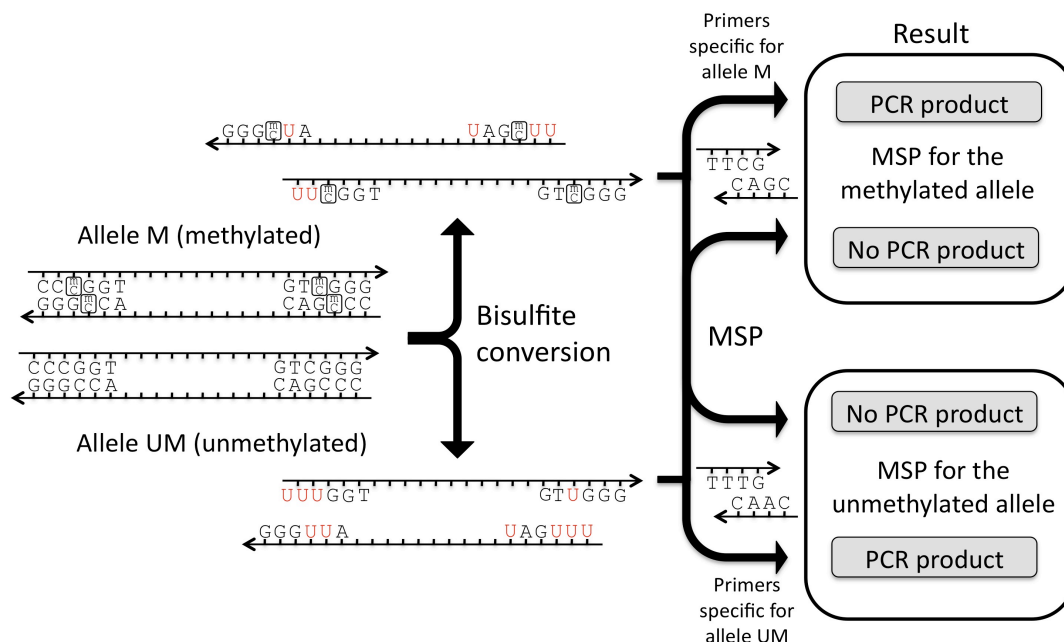


Figure 18: Methylation-specific PCR principal.

Workflow of MSP technique, illustrated with an example of fully methylated (allele M) or unmethylated (allele UM) genomic DNA templates. C^m: methylated cytosine.

This assay consists of an initial chemical DNA modification by sodium bisulfite, converting all unmethylated, but not methylated, cytosines to uracils. For the subsequent PCR amplification, primers are designed to specifically amplify the methylated or the unmethylated allele as well as to discriminate between unmodified and bisulfite modified DNA molecules (Figure 18). To get the highest specificity and provide maximal sensitivity to the assay, primer sequences are chosen for regions containing frequent cytosines and CpG pairs near the 3' end of the primers. The initial report using MSP describes sufficient sensitivity to detect methylation of 0.1% of alleles. In general, MSP and its related protocols are considered to be the most sensitive approach when interrogating the methylation status of a specific locus. Successful amplification from methylated (M) or unmethylated (U) primer pairs indicates the methylated or unmethylated status of the original DNA template, respectively (Figure 18) (Herman, Graff et al. 1996).

MSP conditions for a given gene locus and the corresponding primers set (Table 22) were optimized with fully methylated or unmethylated converted and unconverted DNA, provided with the EpiTect[®] PCR Control DNA Kit. This commercially available DNA was also used as positive and negative controls. MSPs were carried out under specific conditions (Table 42 and Table 43) with methylation-specific primers (Table 22) in a master mix with a final volume of 25 μ l.

Table 42: Composition of the MSP master mix.

Component	Final concentration
10X HIFI Buffer	1X
MgSO ₄	3mM
dNTPs	0.2mM each
Primer R	0.4mM
Primer F	0.4mM
Template	20ng
Platinum <i>Taq</i> DNA polymerase HIFI	1.5U

Table 43: Cycling conditions for methylation-specific PCR.

Phase	Temperature (°C)	Time (minutes)	
Initialization	94	2	
Denaturation	94	0.25	} Number of cycles (see Table 22)
Annealing	Table 22	0.5	
Extension	68	0.5	

Hot Star *Taq* polymerase with the corresponding PCR protocol and annealing temperature was alternatively used to amplify certain gene regions (Table 22).

PCR products were resolved in a 12% polyacrylamide gel, stained with ethidium bromide and documented under UV illumination on Molecular Imager[®] Gel Doc XR[™] System.

Reverse transcription of mRNA

Reverse transcription converts single-stranded RNA into single-stranded cDNA using a RNA-dependent DNA polymerase. This conversion permits the detection of variation in RNA transcription levels. All compounds for reverse transcription of mRNA were provided by Invitrogen.

One microgram of total RNA and 0.5 μ g Oligo(dT) primer were denatured at 70°C for 10 minutes and immediately cooled down at 4°C. The denatured RNA was reverse transcribed in the presence of the following components:

- 5X First strand buffer	1X
- dNTPs	0.5mM (each)
- 0.1M DTT	10 μ M
- Superscriptase Reverse transcriptase RNase (SSII RT)	50U
- RNaseOUT™ Recombinant Ribonuclease Inhibitor	40U

This mixture was incubated in a thermocycler for 90 minutes at 42°C, then heated up to 70°C for 15 minutes and hold at 4°C. Two Units of RNase H were afterwards added to the mixture and incubated for 20 minutes at 37°C. RNase H treatment eliminates mRNA matrix. The cDNA synthesized during this process was diluted with ddH₂O at 40ng/ μ l and stored at -20°C.

Reverse Transcription of miRNA

Unlike mRNAs, miRNAs are not polyadenylated in nature. During this reverse transcription step, miRNAs are polyadenylated by poly(A) polymerase. Reverse transcriptase converts all RNAs (including precursor miRNAs, mature miRNAs, other small non-coding RNAs, and mRNAs) to cDNA using oligo(dT) and random primers. Polyadenylation and reverse transcription are performed sequentially in the same tube. Oligo(dT) primers have a universal tag sequence on the 5' end. This universal tag allows amplification in the following real-time PCR step.

Reverse transcription of 1 μ g of total RNA was done with the miScript® Reverse Transcription Kit (Qiagen) following manufacturer's protocol and cDNA was diluted to 1ng/ μ l.

Real-time PCR

Real-time PCR enables both detection and quantification of a specific DNA sequence in relation to an internal calibration gene (e.g. the housekeeping gene β -actin). Unlike the standard PCR, the accumulation of amplified DNA is detected in real-time during amplification cycles by

fluorescence measurement. Therefore, the double strand-specific DNA intercalant fluorescent dye SYBR[®]Green is used to quantify DNA synthesis.

In this work, real-time PCR was realized using a specific master mix and under stringent conditions (Table 44, Table 45).

Table 44: Composition of the real-time PCR master mix.

Component	Final concentration
Power SybrGreen PCR Master Mix	1X
Primer (reverse and forward)	0.1mM each
Diluted cDNA	8ng

All real-time primers were designed for an annealing temperature of 60°C. Melting curve analysis and electrophoretic gel migration were done to test primers specificity.

Table 45: Cycling program for the real-time PCR.

Phase	Temperature (°C)	Time (minutes)	
Initialization	95	10	
Denaturation	95	0.25	} 40 cycles
Annealing/ Extension	60	1	

For mature miRNA detection, cDNA of total RNA serves as template for real-time PCR analysis using a miRNA specific miScript primer assay (Table 26) in combination with the miScript SYBR[®]Green PCR Kit. MiRNAs are amplified using the miScript universal primer, which primes from the universal tag sequence, together with the miScript primer assay, which is specific for the mature miRNA under study.

For miRNA expression analysis, real-time PCR was realized under stringent conditions using a specific master mix (Table 46 and Table 47).

Table 46: Composition of the real-time PCR master mix for miRNA expression analysis.

Component	Final concentration
QuantiTect SYBR [®] Green PCR master mix	1X
miScript Primer Assay	1X
miScript Universal Primer Assay	1X
Diluted cDNA	2ng

All real-time primers were designed for an annealing temperature of 55°C.

Table 47: Cycling program for the real-time PCR for miRNA expression analysis.

Phase	Temperature (°C)	Time (minutes)	
Initial activating step	95	15	
Denaturation	94	0.25	} 40 cycles
Annealing	55	0.5	
Extension	70	0.5	
Melting curve			

Data from real-time PCR are represented as an amplification curve, derived from the fluorescence intensity plotted against the number of amplification cycles. A threshold was set up in the log-linear range of this amplification curve. The threshold cycle (Ct) value is used to calculate the amount of starting template in each sample. This is the cycle at which the amplification plot crosses the threshold. The raw instrument data (*i.e.* Ct values) were normalized against a reference gene (*i.e.* β -actin for mRNA or RNU1A for miRNA), resulting in “delta Ct”. The relative expression ratio was finally calculated with the comparative Ct method by the arithmetic operation: $2^{-\text{delta Ct}}$.

4.6.14. Bisulfite treatment

Methylated cytosines have nearly the same base pairing characteristics as unmethylated cytosines, and can therefore not be differentiated in normal sequencing reactions. In contrast, selective base conversion called bisulfite mutagenesis allows methylated DNA to be distinguished from unmethylated DNA (Figure 19).

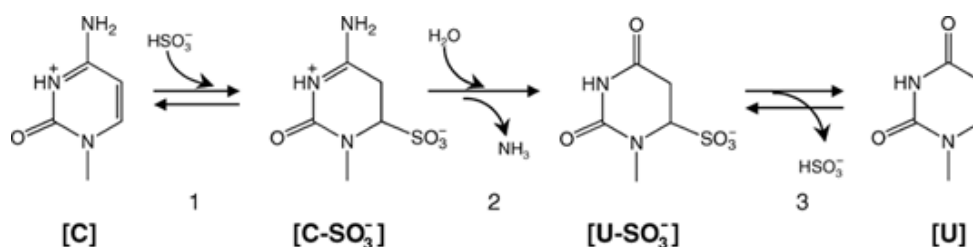


Figure 19: Chemical process of the bisulfite-induced deamination of cytosine to uracil.

Step 1: Sulphonation, Step 2: hydrolytic deamination, Step 3: alkali desulphonation (Hayatsu 2008). C: cytosine, U: uracil, C-SO₃⁻: cytosine-sulphonat, U-SO₃⁻: uracil sulphonate.

Bisulfite has the property to efficiently convert cytosine bases into uracils, whereas methylated cytosines stay unmodified (Figure 19). The initial step of the bisulfite conversion is the denaturation of genomic DNA. The carbon atom in position 6 (C6) of the pyrimidine ring is sterically blocked in double-stranded DNA. Therefore, it has to be denatured to single-stranded DNA. The subsequent chemical process consists in sulphonation of the cytosine to cytosine-sulphonat (C-SO₃⁻) (Figure 19). A methylation-free cytosine possesses in its pyrimidine ring a free C5-C6 carbon bond. This free binding capacity of the C5 atom allows adduct formation with bisulfite ions. In case of a methylated cytosine, this C5 atom is blocked, which is preventing the chemical modification. In aqueous phase, the intermediate sulphonated cytosine gets deaminated and transformed to uracil sulphonate (U-SO₃⁻). The final alkaline treatment causes the desulphonation of the molecule to uracil (Figure 19) (Frommer, McDonald et al. 1992; Clark, Harrison et al. 1994).

Bisulfite conversion was performed using the Epitect Bisulfite Kit as proposed by the manufacturer.

For methylation analysis by deep sequencing, genomic DNA was converted by adding 187 μl of conversion buffer and 73 μl of scavenger solution to 500 ng of genomic DNA in a final volume of 20 μl. After incubation at the following conditions: 99 °C 15 min, 50 °C 30 min, 99 °C 5 min, 50 °C 90 min, 99 °C 5 min and 50 °C for 90 min, the conversion mixture was diluted with 150 μl ddH₂O and loaded on a microcon centrifugal filter Ultracel YM-30 (Milipore). The column was centrifuged for 30 minutes at 11000 g, the flow-through discarded and the column wash once with 500 μl 1X TE, Then, 500 μl

desulphonation solution was added on the column and incubated for 10min at room temperature. After a centrifugation step of 10000 *g* for 18 minutes, the flow-trough was discarded and the column washed with 500 μ l 1X TE. Column was then turned over and placed on a new tube and DNA eluted with 50 μ l of 50°C pre-warmed 1X TE buffer. Converted DNA was stored at 4°C.

4.6.15. Bio-CoBRA

Combined bisulfite restriction assay (CoBRA) relies on the innovation of Sadri and Hornsby who have shown that restriction digestion can be used to reveal DNA methylation-dependent sequence differences in PCR-amplified bisulfite-treated genomic DNA (Sadri and Hornsby 1996). Bisulfite conversion of genomic DNA leads to methylation-dependent formation of new restriction enzyme sites or retention of the pre-existing sites. After PCR amplification, this feature can be exploited to determine DNA methylation levels at specific loci, with a very high quantitative accuracy. However, bisulfite-generated restriction sites are preferred because they allow the simultaneous control of complete bisulfite conversion. It is important to stress that the restriction enzyme cleavage itself is not methylation-dependent because PCR products do not contain 5-methylcytosine. Results of restrictions are classically analyzed by PAGE separation or southern blot. Alternatively, the restriction profile can be quantitatively analyzed by capillary electrophoresis in microfluidics chips (Bio-CoBRA) (Brena, Auer et al. 2006; Brena, Auer et al. 2006).

Conversions of DNA samples as well as PCR amplification of the target sequence were done as previously described (see 4.6.14 and 4.6.13). PCR products were electrophoresed in a 1X TBE-1.5% agarose gel, visualized by ethidium bromide staining and purified with the Qiaex[®] gel extraction Kit. Restriction digestion of 100ng of PCR product was realized as already mentioned (see 4.6.11). Digested samples were next concentrated using a SpeedVac and 20ng were loaded on the Agilent DNA 1000 LabChip as proposed by the manufacturer and analyzed using the Agilent Bioanalyzer 2100.

4.6.16. Crosslinked chromatin immunoprecipitation (X-ChIP)

Crosslinked chromatin immunoprecipitation (X-ChIP) is mainly used to investigate the interactions between proteins (e.g. transcription factors) and specific DNA regions such as gene promoters or other DNA binding domains in cells. In addition, X-ChIP is suitable for the mapping of histone modifications or to detect the recruitment of histone-modifying enzymes to specific gene regions. By incubating cells with a crosslinking agent, *in vivo* reversible cross-linking of proteins with DNA is achieved (Figure 20). After cell lysis, DNA-chromatin is sheared by sonication or using micrococcal nuclease (Figure 20). Protein-DNA complexes are selectively isolated using a specific antibody against the protein of interest (POI), coupled to magnetic, agarose or sepharose beads (Figure 20). Bead-antibody-POI-DNA complexes are then collected, washed and the crosslink reversed. DNA regions associated to the protein are identified by conventional PCR, real-time PCR or by Chip (ChIP on Chip) (Figure 20).

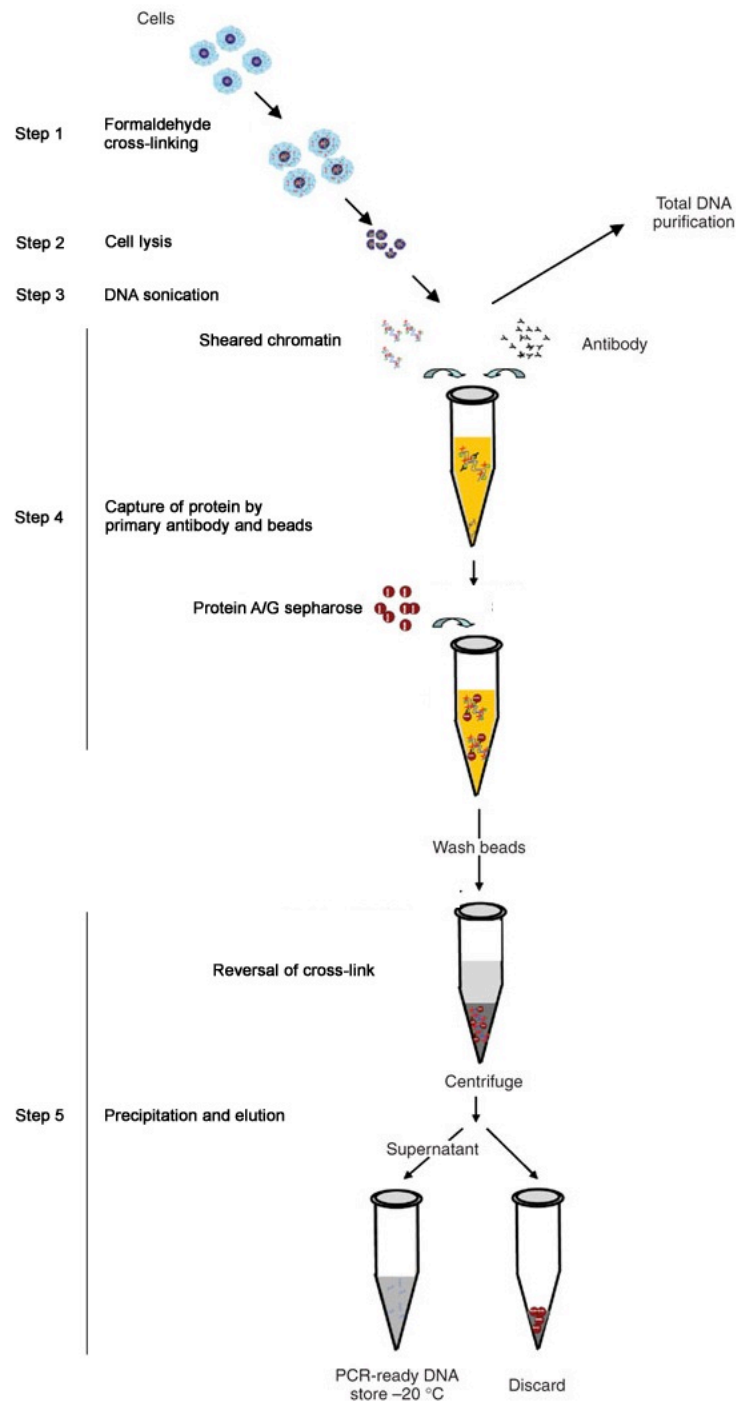


Figure 20: Schematic overview of cross-linked chromatin immunoprecipitation procedure.

For preservation of protein/DNA interactions, intact cells are fixed with formaldehyde (step 1). After cell lysis (step 2), chromatin is sheared (e.g. sonication) into small size uniform fragments (step 3). DNA/Protein complexes are immunoprecipitated with antibodies specific for the protein of interest and recovered using protein A/G sepharose beads (step 4). The cross-link is reversed and DNA purified and analyzed by PCR to determine which DNA regions were interacting with the protein of interest (step 5). Modified from Nelson *et al.* (Nelson, Denisenko *et al.* 2006).

To analyze DNA/protein interactions by X-ChIP, 10^7 cells were cross-linked with 1% formaldehyde for 8 minutes at room temperature. After cross-linking, the reaction was quenched with 0.125M of glycine for 10 minutes at room temperature. Cells were washed twice with ice-cold 1X PBS, pelleted by centrifugation at 350 *g* for 7 minutes at 4°C, resuspended in 1ml of cell lysis buffer (Table 8) and 1X protease inhibitor cocktail and incubated 30 min at 4°C under agitation. After centrifugation at 2500 *g* for 5 minutes at 4°C, nuclei were resuspended in 300 μ l nuclei lysis buffer (Table 8) and incubated for 10 minutes on ice. Chromatin with a size range from 0.5kb to 0.9kb was prepared by sonication using a Bioruptor (Diagenode) at the following settings: mode high, 16 cycles of sonication (30 seconds on / 30 seconds off). Cell debris were removed by centrifugation at 15000 *g* for 10 minutes at 4°C. Supernatant was pre-cleared 1 h at 4°C with 25 μ l of a 50% gel slurry of protein A/G-agarose beads saturated with salmon sperm DNA and bovine serum albumin. After centrifugation at 800 *g* for 3 minutes at 4°C, supernatant was recovered, diluted 10 times in IP dilution buffer (Table 8) and 10% was used as input. The diluted chromatin was incubated overnight at 4°C with 1-2 μ g of the antibody of interest (Table 28) and the immune complexes were recovered by 1h incubation at 4°C with 30 μ l of a 50% gel slurry of protein A/G-agarose beads (Upstate). The precipitated complexes were washed sequentially at 500 *g* for 5 minutes at 4°C with low salt buffer, high salt buffer, LiCl buffer and twice with 1 X TE buffer. Chromatin was eluted twice with 60 μ l of freshly prepared 67°C pre-warmed elution buffer under agitation for 15 minutes at room temperature (Table 8). Cross-link was reversed by an overnight incubation of the elute at 67°C, in presence of 0.3M NaCl and 10 μ g of RNase A (Roche). Samples were then digested with 30 μ g of proteinase K (Roche) in the presence of 40mM Tris-HCL pH 6.5 and 10mM EDTA at 45°C for 1 h. DNA was purified using QIAquick PCR purification kit (Qiagen) and analyzed by real-time-PCR. PCRs were performed using primers that covered different regions of the GSTP1 promoter (Table 25).

4.7. Statistical analysis

Data are presented as means \pm standard deviation (SD), and analyzed by the Student's *t*-test. p-values below 0.05 were considered as statistically significant.

5. Results

Pathological alterations in the native epigenetic pattern, such as aberrant methylation, have great potential for clinical use as promising cancer-specific biomarkers. Tumor biomarkers are useful in the identification of individuals at increased risk of developing cancer and in the early detection of malignant transformations.

The hypermethylated GSTP1 gene is already used as a promising DNA methylation biomarker for prostate cancer diagnosis (Duffy, Napieralski et al. 2009). This aberration reduces or silences GSTP1 expression, decreasing cell detoxification and enhancing consequently the susceptibility of genomic mutations (e.g. breast, prostate and hepatocellular carcinoma). In contrast, DNA hypomethylation leads to high level of GSTP1 expression, improving cell detoxification ability and mediating resistance against cytostatics.

In addition, PTGS2 overexpression is nowadays well accepted as a major player in cancer development by activating cell survival and growth-promoting genes. In contrast, it is now becoming clear that in certain cancer types (e.g. gastric, colorectal), promoter hypermethylation represses PTGS2 expression. In consequence, in these cells both inflammation response and cellular defense are attenuated.

The cases of both epimutated genes demonstrate that a balanced gene expression, regulated by defined epigenetic modification patterns, is very important to avoid for instance prostate or gastric tumor development. This finding may be extended to hematological malignancies but requires therefore further investigations.

Moreover, simultaneous analysis of a broad range of epigenetic biomarker genes will enhance clinical relevance of DNA methylation profiling, for example in the context of individualized medicine. However, aberrant methylation patterns need to be researched further in blood cancer cells in order to pass from a pure laboratory discipline to an area of great bedside relevance to practicing oncologists.

Considering that fact that cancer has an epigenetic etiology, one of the tasks to be tackled in the future will be the efficient and specific modulation of such epigenetic alterations in hematological malignancies as well as in other cancer types. At the moment, nucleoside analogs AZA and DAC are the most effective demethylating compounds. The FDA-approved drug DAC is used for MDS treatment and currently under clinical investigations for treatment of leukemia. However, the demethylation effects seem to be unspecific, leading to activation of genes such as oncogenes or transposable elements. Further investigations are required to elucidate detailed process of DAC-mediated demethylation as well as cellular consequences of DAC treatment.

5.1. Epigenetic regulation of GSTP1 gene expression in hematological malignancies

Since the relationship between epigenetic modifications and GSTP1 expression in leukemia cells remains at the moment poorly understood, the first part of this thesis was focused on the analysis of the epigenetic regulation of GSTP1 expression in leukemia and lymphoma cell lines. Furthermore this study was extended to samples from hematological malignant patients, in order to test the possibility to introduce GSTP1 as a possible cancer biomarker.

5.1.1. Analysis of the constitutive GSTP1 expression in human leukemia/lymphoma cell lines

First, basal GSTP1 gene expression was assessed in various leukemia and lymphoma cell lines. Total mRNA from a panel of 10 leukemia and lymphoma cell lines was reverse transcribed and GSTP1 as well as β -actin mRNA levels analyzed by real-time PCR (Figure 21-A). To compare GSTP1 transcription and translation, GSTP1 protein expression was determined by Western Blot (Figure 21-B).

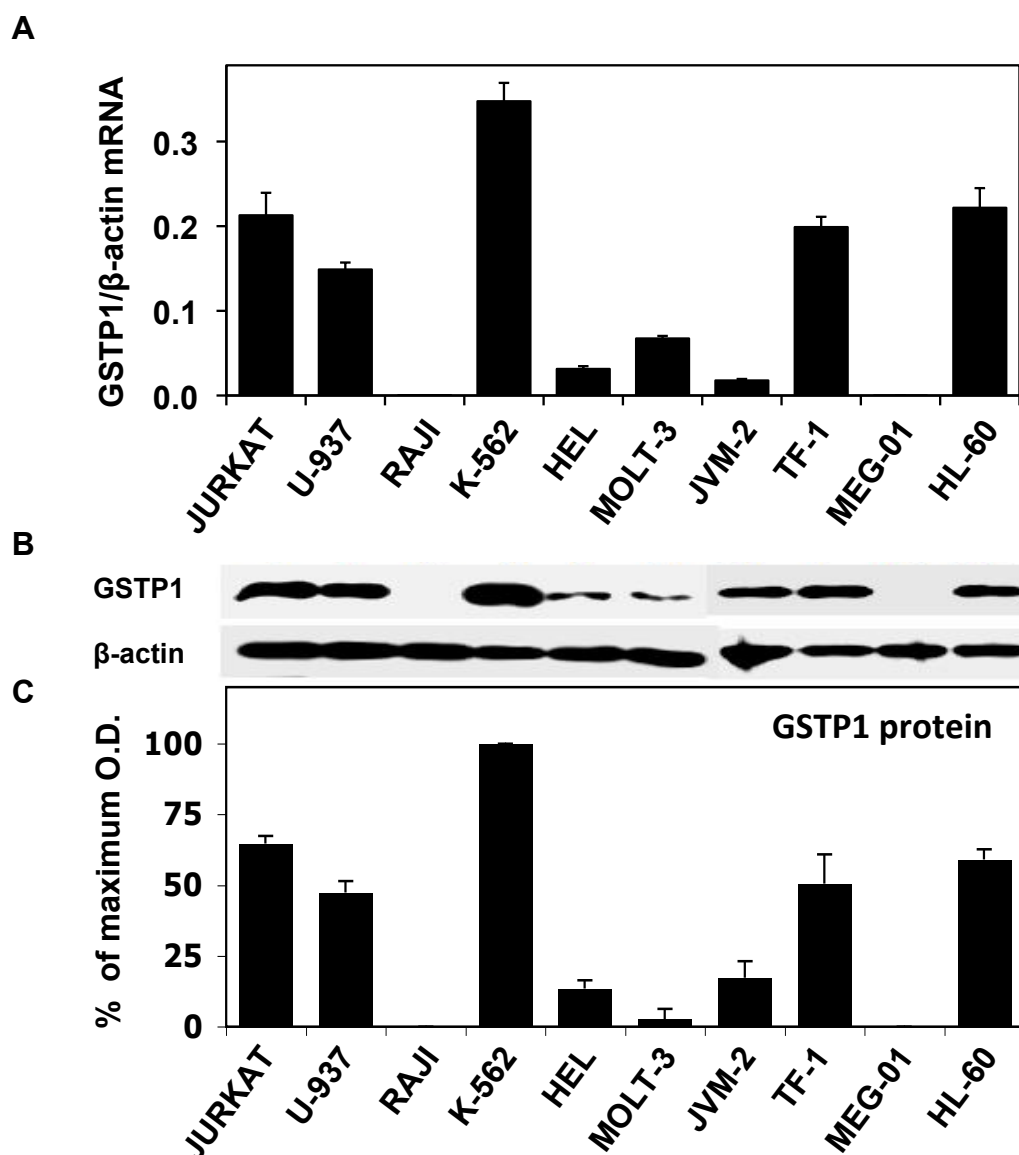


Figure 21: Analysis of basal GSTP1 expression in human leukemia and lymphoma cell lines.

(A) Total RNA extracted from various leukemia and lymphoma cell lines was reverse transcribed into cDNA and analyzed by real-time PCR with primers specific for GSTP1. β -actin was analyzed as a cDNA quantity control. Results represent the ratio of GSTP1/ β -actin mRNA expression. (B) Total protein extractions from the indicated cell lines were analyzed by Western Blot with an antibody specific for GSTP1. β -actin was used as loading control. Pictures are representative of 3 independent experiments. (C) Chemiluminescence was acquired with the Kodak image station 440 CF, quantified with the Kodak 1D image analysis software and normalized to the housekeeping gene β -actin. The relative level of GSTP1 protein in various cell lines is expressed compared to the level in K-562 cells set to 100%. Data are the means \pm SD of 3 independent experiments.

The highest amount of GSTP1, at both mRNA and protein levels, was detected in the CML cell line K-562, whereas GSTP1 was undetectable in RAJI and MEG-01 cells. Furthermore, relatively high basal GSTP1 expression was detected in JURKAT, TF-1, HL-60 and U-937 cell lines, in contrast to the

moderate GSTP1 expression levels detected in JVM-2, HEL and MOLT-3 cell lines (Figure 21).

5.1.2. Effect of DAC treatment on GSTP1 expression in human leukemia/lymphoma cell lines

Previous results about differential levels of GSTP1 expression in blood cancer cell lines and the fact that hypermethylation-mediated GSTP1 silencing is established for other cancer types led to the hypothesis that hypermethylation could be involved in leukemia-specific GSTP1 downregulation. Therefore, we assessed the effects of the DNA demethylating agent DAC on GSTP1 expression. Total mRNA from K-562, RAJI, MEG-01, HEL, MOLT-3 and JVM-2 cells, treated for various time points and doses with DAC was extracted and GSTP1 as well as β -actin mRNA expression quantified by real-time PCR (Figure 22-A, B, C). Moreover, evolution of GSTP1 protein expression was analyzed by Western Blot (Figure 22-D).

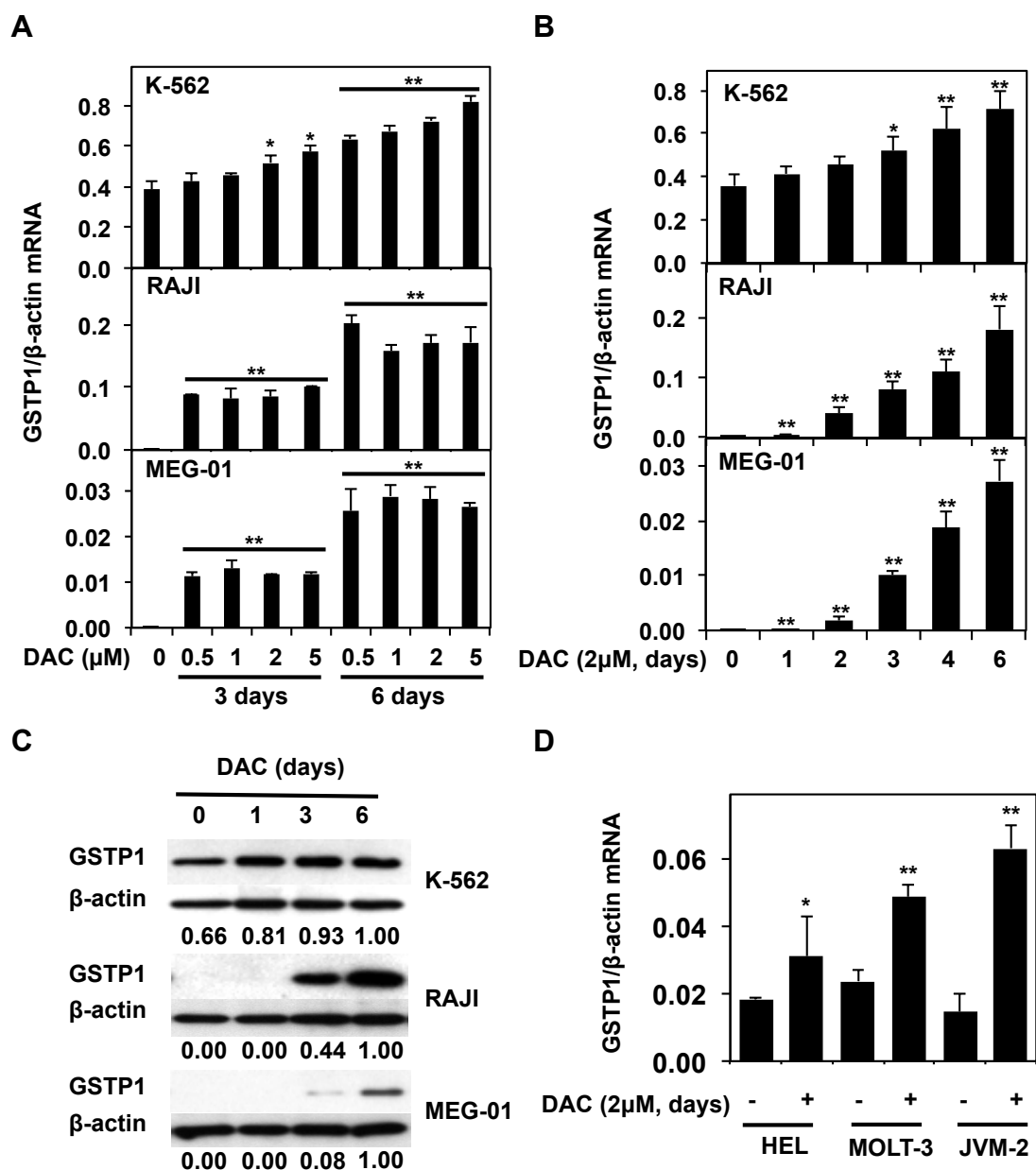


Figure 22: Effect of DAC treatment on GSTP1 expression in leukemia/lymphoma cell lines.

K-562, RAJI and MEG-01 cell lines were treated with various DAC doses at different time periods. Total RNA was isolated and the (A) dose- and (B) time-dependent effects of DAC on GSTP1 mRNA expression were assessed by real-time PCR. Results represent the ratio GSTP1/ β -actin mRNA. (C) Cells were harvested after various time points of DAC treatment and analyzed by Western Blot with an antibody specific for GSTP1. Relative level of GSTP1 protein expression in various blood cancer cell lines is normalized against β -actin and expressed compared to the GSTP1 expression level after 6 days of DAC treatment. Pictures are representative for 3 independent experiments. (D) Total RNA from various untreated (-) and DAC-treated (+) leukemia cell lines was isolated and analyzed by real-time PCR. Results represent the ratio GSTP1/ β -actin mRNA. Data are means \pm SD of 3 independent experiments. * p <0.05, ** p <0.01 vs control.

Results showed that DAC treatment further increased constitutive GSTP1 mRNA and protein expression in a time- and concentration-dependent manner in K-562 cell line. Regarding RAJI cells, DAC treatment drastically induced GSTP1 transcription after two days whereas GSTP1 protein was restored one day later. Similarly, DAC affected GSTP1 expression in MEG-01 cells; however, the induction in MEG-01 was delayed and weaker compared to RAJI cells. In both GSTP1 silenced cell lines, the effect of DAC was time- but not concentration-dependent for the tested range of concentrations (Figure 22-A, C). Furthermore, DAC-mediated induction of GSTP1 expression was delayed in MEG-01 cells compared to RAJI cells. Based on these results, we used 2 μ M DAC to analyze the mechanism of induction of GSTP1 expression in blood cancer cell lines (Figure 22-B). In HEL, MOLT-3 and JVM-2 cells, DAC treatment significantly enhanced the moderate constitutive GSTP1 mRNA expression levels (Figure 22-D).

Western Blot as well as real-time PCR techniques give only an overall of the level of GSTP1 expression in a cell population. To evaluate the localization and cell-specific GSTP1 expression in our models, K-562, RAJI and MEG-01 cells were treated for 3 days with DAC and subsequently immunostained with a GSTP1 antibody. Nucleus were stained with Hoechst and samples analyzed by fluorescence microscopy.

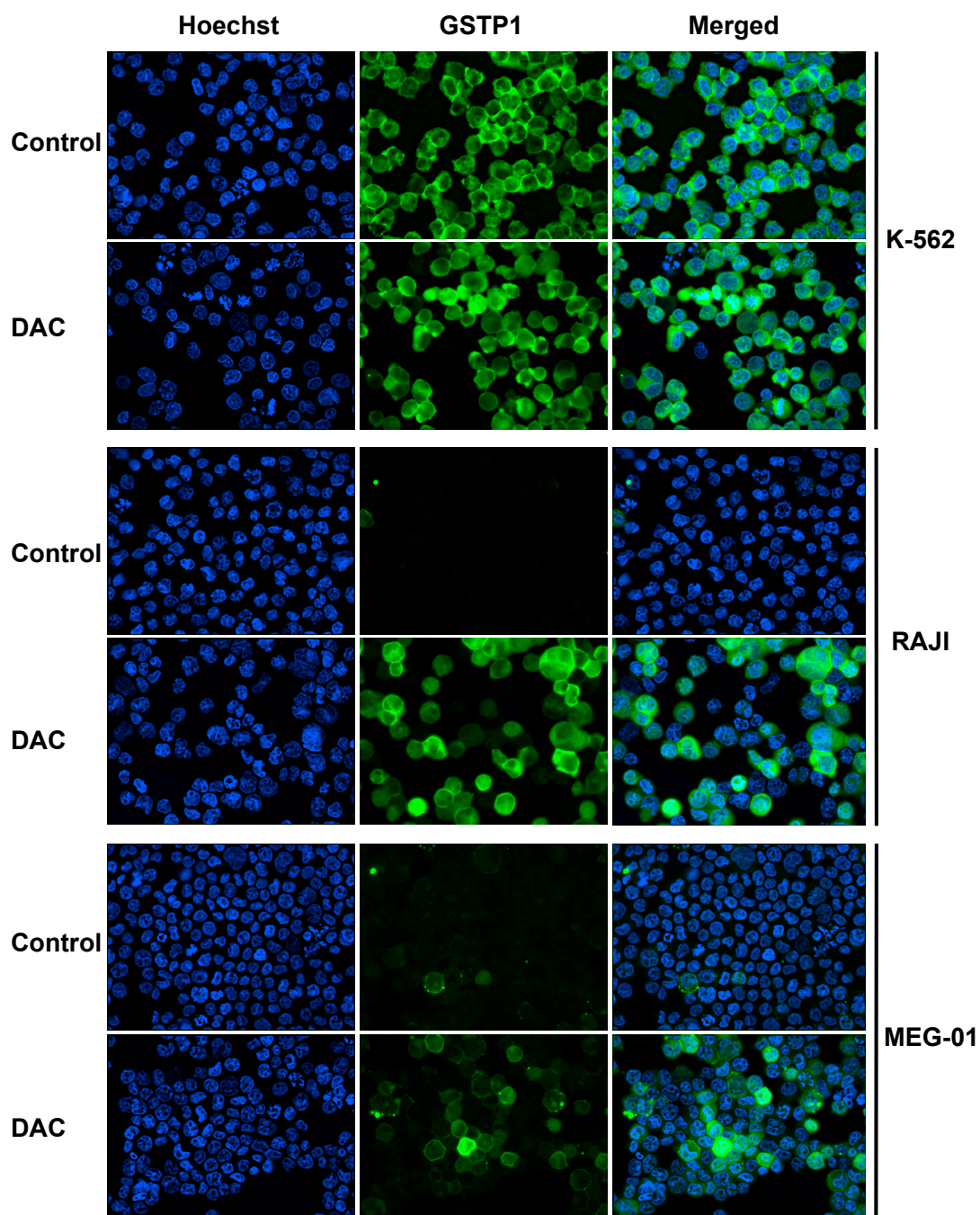


Figure 23: Analysis of GSTP1 expression in control and DAC-treated K-562, RAJI and MEG-01 cells by immunofluorescence.

GSTP1 expression in DAC-treated ($2\mu\text{M}$, 3 days) was assessed by immunofluorescence using primary anti-GSTP1 and secondary Alexa Fluor-488 conjugated (green) antibodies. Hoechst 33342 (blue) was used for nuclear staining. Fluorescence signals were observed with the fluorescence microscope IX81 Olympus microscope under an UPlanFL 40X/0,75 objective and data were acquired by using the CCD camera Olympus XM10. GSTP1 sub-localization was evaluated by overlay (merged). Pictures are representative for 3 independent experiments.

Microscopy images of GSTP1-immunostained K-562 cells showed that all cells express GSTP1. Moreover, DAC treatment further enhanced GSTP1 expression in some K-562 cells (Figure 23). In contrast, untreated RAJI and MEG-01 cell lines did not or expressed undetectable levels of GSTP1 protein. However, images clearly demonstrated that GSTP1 expression is induced in a subpopulation of RAJI and MEG-01 cells after 3 days of DAC exposure (Figure 23). Finally, DAC-induced GSTP1 expression was more pronounced in RAJI compared to MEG-01 cells (Figure 23).

In order to quantify cell-specific GSTP1 expression in K-562, RAJI and MEG-01 leukemia cell lines, GSTP1-immunostained cells were analyzed by flow cytometry. Hence, untreated and DAC-treated K-562, RAJI and MEG-01 cells were fixed, permeabilized and immunostained for GSTP1 (Figure 24).

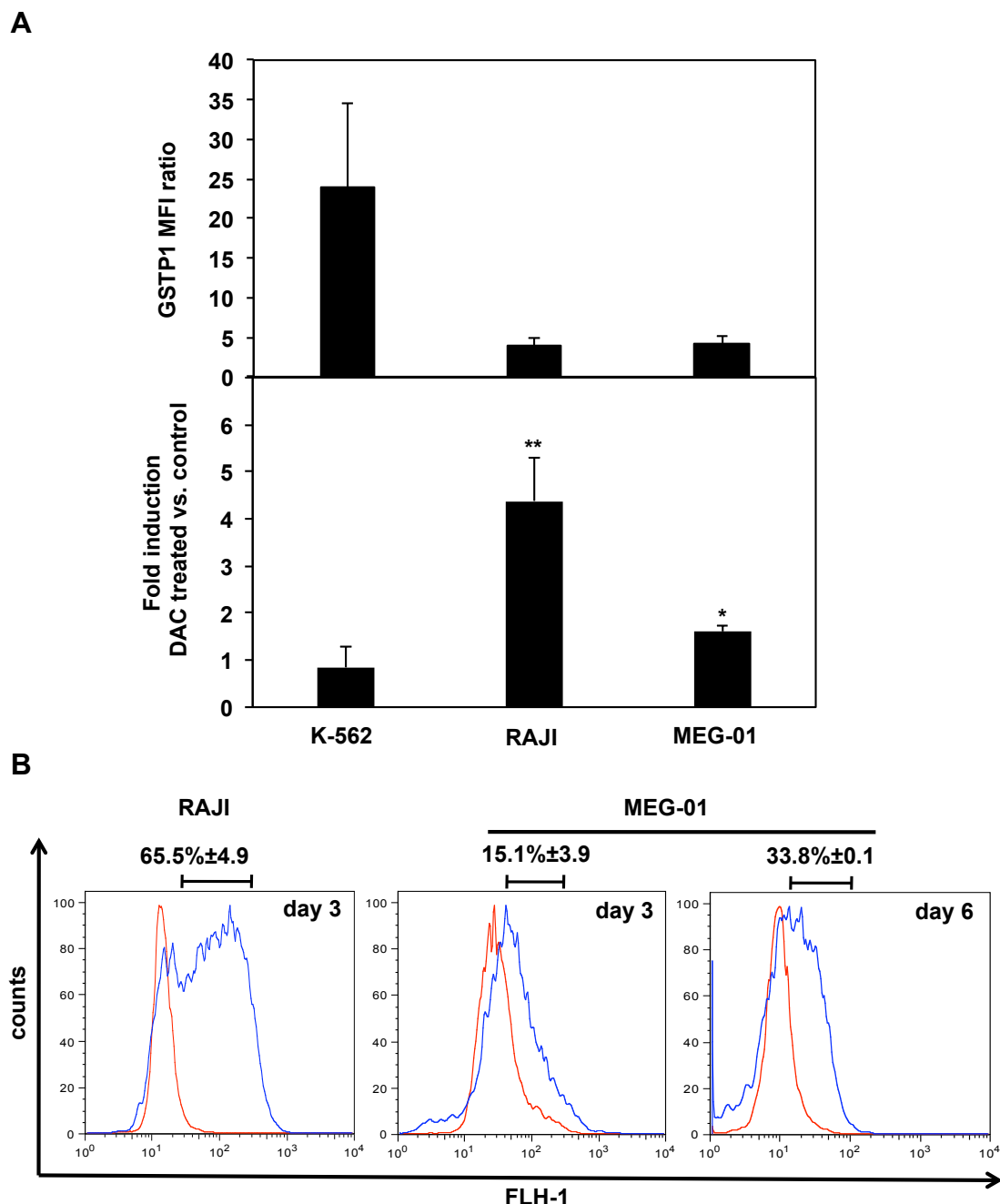


Figure 24: Quantification of GSTP1 expression in DAC-treated K-562, MEG-01 and RAJI cells.

K-562, RAJI and MEG-01 cell lines were treated with 2 μ M DAC for 3 days and GSTP1 stained with primary anti-GSTP1 and secondary Alexa Fluor-488 conjugated anti-mouse antibodies. Fluorescence of 10⁵ immunostained K-562, RAJI and MEG-01 cells was detected by flow cytometry on a FACSCalibur and analyzed by CellQuest Pro. (A) Upper panel: The fluorescence intensity was measured as mean fluorescence intensity (MFI) ratios of immunostained leukemia cells in relation to the IgG. Lower panel: Fold induction of GSTP1 protein expression after 3 days of DAC treatment. (B) One dimensional GSTP1 frequency histogram of 10⁵ wild type (red line) and DAC-treated (blue line) RAJI and MEG-01 cell lines, treated for 3 or 6 days. Data are means \pm SD of 3 independent experiments. * $p < 0.05$, ** $p < 0.01$ vs control.

The highest MFI ratio, representative for the GSTP1 expression level, was measured in K-562 cells (MFI ratio 23.8). In contrast, low MFI ratios were identified in RAJI (MFI ratio: 4) and MEG-01 (MFI ratio: 4.2) cells (Figure 24-A). Quantification of the DAC-induced GSTP1 immunostaining revealed a drastic and significant 4.4-fold increase of GSTP1 expression after 3 days of DAC treatment. In correlation with microscopy results, frequency histogram showed that only a subpopulation of about 65% of the DAC-treated RAJI population was GSTP1-positive compared to untreated cells (Figure 24-B). In MEG-01 cells, 3 days of DAC exposure caused a significant induction of GSTP1 protein expression of about 1.6-fold (Figure 24-A). Moreover, 6 days of DAC exposure were required to induce GSTP1 expression in 33,8% of the MEG-01 cell population (Figure 24-B).

Immunostaining and Western Blot analyses showed that GSTP1 is highly expressed in K-562 leukemia cells and can be induced by DAC treatment in RAJI and MEG-01 cells. Next, we wanted to evaluate the impact of DAC on GST enzymatic activity. Results are presented in Figure 25.

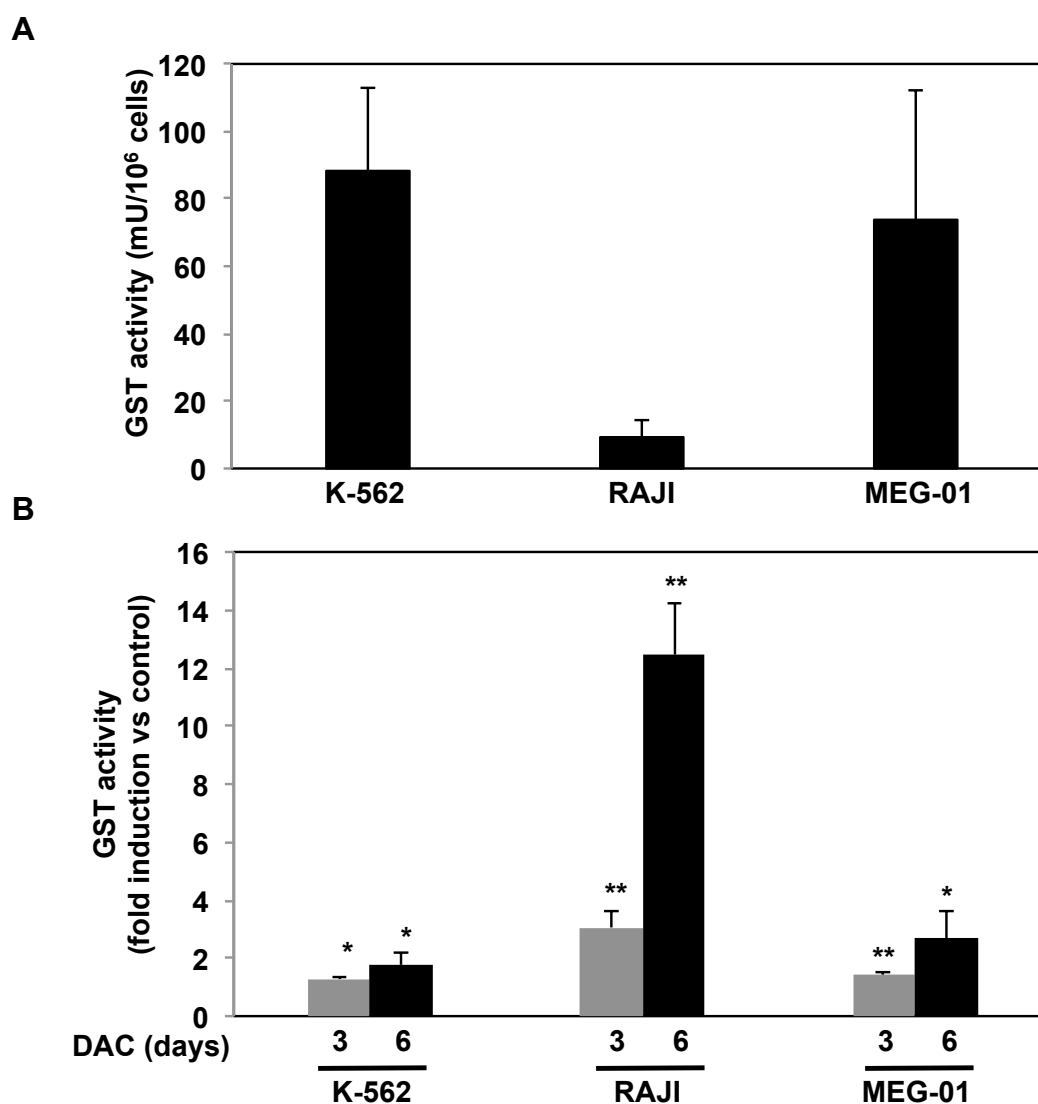


Figure 25: Total glutathione S-transferase activity in DAC-treated leukemia cell lines.

K-562, RAJI and MEG-01 cell lines were treated with for 3 and 6 days with DAC and the intracellular glutathione S-transferase (GST) activity determined by measuring the fluorescence level of monochlorobimane, a dye that reacts with glutathione. Fluorescence results were interpolated by a calibration curve to obtain GST activity values. (A) Constitutive cell line-specific GST activity ($\text{mU}/10^6$ cells). (B) Cell line-specific and time-dependent increase of GST activity was expressed as a fold induction in treated cells vs untreated cells. Data are the means \pm SD of 3 independent experiments. * $p < 0.05$, ** $p < 0.01$ vs control.

The highest basal GST activities were measured in K-562 ($88.5 \text{mU}/10^6$ cells) and MEG-01 ($74 \text{mU}/10^6$ cells) cells in contrast to the lowest GST activity detected in RAJI cells ($9.4 \text{mU}/10^6$ cells) (Figure 25-A). Furthermore, DAC exposure increased GST activity in a time-dependent manner and reached a 3- and 12-fold induction in 3 and 6-day treated RAJI cells,

respectively. A slight but significant GST activity induction was observed in DAC-treated K-562 and MEG-01 cells (Figure 25-B).

5.1.3. Effect of HDAC inhibitors on GSTP1 expression in human leukemia cell lines

In addition to DNA methylation, histone modifications such as acetylation or methylation could be implicated in the epigenetic regulation of GSTP1 transcriptional activity by modifying gene accessibility. Effects of common HDACis on GSTP1 expression in blood cancer cell lines were analyzed. Thus, K-562, RAJI, MEG-01 cells were first treated with DAC for 3 days and subsequently with 1mM VPA or 2 μ M SAHA for 16 hours. Total RNA was extracted and GSTP1 as well as β -actin cDNA amounts were analyzed by real-time PCR (Figure 26). Treatment of K-562, RAJI and MEG-01 cells with HDACis alone lack significant induction of GSTP1 expression. In contrast, sequential treatments with DAC and then HDACis caused a moderate but significant increase of GSTP1 expression in RAJI and MEG-01 cells, compared to DAC treatment alone.

Effectiveness of HDAC inhibition was verified by analyzing the status of histone H4 acetylation (Figure 26). Both HDACi increased total histone H4 acetylation, whereas DAC alone failed to induce histone H4 acetylation.

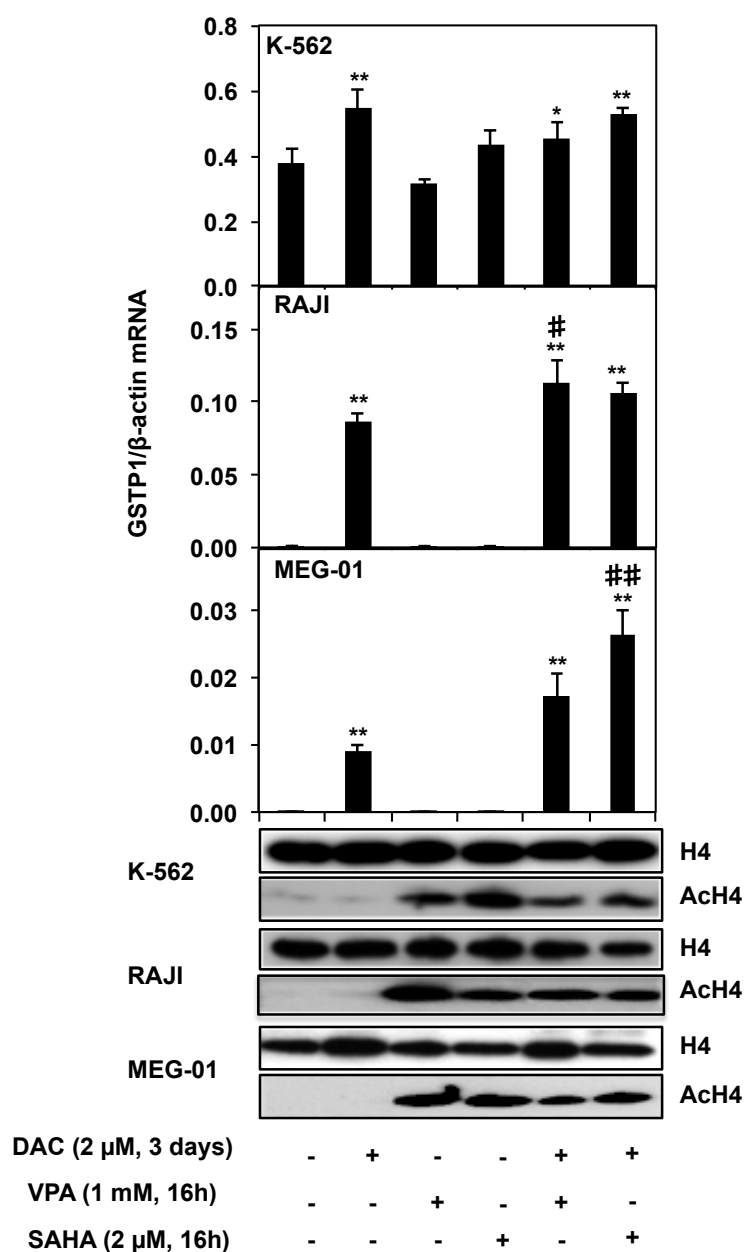


Figure 26: Effects of HDAC inhibitors on GSTP1 expression in leukemia and lymphoma cell lines and on total histone H4 acetylation.

Various leukemia cell lines were treated either with DAC, VPA, SAHA alone or were co-treated with DAC for 3 days followed by 16 hours in presence of VPA or SAHA. Upper panel: total RNA was extracted and GSTP1 mRNA expression assessed by real-time PCR. Results represent the ratio GSTP1/β-actin mRNA expression level and are the mean ± SD of 3 independent experiments. *p<0.05, **p<0.01 vs control; #p<0.05, ## p<0.01 vs DAC. Lower panel: acid extracts were analyzed by Western Blot with antibodies specific for histone (H4) and its acetylated form (AcH4). Pictures are representative for 3 independent experiments. DAC: 5-aza-2'-deoxycytidine, VPA: valproic acid, SAHA: suberoylanilide hydroxamic acid.

5.1.4. DNA methylation analysis of GSTP1 promoter region

The effect of the DNA demethylating agent DAC on GSTP1 expression prompted us to hypothesize that methylation of the GSTP1 promoter region could explain the lack of GSTP1 expression in RAJI and MEG-01 cell lines. *In silico*, CpG density analysis identified 12 CGIs in a region of approximately 20000bp length 5' upstream region of the GSTP1 gene (Figure 27-A). A long CGI, potentially involved in the epigenetic regulation of GSTP1, was identified near the GSTP1 transcription start site.

A

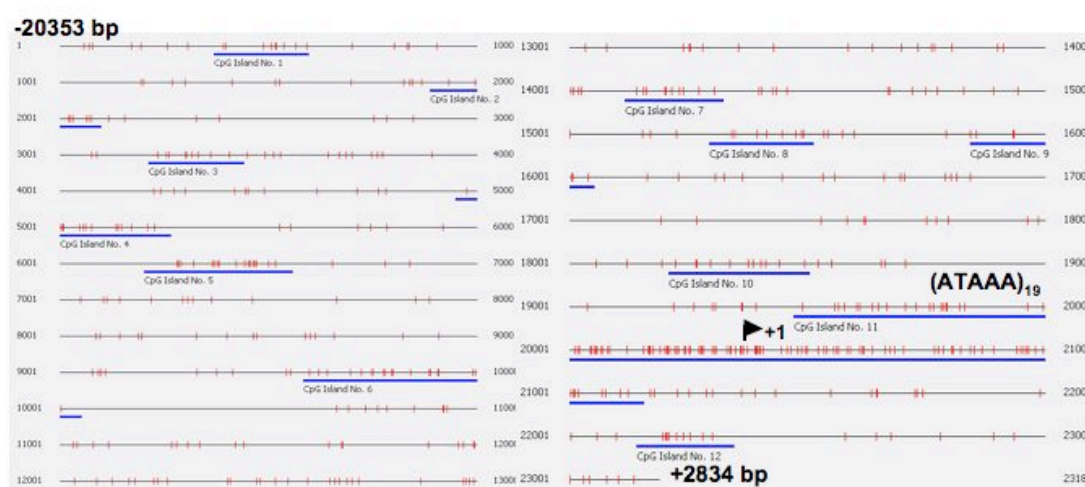
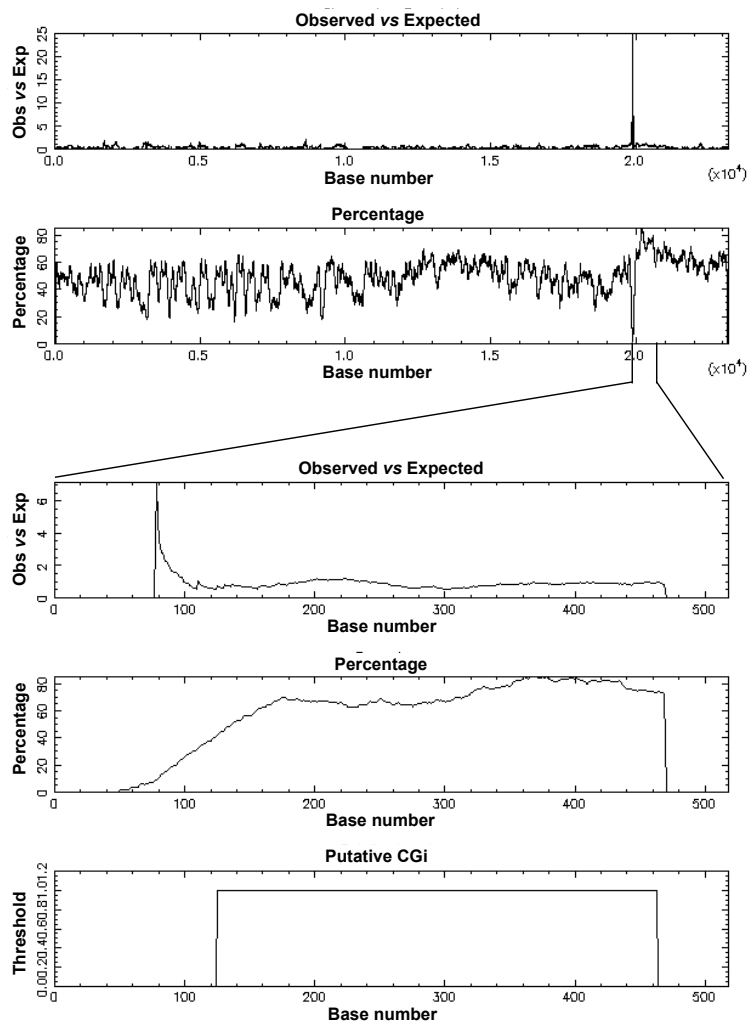


Figure 27: CpG island analysis of the GSTP1 promoter region.

(A) *In silico* CpG density analysis of the GSTP1 promoter region (-20353, +2834) using the Methylprimer express software. Vertical red bars represent CpG dinucleotides and horizontal blue bars indicate CGI positions. Position and length of the (ATAAA)₁₉ repetitive sequence and the transcription start point (+1) are indicated. (B) *In silico* CG analysis of the GSTP1 5' upstream (upper panel) and promoter (lower panel) region with the web-based tool CpGPlot. The observed vs expected ratio, the CG percentage and a putative CGI are represented. (C) Sequence of the putative CGI with the CpG dinucleotides highlighted in red. The positions of the binding sites for GATA-1, NF-κB, AP-1 and SP1 are framed in blue and the transcription start site is underlined and highlighted in green.

B



C

ACTAAAAGGAACCTGATCATGTCCCTTGCAGGGACATGGGTGGAGCTGGAAGCCCTTAGCCTCAGCAAACCTCACACAGGAACAGAAAACCAGCCAGACCCGATGGTCT
 TCACCTTATAAGTGGGAGCTGAACAATGAGAACACATGGTCACATGGCCGATCAACACACACTGGTGCCTGTTGAGCCGGGTGCTGGGAGGGAGAGTACCAGGAA
 GAATAGCTAAGGATATGGGCTTAATACCTGGTGTATGGATGATCTGTACAGCAAACCATCATGGCCGACACACCTATGTAACAAACCTGCACATCCTCTACATG
 TACCCGAGAATCTCAATAAAAAGTTGGAACGGCCAGGCTGGTGGCTCACGCCGTGTAATCCAGCACCTTTGGGAAGCCGAGGCGTGCAGATCACCTAAGGTGAGGAGT
 TCCGAGACCAGCCCGCCCAACATGGTGAACCCCGTCTCTACTAAAAATACAAAAATCAGCCAGATGTGGCACGCACCTATAATCCACCTACTCGGGAGGCTGAAGC
 AGAATTGCTTGAACCCGAGAGGCGGAGGTTGCAGTGAGCCGCGAGATCGCGCCACTGCACCTCCAGCCTGGGCCACAGCGTGAGACTACGTCATAAAAATAAAATAAA
 ATAACAAAAATAAA
 TCTAAGCCGCTCCACCCCTCTCCCTGCCCTGTGAAGCCGGTGTGCAAGCTCCGGATCGCAGCGGTCTTAGGGAATTCGCCCGCATGTCCGGCGCCAGT
 TCGCTGCGCACACTTCGCTGCTCCTCTCTGCTGCTGTTTACTCCCTAGGCCCGCTGGGACCTGGGAAAGAGGGAAAGGCTTCCC CGCCAGCTGCGCGG
 GACTCCGGGACTCCAGGGCCGCCCTCTGCGCCCGACCCCGGGTGCAGCCGCGCGCGGGCTGGGGCCGCGCGGAGTCCGCGGGACCTCCAGAAGAGCCGCGCG
 CGCCCTGACTCAACACTGGGGCGGAGCGGGCGGGAACACCCCTTATAAGGCTCGGAGGC CGGAGGCGCTTCGCTGAGTTTCGCGCGCGAGTCTTCCACCAGTG
 AGTACCGCGCGGCCCGCTCCCGGGATGGGCTCAGAGCTCCAGCATGGGCCAACCCCGCAGCATCAGGCCCGGCTCCCGGCAGGGCTCTCCGCCACTCGAG
 ACCCGGGAACGGGGCTTAGGGACCCAGGACGTCGCCAGTGCCTAGCGGCTTTTCAGGGGGCCCGGAGCGCCTCGGGAGGATGGGACCCCGGGGGCGGGAGGG
 GGGGAGACTGCGCTCACCGCCCTTGCCATCCTCCCGGCTCCAGCAAACCTTTCTTTGTTGCTGCTGAGTCCGCTACACCGTGGTCTATTTCCAGTTTGA
 GGTAGGAGCATGTGCTGGCAGGGAAGGGAGGAGGCGTGGGCTGCAGCCACAGCCCTCCGCCACCGGAGAGATCCGAACCCCTTATCCCTCGTCTGTG
 GCTTTTACC CGGGCTCCTCTGTTCCCGCCTTCCCGCCATGCTGCTCCCGCCAGTGTGTGTAARTCTTCGGAGAACCTGTTCCCTGTTCCCTCC
 CTGCACTCCTGACCCCTCCCGGTTGCTGCGAGGCGAGTCCGCCCGGTCCACATCTCTACTTCTCCTCCCGCAGGCGCTGCGCGGCGCTGCGCATGCTG
 CTGGCAGATCAGGGCCAGAGCTGGAAGGAGGAGGTGGTACCGT

(Figure 27 continued)

The adjacent region to the GSTP1 transcription start site was further analyzed with CpGPlot. The elevated ratio observed *versus* expected (>0,6)

and the high GC percentage indicated, consistently with the Methyl Primer Express software, a CGI in front of the GSTP1 transcription start site (Figure 27-B) (Gardiner-Garden and Frommer 1987). This region includes GATA-1, NF- κ B, AP-1 and SP1 binding sites as well as the GSTP1 transcription start site (Figure 27-C).

BSP was applied to determine the methylation pattern of the CGI in GSTP1 promoter region (-198 to +1) in untreated K-562 and RAJI cells as well as in DAC-treated RAJI cells (Figure 28-A). Genomic DNA was extracted from leukemia cell lines and digested by the restriction enzyme *Bgl*II. After bisulfite conversion, the region of interest was amplified by PCR, cloned into the pGEM-T amplification vector and transformed into *E.coli*. Clones were selected for insert presence based on Blue/White screening and colony PCR. Colony PCR products were also used for subsequent sequencing. Results of the sequencing reaction were bioinformatically processed with QUMA and BIQanalyzer software (Figure 28-B, C, D).

From the 380 analyzed CpG dinucleotides, about 0.3% were methylated in the GSTP1 promoter region of K-562, revealing that the analyzed GSTP1 promoter CGi region was fully unmethylated (Figure 28-B). In contrast, BSP analysis of the GSTP1 promoter region in RAJI cells showed an average DNA methylation percentage of 96.3% (Figure 28-C). In addition, the hypermethylated state of GSTP1 gene in RAJI cells was decreased to 64.5% of methylated CpG dinucleotides. Interestingly, in our model, DAC-induced DNA demethylation was restricted to specific amplicons and therefore demethylation occurred without any CpG position preference (Figure 28-D).

BSP results related to GSTP1 promoter methylation signature in untreated and DAC-treated K-562 and RAJI cells were validated using BioCoBRA. Genomic DNA from untreated and DAC-treated cells was extracted, bisulfite converted and used as template for PCR amplification with BSP primers. The resulting amplicon was digested with the restriction enzyme *RsaI*, which recognizes a unique sequence appearing only in methylated and bisulfite-converted alleles. BioCoBRA was analyzed on the Bioanalyzer from Agilent (Figure 29-A-B).

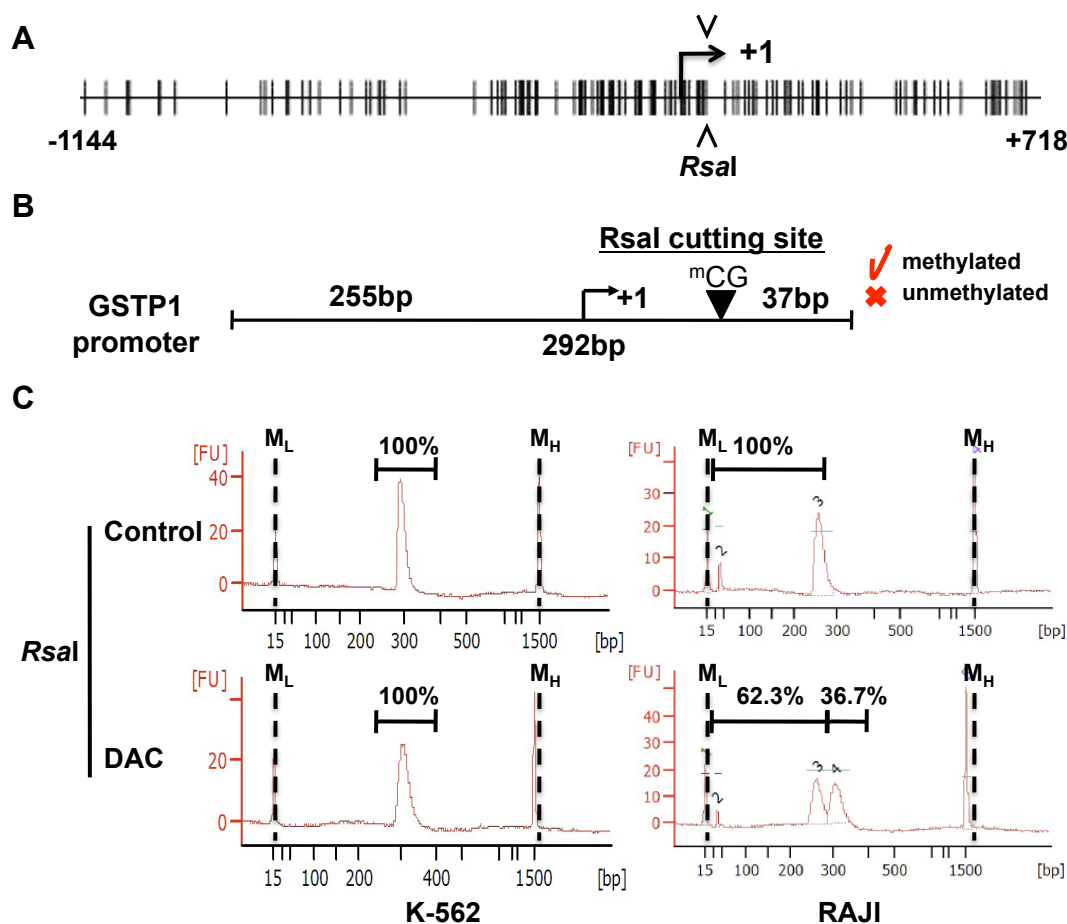


Figure 29: Bio-CoBRA analysis of GSTP1 promoter methylation status.

(A) Physical map generated with the Methylprimer software showing the distribution of CpG dinucleotides (vertical black bars) and the *RsaI* restriction site positions (\wedge/\vee) in GSTP1 promoter. The amplicon obtained by BSP was used to analyze the methylation status of the *RsaI* restriction site in GSTP1 promoter. The localization and the methylation dependent *RsaI* cutting site in the GSTP1 BSP amplicon and the length of the corresponding restriction products are indicated. (B) Results of the Bio-CoBRA assay to determine the methylation status of the *RsaI* restriction site in untreated and DAC (2 μ M, 3 days) treated K-562 and RAJI cell lines. Fluorescence units (FU) are plotted versus DNA fragment length (bp). Partitions of digested and undigested amplicons are indicated in percentage on electropherograms. Electropherograms are representative for 3 independent experiments. +1: transcription start site, Bio-CoBRA: Bioanalyzer combined bisulfite restriction assay, M_L: low marker, M_H: high marker.

The peak at 291bp indicates that the analyzed CpG position in the GSTP1 promoter region of K-562 cells was unmethylated (Figure 29-C). In contrast, *RsaI* digestion of the GSTP1 amplicon from RAJI cells resulted in two fragments of 37bp and 255bp. RAJI restriction pattern and absence of undigested amplicons (292bp) confirmed that the *RsaI* restriction site was hypermethylated in RAJI cells. Decrease of fluorescence intensity peaks of

Empty lanes in the bisulfite conversion control (Bi) evinced that both bisulfite treatments and PCRs were realized without contamination that could affect results. Primer methylation specificity (U or M) was demonstrated by the amplification of GSTP1 PCR product only in presence of the correspondingly methylated and converted DNA template (UMC and MC). Lack of amplification with unconverted DNA (UC) shows that the used oligonucleotides are not mispriming with genomic unconverted DNA (Figure 30-B).

MSP results confirmed previous BSP (Figure 28) and Bio-CoBRA (Figure 29) results, showing that the GSTP1 promoter was unmethylated and methylated in K-562 and RAJI, respectively. Furthermore, MSP analysis revealed that GSTP1 promoter was unmethylated in JVM-2, MOLT-3 and HEL cell lines. Finally, MSP analysis revealed dense methylation on GSTP1 promoter in the CML-derived GSTP1 non-expressing cell line MEG-01 (Figure 30-C).

In a next step, MSP was used to determine the influence of the demethylating agent DAC on the GSTP1 methylation pattern in various leukemia cell lines. Genomic DNA from K-562 and RAJI cells, treated up to 6 days and JVM-2, MOLT-3, MEG-01 and HEL cell lines, treated up to 3 days with DAC, was bisulfite converted and methylation status analyzed by MSP (Figure 31).

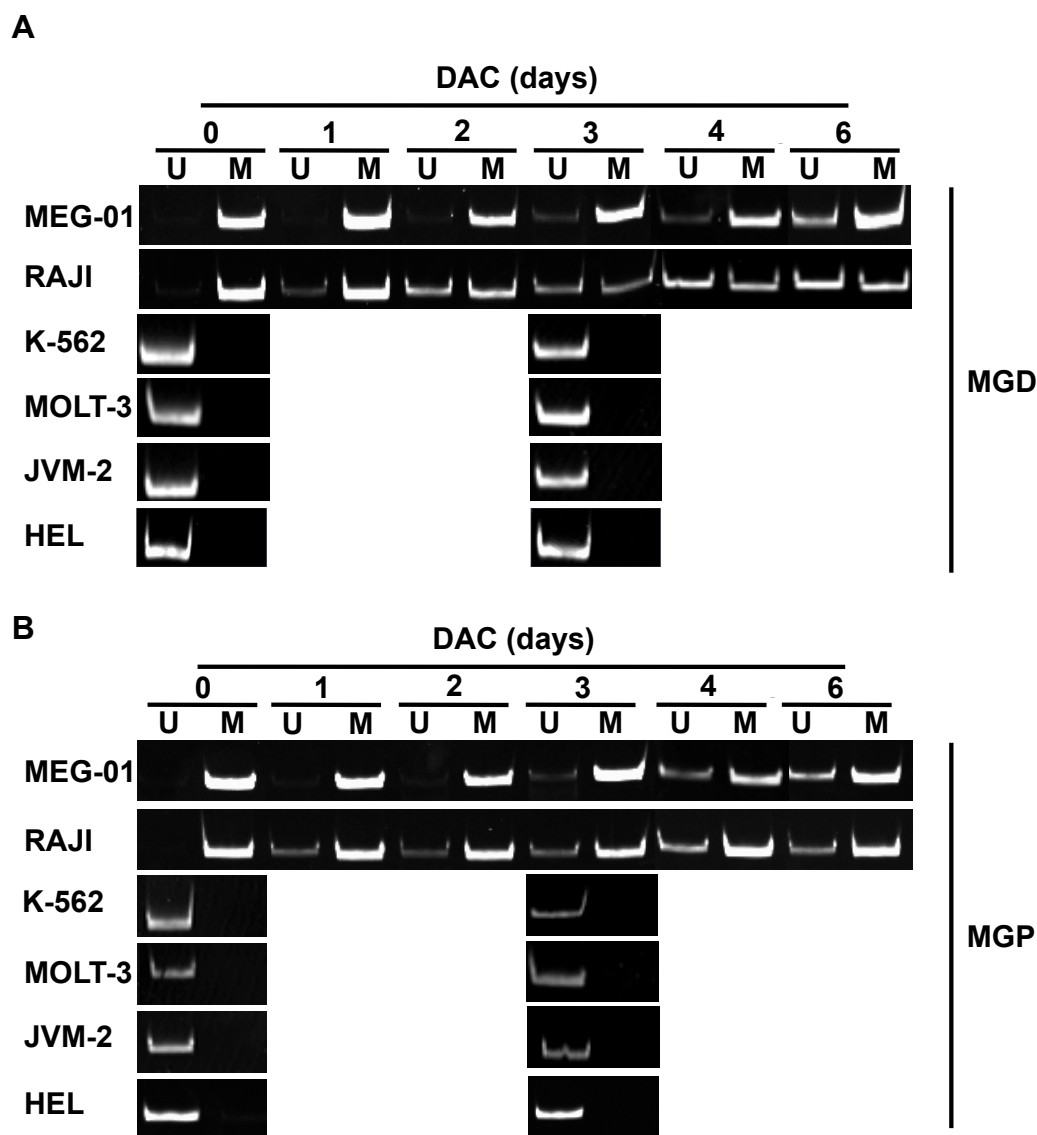


Figure 31: Kinetic analysis of DAC-induced demethylation of GSTP1 promoter in various leukemia and lymphoma cell lines.

Genomic DNA from various leukemia and lymphoma cell lines, treated with DAC were bisulfite converted and analyzed by MSP with primers specific for the unmethylated (U) and methylated (M) state of distal (MGD) (A) and proximal (MGP) (B) GSTP1 promoter regions. MSP amplicons were separated on a 12% PAA gel and stained with ethidium bromide. Images are representative of 3 independent experiments. DAC: 5-aza-2'-deoxycytidine.

In RAJI and MEG-01 cells, DAC treatment induced a time-dependent demethylation of the hypermethylated GSTP1 promoter in both analyzed regions. GSTP1 demethylation was time-delayed in MEG-01 cells compared to RAJI cells. In K-562, MOLT-3, JVM-2 and HEL cell lines, promoter remained unmethylated (Figure 31).

5.1.5. Analysis of the chromatin structure of GSTP1 promoter

In the next step, we performed X-ChIP analysis to determine repressor/activator protein complexes and histone marks associated with GSTP1 promoter. Enrichment of promoter fragments in X-ChIP assays using specific antibodies against various proteins involved in chromatin structure, DNA methylation, histone modifications and transcription were detected by PCR using two primer sets covering GSTP1 basal promoter (CG3) and, as a control, a non-genic 10kb upstream remote region (CG5) (Figure 32-A). The corresponding PCR products were resolved by gel electrophoresis (Figure 32-B).

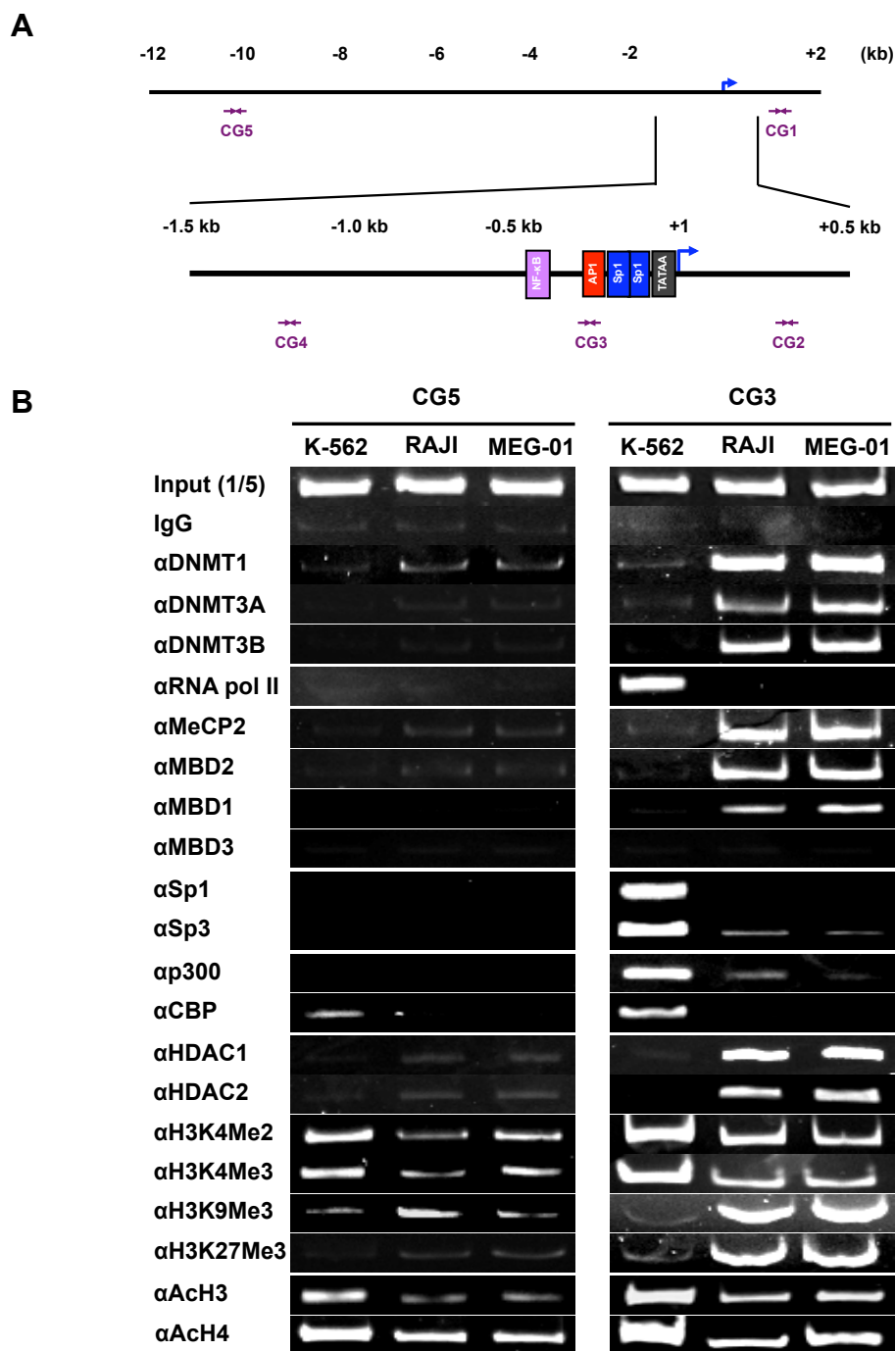


Figure 32: Characterization of GSTP1 chromatin structure in K-562, RAJI and MEG-01 leukemia cell lines by X-ChIP analysis.

(A) Schematic representation of the 5'-upstream region of GSTP1 gene with the positions of PCR primers (CG1 to CG5) used to map the promoter in ChIP analysis. (B) Chromatin from K-562, RAJI and MEG-01 cell lines was immunoprecipitated with specific antibodies. Associated DNA was amplified using CG3 and CG5 primer pairs and PCR products were separated on a gel stained with ethidium bromide. Pictures are representative of 3 independent experiments. Me: methylation, Ac: acetylation, CBP: cAMP-response element binding protein (CREB) binding protein, DNMT: DNA methyltransferase, GSTP1: glutathione S-transferase P1, H4: Histone 4, HDAC: histone deacetylase, MBD: methyl binding protein, MeCP2: methyl CpG binding protein 2, p300: histone acetyltransferase, SP: specificity protein.

As shown in Figure 32, integral components of the transcriptional machinery (RNA pol II, SP1 and SP3) were associated with the hypomethylated and transcriptionally active GSTP1 promoter region in K-562 cells. Moreover, GSTP1 promoter in K-562 cells was highly enriched for di- and trimethylation of lysine K4 on histone H3, for acetylation of histone H3 and H4 as well as for the related HAT proteins (*i.e.* p300 and CBP). In addition, markers for transcriptionally silenced heterochromatin such as HDACs or MBDs were absent in K-562 cells. Concerning RAJI and MEG-01 cells, while GSTP1 silencing was associated to hypermethylation, GSTP1 basal promoter was enriched for repressive histone modifications such as trimethylation of H3K9 and H3K27. In addition, enrichment of acetylated histones H3 and H4 as well as the associated HATs was reduced at this position in RAJI and MEG-01 cell lines. Furthermore, GSTP1 promoter of RAJI and MEG-01 cells was enriched for DNA methylation- and heterochromatin-associated proteins (*e.g.* DNMTs, MBDs and HDACs), respectively (Figure 32). Finally, we used primers targeting a region 10kb upstream of the basal GSTP1 promoter as a negative control (CG5). As expected, this region was not enriched for proteins related to active transcription (Figure 32).

5.1.6. Analysis of the DAC-induced acquisition of a GSTP1 transcriptional permissive state in GSTP1 non-expressing cells

In order to evaluate DAC-induced molecular reprogramming of the GSTP1 promoter complex associated to demethylation and transcriptional activation of GSTP1 gene, X-ChIP assay was performed. Using primers covering the GSTP1 promoter region (CG2 to CG4), the first coding region (CG1) in the gene body and a primer pair (CG5), specific for a transcriptionally silenced region 10kb upstream of the GSTP1 TSS, enrichment of DNA fragments was quantified by real-time PCR (Figure 32-A).

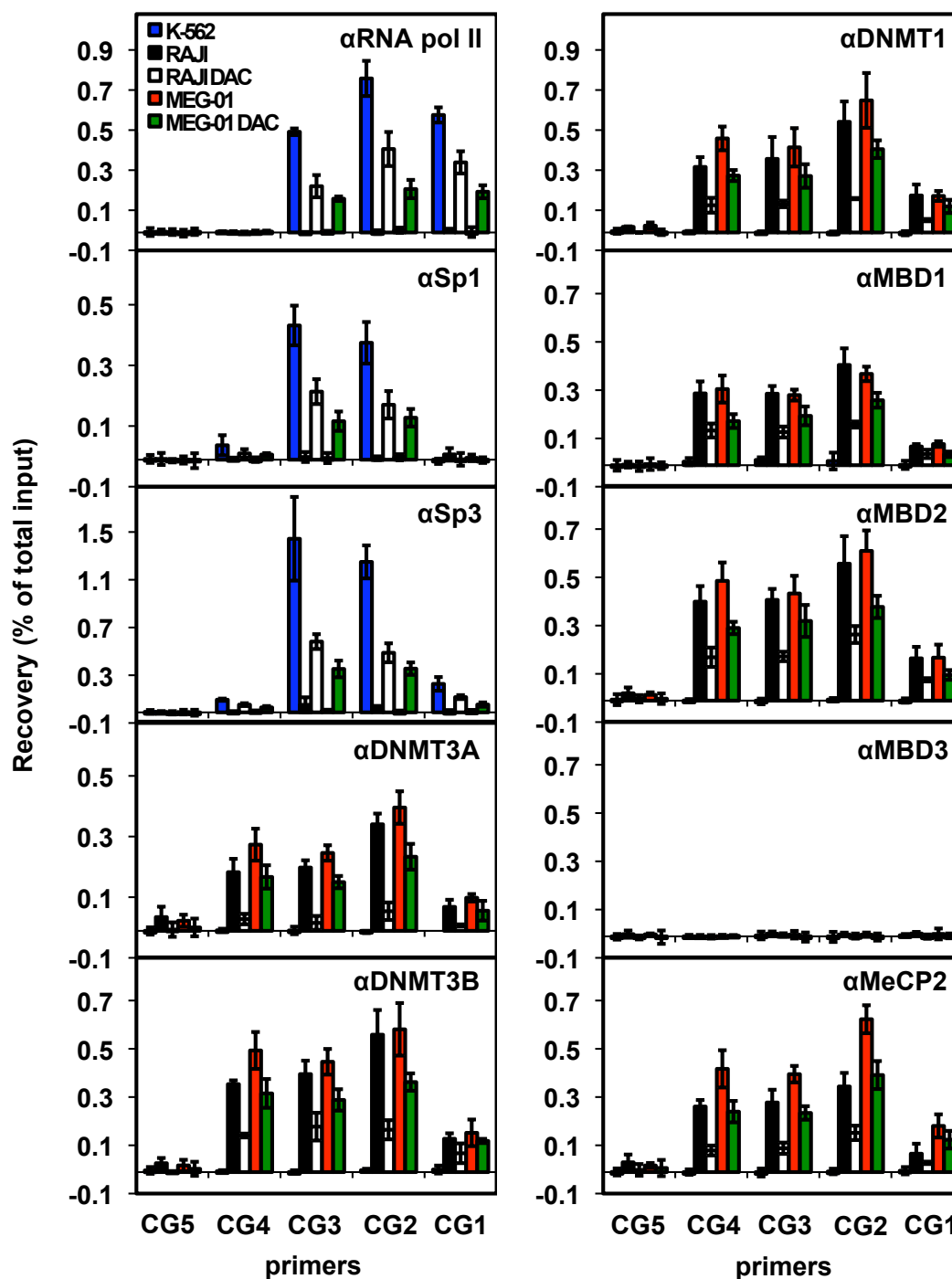
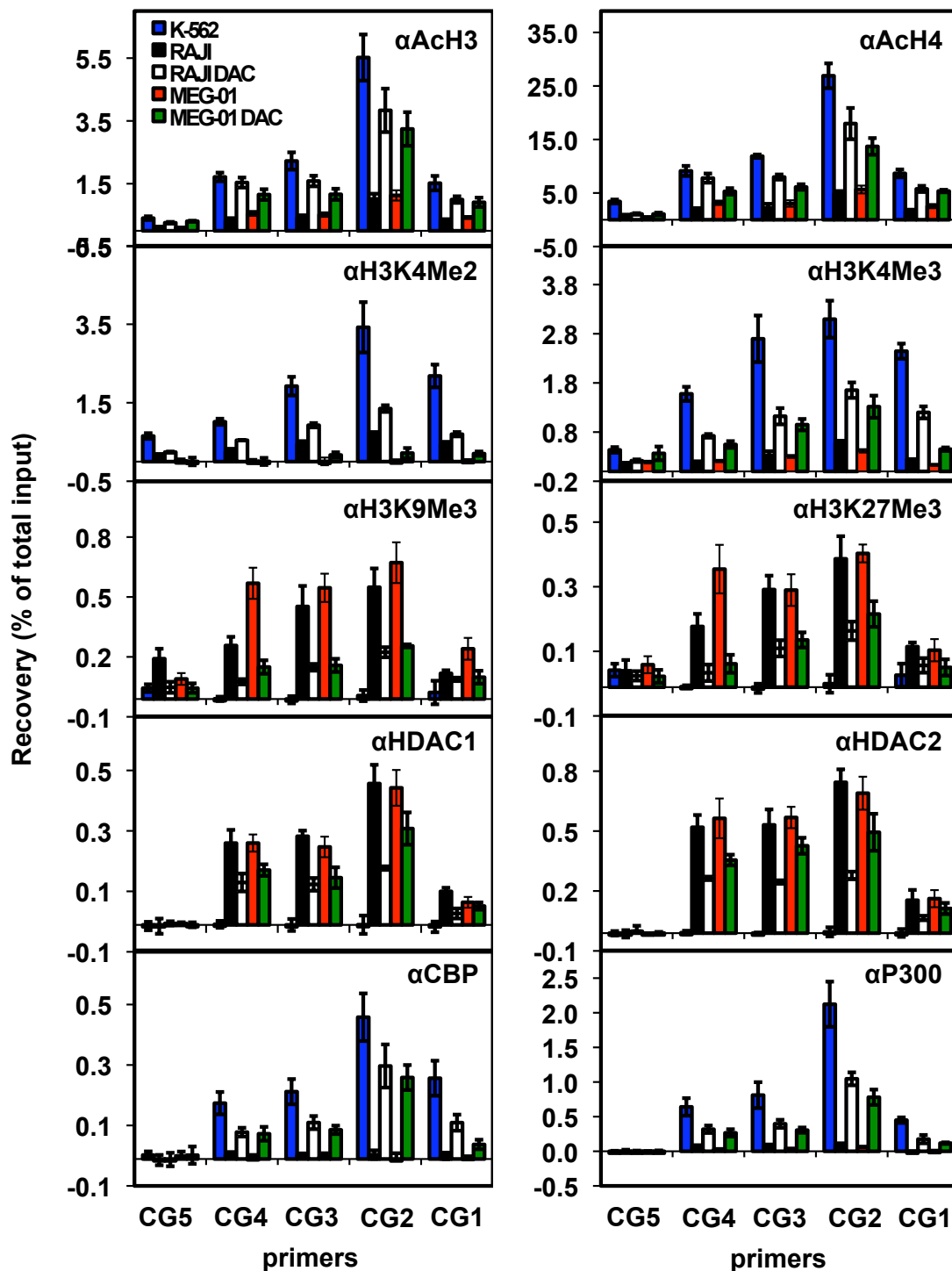


Figure 33: Analysis of the evolution of GSTP1 chromatin structure after DAC treatment of K-562, RAJI and MEG-01 leukemia cell lines by X-ChIP assay.

Chromatin from untreated K-562, RAJI and MEG-01 cell lines as well as in RAJI and MEG-01 cells treated with 2 μ M DAC for 3 days was immunoprecipitated with specific antibodies. The enrichment was measured by real-time PCR and results expressed as recovery (% of total input) = $((Ct_{IP} - Ct_{IgG})/Ct_{input})$. Data are the mean \pm SD of 3 independent experiments. CBP: cAMP-response element binding protein (CREB) binding protein, DNMT: DNA methyltransferase, GSTP1: glutathione S-transferase P1, H4: Histone 4, HDAC: histone deacetylase, MBD: methyl binding protein, MeCP2: methyl CpG binding protein 2, p300: histone acetyltransferase, SP: specificity protein.



(Figure 33 continued)

Results demonstrated that DAC treatment leads to the release of both DNMT and MDB proteins from the analyzed region on the GSTP1 promoter. Furthermore, DAC exposure led to the enrichment of acetylated histone H4 and H3, the recruitment of HATs and the release of HDAC1 and 2 from GSTP1 promoter in RAJI and MEG-01 cells. In addition, in the same cells,

DAC reduced the occupancy of lysine K9 and K27 trimethylation on histone H3 and enhanced the presence of lysine K4 di- and tri-methylation on histone H3 in GSTP1 promoter (Figure 33-B). Moreover, DAC treatment increased the association of the transcription factors SP1 and SP3 as well as the RNA polymerase II on the GSTP1 promoter in non-expressing cells (Figure 33-B). In summary, these results showed that DAC treatment induced important changes in histone modification marks and protein recruitment to the GSTP1 promoter in RAJI and MEG-01 cells, which correspond to a shift from a repressive to a more permissive chromatin state, close to the one observed in K-562 cell line.

Lack of protein binding on DNA as well as cell line-dependent variations in protein expression could be responsible for low or absence of chromatin enrichment in X-ChIP analysis. Therefore, we assessed the constitutive expression of proteins analyzed by ChIP in K-562, RAJI and MEG-01 cell lines. Western Blot showed that lack of protein recruitment was not due to lack or high variance in protein expression (Figure 34).

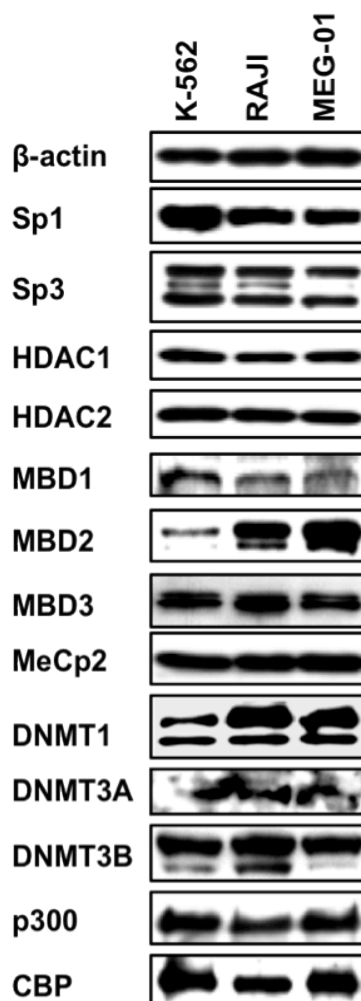


Figure 34: Immunoblot detection of proteins analyzed in X-ChIP experiments.

Total or nuclear proteins were extracted from K-562, RAJI and MEG-01 cell lines and analyzed by Western Blot with the indicated antibodies. Pictures are representative for three independent experiments. CBP: cAMP-response element binding protein (CREB) binding protein, DNMT: DNA methyltransferase, GSTP1: glutathione S-transferase P1, H4: Histone 4, HDAC: histone deacetylase, MBD: methyl binding protein, MeCP2: methyl CpG binding protein 2, p300: histone acetyltransferase, SP: specificity protein.

5.1.7. GSTP1 promoter methylation status in leukemia patient samples

For a transition from research to clinical application and the potential use of the epigenetic disruption of GSTP1 regulation and expression as a biomarker for hematological malignancies, patient samples have to be included into the study in order to evaluate the role of methylation-associated

GSTP1 silencing in development, progression or subsistence of malignant homeopathies.

Leukemia and lymphoma patient biopsies as well as healthy PBMCs and CD34+ blood stem cells were used to extract genomic DNA. After bisulfite conversion, the methylation profile of the GSTP1 promoter region was determined by MSP analysis and summarized in Table 48.

Table 48: Analysis of the GSTP1 methylation status in leukemia and lymphoma patient samples.

Genomic DNA from 81 patients and 9 healthy donor samples was bisulfite converted and the GSTP1 methylation pattern analyzed by MSP. The table summarizes the GSTP1 methylation status.

GSTP1 Methylation status	CLL	CML	ALL	AML	MDS	DLBCL	MCL	FL	BL	CD34+	PBMC
Unmethylated	16	4	6	17	2	9	9	10	4	3	6
Methylated	0	0	0	0	0	2	2	0	0	0	0
∑ of samples	16	4	6	17	2	11	11	10	4	3	6

ALL: acute lymphoblastic leukemia, AML: acute myeloid leukemia, BL: Burkitt's lymphoma, CD34+: hematological stem cells, CLL: chronic lymphocytic leukemia, CML: chronic myeloid leukemia, DLBCL: diffuse large B-cell lymphoma, FL: follicular lymphoma, MCL: mantle cell lymphoma, MDS: myelodysplastic syndrome, PBMC: peripheral blood mononuclear cell.

Almost every analyzed leukemia and lymphoma patient samples as well as PBMC samples from supposed healthy donors presented an unmethylated GSTP1 promoter (Table 48). However, out of 81 patients samples analyzed, a partially methylated GSTP1 promoter was identified in two mantle cell lymphoma (18%) and two diffuse large B-cell lymphoma (18%) samples (Table 48). Tumor samples were prepared without microdissection, possibly leading to the coexistence of methylated and unmethylated alleles.

5.1.8. Involvement of micro RNAs in regulation of GSTP1 expression

As mentioned in the introduction, miRNA is an additional epigenetic mechanism dysregulated in cancer. Moreover, we showed previously that certain leukemia cell lines (e.g. HEL and MOLT-3) moderately express GSTP1 in contrast to the highly expressing K-562 and JURKAT cell lines. It is reasonable to assume that overexpression of a GSTP1 targeting miRNA could silence GSTP1 gene expression, reducing cell detoxification and promoting genomic damages. In contrast, silencing of a GSTP1 repressing miRNA would lead to GSTP1 upregulation associated with enhanced detoxification potential and therefore possibly confers chemoresistance to cancer cells. Accordingly, the analysis of miRNA signatures in leukemia and normal cells could possibly contribute to the knowledge of the epigenetic regulation of GSTP1 expression and offer new promising approaches to control its expression.

To the best of our knowledge, no published study has investigated the potential of miRNA-mediated post-transcriptional regulation of GSTP1 in leukemia cells or other cancer types. Thus, we investigated the potential of GSTP1 3'UTR for miRNA regulation as well as the possibility for GSTP1-miRNA interactions using online prediction tools. Results of the screening of miRNA target databases are summarized in Figure 35.

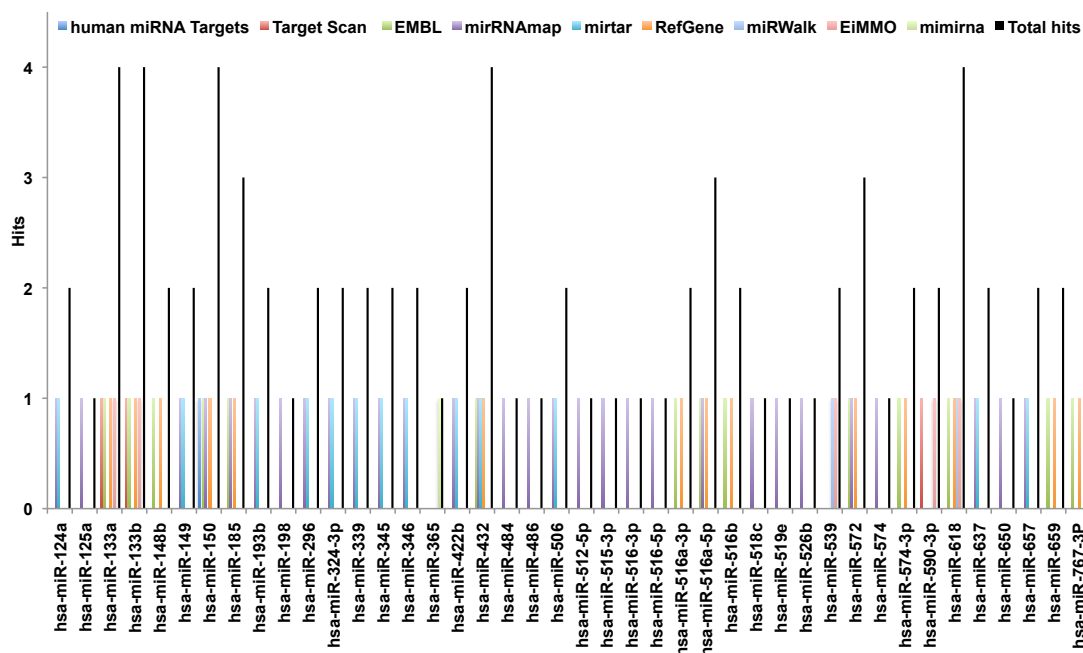


Figure 35: Prediction of miRNA-GSTP1 mRNA interaction.

Computational target prediction tools were used to screen miRNA databases and to assess miRNAs targeting GSTP1 mRNA. A positive hit in a database is represented by a colored bar and the cumulative number of prediction hits is represented by a black bar. *hsa*: *homo sapiens*.

Using 9 different online miRNA target prediction tools, up to 42 miRNAs were predicted as potentially involved in the post-transcriptional regulation of GSTP1 expression. Considering that almost every software use a different prediction algorithm or method, prediction results were not homogenous, *i.e.* *hsa-miR-150* was predicted by 4 prediction tools and *hsa-miR-365* by only one (Figure 35).

To detect a potential negative relationship between the miRNA and GSTP1 expression profile, total RNA of cell lines with high (K-562, JURKAT), moderate (HEL, MOLT-3) and no (RAJI, MEG-01) GSTP1 expression was extracted. PBMC cells were also included in the analysis. After conversion by reverse transcription, the expression profile of miRNAs that were predicted at least twice by bioinformatical tools was analyzed by real-time PCR and a heat map represented the results (Figure 36).

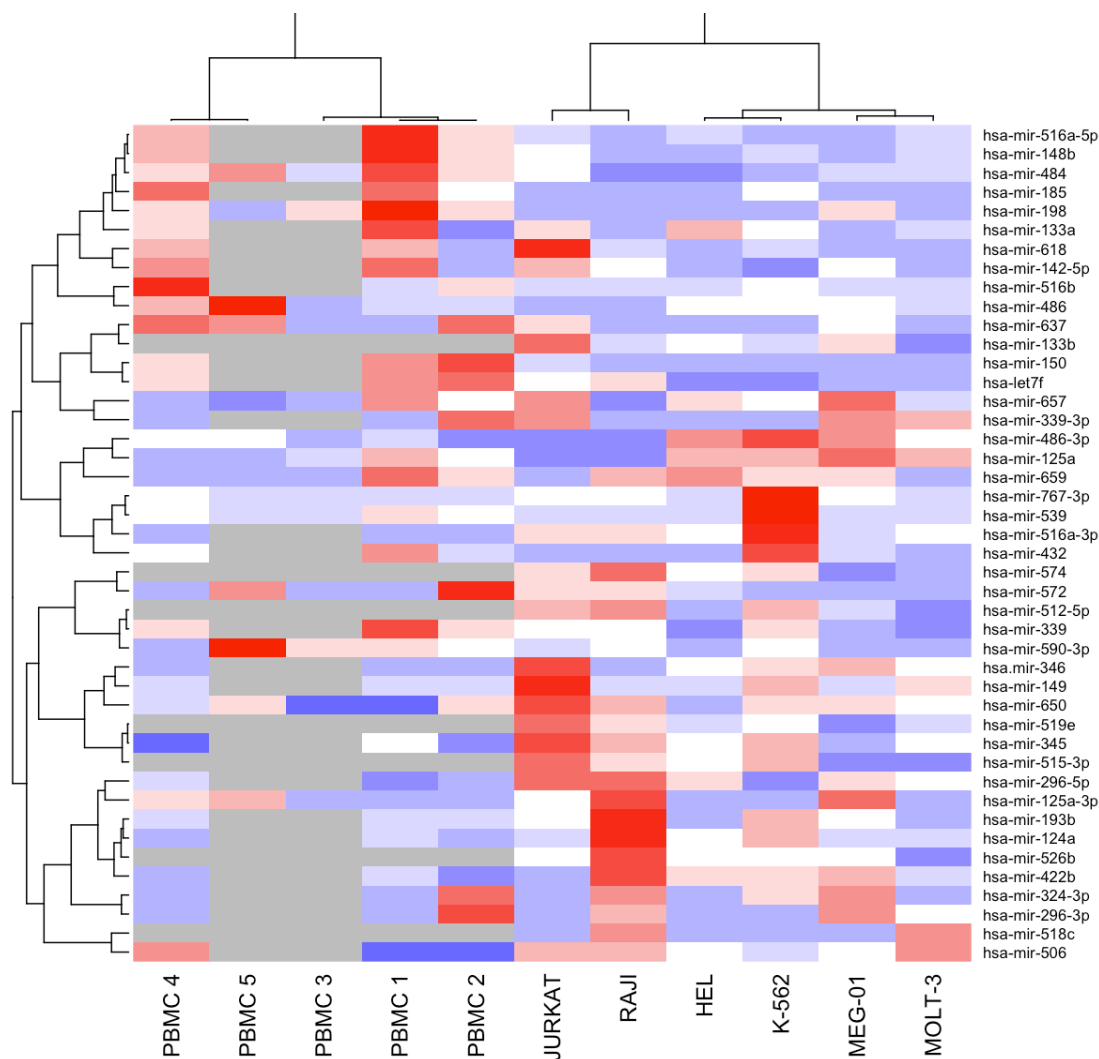


Figure 36: Expression pattern of potential GSTP1 silencing miRNAs in leukemia cell lines with high, moderate and low GSTP1 expression levels.

Total RNA from leukemia and lymphoma cell lines and from healthy donors cells was reverse transcribed and analyzed by real-time PCR with specific primers for various miRNAs. The small nuclear RNA RNU1A was analyzed as a quantity control in each reaction. The heat map summarizes the expression levels of predicted GSTP1 targeting miRNAs in various leukemia and lymphoma cell lines. For a better illustration, expression levels were normalized for each miRNA, going from blue (low expression) to red (high expression). White bars indicate moderate expression level and gray bars represent missing values. Correlations were used for data clustering. Data are the mean \pm SD of 3 independent experiments. hsa-miR: *homo sapiens* micro RNA.

The heat map shows a very heterogeneous expression pattern of the various miRNAs analyzed in the different cell lines (Figure 36). Correlation analysis between the analyzed miRNAs led to the definition of two main clusters, separating miRNAs upregulated in healthy samples from miRNAs upregulated in blood cancer cell lines. Several miRNAs were highly expressed

in samples derived from healthy donors (e.g. miR-516a-5p, -148b, -484 and -185), whereas they were repressed in blood cancer cell lines and *vice versa*. Moreover, subclustering revealed high variations in miRNA expression pattern between the various analyzed cell lines. For example miR-346, -149, -650, -519e, -345 and -515-3p are highly expressed in JURKAT cell line in contrast to RAJI, HEL, K-562, MEG-01 and MOLT-3 (Figure 36).

5.2. DNA hypermethylation as a key player in PTGS2 expression silencing in hematological malignancies

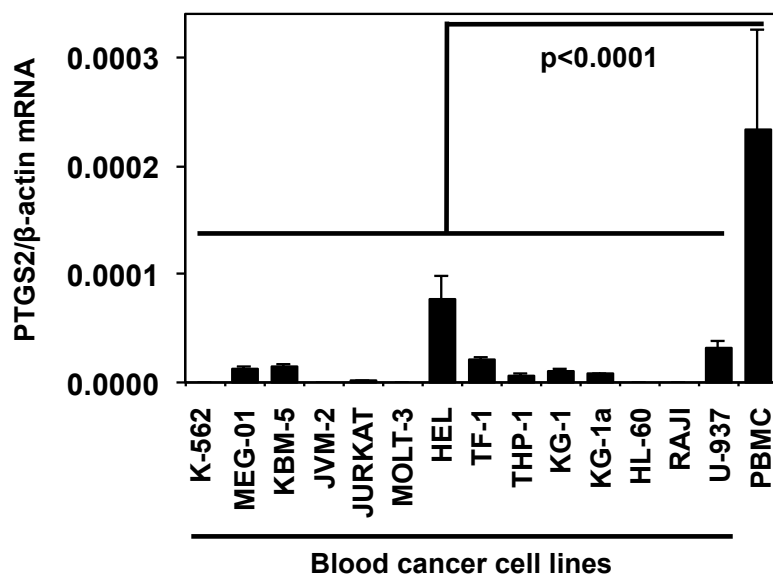
As mentioned in the introduction, it is widely recognized that various cancer cells are associated with PTGS2 overexpression, which contributes thereby to the cancer phenotype by activating prosurvival and cell proliferation genes. In contrast, DNA hypermethylation-mediated silencing of PTGS2 was already observed for esophageal, prostate or epithelial cancer.

In the second thesis part, the possibility of DNA methylation on regulation of PTGS2 expression in hematological malignancies was evaluated. The implication of promoter hypermethylation in the regulation of PTGS2 expression was, to our knowledge, never reported for cell lines and patient samples, derived from or with hematological malignancies, respectively.

5.2.1. PTGS2 expression in leukemia/lymphoma cell lines and healthy blood cells

First, the constitutive PTGS2 gene expression was assessed in various blood cancer cell lines and compared to PBMCs from healthy donors. Total mRNA from various leukemia and lymphoma cell lines was reverse transcribed and the cDNA amount of PTGS2 and β -actin quantified by a real-time PCR assay (Figure 37).

A



B

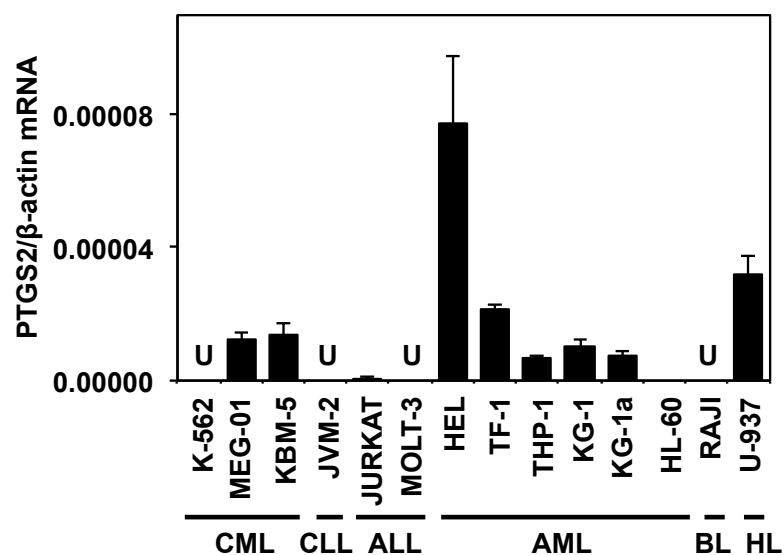


Figure 37: PTGS2 expression in various leukemia/lymphoma cell lines and in healthy donor blood cells.

Total RNA was extracted from various blood cancer cell lines and PBMCs, reverse transcribed into cDNA and analyzed by real-time PCR with primers specific for PTGS2. β -actin was also analyzed as a control of cDNA quantity in each reaction. Results represent the ratio PTGS2/ β -actin mRNA expression level in PBMCs (A) and leukemia and lymphoma cell lines (A, B). Data are the means \pm SD of 3 independent experiments. ALL: acute lymphoid leukemia, AML: acute myeloid leukemia, BL: Burkitt's lymphoma, CML: chronic myeloid leukemia, CLL: chronic lymphoid leukemia, HL: histiocytic lymphoma, U: Ct value undetermined after 45 cycles of amplification.

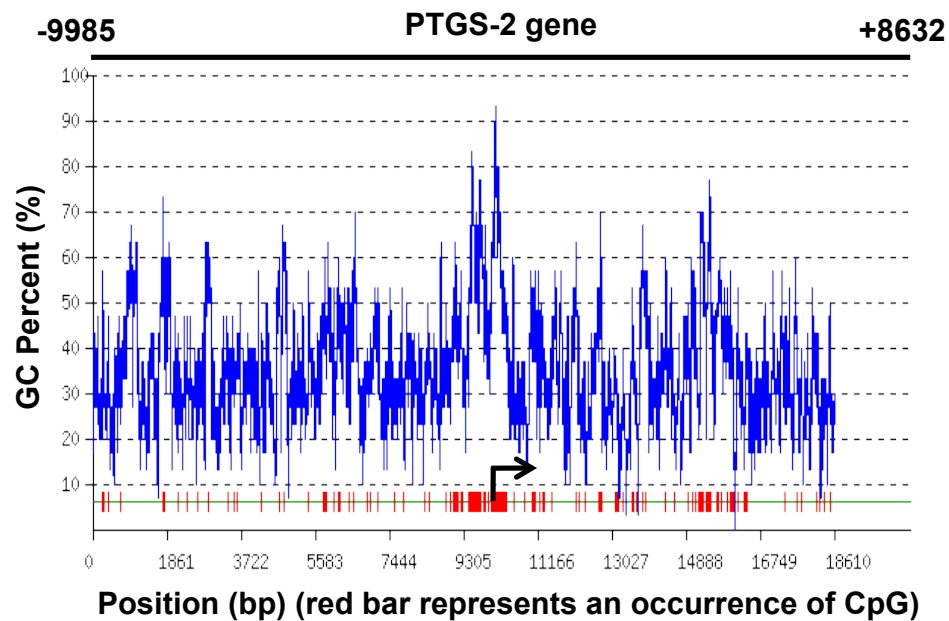
PTGS2 expression is significantly higher in PBMCs, compared to the analyzed leukemia cell lines (Figure 37-A). Among the 14 leukemia- or lymphoma-derived cell lines, the highest expression of PTGS2 mRNA was

observed in the HEL cell line. MEG-01, KBM-5, TF-1, THP-1, KG-1, KG-1a and U-937 cell lines express relatively moderate level of PTGS2 mRNA compared to normal PBMCs. In addition, K-562, JVM-2, JURKAT, MOLT-3, HL-60 and RAJI cell lines showed very low or undetectable transcriptional activity for the PTGS2 gene (Figure 37-B).

5.2.2. CpG density analysis of PTGS2 promoter and gene body

For methylation-associated silencing, a CGi is required in the promoter or the first exon-intron region of PTGS2. In order to determine the CpG dinucleotide density, PTGS2 gene body (≈ 10000 bp) as well as a promoter region upstream of the transcription start site (≈ 9000 bp) were bioinformatically analyzed with the EMBOSS CpGPlot/CpGReport online tool (Figure 38).

A



B

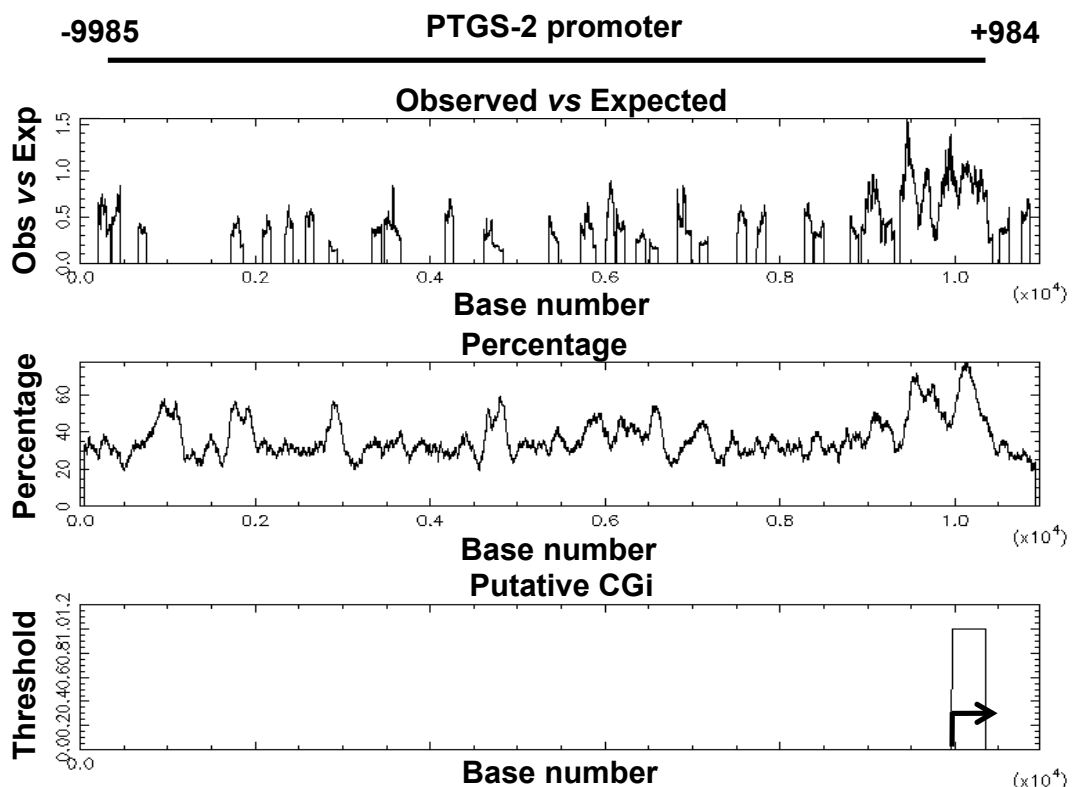


Figure 38: CpG island prediction for PTGS2 promoter region.

(A) *In silico* analysis of the GC content and the CpG dinucleotide positions (red bars) in the PTGS2 promoter and coding region (-9985 - +8632). (B) *In silico* CG analysis of the PTGS2 promoter region (-9985 - + 984) with the web based tool CpGPlot. The observed vs. expected ratio, the CG percentage and the putative island are plotted against the base position within PTGS2 sequence. \blacktriangleright : transcription start site.

In silico assessment of the CG dinucleotide distribution in PTGS2 gene uncovered a large accumulation of CpG in the promoter region (relative position: 9000 to 11000bp) as well as in the coding region (relative position: 14000 to 16000bp) (Figure 38-A). Close examination of PTGS2 promoter revealed a 394-bp long putative CGI with a CpG ratio of over 0.6 and a percentage of CG higher than 50%, satisfying the criteria of Gardiner-Garden for a CGI (Gardiner-Garden and Frommer 1987). The CGI starts just after the PTGS2 TSS and includes 34 CpG dinucleotides (Figure 38-B).

5.2.3. Methylation status of PTGS2 promoter in leukemia and lymphoma cell lines

To determine if lack of PTGS2 expression in certain leukemia and lymphoma cell lines was associated with PTGS2 promoter hypermethylation, DNA methylation profile of PTGS2 promoter was analyzed by MSP (Figure 39).

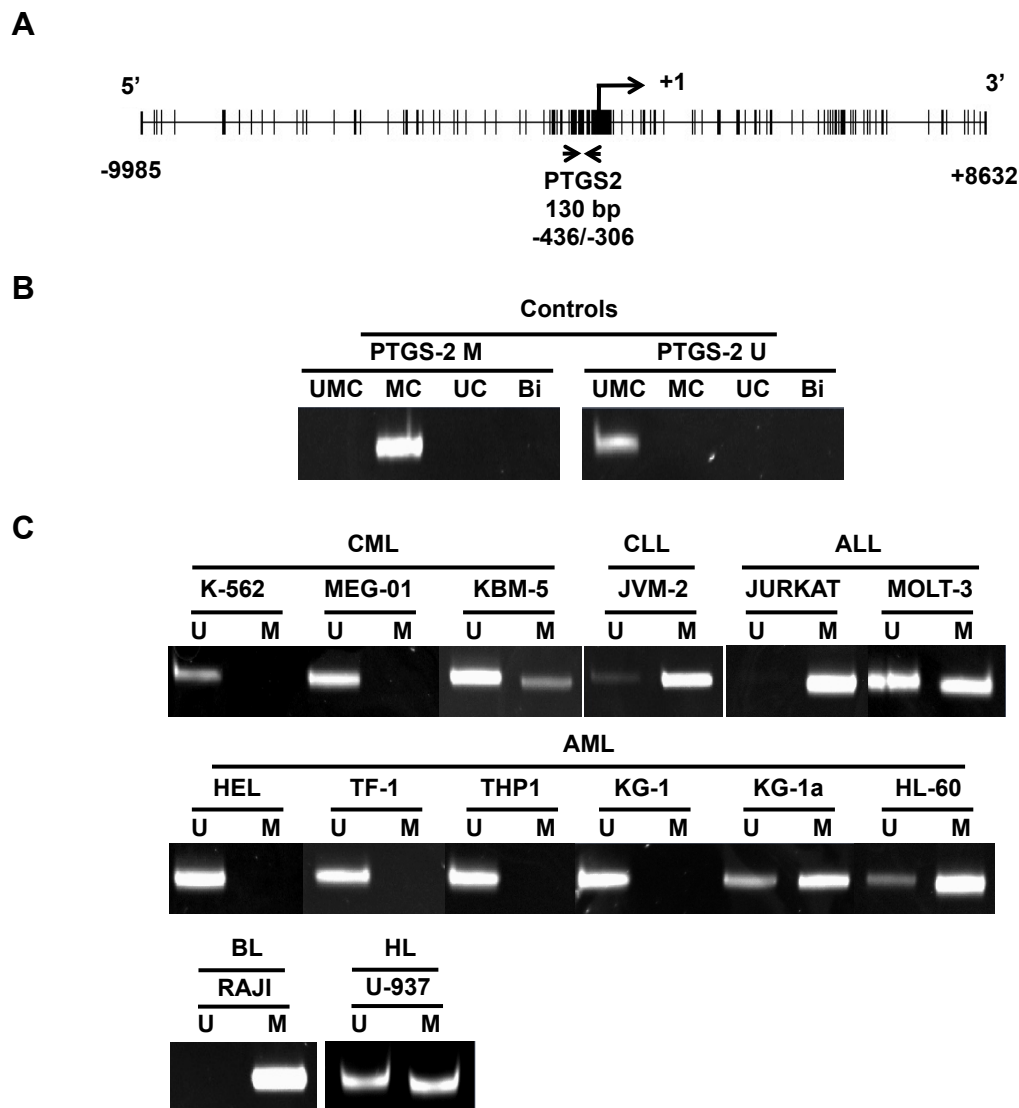


Figure 39: Analysis of PTGS2 promoter methylation in leukemia and lymphoma cell lines.

(A) Physical map generated with the Methylprimer software shows the distribution of CpG dinucleotides (vertical black bars) and MSP primer pair positions relative to the transcription start site (Γ) on PTGS2 promoter. (B) To check primer specificity, MSP assays with the following control samples as templates were carried out: complete bisulfite conversion procedure without genomic DNA (Bi), unmethylated converted DNA (UMC), methylated converted DNA (MC), unconverted unmethylated DNA (UC). (C) Genomic DNA was extracted from various leukemia/lymphoma cell lines, bisulfite converted and used as templates for MSP with primers specific for the unmethylated (U) and methylated (M) state of PTGS2 promoter. MSP amplicons were separated on a 12% PAA gel and stained with ethidium bromide. Pictures are representative for 3 independent experiments. ALL: acute lymphoid leukemia, AML: acute myeloid leukemia, BL: Burkitt's lymphoma, CML: chronic myeloid leukemia, CLL: chronic lymphoid leukemia.

MSP primers were designed to analyze the methylation profile of CG dinucleotides pertaining to a region 5' upstream of the transcription start site (-436bp/-306bp) (Figure 39-A). Control reactions showed methylation specificity

of the MSP primers (Figure 39-B). Hypomethylation of the PTGS2 promoter region was detected for the CML-derived K-562 and MEG-01 cell lines as well as the AML-derived HEL, TF-1, THP-1 and KG-1 cell lines. PTGS2 promoter was hemi-methylated in JVM-2, MOLT-3, KBM-5, KG-1a, U-937 and HL-60 cell lines, and hypermethylated in RAJI and JURKAT cell lines (Figure 39-C).

5.2.4. Effect of DAC treatment on PTGS2 methylation and expression

To determine the effect of the demethylating agent DAC on PTGS2 promoter methylation status, cell lines presenting various hypermethylated and partially methylated PTGS2 promoters were treated with 2 μ M DAC. Genomic DNA was extracted, bisulfite converted and the methylation pattern of PTGS2 analyzed by MSP (Figure 40).

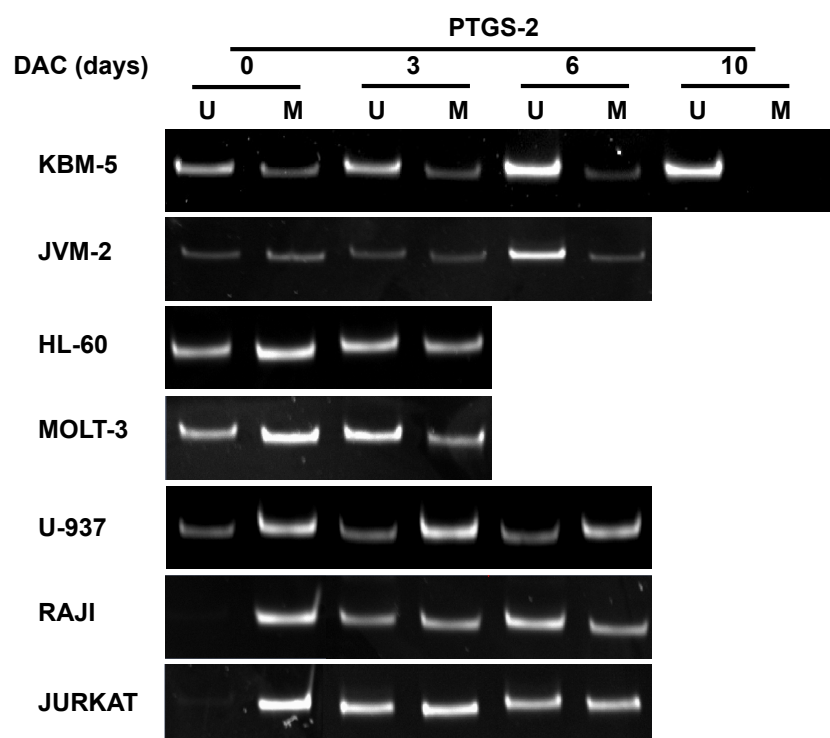


Figure 40: Kinetic analysis of the DAC-mediated demethylation of PTGS2 promoter in leukemia and lymphoma cell lines.

Genomic DNA from various DAC-treated leukemia and lymphoma cell lines was bisulfite converted and PTGS2 promoter methylation status analyzed by MSP with primers specific for the unmethylated (U) and methylated (M) state. MSP amplicons were separated on a 12% PAA gel and stained with ethidium bromide. Images are representative of three independent experiments. DAC: 5-aza-2'-deoxycytidine.

DAC treatment of KBM-5 cell line led to a time-dependent and complete demethylation of PTGS2 promoter region. Similarly, partially methylated JVM-2, HL-60, MOLT-3 and U-937 as well as fully methylated RAJI and JURKAT cell lines get demethylated by DAC exposure but not completely (Figure 40).

To evaluate the consequences of DAC-induced PTGS2 promoter demethylation for the transcriptional activity, total mRNA from DAC-treated KG-1a, JVM-2, RAJI, JURKAT, HEL, MOLT-3 and KBM-5 cells was extracted. After reverse transcription, the cDNA amount of PTGS2 and β -actin was quantified by a real-time PCR assay. In addition, the effect of DAC treatment on the hypomethylated but silenced PTGS2 expression in K-562 was analyzed (Figure 41).

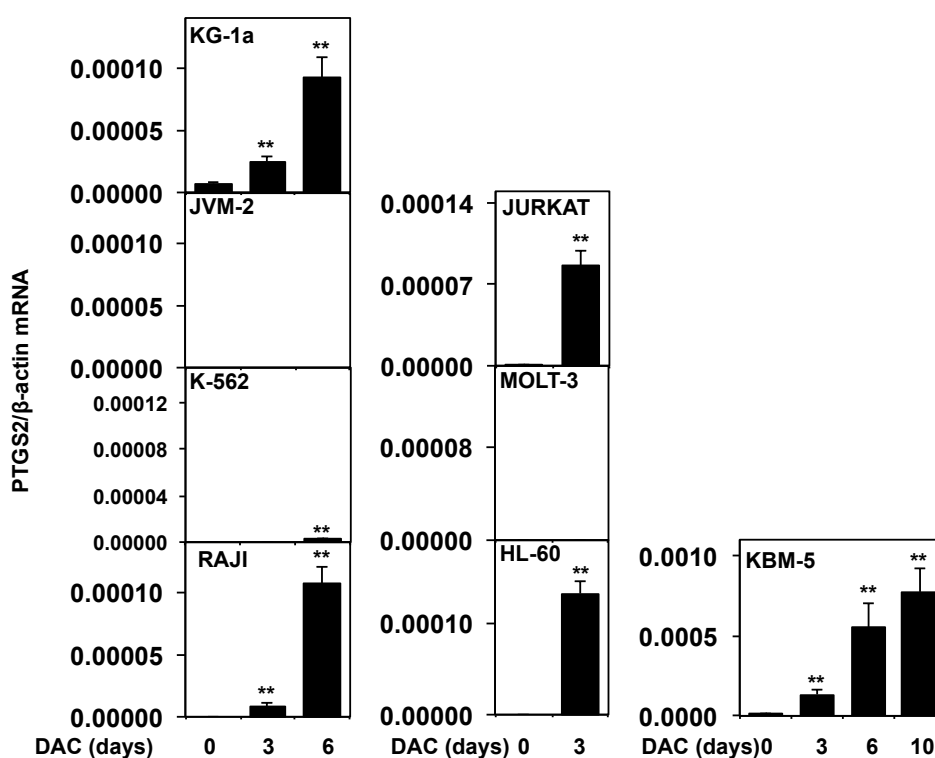


Figure 41: Kinetic analysis of PTGS2 expression after DAC treatment.

Cell lines, derived from various hematological malignancies, were treated with $2\mu\text{M}$ DAC for the indicated times. Total RNA was extracted and $1\mu\text{g}$ was reverse transcribed into cDNA, and then analyzed by real-time PCR with primers specific for PTGS2. β -actin was also analyzed as a control of cDNA quantity in each reaction. Results represent the ratio PTGS2/ β -actin mRNA expression level and are plotted for the various human leukemia cell lines and the time interval of DAC-treatment. Data are the means \pm SD of 3 independent experiments.

Real-time PCR results demonstrated that DAC treatment reversed in a time-dependent manner DNA methylation-mediated silencing of PTGS2 expression and induced transcriptional activity in most analyzed cell lines. Independently of the DAC exposure time, partially methylated JVM-2 and MOLT-3 cell lines as well as the unmethylated K-562 cell line staid repressed for PTGS2 expression.

5.2.5. Methylation analysis of PTGS2 promoter in leukemia and lymphoma patient samples

For a possible later clinical application of the preliminary results obtained in this work, the study was enlarged to blood and bone marrow samples from patients with hematological malignancies. Samples from leukemia patients (ALL, AML, CLL and CML), and lymphoma biopsies (DLBCL, FL, MCL, BL and MDS) as well as PBMCs from healthy donors were used for DNA extraction and bisulfite conversion. The methylation profile of PTGS2 was detected by MSP (Figure 42).

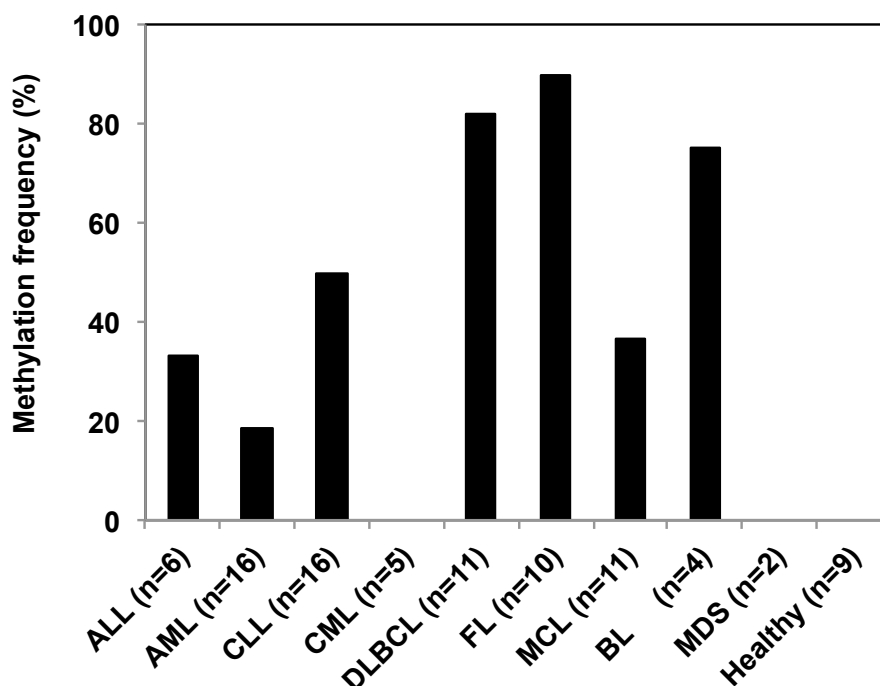


Figure 42: Frequency of PTGS2 promoter methylation in samples of patients with a hematological malignancy.

Genomic DNAs from 81 patient samples and 9 healthy donor samples were extracted, bisulfite converted and PTGS2 promoter methylation patterns analyzed by MSP. Frequency (%) of PTGS2 promoter methylation was plotted against the type of hematological malignancy. ALL: acute lymphoblastic leukemia, AML: acute myeloid leukemia, BL: Burkitt's lymphoma CLL: chronic lymphocytic leukemia, CML: chronic myeloid leukemia, DLBCL: diffuse large B-cell lymphoma, FL: follicular lymphoma, MCL: mantle cell lymphoma, MDS: myelodysplastic syndrome.

Except CML and MDS patients samples that were completely unmethylated, 77% of the analyzed leukemia and lymphoma patient samples showed a certain percentage of PTGS2 methylation (Figure 42). The highest methylation frequency was detected in diffuse large B-cell, follicular and Burkitt's lymphoma samples. Regarding the leukemia samples, most PTGS2 promoter methylation was found in CLL samples. Moreover, PTGS2 hypermethylation was not detected in healthy control PBMCs (Figure 42).

5.2.6. Correlation between PTGS2 methylation and expression in samples from patients with hematological malignancies

In complement to the PTGS2 methylation profiling, the PTGS2 expression level in leukemia and lymphoma patient samples was determined.

Total RNA was extracted from leukemia/lymphoma biopsy samples and healthy donor PBMCs as well as CD34+ cells from cord blood. Messenger RNA was reverse transcribed and the cDNA amount of PTGS2 and β -actin quantified by real-time PCR assay (Figure 43).

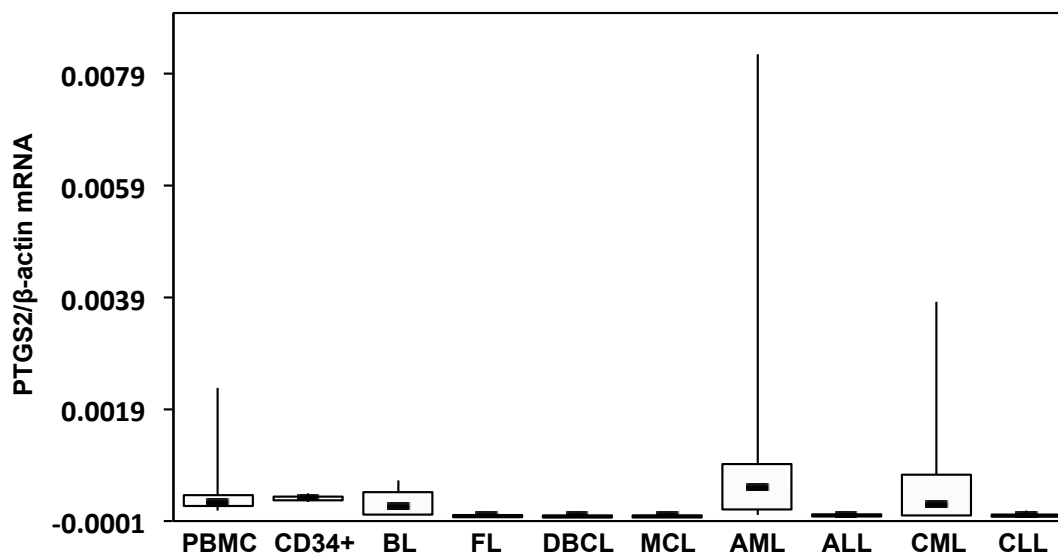


Figure 43: Distribution of PTGS2 mRNA expression levels in blood cells from healthy donors and patients with hematological malignancies.

Total RNAs from lymphoma/leukemia biopsies and blood cells from healthy control groups (PBMC, CD34+) were extracted and cDNA analyzed by real-time PCR with primers specific for PTGS2. β -actin was analyzed as a control of cDNA quantity in each reaction. Results represent the distribution of the ratio PTGS2/ β -actin mRNA expression level and are plotted for the healthy control cells as well as the various blood cancer types. The line indicates the median, the box is the interquartile range and the outer whiskers represent the maximum and minimum range including extreme outliers. Data are the means \pm SD of 3 independent experiments. ALL: acute lymphoblastic leukemia, AML: acute myeloid leukemia, BL: Burkitt's lymphoma CLL: chronic lymphocytic leukemia, CML: chronic myeloid leukemia, DLBCL: diffuse large B-cell lymphoma, FL: follicular lymphoma, MCL: mantle cell lymphoma, PBMC: peripheral blood mononuclear cell.

Distribution and median PTGS2 expression levels were similar in PBMCs and CD34+ cells from supposed healthy donors. Moreover, median PTGS2 expression in Burkitt's lymphoma, AML and CML samples was comparable to healthy controls. Noteworthy, PTGS2 transcriptional activity was highly variable in Burkitt's lymphoma, AML and CML samples. In contrast, reduced or silenced PTGS2 expression was detected in lymphoid lineage derived leukemia and lymphoma samples, compared to the healthy controls.

Simultaneous DNA and RNA preparations from the same patient samples (n=52) and subsequent PTGS2 methylation and expression analysis allowed assessing a possible correlation between the methylation status and the expression level of PTGS2. For this purpose, patient samples were classified by their PTGS2 promoter methylation status and plotted for their PTGS2 expression (Figure 44).

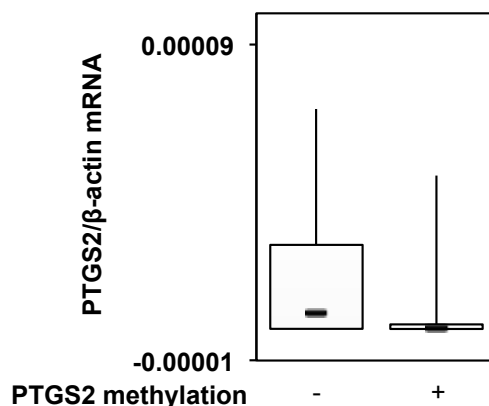


Figure 44: Analysis of PTGS2 mRNA expression in relation to the promoter methylation state.

Box whisker plots show the variations of PTGS2 expression depending on the methylation status of the PTGS2 promoter region in leukemia and lymphoma patient samples. Box denotes interquartile range, line within the box denotes the median, and whiskers denote the maximum and the minimum range. Outliers were excluded from the analysis (n=52).

Patient samples with hypomethylated PTGS2 promoter region had highly variable PTGS2 expression levels. However, samples with hypermethylated PTGS2 promoter configuration presented reduced PTGS2 expression.

5.3. DNA methylation fingerprint of blood cancer cells

Epigenetic alterations such as DNA hypermethylation (e.g. GSTP1 and PTGS2), lead to aberrant gene expression and are implicated in cancer initiation and progression. The epigenetic hype of the past decade allowed to compile a long list of epimutation hotspots, including genes involved in tumor suppression, DNA repair, cell metabolism, apoptosis or hormonal receptor.

With the objective to establish a map of epigenetic signatures of hematological malignancies, the third part of this thesis mainly dealt with the DNA methylation analysis of genes. Methylation status of some of the selected genes were already determined independently of each other, whereas the methylation states of other genes were never analyzed in blood cancer cell lines. However, in order to improve sensitivity and specificity of early cancer detection, it is an existential necessity to analyze a whole range of epigenetic marks. Moreover, the evaluation of distinctive aberrant methylation pattern can deliver potentially usable clinical insights concerning cancer progression (e.g. metastatic potential, chemosensitivity) and treatment.

5.3.1. Methylomic profiling of hematological malignancies

In order to establish a map of DNA methylation aberrations in various leukemia and lymphoma cell lines, the methylation of genes already established as cancer biomarkers for other cancer types was analyzed by MSP and represented by a heat map. Moreover, methylation frequency of each blood cancer cell line was calculated based on the gene-specific MSP results (except LINE1) (Figure 45).

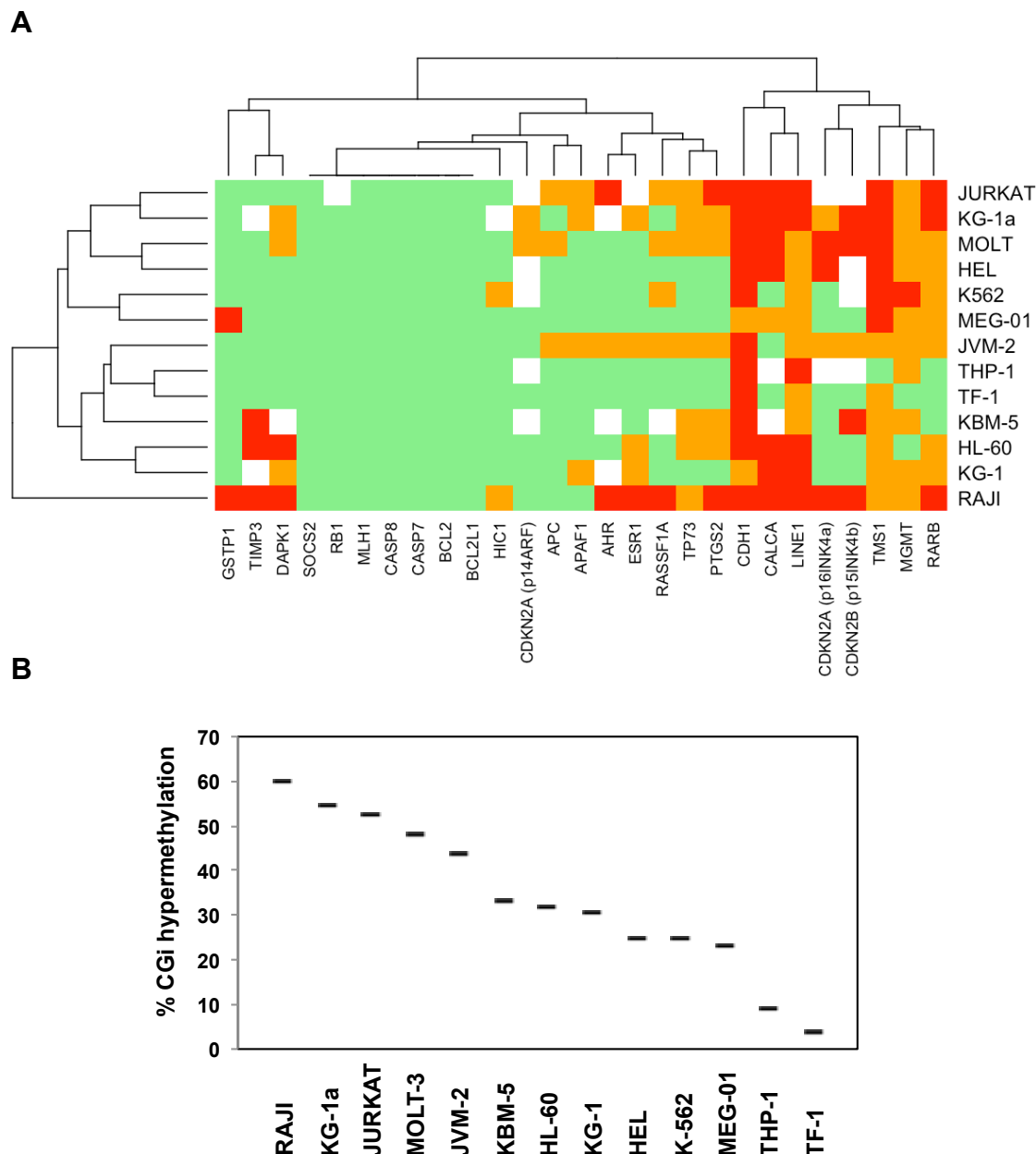


Figure 45: Unique methylation signature of leukemia and lymphoma cell lines.

Gene-specific methylation profile of various blood cancer cell lines was determined by MSP. Aryl hydrocarbon receptor (AHR), apoptotic peptidase activating factor 1 (APAF-1), adenomatous polyposis coli (APC), B-cell CLL/lymphoma 2 (BCL-2), apoptosis regulator Bcl-X (BCL-XL, BCL2L1), calcitonin-related polypeptide alpha (CALCA), caspase 7 and 8 (CASP7 and 8), epithelial cadherin (CDH1), cyclin-dependent kinase inhibitor (CDKN) 2A (p16/14^{INK4a}), CDKN 2B (p15^{INK4b}), death-associated protein kinase 1 (DAPK1), estrogen receptor (ESR1), glutathione S-transferase P1 (GSTP1), hypermethylated in cancer 1 (HIC1), long interspersed repetitive element 1 (LINE1), O6-methylguanine-DNA methyltransferase (MGMT), human MutL protein homolog 1 (MLH1), prostaglandin-endoperoxide synthase 2 (PTGS2), retinoic acid receptor beta (RARβ), Ras association domain family protein 1A (RASSF1A), retinoblastoma 1 (RB1), suppressor of cytokine signaling (SOCS), tissue inhibitor of metalloproteinase 3 (TIMP3), target of methylation-induced silencing 1 (TMS1) and tumor protein p73 (TP73). MSP amplicons were separated on a 12% PAA gel and stained with ethidium bromide. (A) Results were represented on a heat map with clustering, indicating the DNA methylation status (green:

unmethylated, orange: partially and red: fully methylated, white: not analyzed or mutated) by gene and blood cancer cell line. (B) Representation of methylation frequency from the most hypermethylated to the least based on the methylation of the analyzed genes in leukemia and lymphoma cell lines. The repetitive element LINE1 was excluded from this analysis. Data are the mean of 3 independent experiments.

Methylation analysis results show that the methylation pattern is highly variable and is different for each blood cancer type, cell line or gene. In hematological malignancies-derived cell lines, promoter methylation was never or rarely detected in the following genes: human MutL protein homolog 1 (MLH-1), CDKN2A (p14ARF) and retinoblastoma 1 (RB1) as well as caspases 7 and 8, B-cell CLL/lymphoma 2 (BCL-2), apoptotic peptidase activating factor 1 (APAF-1) and apoptosis regulator Bcl-X (BCL-XL). Furthermore, HIC1 and suppressor of cytokine signaling (SOCS2) genes showed no methylation in their promoter region in the analyzed blood cancer cell lines (Figure 45-A). In contrast, moderate methylation frequency (15-40% of the analyzed leukemia and lymphoma cell lines) was measured for the promoters of MGMT, CDKN2A (p16^{INK4a}), estrogen receptor (ESR1), aryl hydrocarbon receptor (AHR), GSTP1, PTGS2, tumor protein p73 (TP73), death-associated protein kinase 1 (DAPK), Ras association domain family protein 1 (RASSF1A), adenomatous polyposis coli (APC) and tissue inhibitor of metalloproteinase 3 (TIMP3) (Figure 45). High methylation frequency (40%-70%) was detected for the promoter regions of CDKN2B (p15^{INK4b}), RARB, calcitonin-related polypeptide alpha (CALCA) and target of methylation-induced silencing 1 (TMS1). Genes encoding epithelial cadherin (CDH1) as well as the transposable long repetitive element LINE1 had the highest methylation frequency and were at least hemi-methylated in all 13 leukemia and lymphoma cell lines (Figure 45-A).

The AML cell lines TF-1 and THP-1 showed the weakest methylation frequencies for the analyzed set of genes (4% and 9%, respectively), followed by the AML cell line HEL (25%) and the CML cell lines K-562 (25%) and MEG-01 (23%). Moderate amount of methylation (30-33%) was detected in KBM-5 cells (CML) and in the AML-derived cells KG-1 and HL-60. Methylation frequency was further increased in JVM-2 (CLL, 43%), MOLT-3 (ALL, 48%) and JURKAT (ALL, 52%) cell lines. The highest methylation frequencies for

the analyzed set of genes were detected in the AML cell line KG-1a (54%) and the Burkitt's lymphoma cell line RAJI (60%) (Figure 45-B). Hierarchical clustering of the human leukemia and lymphoma cell lines by their CGI hypermethylation profiles clearly clustered lymphoma cell line RAJI outside of the leukemia cell lines. On the next cluster level JURKAT, KG-1a, MOLT-3 and HEL were separated from the K-562 and MEG-01. Furthermore, JVM-2, THP-1, TF-1 and KBM-5 cells were separately clustered from the HL-60 and KG-1 cell lines (Figure 45-A).

In addition, screening of methylation pattern in cell lines derived from hematological malignancies pointed out that the promoter region of CDKN2B was mutated (no amplification with both methylated and unmethylated primer sets) in K562, JURKAT and HEL cell lines. JURKAT cells possessed a further mutation in the CDKN2A promoter region (Figure 45-A).

5.4. Analysis of DAC treatment response in blood cancer cell lines

Since epigenetic lesions are potentially reversible, epimutations are promising therapeutic targets for DNA demethylating drugs (e.g. DAC). The nucleoside analog DAC binds covalently DNMTs after integration into DNA. Hence, maintenance of methylation is dysregulated leading to a passive loss of DNA methylation. This demethylation may lead to a restoration of TSG functions and therefore of growth-control and apoptosis mechanisms in tumors. However, it is assumed that DAC-mediated DNA demethylation is unspecific and can further enhance global hypomethylation, activating hypermethylated harmful elements such as transposons. Since DNA methylation is a main player in gene regulation, demethylation influences a broad range of cellular mechanisms, leading to a complex phenotypical response. Therefore, a side part of this thesis was focused in the genome-wide and regional gene-specific effects of DAC-mediated demethylation as well as in the characterization of the cellular response to DAC exposure in leukemia and lymphoma cell lines.

5.4.1. Effect of DAC treatment on leukemia/lymphoma cell survival

To analyze the impact of DAC treatment on leukemia cell survival, K-562, RAJI, HEL, MOLT-3, MEG-01 and JVM-2 cells were treated with different DAC concentrations for 3 days and cell survival evaluated with the trypan blue exclusion test (Figure 46).

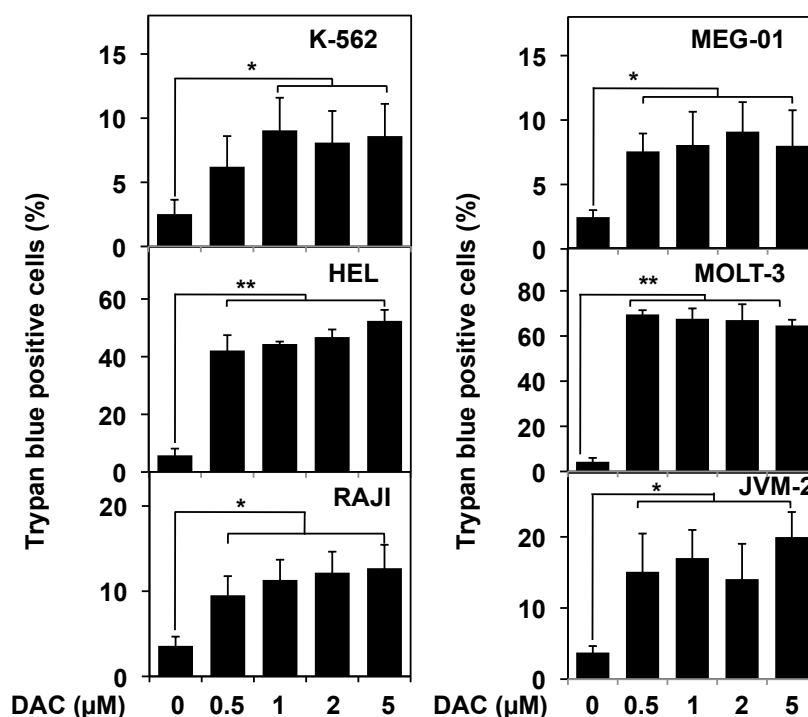


Figure 46: Analysis of DAC exposure on cell viability.

Leukemia and lymphoma cell lines K-562, RAJI, MEG-01, HEL, MOLT-3 and JVM-2 were treated with DAC at the indicated concentrations for 3 days. Cell viability was determined by trypan blue exclusion test. Results indicate the percentage of cell death plotted against the DAC concentration. Data are the mean \pm SD of 3 independent experiments. * $p < 0.05$, ** $p < 0.01$ vs control. DAC: 5-aza-2'-deoxycytidine.

Both CML cell lines K-562 and MEG-01 had only a reduced sensitivity to DAC treatment and showed in average 7.9% and 8.2% of cell death, respectively, after 3 days. In addition, minor proportions of dead cells were identified in RAJI (11.4%) and JVM-2 (16.5%) cell lines after DAC treatment. The highest rate of DAC-induced cell death was measured for the T-cell leukemia cell line MOLT-3 (67.2%) and the erythroleukemia cell line HEL (46.4%). Nevertheless, no significant variation in cell death was detected for the tested DAC concentration range (Figure 46).

Moreover, previous results showed that 2 μ M DAC was sufficient to induce GSTP1 promoter demethylation and expression in RAJI and MEG-01 cells. Therefore, the evolution of cell growth and cell death was followed during 4 days of treatment with 2 μ M DAC. Various blood cancer cell lines were treated with DAC over a defined period of time. Progress of cell viability was determined by trypan blue exclusion test. Growth inhibition was determined by comparing cell growth of untreated and DAC-treated cells (Figure 47).

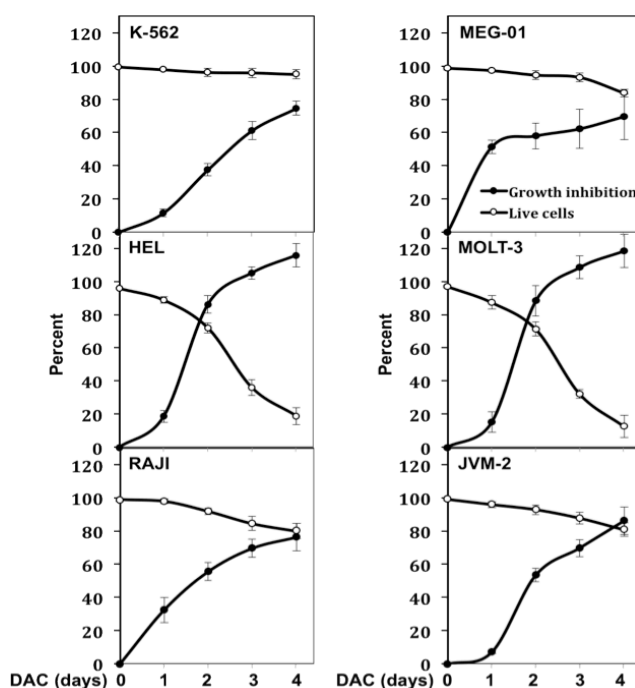


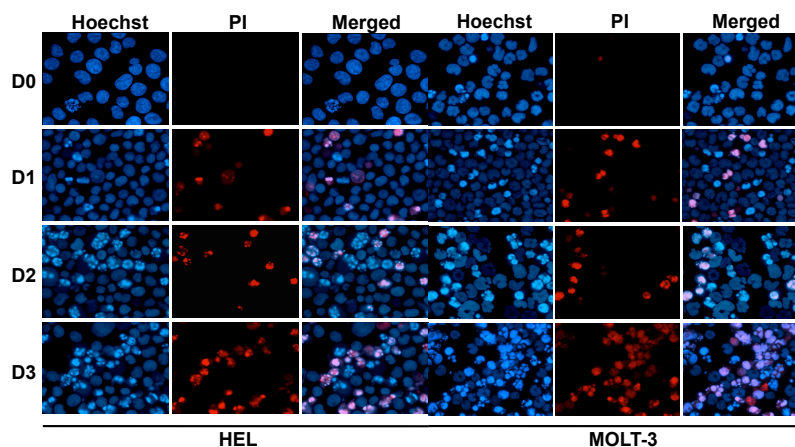
Figure 47: Effect of DAC on leukemia and lymphoma cell growth and viability.

Blood cancer cell lines were treated daily with 2 μ M DAC for 4 days. Cell survival was assessed by trypan blue exclusion test and growth inhibition was calculated by comparing the cellular growth of treated and untreated cells. Data are means \pm SD of 3 independent experiments. DAC: 5-aza-2'-deoxycytidine.

Results demonstrated that DAC moderately decreased (<20%) cell viability of K-562, MEG-01, RAJI and JVM-2 cells. In contrast, DAC treatment robustly decreased in time-dependent manner cell viability in HEL and MOLT-3 to reach at 4 days 19% and 12%, respectively (Figure 47). Moreover, in all tested blood cancer cell lines, DAC strongly induced, in a time-dependent manner, growth inhibition and reached for example 86% in JVM-2 cells.

Since DAC treatment induced cell death in various leukemia cell lines, we then aimed to characterize the type of cell death induced after DAC exposure. K-562, RAJI, JVM-2, MEG-01, HEL and MOLT-3 cell lines were treated with 2 μ M DAC for 4 days and cells stained with Hoechst and PI dyes. Apoptosis and necrosis were assessed by nuclear morphology analysis (Figure 48).

A



B

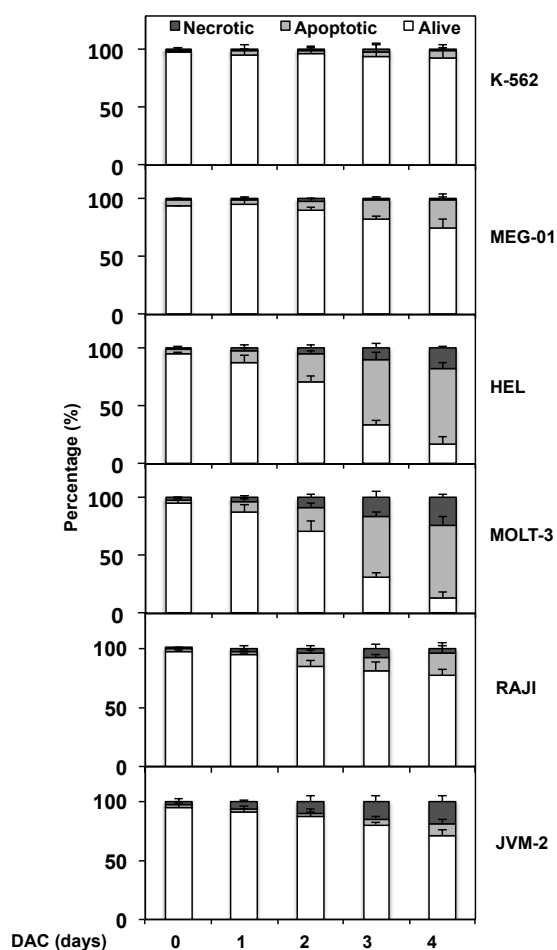


Figure 48: Morphology analysis of cell death in DAC-treated leukemia and lymphoma cell lines.

Leukemia and lymphoma cell lines were treated with $2\mu\text{M}$ DAC for 4 days. Every day, cells were stained with Hoechst and PI, visualized under fluorescence microscopy (HEL and MOLT-3 cell lines as example, A) and apoptotic and necrotic cell death quantified (B). Pictures are representative of 3 independent experiments and data are the mean \pm SD of 3 independent experiments. * $p < 0.05$, ** $p < 0.01$ vs control.

DAC treatment of HEL and MOLT-3 cells resulted in a robust and time-dependent increase of apoptosis and necrosis (Figure 48-A). After 4 days of DAC treatment, 65% of the HEL cells presented characteristic features (fragmented nuclei, condensed chromatin) of apoptosis and 18% of necrosis. In the case of MOLT-3 cells, 62% and 24% of the population was apoptotic and necrotic, respectively. In contrast, after 4 days of DAC treatment, only a slight percentage of K-562 (6%) and a moderate proportion of MEG-01 (25%) and RAJI (19%) cells showed apoptotic features. Moreover, DAC exposure led to a moderate increase of necrosis (19%) and slight occurrence of apoptotic nuclear morphologies (9%) in JVM-2 cell lines (Figure 48-B)

In conclusion, leukemia and lymphoma cell lines presented a differential response to DAC exposure, from the highly sensitive (*e.g.* HEL) to the moderately sensitive (*e.g.* K-562) cells. Moreover, results showed that independently of the cell line considered, cell death was limited to a part of the DAC-treated cell population.

5.4.2. Influence of DAC treatment on global DNA methylation in leukemia/lymphoma cells

To unveil possible relationships between DAC-induced cellular response and genome-wide demethylation, global DNA methylation profile of various cell lines was determined by methylation-specific restriction assay (Figure 49).

	K562			RAJI			JVM-2			MOLT-3			HEL			MEG-01		
<i>HpaII</i>	-	-	+	-	-	+	-	-	+	-	-	+	-	-	+	-	-	+
<i>MspI</i>	-	+	-	-	+	-	-	+	-	-	+	-	-	+	-	-	+	-

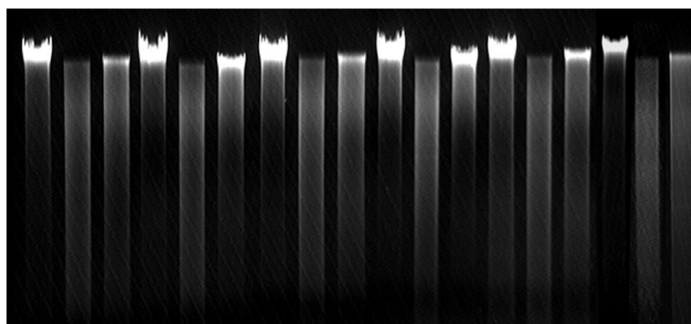


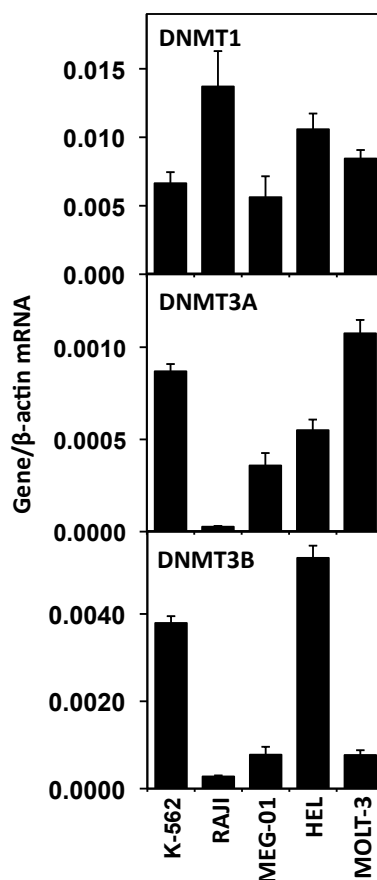
Figure 49: Evaluation of global methylation in various leukemia cell lines by MSRA.

Genomic DNA from various leukemia cell lines was digested by *HpaII* or *MspI*. Digested and undigested control DNA were separated on a 0.8% agarose gel and stained with ethidium bromide. The picture is representative of 3 independent experiments. MSRA: methylation sensitive restriction assay.

Results of the methylation-sensitive restriction assay with *HpaII* are showing that the genomic DNA from RAJI, MOLT-3 and HEL cells is more methylated than the genomic DNA from K-562, JVM-2 and MEG-01 cells.

In order to explain the cell line-specific variations in genome-wide methylation occurrence, constitutive expression of enzymes responsible for DNA methylation maintenance (DNMT1) and establishment (DNMT3A and DNMT3B) was analyzed on mRNA and protein levels. Total mRNA from K-562, RAJI, MEG-01, HEL, MOLT-3 and JVM-2 was extracted and expression of DNMT1, 3A and 3B analyzed by real-time PCR assay (Figure 50-A). Moreover, evolution of DNMT1 protein expression after DAC exposure was analyzed by Western Blot (Figure 50-B).

A



B

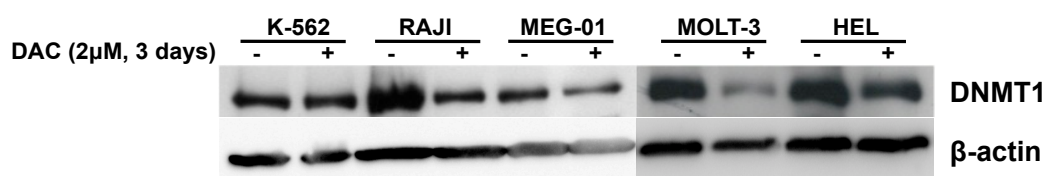


Figure 50: Analysis of the effect of DAC on DNMT1 expression.

(A) Total RNA from various human leukemia cells was analyzed by real-time PCR with primers specific for DNMT1, DNMT3A and DNMT3B. β -actin was analyzed as a control of cDNA quantity in each reaction. Results represent the ratio DNMT/ β -actin mRNA expression levels. Data are mean \pm SD of 3 independent experiments. (B) Proteins from untreated and DAC-treated cells were analyzed by Western Blot with an antibody against DNMT1. β -actin was used as loading control. Pictures are representative of 2 independent experiments. DNMT: DNA methyltransferase.

Compared to K-562 and MEG-01 cell lines, leukemia and lymphoma cell lines RAJI, HEL and MOLT-3 expressed more DNMT1 mRNA and protein. The lowest DNMT1 mRNA level was identified in JVM-2 cells. Globally, the *de novo* DNMT3A and 3B expression rates are much lower than for DNMT1 in all analyzed leukemia cell lines. The highest expression for DNMT3A was

measured in K-562, MEG-01, HEL and MOLT-3 cells. For DNMT3B, the highest mRNA level was determined in K-562 and HEL cell lines (Figure 50-A). Treatment of leukemia cell lines with 2 μ M DAC for 3 days reduced the DNMT1 protein amount in all analyzed cell lines except in K-562 cells. Following DAC exposure, the highest reduction of DNMT1 protein expression was observed in RAJI, HEL and MOLT-3 cell lines (Figure 50-B).

Due to the inhibitory effect of DAC on DNMT1 protein expression, the influence of DAC treatment on global DNA methylation was assessed in various hematological malignancies. Genomic DNA from leukemia cell lines treated with DAC was analyzed by MSRA (Figure 51).

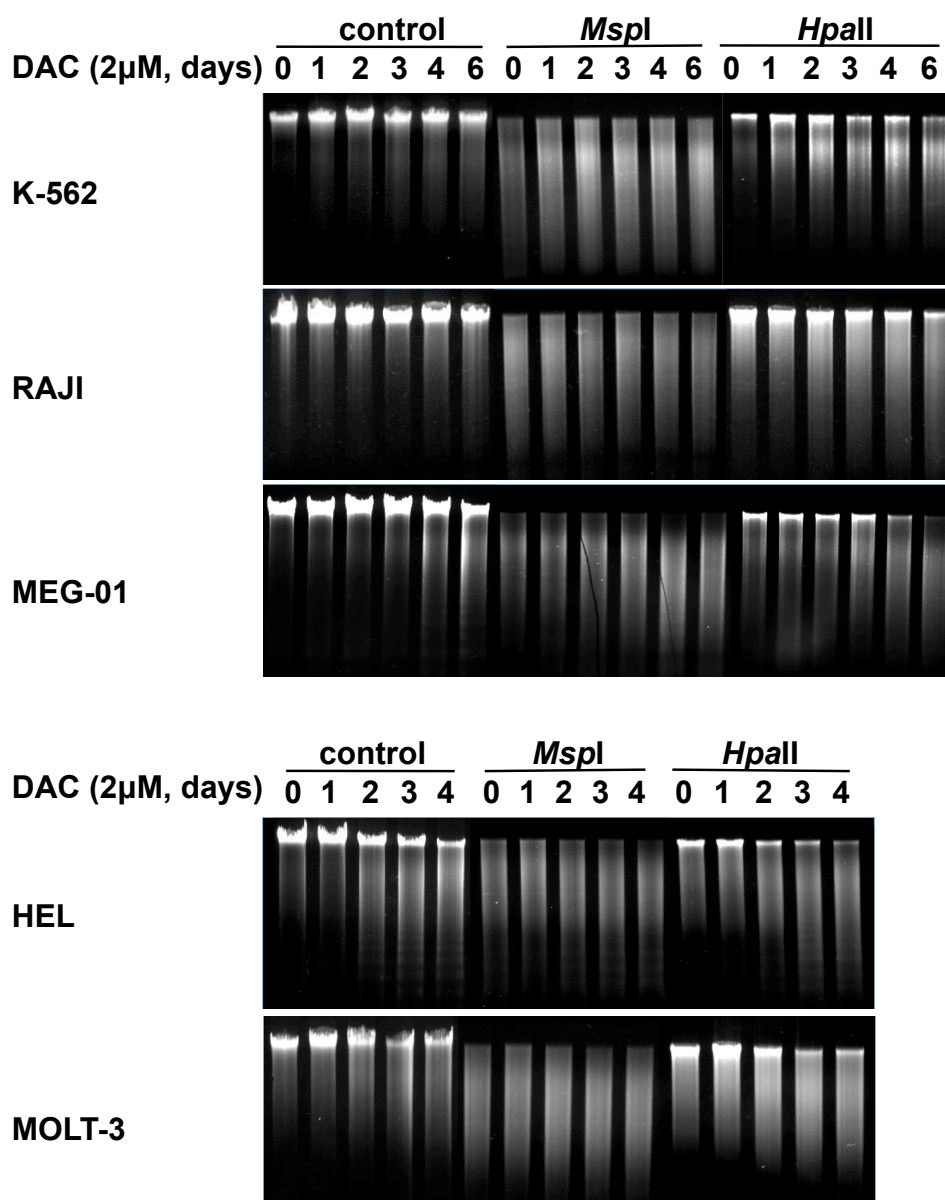


Figure 51: Kinetic analysis of the global DAC-induced DNA demethylation by MSRA.

Various leukemia and lymphoma cell lines were treated for the indicated time with DAC, genomic DNA extracted and digested with *MspI* or the methylation sensitive *HpaII* enzymes. Separation profile was visualized on a 0.8% agarose gel, stained with ethidium bromide. Images are representative for 3 independent experiments. MSRA: methylation sensitive restriction assay.

The high molecular band intensity in the *HpaII* digestion lane decreased and has a similar pattern as the *MspI* control digestion after DAC treatment, indicating global demethylation in all analyzed leukemia and lymphoma cell lines. In addition, demethylation efficiency was cell line-specific and time-dependent (Figure 51).

In conclusion, amounts of DNA methylation of the various leukemia and lymphoma cell lines correlated with their DNMT1 expression levels. Depending on the blood cancer cell line, DAC treatment led to partial repression of DNMT1 protein expression and global demethylation.

5.4.3. Analysis of DAC-induced growth inhibition by a single cell approach

Previous results showed that DAC treatment leads to differential growth inhibition, cell death and global demethylation in various cell lines derived from hematological malignancies. Nevertheless, these results only provide an overall impression of the effects of DAC in a given population. RAJI cell line was selected as a cellular model in order to study the effects of DAC-treatment on growth behavior on a single cell level. Decisive factors for this choice were linked to the fact that the RAJI genome is relatively high methylated and can be efficiently demethylated by DAC. Phenotypically, DAC treatment leads to growth inhibition of RAJI cells without inducing pronounced cell death.

Cell division tracking using intracellular CFSE staining and flow cytometry analysis was used to determine the influence of DAC on proliferation of each single RAJI cell. During the first 24 hours of culture, cell proliferation patterns were similar in DAC- and mock-treated RAJI cells (Figure 52).

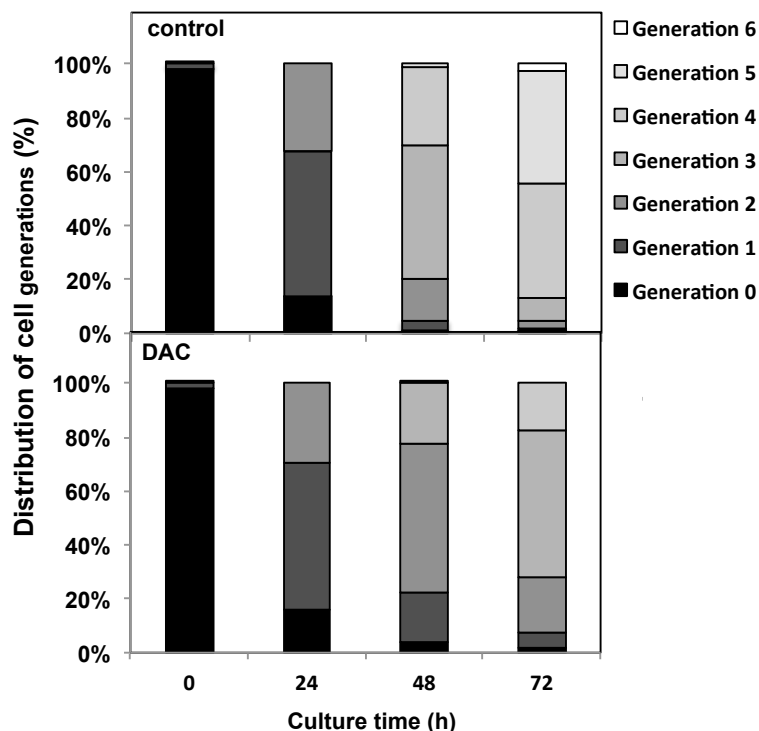


Figure 52: Evaluation of the influence of DAC treatment on RAJI cell proliferation.

RAJI cells in exponential growth phase were stained with 0.2 μ M CFSE (CellTrace™CFSE Cell Proliferation Kit, Invitrogen) as proposed by the manufacturer. After a recovery phase of 24 hours, cells were treated for 72 hours with 2 μ M DAC. Cells were harvested at the indicated time points and CFSE staining analyzed by flow cytometry. Data were processed by FlowJo and represented as the mean of 3 independent experiments.

After 72 hours under normal culture conditions, 42.5, 41.5 and 2.7% of the initial RAJI cell population had divided 4, 5 and 6 times, respectively. In contrast, 72 hours of DAC treatment were sufficient to consistently decrease cell proliferation activity in RAJI cells. Indeed, about 7.6% of the initial RAJI cells population stayed undivided or had divided only once during 72 hours of DAC treatment. The major amount of cells was found in generation 2 (20.3%) and generation 3 (54.9%). Generation 4 was only represented by 17.2% of the DAC-treated RAJI cells (Figure 52).

In addition, the impact of DAC treatment on average RAJI cell growth and doubling time was compared between control and DAC-treated cells. As previously observed by the cell tracking method, the doubling time during the first 24 hours of cell culture was similar in control and DAC-treated RAJI cells (Figure 53).

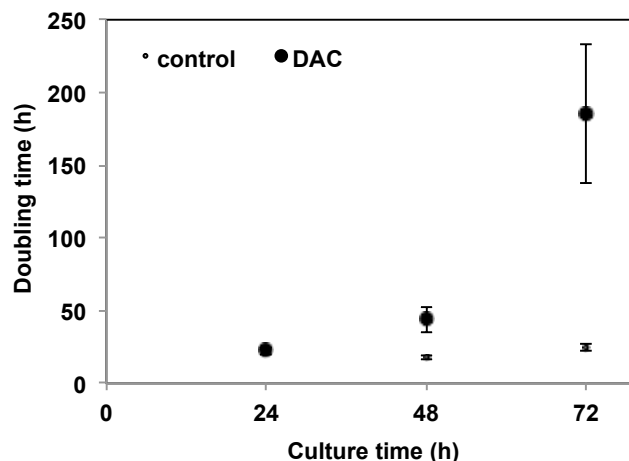


Figure 53: Effect of DAC treatment on the doubling time of RAJI cells.

RAJI cells were treated with 2 μ M DAC for 72 hours and cells were counted using trypan blue exclusion test. Doubling time was calculated using the doubling time software (<http://www.doubling-time.com/index.php>). Data are the mean \pm SD of 3 independent experiments.

However, in correlation with previous results about DAC-induced growth inhibition (Figure 47), doubling time of RAJI cells was moderately attenuated during the following day of culture and drastically affected at 72 hours. In contrast, the proliferation rate of untreated RAJI cells stayed constant (Figure 53).

5.4.4. Simultaneous analysis of DAC-induced GSTP1 expression and cell proliferation

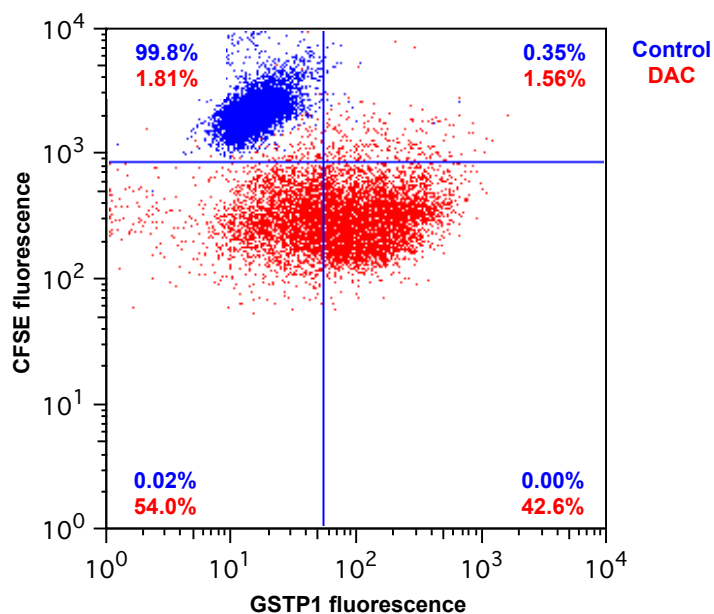
As previously shown, DAC-mediated demethylation is replication-dependent and induces cell-specific growth arrest at different cell generations. These findings leads to the assumption that differential cell division may lead to differential gene demethylation and induction of expression, as already reported by the previous data about the heterogeneous induction of GSTP1 expression in DAC-treated RAJI cells.

In order to investigate more deeply the role of cell division in DAC-induced demethylation and gene expression, we selected GSTP1 gene, which is hypermethylated in the RAJI cells as a model to analyze DAC-induced single cell-specific GSTP1 expression in relation to cell division. GSTP1

immunostaining was combined with the analysis of cell division by CFSE-mediated cell tracking.

At the beginning of DAC treatment, 99.8% of the control cells were CFSE-positive and GSTP1-negative (Figure 54-A).

A



B

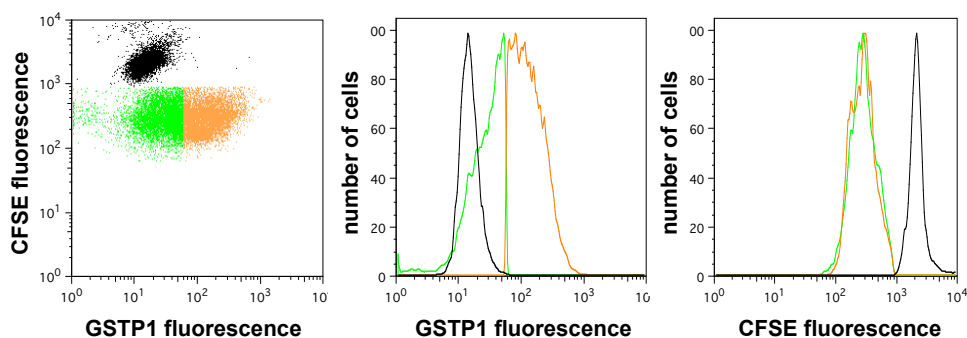


Figure 54: Analysis of the link between cell division and GSTP1 expression in DAC-treated RAJI cells.

RAJI cells were stained with CFSE and after 24 hours of recovery, treated for 72 hours with DAC. GSTP1 expression was assessed by immunostaining using primary anti-GSTP1 and secondary Alexa-Fluor 647-conjugated antibodies. CFSE and GSTP1 fluorescence intensity were detected by flow cytometry and processed by FlowJo. (A) Dot plots, representative of three independent experiments, show the distribution of CFSE and GSTP1 fluorescence intensity relative to each cell. Percentages of control (blue) or DAC-treated (red) cells, present in each quadrant, are indicated and represent the mean of 3 independent experiments. (B) Untreated (black), DAC-treated GSTP1-negative (green) and GSTP1-positive (orange) cells were gated (left panel) and analyzed based on GSTP1 fluorescence (middle panel) or CFSE presence (right panel). Data are representative of 3 independent experiments.

After 72 hours of DAC treatment, 96.6% of the cell population had divided (represented by the sum of cells in the lower left and right quadrants) and about 54% of the whole RAJI cell population was presenting low intensities for CFSE and GSTP1 staining. In contrast, 42.6% of the DAC-treated RAJI cells were presenting a low intensity of CFSE but were also positive for GSTP1 expression (Figure 54-A). To get a better overview of CFSE- and GSTP1-positive cell distributions, subsets of GSTP1 expressing (green) and non-expressing (orange) DAC-treated RAJI cells were gated and CFSE pattern separately analyzed. Results show that both subpopulations had, independently of the GSTP1 expression level, the same cell proliferation pattern (Figure 54-B).

In conclusion, all RAJI cells that were exposed to DAC were still dividing; even though the cell proliferation rate was slowed down. However, DAC-mediated induction of GSTP1 expression was heterogeneously distributed over the RAJI cell population. In consequence, DNA demethylation is cell division-dependent but cell proliferation is not sufficient to induce GSTP1 expression in all RAJI cells.

5.4.5. Analysis of the relationship between GSTP1 expression and methylation pattern in DAC-treated RAJI cells

As previously shown, DAC treatment induces GSTP1 expression in only a subpopulation of RAJI and MEG-01 cell lines. In order to study a possible link between DAC-mediated heterogeneous GSTP1 expression and promoter demethylation, RAJI cells were treated with DAC for 3 days, immunostained and sorted based on GSTP1 expression level (high, low and intermediate). Then the methylation status of each sorted cell subpopulations was analyzed by MSP (Figure 55).

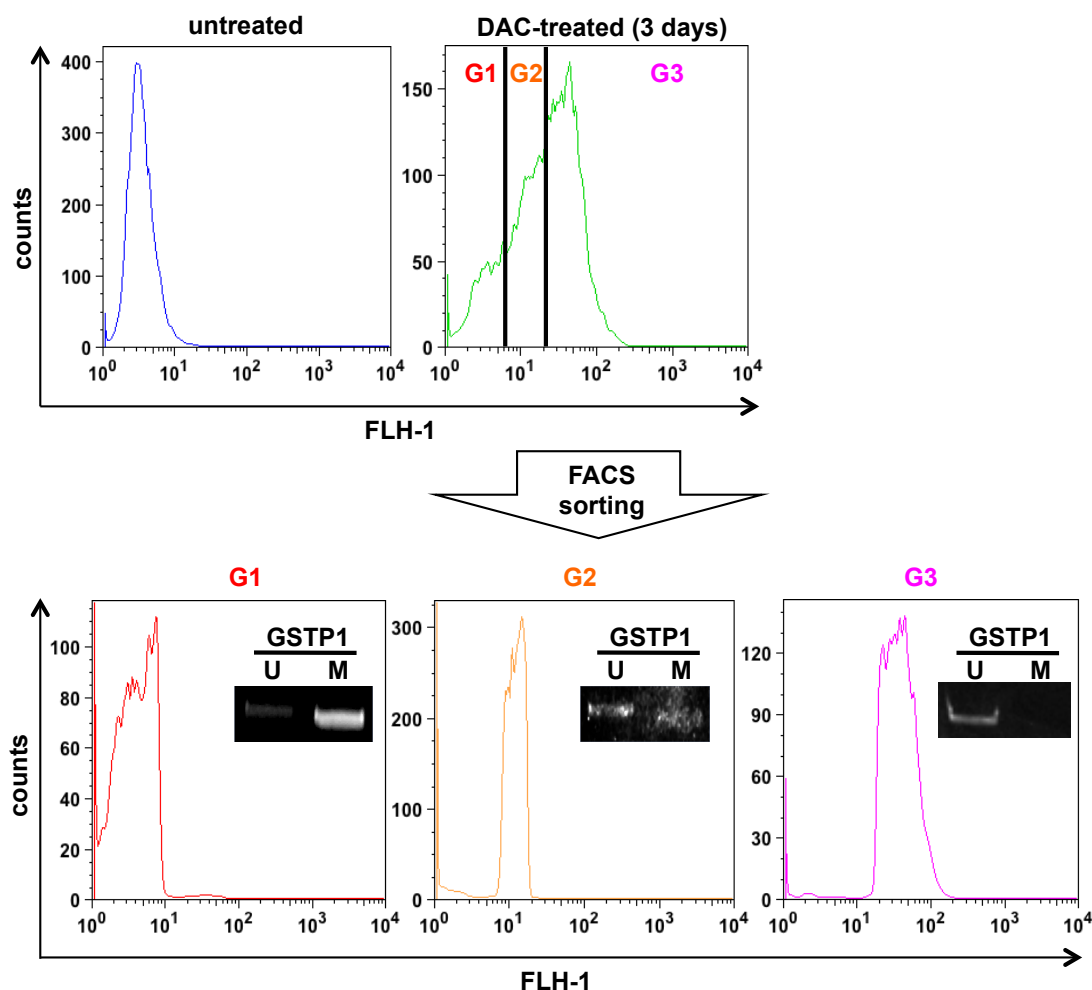


Figure 55: Analysis of GSTP1 promoter methylation after cell sorting based on GSTP1 expression in DAC-treated RAJI cells.

Untreated and DAC-treated ($2\mu\text{M}$, 3 days) cells were indirectly stained with primary anti-GSTP1 and secondary Alexa Fluor 488-conjugated antibodies. The fluorescence amount of 10^5 immunostained RAJI cells was detected by flow cytometry on a FACSCalibur and analyzed by CellQuest Pro. Upper panel: one-dimensional GSTP1 frequency histogram of 10^5 untreated (blue) and DAC-treated RAJI cell lines (green). Cells were gated by their fluorescence intensity and separated by fluorescence assisted cell sorting. Lower panel: one-dimensional GSTP1 frequency histogram of 10^5 DAC-treated and sorted RAJI cells (G1 (red): GSTP1-negative, G2 (orange) GSTP1 intermediate and G3 (pink): GSTP1-positive cells). Genomic DNA was extracted from the different fractions (G1 to G3), bisulfite converted and GSTP1 promoter methylation status determined by MSP. A representative picture of MSP analysis is inserted in each corresponding histograms. Results are representative of 3 independent experiments. DAC: 5-aza-2'-deoxycytidine, U: unmethylated, M: methylated.

As shown in Figure 55, it was possible to separate DAC-mediated GSTP1 expressing (G3) from non-expressing (G1) RAJI cells as well as to enrich a mixed fraction (G2). MSP analysis of the GSTP1 expressing cells

fraction (G3) revealed a hypomethylated state of GSTP1 promoter in these cells. In contrast, analysis of cells from the fraction regrouping GSTP1 non-expressing cells (G1) showed that despite DAC exposure, DNA hypermethylation remained unaffected in the GSTP1 promoter region. Accordingly, the intermediate fraction composed by GSTP1-negative and GSTP1-positive cells showed a mix of hypo- and hyper-methylated GSTP1 promoters.

In conclusion, cell-sorting results showed that methylation status correlates with GSTP1 promoter activity in DAC-treated RAJI cells.

5.4.6. Analysis of gene-specific demethylation in DAC-treated RAJI cells.

DAC treatment led to a heterogeneous RAJI cell population consisting of cells with differential methylated promoter region and GSTP1 expression pattern. To analyze whether this unequal demethylation of RAJI cells is specific for GSTP1 gene, the study was extended on further genes for which methylation patterns were analyzed by deep-sequencing on a GS FLX Titanium platform. Based on literature and own methylation analysis, genes that are hypermethylated in RAJI cells were analyzed. Results of these experiments were represented and presented in the form of a heat map, showing the evolution of DAC-induced demethylation. By comparing the mean methylation of each analyzed gene before and after DAC treatment, the demethylation efficiency was assessed (Figure 56).

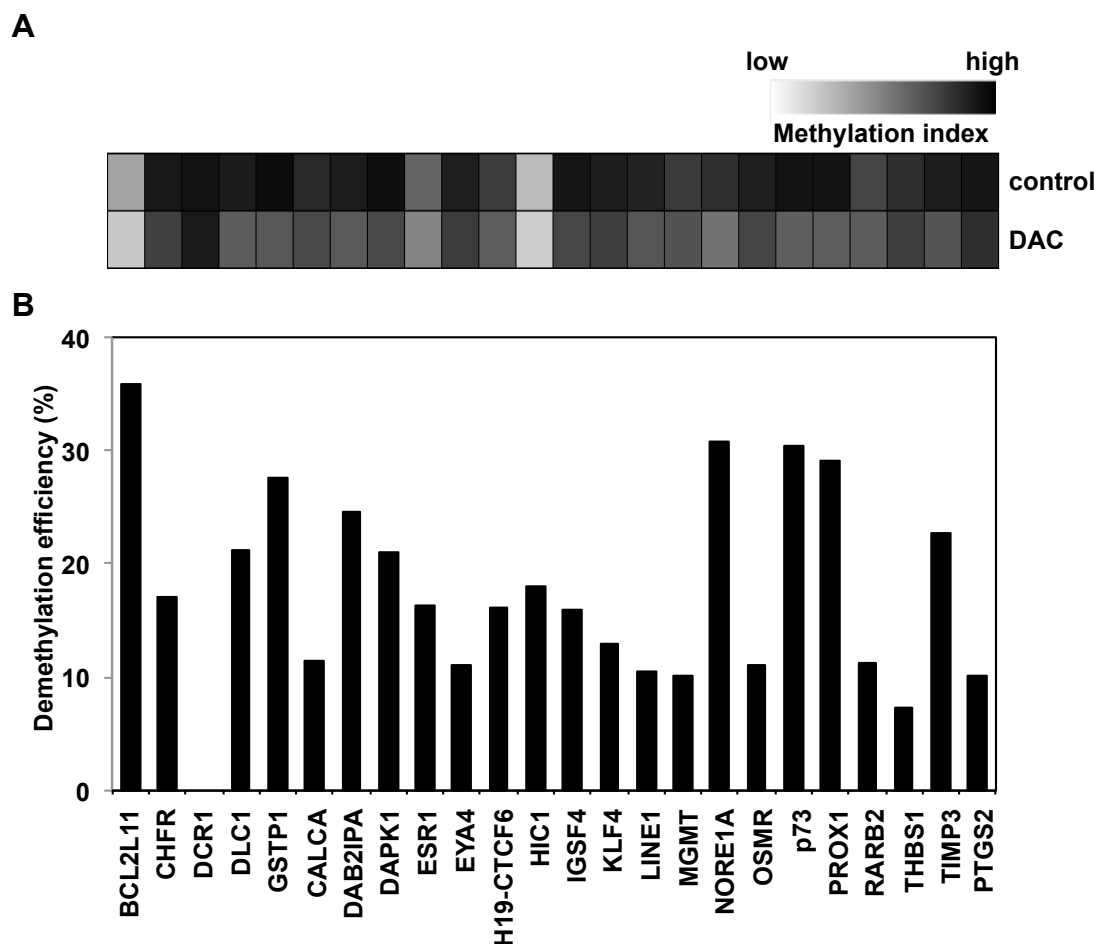
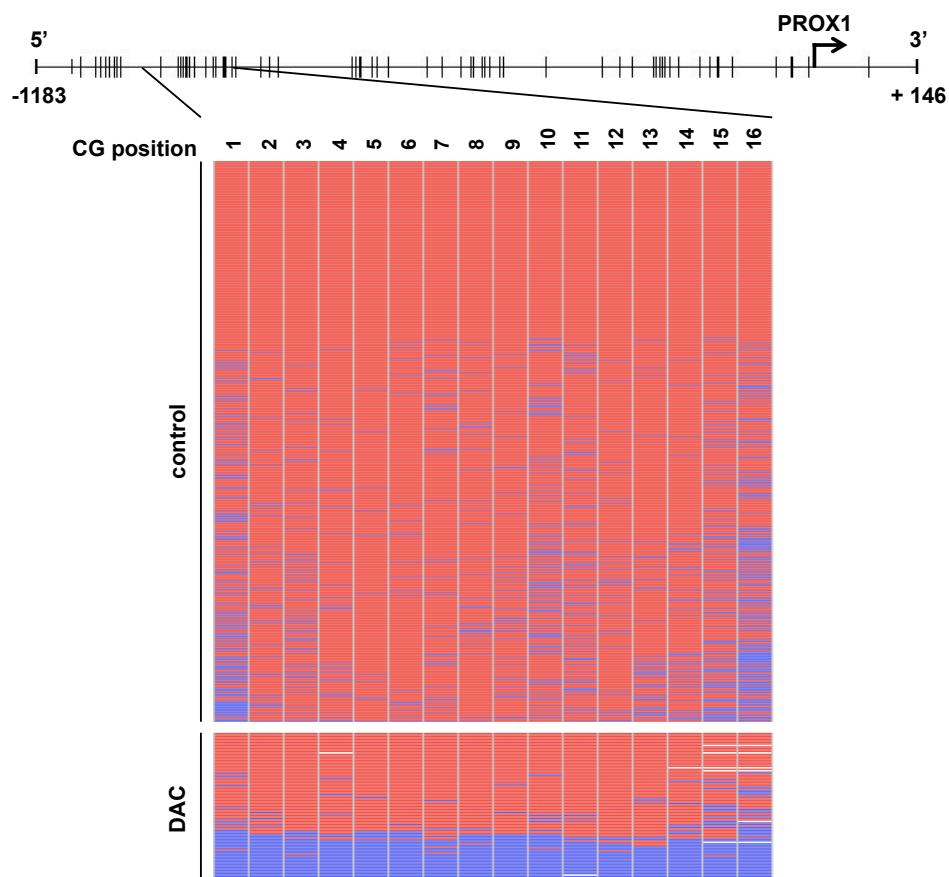


Figure 56: Methylation analysis of various genes in control and DAC-treated RAJI cells.

Genomic DNA from RAJI cells, treated for 3 days with 2 μ M DAC was bisulfite converted and regions of interest amplified by PCR. Methylation pattern was determined by next generation sequencing on a GS FLX platform. (A) Panel shows the methylation pattern before and after DAC treatment of all analyzed genes in RAJI cells. (B) Figure indicates the demethylation efficiency for each analyzed genes, calculated by comparing the mean methylation before and after DAC exposure. Mapping of the CpG dinucleotide distribution and detailed view on the sequence reads of (C) PROX1, (D) GSTP1 and (E) NORE1A genes, before and after 3 days DAC treatment. n=1, Blue: unmethylated, red: methylated CG dinucleotide. Results from one experiment. BCL2L11: BCL2-like 11, CALCA: calcitonin-related polypeptide alpha, CHFR: checkpoint with forkhead and ring finger domains, DAB2IBA: DAB2 interacting protein, DAPK1: death-associated protein kinase 1, DCR1: decoy receptor 1, DLC1: deleted in liver cancer 1, GSTP1: glutathione S-transferase P1, ESR1: estrogen receptor 1, EYA4: eyes absent homolog 4, H19-CTCF6: H19 imprinting control region, HIC1: hypermethylated in cancer 1, IGSF4: cell adhesion molecule 1, KLF4: krueppel-like factor 4, LINE1: long interspersed nuclear element 1, MGMT: O6-methylguanine-DNA methyltransferase, NORE1A: Ras association (RaIGDS/AF-6) domain family 5, OSMR: oncostatin M receptor, TP73: tumor protein P73, PROX1: prospero homeobox 1, PTGS2: prostaglandin-endoperoxide synthase 2, RARB2: retinoic acid receptor beta, THBS1: thrombospondin 1, TIMP3: tissue inhibitor of metalloproteinase 3.

C



(Figure 56 continued)

D

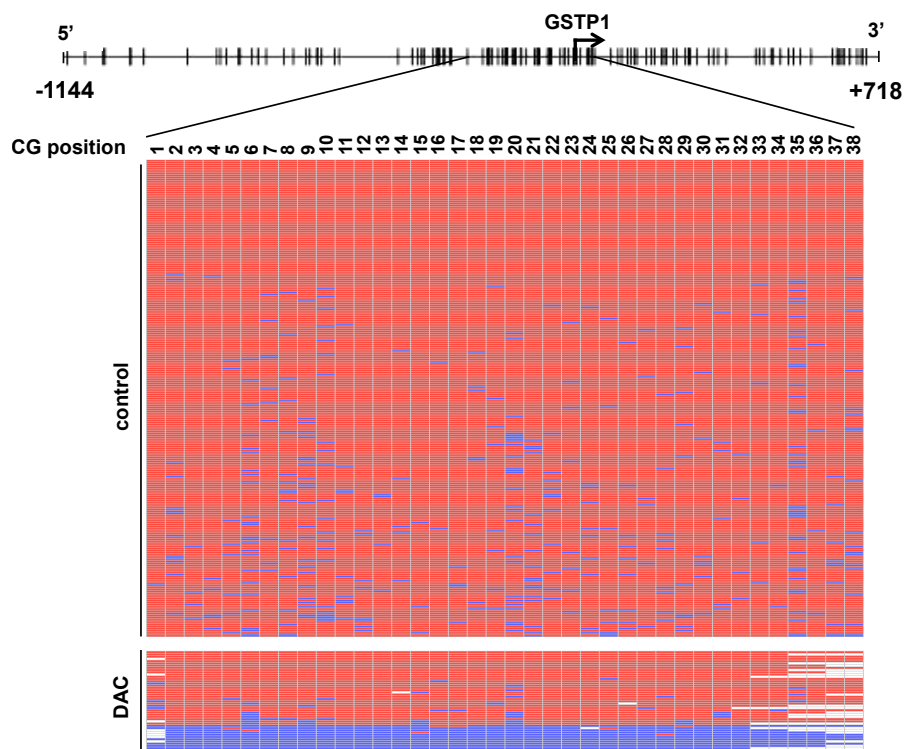


(Figure 56 continued)

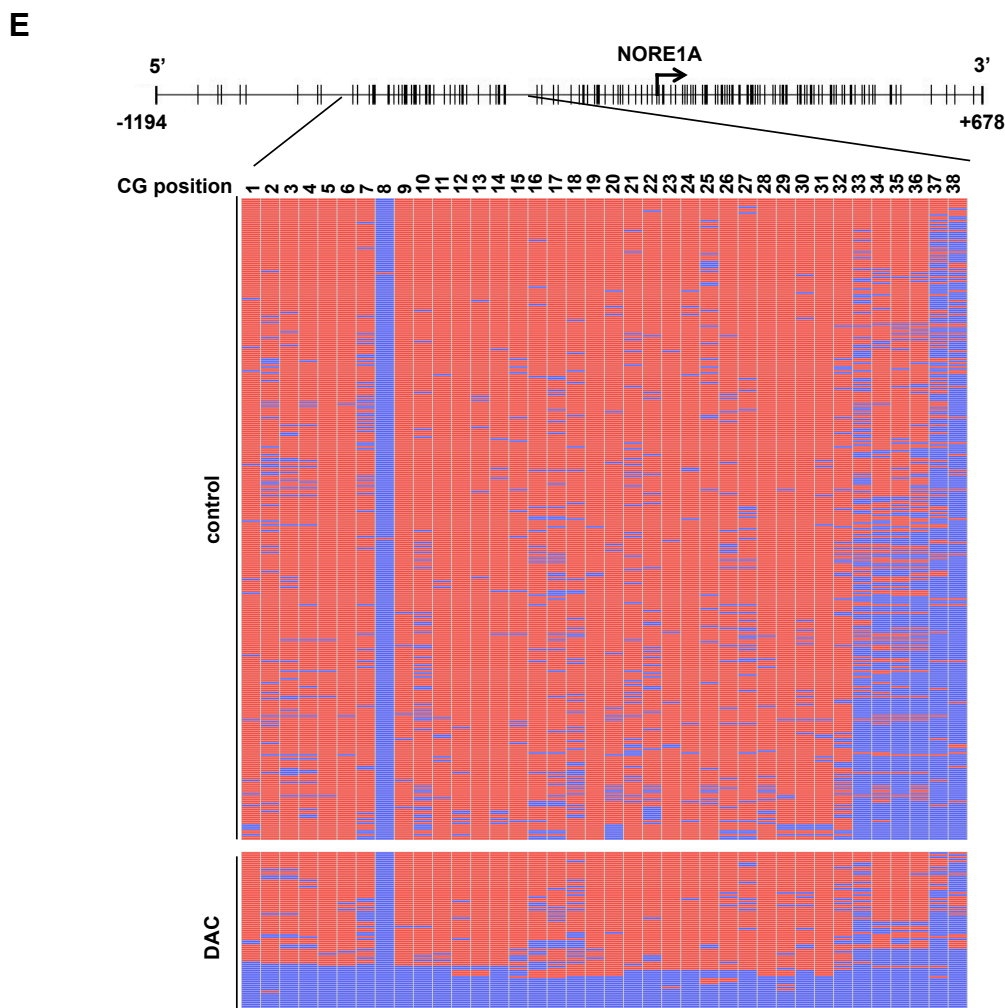


(Figure 56 continued)

Sequencing results indicated that the analyzed genes were differentially methylated in RAJI cells. The bulk of the genes (e.g. DCR1, DAPK1, GSTP1) were hypermethylated while some genes were moderately methylated (i.e. BCL2L11, ESR1, HIC1 and RARB2). Average methylation decreased after 3 days of DAC treatment whereas the unequal methylation distribution was maintained (Figure 56-A). Furthermore, results showed that demethylation efficiency was specific for each gene. For example, the highest demethylation efficiencies were detected for BCL2L11, NORE1A, TP73 and PROX1 genes. In contrast, DCR1 gene was resistant against DAC-induced DNA demethylation. Remaining genes were moderately demethylated by DAC treatment associated with a demethylation efficiency that was highly variable between 7 to 28 % (Figure 56-B). Furthermore, detailed mapping of PROX1,

GSTP1 and NORE1A methylation patterns revealed that DAC-induced demethylation was CpG position-independent but read-specific (Figure 56-B, -C, -D). Only a small subset of the sequencing reads was completely demethylated, whereas the rest remained hypermethylated. Detailed results of the remaining analyzed genes are summarized in the appendix.

Taking together, these findings showed that the analyzed genes are individually methylated in RAJI cells and get differentially demethylated in response to DAC. Moreover, individual analysis of the methylation pattern showed that DAC induced complete demethylation of certain reads, indicating that demethylation was restricted in certain cells.

5.4.7. Analysis of GSTP1 promoter methylation recovery after DAC treatment

As previously shown, DAC treatment can partially reverse DNA hypermethylation on GSTP1 promoter in RAJI and MEG-01 cells. To investigate whether DAC stably demethylates GSTP1 promoter or whether methylation is recovered after DAC exposure, leukemia cell lines RAJI and MEG-01 were exposed up to 3 days with DAC, cells washed and the medium subsequently exchanged by drug free medium. GSTP1 promoter methylation status during treatment and recovery phases was investigated by MSP analyses (Figure 57).

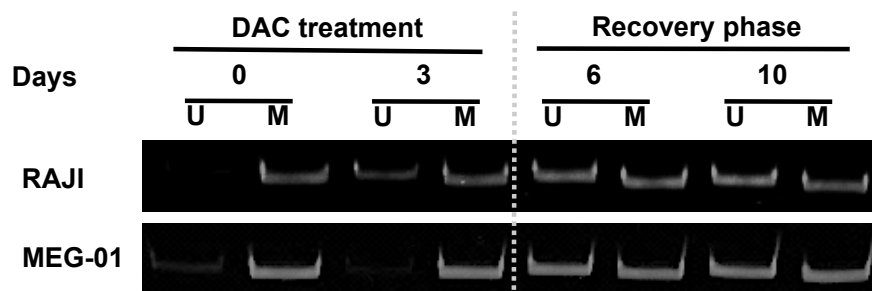


Figure 57: Analysis of GSTP1 promoter methylation pattern after DAC recovery.

RAJI and MEG-01 cells were treated for 3 days with 2 μ M DAC. After a washing step, highlighted by a dotted line, medium was replaced by fresh medium without DAC. Samples were collected during the treatment phase at day 0 and 3, and during the recovery phase at day 6 and 10. Genomic DNA was then extracted, bisulfite converted and used as template for MSP with primers specific for the unmethylated (U) and methylated (M) state of GSTP1 gene. MSP amplicons were separated on a 12% PAA gel and stained with ethidium bromide. Pictures are representative of 2 independent experiments.

Results showed that DAC-induced GSTP1 promoter demethylation in RAJI and MEG-01 cells was not stopped after removal of the demethylating drug but even continued up to a certain degree and then remained constant. Noteworthy, induction of GSTP1 demethylation was delayed, compared to RAJI cells.

In conclusion, remethylation of the GSTP1 promoter was not observed in DAC-treated RAJI and MEG-01 cells.

6. Discussion

In 1989, Greger *et al.* described for the first time the association between DNA hypermethylation and TSG silencing in human cancer based on a study on Retinoblastoma gene (Greger, Passarge *et al.* 1989). Nowadays, long lists of TSGs (*e.g.* DNA repair or metastasis genes) are showing aberrant methylation and thus gene silencing in cancer cells (Esteller 2011). Analysis of the cancer-specific epigenetic fingerprint, based on the evaluation of alterations in the methylation pattern, is a promising approach for cancer detection, assessment of individual's risk for post-diagnosical recurrence and progression as well as for cancer therapy. Epigenetic disruptions occur during early carcinogenesis and are often responsible for loss of gene expression. Accordingly, methylation-associated silencing frequently affects genes, involved in DNA damage repair, tumor suppression, detoxification, inflammation, cell cycle regulation and motility. This inventory includes the detoxification gene GSTP1, which is hypomethylated and widely expressed in benign tissues, but hypermethylated and transcriptionally silenced in prostate, breast and kidney cancer cells (Dulaimi, Ibanez de Caceres *et al.* 2004; Hopkins, Burns *et al.* 2007; Lasabova, Tilandyova *et al.* 2010). Moreover, PTGS2, a key player in inflammation, was reported to be hypermethylated in several cancer types (*e.g.* breast, colon) and is newly used as a prognostic marker for prostate cancer (Phe, Cussenot *et al.* 2010). However, to the best of our knowledge, methylation-associated epigenetic silencing of GSTP1 and PTGS2 genes have never been studied in details for hematological malignancies. Hence, this study will provide compelling evidences for the role of DNA methylation in GSTP1 and PTGS2 repression in leukemia and lymphoma cells and can open up new strategies to detect, evaluate and treat hematological malignancies.

Reversible epigenetic fingerprint is associated to glutathione-S-transferase P1 gene silencing in human leukemia cell lines.

In the first part of this study, we investigated GSTP1 promoter methylation and the contribution of chromatin structure (*i.e.* histone modifications), chromatin-modifying enzymes and transcriptional regulators in relation to GSTP1 expression levels. Screening of various human leukemia and lymphoma cell lines confirmed the constitutively high level of GSTP1 expression in K-562 and JURKAT cells and the lack of expression in RAJI cell line (Shea, Kelley et al. 1988; Borde-Chiche, Diederich et al. 2001). Moreover, our results identified several leukemia cell lines (JVM-2, HEL, MOLT-3) with moderate GSTP1 expression as well as an additional GSTP1-negative CML cell line (MEG-01). Methylation analysis by BSP, MSP and CoBRA as well as time-dependent but concentration-independent induction of GSTP1 expression after DAC treatment pointed out accordingly the hypermethylation of the GSTP1 regulatory region in RAJI and MEG-01 cells. However, DAC-mediated demethylation and induction of GSTP1 expression was time-delayed in MEG-01 cells compared to RAJI cells. Since the proliferation rate of RAJI cells is higher than the one of MEG-01 cells, results are confirming that DAC-induced demethylation is a passive and replication-dependent process (Jones and Taylor 1980). In contrast, GSTP1 promoter was hypomethylated in K-562 cells. Therefore, promoter methylation status and GSTP1 expression pattern are correlated in blood cancer cell lines.

These results prompt us to assume that, in accordance to prostate cancer, aberrant GSTP1 methylation could be linked to early leukemogenesis. Regarding its 'caretaker' gene function, DNA methylation-mediated GSTP1 silencing might promote susceptibility to somatic genome alterations caused by electrophilic or oxidative carcinogens and thus provides cancer-associated growth advantages (Kinzler and Vogelstein 1997; Lin, Tascilar et al. 2001). Therefore, reactivation of the dormant GSTP1 gene and avoidance of its hypermethylation are not only beneficial for cell detoxification, integrity and survival but also for cancer prevention. This statement is confirmed by enhanced cancer susceptibility, detected in GSTP1 deficient mice (Ketterer 1998). In non-malignant cells, DNA methylation is responsible for the long-

term silencing of harmful tumor promoting genes and repetitive non-protein-coding DNA regions (e.g. transposable elements) (Jones and Takai 2001). Apparently, gene-directed DNA methylation is truncated in cancer cells but the mechanistic reasons have still to be elucidated.

Previous studies discussed the possibility to detect aberrant methylation on cell free DNA, extracted from serum, plasma or urine of prostate, lung and colon cancer patients (Esteller, Sanchez-Cespedes et al. 1999; Goessl, Krause et al. 2000; Cairns, Esteller et al. 2001; Grady, Rajput et al. 2001). This idea was adopted to detect urological malignancies during a minimal invasive DNA-based routine screening by analyzing GSTP1 methylation pattern on circulating DNA (Cairns, Esteller et al. 2001; Goessl, Muller et al. 2001). According to our results, aberrant GSTP1 methylation could also be a characteristic of certain leukemia cells, implying that the detection of GSTP1 hypermethylation in serological biopsies could not only stem from prostate cancer but could also originate from hematological malignancies. To prevent misdiagnosis, we propose to use aberrant GSTP1 methylation in various body fluids (e.g. blood, urine, ejaculate) as a first indication for cancer development whereas the analysis should be completed with further cancer-specific biomarkers.

Although the herein used assay was not specific for the GSTP1 isoform, it was shown that DAC treatment had an enhancing effect on the enzymatic activity of the GST superfamily members in K-562, RAJI and MEG-01 cells. Basal GST activity was higher in K-562 and MEG-01 than in RAJI cells whereas DAC-mediated induction was higher in RAJI than in K-562 and MEG-01 cells. We assume that, in addition to GSTP1, other GST isoforms, which are preceded by CGIs, are hypermethylated in RAJI cells (Peng, Razvi et al. 2009). Indeed, DAC induces simultaneous demethylation of GST genes and leads to a massive increase of GST activity. Regarding K-562 and MEG-01 cells, GST genes except GSTP1 are probably hypomethylated and expressed, leading to the observed high basal GST activity. Moderate increase of GST activity in DAC-treated MEG-01 cells is probably due to the demethylation of GSTP1.

GSTP1 immunostaining followed by microscopy and flow cytometry analyses showed that DAC treatment of RAJI and MEG-01 cells led to GSTP1

re-expression in only a limited subpopulation of cells, resulting in an heterogeneous mix of GSTP1 expressing and non-expressing cells. Furthermore, only a limited number of entirely demethylated GSTP1 promoter sequences were observed in DAC-treated RAJI cells. Fluorescence-assisted cell sorting of GSTP1-positive and GSTP1-negative DAC-treated RAJI cells and analysis of their methylation pattern revealed a correlation between DAC-induced demethylation and GSTP1 expression in the heterogeneous cell population. This limited demethylation could be explained by a partial genomic demethylation related to a low efficiency of DAC in those cells. However, methylation-specific restriction assay showed a strong genomic demethylation. Interestingly, DAC-mediated heterogeneous cell population was already reported in a publication from dos Santos *et al.* about synovial sarcoma X gene expression in human melanoma cell lines (dos Santos, Torensma et al. 2000). Currently, it remains unclear why only a part of the DAC-treated cells loses GSTP1 promoter methylation and thereupon re-expresses GSTP1. We assume that the GSTP1 surrounding heterochromatin structure could be responsible for the delayed demethylation. Another hypothesis is that differential DAC-mediated demethylation and GSTP1 re-expression are cell cycle-related. At the moment of DAC treatment, asynchronous cells are in different cell cycle phases. Depending on their progress in cell division, cells either directly incorporate DAC leading to DNA demethylation or have to complete cell division before incorporation of DAC at the following cycle, leading to delayed demethylation in these cells.

Although DNA methylation and histone acetylation act as synergistic layers in tumor-associated gene silencing, we demonstrate that HDACi alone failed to restore GSTP1 expression in non-expressing cell lines. Our findings are in agreement with a former study on CDKN2A (p15) and CDKN2B (p16), TIMP3 and MLH1 (Cameron, Bachman et al. 1999). HDACi had only an impact on GSTP1 expression after pre-incubation with the demethylating agent DAC. However, the incapacity of HDACis to restore GSTP1 expression was not due to lack of inhibitory activity. Therefore, our results demonstrate that dense CGi methylation of GSTP1 promoter is dominant for the permanent transcriptional silencing of the GSTP1 loci and has to be removed before HDACi can affect GSTP1 expression. Nevertheless, a recent publication

reported that treatment of the LNCaP prostate cancer cell line with the HDACi depsipeptide induced HDAC inhibition, DNA demethylation and GSTP1 re-expression. However, it was published that besides HDAC inhibition, depsipeptide also decreases the recruitment of DNMT1 to the hypermethylated CDKN2B gene, which can be the origin of the discrepancies between the observations (Hauptstock, Kuriakose et al. 2011).

The two SP1 binding sites on the GSTP1 proximal promoter region are essential *cis*-elements required for basal gene activity (Jhaveri and Morrow 1998; Morceau, Duvoix et al. 2004). Although, the binding of the SP1 transcription factor to its recognition site has been shown to be insensitive to cytosine methylation, our study showed that neither SP1 nor SP3 are associated to hypermethylated GSTP1 promoter region of RAJI and MEG-01 cell lines (Harrington, Jones et al. 1988; Holler, Westin et al. 1988). This finding is in accordance to the current hypothesis that DNA methylation can induce conformational changes in chromatin structure, which block the accessibility of SP1 to its binding site and contribute to GSTP1 transcriptional silencing.

GSTP1 expression and gene methylation patterns are correlated to the chromatin structure of its promoter. Indeed, ChIP analysis identified typical proteins and histone marks associated to a transcriptional active GSTP1 promoter in K-562 cells. In addition, the hypermethylated GSTP1 promoter region of RAJI and MEG-01 cells was enriched for repressive proteins and histone marks, correlating with the lack of GSTP1 expression. GSTP1 expression is therefore not exclusively regulated by DNA methylation, but also synergistically on level of histone modifications and transcription factor recruitments. In addition, the effect of DAC was not limited on GSTP1 methylation pattern. Indeed, GSTP1 demethylation is associated with drastic changes of GSTP1 promoter-associated proteins including MBDs, HDACs and DNMTs in both non-expressing RAJI and MEG-01 cell lines, which correlate with GSTP1 re-expression (Jones, Veenstra et al. 1998; Nan, Ng et al. 1998; Jones and Baylin 2002). Thus, we clearly confirmed that DAC treatment triggered DNA demethylation and induced a substitution of repressive marks by active ones on GSTP1 promoter in RAJI and MEG-01 cells.

The present study described methylation-associated silencing of GSTP1 promoter and DAC-induced release of its repression. Moreover, it was shown that GSTP1 silenced cells are more vulnerable to somatic mutations after exposure of genome-damaging stress (Kinzler and Vogelstein 1997; Lin, Tascilar et al. 2001; Coughlin and Hall 2002). However, GSTP1 does not meet all criteria of Esteller's candidate gene approach to identify new biomarkers (Esteller 2002). For a later potential clinical application of GSTP1 as an epigenetic biomarker, the aberrant GSTP1 DNA methylation pattern should be detected in biopsies from patients with hematological malignancies. Unfortunately, GSTP1 promoter hypermethylation was not detected in leukemia patient samples and was clearly underrepresented in lymphoma patient samples. These observations are in contrast with results obtained by Rossi *et al.* and Amara *et al.*, reporting that GSTP1 hypermethylation was common in patient samples derived from DLBCL, hairy cell leukemia, follicular lymphoma, Burkitt's lymphoma and MALT lymphoma (Rossi, Capello et al. 2004; Amara, Trimeche et al. 2008). Extending our analyses with further leukemia (*e.g.* CML) and lymphoma patient (*e.g.* Burkitt's lymphoma) samples could reveal the presence of GSTP1 methylation in these specific hematological malignancy subtypes.

Cell lines with high (*i.e.* K-562, JURKAT) and moderate (*i.e.* HEL and MOLT-3) GSTP1 expression possessed a hypomethylated promoter region. These data demonstrate that DNA methylation is not the only mechanism regulating the level of GSTP expression. Publications about miRNA expression and target prediction postulated that GSTP1 is post-transcriptionally regulated by miRNAs in lung and ovarian cancer (Dahiya, Sherman-Baust et al. 2008; Wang, Xu et al. 2009). Screening of the GSTP1 3'UTR by several online databases and prediction tools led to a long list of potential GSTP1 regulating miRNAs. It is assumed that in normal cells, native miRNA expression levels lead to moderate GSTP1 expression. In contrast, aberrant downregulation of an aforementioned GSTP1 targeting miRNA in cancer cells may enhance GSTP1 expression as observed in K-562 or JURKAT cell lines. In consequence, detoxification potential of these cancer cells is improved and possibly confers chemoresistance. Nevertheless, this hypothesis was never tested for hematological malignancies. Mutallip *et al.*

recently reported the post-transcriptional regulation of GSTP1 by miR-133a in head and neck squamous cell carcinoma (HNSCC), showing that artificial repression or induction of miR-133a expression leads to GSTP1 up- or down-regulation, respectively (Mutallip, Nohata et al. 2011). However, an inverse correlation between GSTP1 and miRNA expression levels remained undetected in the analyzed leukemia and lymphoma cell lines and for the considered miRNAs, including miR-133a. The discrepancy between our observations and the finding of Mutallip *et al.* might be explained by possible minor effect of miR-133a in leukemia and lymphoma cells.

Aberrant epigenetic silencing and reduced expression of prostaglandin-endoperoxide synthase 2 gene are common events in human hematological malignancies.

In the second part of this thesis, the correlation between PTGS2 promoter methylation and expression in leukemia and lymphoma cells was assessed. Results showed that PTGS2 was differentially expressed in a broad range of leukemia and lymphoma cell lines. Our study pointed out that hypermethylation of the promoter region was associated to PTGS2 expressional silencing in RAJI cells. Accordingly, the demethylating effect of DAC on PTGS2 promoter region, leading to the induction of PTGS2 expression in RAJI cells, indicates that promoter methylation plays an important role in PTGS2 silencing. In contrast, Toyota *et al.* reported, in a publication about colorectal cancer, a partial methylation of the first PTGS2 exon in RAJI cells. Moreover, they showed that hypermethylation of this region was responsible for the PTGS2 expressional deficiency in colorectal cancer cell lines (Toyota, Shen et al. 2000). The different locations of the analyzed regions (*i.e.* gene-body and promoter region) are likely responsible for the differing methylation results. According to Mori *et al.*, PTGS2 was found to be hypermethylated and transcriptionally silenced in JURKAT cells (Mori, Inoue et al. 2001). The identification of leukemia cell lines that are methylated and thus do not express PTGS2 may be a good experimental model to study PTGS2-independent effects of non-steroidal anti-inflammatory drugs.

PTGS2 is highly expressed in various cancer types, including breast, gastric, colorectal, lung, liver and prostate (Eberhart, Coffey et al. 1994; Liu and Rose 1996; Ristimaki, Honkanen et al. 1997; Liu, Yao et al. 1998; Wolff, Saukkonen et al. 1998). However, in this study we demonstrated that in comparison to PBMCs from healthy donors PTGS2 is downregulated in all blood cancer cell lines. The leukemia cell line HEL showed the highest expression of all leukemia and lymphoma cell lines associated with a hypomethylated promoter. Moreover, moderate PTGS2 expression was detected in blood cancer cell lines with either partially methylated (e.g. KBM-5, HL-60) or unmethylated (e.g. MEG-01, TF-1) PTGS2 promoter. Finally, unmethylated and methylated PTGS2 promoters were detected in non-expressing K-562 and MOLT-3 cells, respectively. PTGS2 silencing in K-562 was already reported by Waskewich *et al.* (Waskewich, Blumenthal et al. 2002). In contrast, previous studies showed that the CML cell line K-562 as well as chronic-phase CML patients were positive for PTGS2 (Giles, Kantarjian et al. 2002; Zhang, Liu et al. 2006). Due to these discrepancies, it remains to be confirmed if, despite of promoter hypomethylation, PTGS2 is silenced in K-562 cells.

Independently of the methylation status, DAC exposure induced PTGS2 promoter demethylation and led to increased PTGS2 transcriptional activity in JURKAT, RAJI, HL-60 and KBM-5 cells. It is conceivable that in contrast to K-562 cells, promoter regions of these cell lines are constitutively activated by cell line-specific overexpression of growth factors, tumor promoters or cytokines. Alternatively, it was reported that ALL-associated HTLV-1 infection might be responsible for the permanent induction of PTGS2 expression by the viral Tax protein via CREB and NF- κ B pathways. For instance, Mori *et al.* associated lack of PTGS2 expression to the absence of HTLV-1 in JURKAT cells (Mori, Inoue et al. 2001). However, the current study clearly shows that promoter methylation is causal for PTGS2 repression and that DAC exposure can reverse PTGS2 silencing by demethylation in HTLV-1-negative JURKAT, RAJI and HL-60 cells (Uphoff, Denkmann et al. 2010). These results imply that HTLV-1 does not affect PTGS2 expression in the analyzed cell lines. It is possible that DAC-induced demethylation increases PTGS2 promoter accessibility for other regulatory factors that are either

constitutively expressed or DAC-induced in JURKAT, RAJI and HL-60 cells. Moreover, our results are consistent with the role of promoter hypermethylation in PTGS2 silencing.

In contrast to DAC-mediated induction of PTGS2 expression in JURKAT, RAJI and HL-60, DAC exposure was not sufficient to induce PTGS2 expression in partially methylated JVM-2 and MOLT-3 cell lines. In these cell lines, DNA methylation release is obviously not enough to induce PTGS2 expression. Similarly to K-562 cells, JVM-2 and MOLT-3 cells probably require an additional signal to be activated even after PTGS2 promoter demethylation. In addition to PTGS2-regulating factors, it has been demonstrated that oncogenes such as H-RAS and c-MYB can positively regulate PTGS2 expression (Sheng, Shao et al. 1998; Ramsay, Friend et al. 2000; Sheng, Shao et al. 2000). It is presumed that JVM-2, MOLT-3 and even K-562 cells do not constitutively express such PTGS2-inducing factors or onco-proteins.

Incidence of PTGS2 promoter hypermethylation was high in biopsies derived from leukemia patients and was even higher in lymphoma patient samples. In accordance, malignant samples were frequently PTGS2 deficient or depleted compared to blood cells from healthy donors. Moreover, PTGS2 promoter hypermethylation was correlated to PTGS2 transcriptional silencing in blood cancer patient samples. In comparison, patients with hypermethylated PTGS2 promoter showed consistently the absence of PTGS2 expression, whereas PTGS2 expression was highly variable in patient samples with unmethylated PTGS2 promoter region. Since PTGS2 expression is highly inducible by factors for instance from the inflammatory processes, PTGS2 expression variations are possibly caused by population-based differences.

As shown in this study, PTGS2 is epigenetically silenced in leukemia and lymphoma cell lines and can be induced by treatment with the DNA demethylating agent DAC. Similarly, PTGS2 is hypermethylated and transcriptionally inactive in samples derived from patients with hematological malignancies. Hence, PTGS2 promoter region fulfills all requirements of Esteller's candidate gene approach for the identification of new biomarkers (Esteller 2002). However, a cohort study with a large number of samples,

especially CML, AML and Burkitt's lymphoma, could improve the previous results. Noteworthy, methylation-associated PTGS2 silencing is mainly limited to lymphoid lineage-derived blood cancer patient samples. If this is confirmed in further lymphoma and lymphoid leukemia patient samples, PTGS2 methylation could be used as a blood cancer classification marker.

The role of epigenetic PTGS2 silencing in tumorigenesis is still under discussion. It is commonly assumed that PTGS2 is overexpressed, promoting carcinogenesis by inducing genes such as cell survival genes (Eberhart, Coffey et al. 1994; Liu and Rose 1996; Ristimaki, Honkanen et al. 1997; Liu, Yao et al. 1998; Wolff, Saukkonen et al. 1998). Accordingly, disruption of PTGS2 expression decreases tumorigenicity (Oshima, Dinchuk et al. 1996). However, it must be taken into account that loss of PTGS2 expression seriously affects pathways, in which PTGS2 is involved (e.g. attenuated inflammation reaction). Further studies needs to clarify the biological roles of altered PTGS2 expression in cancer development and progression.

Moreover, the time point of PTGS2 overexpression is debated, assuming that it is an early event during carcinogenesis. PTGS2 overexpression may suppress at short-term cell progression but contribute at long-term to cell growth, invasion and metastasis (Fosslien 2001; Murata, Tsuji et al. 2004). Accordingly, epigenetic silencing of PTGS2, as reported in this study, could possibly be a very late event in carcinogenesis. However, this would exclude PTGS2 as an early epigenetic cancer biomarker. Nevertheless, Ma *et al.* reported that the metastatic potential of breast cancer cells is positively correlated with increased PTGS2 expression and enzymatic activity (Ma, Yang et al. 2004). Since PTGS2 could be used as a prognostic metastasis marker, analysis of the methylation pattern of hematological malignancies after diagnosis could help to evaluate potential cancer progression and invasiveness of cancer cells. Regarding PTGS2 as a therapeutic target, it was reported that treatment of lung and colorectal cancer patients with selective PTGS2 inhibitors had a strong chemoprevention potential and reduced cancer incidence, respectively. (Sandler, Halabi et al. 2003; Harris, Beebe-Donk et al. 2007). Furthermore, inhibition of PTGS2 in prostate cancer showed delay and prevention of disease progression (Pruthi, Derksen et al. 2006). Consequently, the analysis of early PTGS2 methylation

pattern of high-risk population for blood cancer development could predict success of cancer prevention and cancer treatment by PTGS2 inhibitors.

DNA methylation profiling of leukemia and lymphoma cell lines: promising results for blood cancer detection and assessment.

The systematic study of DNA methylation profiles of selected genes unveiled a map of frequent and distinct epigenetic aberrations in DNA methylation, specific for each leukemia and lymphoma cell line. DNA hypermethylation was detected in genes involved in normal cell physiology such as DNA repair (e.g. MGMT), cell cycle control (e.g. CDKN2A) or cell detoxification (e.g. GSTP1).

By using gene-non-specific approaches (e.g. restriction landmark genomic scanning) and gene-specific high-resolution studies (e.g. DNA methylation microarray), several studies already reported differential methylation amount in cancer cells (Costello, Fruhwald et al. 2000; Ehrich, Turner et al. 2008; Figueroa, Lugthart et al. 2010). The present study extends this knowledge on hematological malignant cells, showing by a gene-specific technique (i.e. MSP) that methylation frequency was highly variable. Accordingly to Paz *et al.* the highest gene methylation frequency was detected in the RAJI (BL) cells, followed by the KG-1a (AML) cell line (Paz, Fraga et al. 2003). Furthermore, ranking cell lines based on descending CGI methylation levels led to the following order: JURKAT (ALL), MOLT-3 (ALL), JVM-2 (CLL), KBM-5 (CML), HL-60 (AML), KG-1 (AML), HEL (AML), K-562 (CML) and MEG-01 (CML) cell lines. The lowest methylation frequency was detected for the cell lines THP1 (AML) and TF-1 (AML). Although the candidate gene approach in our study was more extensive (26 genes) than in the publication of Paz *et al.* (15 genes) and that gene lists slightly differ between both studies, ranking of leukemia and lymphoma cell lines by their amount of methylation was in line with the results of Paz *et al.* Moreover, both studies consistently reported equal percentage of hypermethylation for K-562 and HL-60 cell lines (Paz, Fraga et al. 2003).

Currently, histology and cytology are still important diagnostic tools for cancer management, detection and staging of neoplasia. Hence, the current

study should evaluate if the methylation pattern could be used for blood cancer classification. Hierarchical clustering of blood cancer cell lines according to their methylation profile revealed differences between the analyzed blood cancer cell lines and clustered the lymphoma cell line RAJI outside of the leukemia cell lines. Furthermore, microarray-based study for DNA methylation analysis reported the promising possibility to use methylation to differentiate healthy from leukemia samples and to classify leukemia samples (Adorjan, Distler et al. 2002). However, leukemia cell lines were often misclassified and thus only partially grouped together in their theoretical cell type branches. Noteworthy, K-562 and MEG-01 CML cell lines were closely grouped in the same cluster, whereas KBM-5 was excluded from this cluster. In addition, HL-60 and KG-1 AML cell lines were clustered, whereas for instance HEL was located in another cluster. Strikingly, the candidate gene approach separately clustered the parental KG1 cell line from its less differentiated subline KG-1a (Furley, Reeves et al. 1986). It might be possible that this study uncovered a cell line for which cell type was incorrectly classified in literature such as for MDA-MB-435, which has long been believed to be a breast cancer cell line (Paz, Fraga et al. 2003). Indeed, while in the past, MDA-MB-435 was used as a breast cancer model, a lot of studies later showed that this cell line is of melanocyte nature (Lacroix 2009). However, the restrictive factors of the present study are, on the one hand, the number of the analyzed genes and on the other hand the selection of these genes. Thus, differences between the methylation patterns are not significant enough to classify the various hematological malignancies. Therefore, the use of additional genes in this candidate gene approach or a methylome-wide analysis would increase the stringency of the approach and should allow the classification of hematological hemopathies based on their methylation profiles (Adorjan, Distler et al. 2002).

From a qualitative point of view, a broad range of genes were frequently hypermethylated in the analyzed leukemia and lymphoma cell lines, including CDH1, CALCA, LINE1, CDKN2A, CDKN2B, TMS1, MGMT and RARB. Due to the extensive hypermethylation of these genes in leukemia cell lines, they could theoretically be used as markers for blood cancer detection, even in the background of other cell types (*i.e.* tumor or normal cells). However, the

analysis of these genes is largely inadequate to subclassify hematological neoplasms, for instance based on their lineage. Another subset of genes (*i.e.* GSTP1, TIMP3, DAPK1, HIC-1, CDKN2A, APC, AHR, ESR1, RASSF1A TP73 and PTGS2) was occasionally methylated on various blood cancer cell lines. These genes are potentially good biomarkers for clinical stratification of blood cancer cells into their different subtypes. Finally, promoter regions of SOCS-1, RB1, MLH1, CASP8, CASP7, BCL2 and BCL2L11 genes were unmethylated in our cancer cell lines, clustering amongst others apoptosis-related genes. Even though the methylation state of these genes indicates the conservation of the apoptosis potential, they are useless for an application as epigenetic biomarkers. Cell lines are often used in basic research without taking into account the epigenetic environment. However, if we want to analyze apoptosis, it would be worth to know the epigenetic silencing of apoptosis-associated genes. This study may serve as a starting point, extending our knowledge on the field of cancer cell lines.

In addition to cancer detection and diagnosis, the analysis of DNA methylation alterations is a valuable source for information about the constitution of the cancer cells. DNA methylation-associated silencing of GSTP1 in RAJI and MEG-01 was described in detail for the first time in the present study. In accordance to Paz *et al.*, we reported TIMP3 promoter hypermethylation in RAJI cells (Paz, Fraga *et al.* 2003) and additionally in the KBM-5 cell line. Regarding the HL-60 cell line, TIMP3 methylation results were controversial (Paz, Fraga *et al.* 2003). In consistence with former studies, DAPK1 hypermethylation was detected in RAJI, HL-60 and KG-1a cells and hypomethylation in K-562 and KG-1 cells (Paz, Fraga *et al.* 2003; Takahashi, Shivapurkar *et al.* 2004; Raval, Tanner *et al.* 2007; Chim, Chan *et al.* 2008). Moreover, Paz *et al.* reported that DAPK1 promoter is hypermethylated in JURKAT cell line. However, our results in accordance with other publications reported DAPK1 hypomethylation in JURKAT cells (Katzenellenbogen, Baylin *et al.* 1999; Takahashi, Shivapurkar *et al.* 2004; Chim, Chan *et al.* 2008). Raval *et al.* showed that DAPK1 promoter is methylated in the gene body region, whereas the promoter remains unmethylated (Raval, Tanner *et al.* 2007). Thus, differences in the analyzed gene loci might be at the origin of such discrepancies between studies.

In accordance with an earlier study, we showed HIC1 promoter hypermethylation in RAJI and K-562 cell lines (Issa, Zehnbaauer et al. 1997). Moreover, Paz *et al.* and Guo *et al.* already published HIC1 hypomethylation in JURKAT, K-562, KG-1a, HL-60 and RAJI cell lines (Paz, Fraga et al. 2003; Guo, Burger et al. 2005). In line with previous data, we reported CDKN2A (p14^{ARF}) promoter hypomethylation in RAJI and HL-60 cells and hypermethylation in KG-1a cells (Paz, Fraga et al. 2003; Chim, Chan et al. 2008). However, predominant methylation of this cell cycle regulator in MOLT-3 cells was unpublished. Furthermore, lack of MSP products for K-562, HEL and JURKAT cells were consistent with homozygous deletion of the CDKN2A (p14^{ARF}) locus. Moreover, hypermethylation of APC gene was reported for several solid tumor cancer cell lines, whereas its DNA methylation was mainly unknown in blood cancer cells. In correlation with our results, Wu *et al.* reported hypermethylation of the APC promoter in JURKAT cells (Wu, Shen et al. 2009). In addition, we showed APC methylation in JVM-2 and MOLT-3 cell lines. Regarding the methylation status of APAF-1 gene, widely differing results were obtained. Furakawa *et al.* reported hypermethylation of APAF-1 gene in RAJI and K-562 cell lines and hypomethylation in JURKAT, and HL-60 cell lines. In contrast, our data correlate with results from Chim *et al.*, showing that APAF-1 is unmethylated in RAJI, HL-60 and JURKAT cells (Chim, Chan et al. 2008). Hypermethylation of AHR promoter was also detected in RAJI and JURKAT cells in this study. In contrast, Mulero-Navarro *et al.* reported AHR promoter hypermethylation in K-562 cells (Mulero-Navarro, Carvajal-Gonzalez et al. 2006). Moreover, hypermethylation of ESR1 gene was extensively described in former publications (Guo, Burger et al. 2005; Gebhard, Schwarzfischer et al. 2006; Gebhard, Schwarzfischer et al. 2006). However, our data demonstrated in contrast to Gebhard *et al.*, that ESR1 promoter was hypomethylated in THP-1 and K-562 cell lines (Gebhard, Schwarzfischer et al. 2006). In line with previous data published by Paz *et al.*, we showed RASSF1A promoter methylation in JURKAT, K-562 and RAJI cell lines as well as promoter hypomethylation in KG-1a and HL-60 cells (Paz, Fraga et al. 2003). In accordance to results from Corn *et al.*, we observed TP73 methylation in KG-1a, HL-60 and RAJI cells. However, methylation of TP73 in JURKAT and KBM-5 cell lines has never been mentioned before.

Interestingly, methylation-associated silencing of PTGS2 has never been considered as epigenetic mark in hematological malignancies and was described for the first time in this study.

E-cadherin is one the most commonly methylated genes in hematological malignancies. As proven by Paz *et al.* and Corn *et al.*, we confirmed CDH1 hypermethylation in JURKAT, K-562, KG-1a, HL-60 and RAJI cells (Corn, Smith *et al.* 2000; Paz, Fraga *et al.* 2003). Moreover, Lakshmikuttyamma *et al.* revealed a partial methylation and complete methylation of CDH1 in KG1 and KG-1a cells, respectively (Lakshmikuttyamma, Scott *et al.* 2010). We further completed the list of CDH1 promoter methylation-positive cell lines with MOLT-3, HEL, MEG-01, JVM-2, THP-1, TF-1 and KBM-5. Even though, CALCA gene is found hypermethylated in various hematological neoplasia (Ismail, El-Mogy *et al.* 2011). We determined CALCA hypermethylation in RAJI, KG-1, HL-60, Hel, MOLT-3, KG1a and JURKAT cell lines. In correlation with Paz *et al.*, the cell cycle regulating gene CDKN2A (p16^{INK4a}) and CDKN2B (p15^{INK4a}) were shown here to be methylated in RAJI and KG-1a cells and the promoter deleted in THP-1 and JURKAT cells (Dodge, Munson *et al.* 2001; Paz, Fraga *et al.* 2003; Galm, Herman *et al.* 2006M; Gebhard, Schwarzfischer *et al.* 2006). Moreover, CDKN2A (p16^{INK4a}) gene methylation was detected in JVM-2, HEL as well as KG-1a cells and for CDKN2B (p15^{INK4a}), methylation was observed in KBM-5, JVM-2 and MOLT-3 cells. TMS1 gene is often found methylated in breast cancer cells (Levine, Stimson-Crider *et al.* 2003). However, methylation-associated silencing in leukemia and lymphoma cell lines remained so far undescribed. Surprisingly, here, TMS1 promoter was hypermethylated or partially methylated in all analyzed blood cancer cell lines with the exception of THP-1 cells. In accordance with Paz *et al.*, the present study also revealed the hypermethylation of MGMT promoter region in RAJI, K-562, KG-1a and JURKAT cells, whereas its methylation status in HL-60 was different in both studies. Moreover, discordant results were published for the methylation status of RARB in HL-60, K-562 and JURKAT cell lines (Paz, Fraga *et al.* 2003). The causes for these divergences between both studies are not clear, but as it has already been emphasized, region specific differences may be at the origin of such discrepancies.

Determination of the methylation status of the above mentioned genes could provide important information about chemosensitivity, cell motility, inflammation, hormone response, cell cycle regulation and apoptosis of cancer cells, improving cancer therapy. However, DNA methylation analysis in leukemia and lymphoma patient samples was so far done for only several genes (Galm, Herman et al. 2006; Boultwood and Wainscoat 2007). Therefore, the expansion of DNA methylation analysis to patient samples could reveal new path in blood cancer treatment.

The use of a single gene locus to discriminate malignant from benign cells as well as to classify cancer cells has several drawbacks. The sensitivity is restricted by the hypermethylation frequency at a specific CpG locus. Moreover, as CGi methylation is not specific for blood cancer cells, hypermethylation of a specific gene can also occur in non-cancerous tissue or in other cancer types. Indeed, methylation analysis of several genes has more discriminatory power for detection of a specific cancer. A combinatorial approach with several of often but differential hypermethylated genes in leukemia cell lines could improve cancer detection and treatment. For example, combined detection of GSTP1 and APC hypermethylation in prostate cancer achieved a theoretical sensitivity of 98.3% as compared to benign prostatic hyperplasia and had a specificity of 100% (Jeronimo, Henrique et al. 2004).

Even if the methylation status of some of the genes reported in this study were already published, combined analysis of these genes and blood cancer cell lines was never reported. In addition, this study extends the knowledge about blood cancer-associated hypermethylation to further target genes. As described above, cancer-associated DNA methylation changes were mostly analyzed on a gene-by-gene basis, metaphorically speaking, from a frog perspective (Schulz and Goering 2011). However, the development of new techniques allows today the eagle's view, an overview of the whole methylome. In conclusion, simultaneous methylation analysis of selected and highly informative genes or genome-wide methylation patterns within the scope of individualized medicine could be used as a molecular fingerprint of cancer cells, enabling premalignant cancer detection, prediction and prognosis in the same manner as mRNA expression profiling is already

applied in molecular cancer diagnosis. Finally, DNA hypermethylation is nowadays a promising target for epigenetic drugs (e.g. DAC).

Demethylation efficiency and specificity of 5'-aza-2'-deoxycytidine in hematological malignant cells.

Initially synthesized as an anticancer cytotoxic agent in 1968 by Sorm *et al.*, the later use of 5'-aza-2'-deoxycytidine (DAC) at low doses revealed its differentiation- and DNA demethylation-inducing activities (Piimi 1964; Pískala 1965; Jones, Taylor *et al.* 1982). Interestingly, DAC is used as a molecular demethylation tool to analyze DAC-mediated induction of gene expression. It is known that in cell culture, high doses of DAC trigger cell death, whereas low doses lead to loss of DNMT activity and DNA demethylation (Christman 2002). In addition, multiple clinical trials underlined the promising effect of low-dose DAC in leukemia, leading to FDA approval for the medication of MDS (Kantarjian, O'Brien *et al.* 2003; Issa, Garcia-Manero *et al.* 2004; Schmelz, Sattler *et al.* 2005). Even if DAC is routinely used in research and is newly used for MDS treatment, statements about DAC-induced molecular and cellular effects in hematological malignancies are still vague. Hence, the last part of this thesis wanted to elucidate the cellular response as well as the demethylation efficiency and specificity of DAC treatment in leukemia cell lines at clinical relevant low doses (Aparicio, Eads *et al.* 2003).

The present study showed that independently of the tested DAC concentrations, 4 days of DAC treatment were not sufficient to induce pronounced cell death in K-562 and MEG-01 cells (<10%). In contrast, HEL cells were more sensitive to DAC exposure (>40%) than K-562 cells whereas MOLT-3 cells were the most sensitive (>60%). Noteworthy, other results from our laboratory showed delayed apoptosis in K-562 and MEG-01 cells after sustained DAC exposure (data not shown). This study was extended to further cell lines, reporting moderate cell death in the DAC-treated RAJI Burkitt's lymphoma and the JVM-2 CLL cell lines. Moreover, the present study showed that sustained DAC exposure decreased cell proliferation and increased growth inhibition in a time-dependent manner. In addition, DNMT1 expression and global DNA methylation analysis showed that K-562, JVM-2

and MEG-01 genomes were relatively hypomethylated, compared to the hypermethylated RAJI and MOLT-3 genomes. In between, HEL genome is moderately methylated. Globally, cell death and methylation results indicate a direct link between the amount of DNA methylation, the level of DNMT1 expression and DAC-sensitivity. We assume that cells with high amount of methylation and DNMT1 expression are more sensitive to DAC treatment than cells with hypomethylated genome. Since DAC induced global demethylation and DNMT1 depletion, alterations in DAC metabolism, leading to DAC resistance, can be excluded as reasons for differential DAC response of blood cancer cell lines (Qin, Jelinek et al. 2009). Since DAC-mediated demethylation is related to cell replication, cell proliferation could be a decisive factor influencing DAC response. However, all cell lines divide more or less at the same rate, leading to a similar demethylation pattern. It is conceivable that, in addition to the epigenetic background, genetic differences are responsible for the differential response of the analyzed leukemia cell lines to DAC treatment.

It is commonly accepted that DAC is incorporated into the daughter strand during replication, subsequently DNMT1 is trapped, ubiquitinated and finally degraded. Goshal *et al.* reported that DAC exposure (2.5 μ M) of HELA cells led to a entire loss of DNMT1 protein after 24 hours (Goshal, Datta et al. 2005). Moreover, complete decline of DNMT1 protein expression after 24 hours of AZA treatment was reported in K-562, HL-60 and HEL cell lines. Despite sustained AZA exposure, DNMT1 protein increased again during the next 48 hours of treatment (Stresemann, Bokelmann et al. 2008). Moreover, another study described complete depletion of DNMT1 protein after 48 hours of DAC treatment in KG-1a and THP-1 cell lines at concentrations of 0.1 μ M and 0.3 μ M, respectively (Hollenbach, Nguyen et al. 2010). However, we observed in all analyzed cell lines a partial loss of DNMT1 protein after 72 hours of DAC treatment. Since DAC and AZA have to be metabolized and integrated during replication, the question arises how DAC can induce complete removal of DNMT1 after maximal one cell division. Our data show moderate DAC-induced depletion of DNMT1, which is in accordance to passive loss of DNA methylation.

Numerous studies have already discussed the cellular consequences of DAC treatment. DNA damage-related and DNA methylation-independent activation of CDKN1A (p21) *via* p53 as well as G1 cycle arrest were reported in various DAC-treated AML cell lines (Jiemjit, Fandy et al. 2008). It is assumed that in p53-proficient cells, DAC-mediated DNA damages induce cell cycle arrest, whereas they lead to cell death in p53-deficient cells (Nieto, Samper et al. 2004). On the basis of literature, we found out that K-562 cells are p53 negative and HEL cells p53 positive. However, p53 status did not correlate with cell survival after DAC exposure (Durland-Busbice and Reisman 2002). Alternatively, Tamm *et al.* have attributed the induction of DAC-mediated apoptosis in AML cell lines to the demethylation-associated induction of the p53 sequence homolog and apoptosis inducer TP73 (Tamm, Wagner et al. 2005). However, the TP73 methylation signature of the blood cancer cell lines used in this study did not correlate with DAC-induced cell death (*e.g.* high DAC responsive cell lines are differentially methylated in the TP73 locus). Furthermore, it was reported that DAC could induce G2/M cell cycle arrest *via* the p38 MAP kinase pathway (Lavelle, DeSimone et al. 2003). As previously described, DAC induces the expression of p53 inducible apoptotic proteins Puma and Noxa, leading to the activation of both the intrinsic mitochondrial apoptosis pathway and caspase 3 or leading to a caspase-independent cell death pathway (Tamm, Wagner et al. 2005; Brodska, Otevrelva et al. 2011). In addition, DAC-mediated demethylation and induction of other genes, involved in cell death signaling or cell cycle regulation are probably at the origin for DAC-induced cell death in our cell models. For example, Furukawa *et al.* described induction of the cell death-associated APAF-1 gene in DAC-treated acute leukemia cells (Furukawa, Sutheesophon et al. 2005). However, methylation profiling of blood cancer cell lines showed that APAF-1 is not differentially methylated between DAC-sensitive and less sensitive cell lines. An alternative model for DAC-mediated cancer cell death is related to formation of covalent DNMT-DNA adducts in DAC containing DNA, leading to DNA damages and cytotoxicity (Juttermann, Li et al. 1994). Noteworthy, it is reported that DAC-induced demethylation and gene expression is rather unspecific. Thus, loss of gene regulation and simultaneous release of gene expression probably lead to activation of

several pathways. Therefore, it is most likely that DAC-induced cell death results of a combination of effects reflecting the sum of induced genes.

The previous part of the study provided insights into DAC-induced cellular effects in blood cancer cell population. Noteworthy, results revealed that DAC exposure initiates heterogeneously apoptosis and DNA demethylation in the same cell population. However, significance of the MSRA approach is limited to global methylation and does not allow elucidating the causes for heterogeneous demethylation. Therefore, the existing question is: Does DAC exposure induce uniform but partial demethylation in the entire cell population or does it affect only certain cells and initiate subsequently cell death in these unmethylated cell subpopulation? Moreover, it remains to determine whether DAC-induced DNA demethylation is gene specific.

To investigate these issues, RAJI cell line was selected as a suitable model based on its relatively high global DNA methylation level and low sensibility to DAC-induced cell death. Moreover, GSTP1 gene that is hypermethylated in RAJI cells was chosen as reference gene. Since DAC-treated cells were not synchronized in previous experiments, we assumed that cell cycle distribution could be responsible for the differential DAC response. Theoretically, cells in G1 phase can integrate DAC during the first replication, leading to DNA demethylation from the very beginning of the treatment. In contrast, demethylation of cells in G2 is delayed because they have first to complete their division before they can subsequently integrate DAC. However, results showed that even if doubling time was continuously increasing, only an infinitesimal part of the cell population remained undivided or was blocked in the first cell division after 3 days of DAC treatment. At that time, most of the DAC-treated RAJI cells had divided 3 times. Absence of cell proliferation arrest and decreased cell proliferation rate in DAC-treated RAJI cells are in contrast to the commonly reported DAC-induced cell cycle arrest (Lavelle, DeSimone et al. 2003; Tamm, Wagner et al. 2005; Jiemjit, Fandy et al. 2008). Differences in the genetic and epigenetic background of leukemia and lymphoma cell lines as well as differences in applied DAC concentrations could be at the origin of the differences observed in this study. Moreover, combination of cell proliferation assay and GSTP1 immunostaining of DAC-treated RAJI cells showed that all treated cells were dividing, whereas

demethylation-associated induction of GSTP1 expression was detected only in a subpopulation. In conclusion, cell proliferation is necessary but not sufficient to induce homogeneously demethylation and transcriptional activity. It is presumed that DAC does not directly affect cell proliferation and DNA demethylation of blood cancer cells, but probably has to be first absorbed and metabolized. In line with this assumption, the effect that we observed in this study is probably just the beginning of DAC-mediated demethylation. Some cells are probably not yet affected by DAC and continue to proliferate, whereas another cell subpopulation is demethylated and GSTP1 expression concomitantly induced. It is also possible that GSTP1 demethylated cells undergo in a next step cell cycle arrest and apoptosis.

In order to exclude that the heterogeneous demethylation, observed in DAC-treated RAJI cells was specificity for the GSTP1 gene locus, further genes were included into this study. Deep sequencing results revealed that the analyzed genes were differentially demethylated in presence of DAC. For example, DCR1 and THBS1 genes were mainly resistant to DAC-induced demethylation, in contrast to BCL2L11 and NORE1A genes, which were more efficiently demethylated. Moreover, DAC-response was independent of the initial gene methylation since partial methylated BCL2L11 and hypermethylated GSTP1 promoter regions showed similar demethylation efficiency. In addition, deep sequencing results were consistent to GSTP1 promoter BSP results, showing completely hypermethylated as well as fully unmethylated reads, indicating that only a part of cells was demethylated. Post-sorting analysis confirmed this statement, showing that GSTP1 promoter region was only unmethylated in GSTP1 expressing cells, and accordingly GSTP1 was hypermethylated in non-expressing cells. By using a DNA methylation reporter gene assay, Si *et al.* also reported heterogeneous gene reactivation by DAC treatment (Si, Bumber *et al.* 2010). In line with our previous hypothesis about delayed and stepwise loss of DNA methylation, we assume that heterogeneous re-expression could be explained by the existence of a mixed cell population consisting of cells with fully demethylated and transcribed DNA and other cells with fully methylated and silenced DNA.

Finally, the current study showed that GSTP1 methylation was not recovered after DAC withdrawal. However, with a similar experimental setup,

Qin *et al.* showed recovery of LINE1 methylation. Indeed, 4-days of DAC exposure decreased initial LINE1 methylation to 25% whereas after 10 days of DAC withdrawal LINE1 methylation was recovered at 75% of the initial density in HL-60 cells (Qin, Youssef *et al.* 2007). Furthermore, a publication about hypermethylation of DAPK1 showed complete recovery of DAPK1 methylation in RAJI cells after 7 days of DAC exposure (0.3 μ M) followed by 11 days in fresh media (Katzenellenbogen, Baylin *et al.* 1999). Moreover, a recent study that used a DNA methylation reporter gene assay to analyze evaluation of methylation after DAC exposure showed a time-dependent recovery of methylation and reporter gene silencing after DAC withdrawal (Si, Bumber *et al.* 2010). We assume that in the experimental conditions of our study, the level of DAC-induced DNA demethylation exceeded a certain threshold leading to a decrease of cell proliferation, which is impairing DNA remethylation. In addition, it is possible that high quantity of DAC was already entered into cells and/or metabolized, sustaining DNMT1 inhibition. Moreover, it is possible that lack of recovery is cell line- or gene-specific. In conclusion, further experiments are required to understand the gradual loss of DNA methylation and explain heterogeneous cell behavior after DAC exposure.

7. Conclusions and perspectives

Reversible epigenetic fingerprint is associated to glutathione-S-transferase P1 gene silencing in human leukemia cell lines.

Results of this thesis part gave new insights into the regulation of GSTP1 gene expression by epigenetic mechanisms in leukemia. GSTP1 promoter hypomethylation and the associated euchromatin structure correlate with GSTP1 transcriptional activity (e.g. K-562). In contrast, heterochromatin configuration and the hypermethylated state of the GSTP1 promoter region lead to expressional silencing (e.g. RAJI, MEG-01). Treatments with the DNA hypomethylating agent DAC decrease the hypermethylated state of GSTP1 promoter, inducing chromatin decondensation of this region and thus restoring GSTP1 expression in a subset of GSTP1-negative leukemia cells. Furthermore, screening of CLL, AML, ALL and lymphoma patient samples did not identify any DNA hypermethylation in the GSTP1 promoter region. This epimutation may be CML or Burkitt's lymphoma specific or the sample frequency may be too reduced. Consequently, we will try to further collect and enlarge our pool of leukemia patient samples. In conclusion, these data demonstrate that cytosine methylation can repress GSTP1 gene expression in leukemia and lymphoma cells. Hence, we can consider the investigation of GSTP1 methylation marks as a prognostic factor for hematological malignancies. Furthermore, these data support the concept of the dominance of DNA methylation over HDAC inhibitor-sensitive histone deacetylation in silencing genes with a high CpG density in the promoter region.

In perspective, this study has to be completed with further leukemia and lymphoma patient samples to validate GSTP1 as an epigenetic biomarker. Moreover, the biological role of GSTP1 epigenetic silencing in early carcinogenesis has to be clarified. For this purpose, we suggest to analyze the effects of GSTP1 repression in non-cancerous cell lines. Indeed, analysis of GSTP1 methylation pattern could allow to anticipate for instance chemosensitivity or improve individualized cancer medicine on the field of diagnostic, optimized prevention and therapeutic care.

Moreover, genome-wide miRNA expression profiling may identify miRNAs of importance for GSTP1 gene regulation in hematological malignancies. If a potential GSTP1 targeting miRNA is newly identified, the study will be completed with an analysis, studying the effect of miRNA downregulation or overexpression on GSTP1 expression.

Aberrant epigenetic silencing and reduced expression of prostaglandin-endoperoxide synthase 2 gene are common events in human hematological malignancies.

Results showed that PTGS2 expression is markedly decreased or absent in leukemia and lymphoma cell lines. PTGS2 downregulation is closely associated with DNA hypermethylation, which can be reversed by DAC to increase PTGS2 expression. In patients, PTGS2 promoter methylation is identified in numerous blood cancer patients, which significantly contributes to PTGS2 downregulation. Noteworthy, PTGS2 downregulation occurs mainly in tumors from the lymphoid lineage. In conclusion, PTGS2 promoter methylation represents a promising biomarker for diagnosis in hematological malignancies.

In perspective, PGE2 production in DAC-treated cells presenting PTGS2 demethylation/overexpression will be analyzed in order to determine functionality of the DAC-induced protein. In order to evaluate the specificity of PTGS2 methylation regarding blood cancer cells, other cancer types will be included in this study. To investigate whether DNA methylation is sufficient to repress PTGS2 expression, effects of HDACis alone or in combination with a canonical inducer of PTGS2 expression such as phorbol myristate acetate (PMA) will be analyzed on PTGS2 expression in PTGS2-negative cells. Moreover, the biological role of PTGS2 methylation-associated silencing has to be clarified. Therefore, PTGS2 knock-out or overexpression in undifferentiated blood stem cells or normal non-malignant cells will give new insight into the roles of PTGS2 repression in cancer development. In addition, we plan to analyze the effects of PTGS2-specific inhibitors on cell chemosensitization, which should provide important information for cancer treatment and management. Similarly to the experiments carried out on

GSTP1 promoter, chromatin structure will be analyzed in PTGS2 hyper- and hypo-methylated blood cancer cell lines.

To validate PTGS2 as a an epigenetic blood cancer marker, additional samples (especially CML, ALL and BL) and further leukemia and lymphoma subtypes have to be included in this study. To analyze the evolution of PTGS2 methylation during cancer progression, samples from different blood cancer progression states should be included in the study. Finally, the study should be extended to other cancer types (e.g. prostate, lung, breast, colon) in order to determine for which cancer types PTGS2 methylation is characteristic.

DNA methylation profiling of leukemia and lymphoma cell lines: promising results for blood cancer detection and assessment.

Results of this study revealed high qualitative and quantitative variations in the leukemia and lymphoma cell line-specific methylomes.

In perspective, this study should be extended to further genes by using methods investigating the whole methylome (e.g. next generation sequencing) instead of MSP analyses, thereby increasing the stringency of the approach. In addition, methylation pattern of miRNAs, which are the main players in the post-transcriptional regulation of gene expression, has to be included in the approach. Further leukemia, lymphoma and myeloma cell lines should be included in this study as well as healthy cells as reference. Moreover, this candidate gene approach should be applied to a large set of patient samples. The present study only served as a starting point, extending our knowledge on the field of blood cancer cell lines. However, the use of such a candidate gene approach for individualized blood cancer medicine remains a long-term objective.

Demethylation efficiency and specificity of 5'-aza-2'-deoxycytidine in hematological malignant cells.

The present study pointed out the differential sensitivity of blood cancer cell lines to DAC exposure. Furthermore, it was shown that DAC treatment leads to heterogeneous induction of DNA demethylation and cell death in a

cell population. Moreover, this study showed that cell proliferation is necessary to induce DNA demethylation but is not sufficient to cause complete loss of methylation in a cell population. However, the precise mechanisms and dynamics of DAC about induction of cell death are still not well understood. We assume that heterogeneous cell behavior, regarding demethylation, gene induction and apoptosis, is due to a gradual impact of DAC on the cells. Our model proposes that DAC treatment induces complete demethylation in a part of the cell population, whereas the rest of the cells remain DAC-unaffected and maintain their cancer-specific methylation pattern. Subsequently, methylation poor cells undergo apoptosis, whereas methylated cells continue to proliferate. Thus, this study leaves a lot of questions unanswered. In consequence, further experiments may be needed to verify the above-mentioned presumptions.

In perspectives, comprehensive analyses of intrinsic and DAC-induced expression of various cell cycle and apoptosis regulators, the epigenetic pattern of these genes as well as their mutation status have to be included to finalize this study and determine the mode of action of DAC in blood cancer cell lines. Moreover, kinetic analysis of DAC integration into DNA, possibly by HPLC analysis could provide information about DAC-induced demethylation dynamics. In order to validate previous demethylation results, deep-sequencing will be repeated. To investigate whether the heterogeneous induction of GSTP1 expression in RAJI cells is caused by complete demethylation of certain cells, we will perform post-sorting methylation analyses of further genes in DAC-treated RAJI cells. Moreover, the minimum degree of hypomethylation required for gene activation is largely unknown. GSTP1 expression-based sorting and analysis of both DNA strands by BSP or the use of hairpin-bisulfite PCR should elucidate whether DAC-induced promoter hemimethylation is sufficient to induce GSTP1 expression. In order to reveal a relationship between DAC-mediated demethylation and subsequent cell death, induction of membrane proteins by DAC exposure, coded by hypermethylated genes (*i.e.* cadherins or interleukins) will be analyzed and used to immunosort cells. In the next step, target membrane protein-positive and -negative cells will be separately cultured. Subsequent analyses of cell death will provide information about the link between

methylation loss and apoptosis. In addition, methylome analysis of both fractions can provide information about the quality and quantity of DAC-mediated demethylation that is needed to induce apoptosis. Alternatively, a DNA methylation reporter gene assay (green fluorescent protein (GFP) under the control of a methylated cytomegalovirus promoter) could be used to analyze DAC-mediated demethylation and induction of expression. Moreover, this non-destructive technique allows post-sorting cell culture and subsequent cell death assessment. To exclude the presence of different cell-cycle stages as a reason for differential demethylation, RAJI cells should be synchronized, treated with DAC and demethylation-associated induction of gene expression evaluated. Finally, in order to exclude a RAJI cell-specific effect, all experiments should be repeated in other leukemia and lymphoma cell lines.

Summary

Glutathione S-transferase P (GSTP) 1 and prostaglandin-endoperoxide synthase (PTGS) 2 genes are commonly silenced by promoter hypermethylation in various cancers. However, these epimutations remain poorly investigated in leukemia and lymphoma. We hypothesized that DNA methylation-induced GSTP1 and PTGS2 silencing may be involved in hematological malignancies. Our results demonstrated that methylation-associated silencing of GSTP1 and PTGS2 was found in various leukemia and lymphoma cell lines. A correlation was found between GSTP1 chromatin structure and GSTP1 transcriptional state. Interestingly, PTGS2 hypermethylation was observed in many samples from patient with hematological malignancies presenting reduced PTGS2 expression levels. By extending our study to other epigenetically regulated genes, we observed differential proliferation, cell death and DNA demethylation responses of blood cancer cell lines to the DNA demethylating agent 5-aza-2'-deoxycytidine. In conclusion, we identified DNA methylation signatures that could be promising clinical biomarkers in hematological malignancies. Finally, our study provides critical data for a better understanding of the mechanism of action and effects of 5-aza-2'-deoxycytidine that could provide guidance to predict sensitivity and response for a therapeutic use of this compound against hematological malignancies and potentially other cancers.

Zusammenfassung

In Krebszellen liegen die Gene Glutathion-S-transferase P1 (GSTP1) und Prostaglandinsynthase-2 (PTGS2) häufig methyliert vor, jedoch wurden diese Epimutationen in Blutkrebszellen noch kaum untersucht. Wir vermuteten allerdings, dass fehlerhafte Methylierungen eine wichtige Rolle beim Ausschalten dieser Gene in Leukämie- und Lymphomzellen spielen könnte. Unsere Ergebnisse bestätigten diese Annahme und zeigten, dass die Genexpression von GSTP1 und PTGS2 durch die Hypermethylierung der DNA unterdrückt wird. Weiterhin konnte ein Zusammenhang zwischen der GSTP1 Genexpression und Chromatinstruktur hergestellt werden. Interessanterweise konnte die Methylierung des PTGS2 Gens auch in Zellen von Blutkrebspatienten nachgewiesen werden. Die Analyse weiterer epigenetisch regulierter Gene und die Untersuchung der Zellteilung, des Zelltods und der DNA Demethylierung in Blutkrebszellen, welche mit der demethylierenden Substanz 5-Aza-2'-Deoxycytidin behandelt wurden, zeigte dass jede Zelle unterschiedlich auf den Verlust der Methylierung reagiert. Schlussfolgernd sind die Methylierungsmuster der hier beschriebenen Gene vielversprechende Blutkrebsmarker. Weiterhin ermöglichen die Ergebnisse dieser Studie einen Einblick in die Wirkungsweise von 5-Aza-2'-Deoxycytidin in Blutkrebszellen. Diese Erkenntnisse könnten nicht nur eine wichtige Rolle für die Diagnose sondern auch für die Behandlung von Blutkrebs oder anderen Krebsarten mit dieser demethylierenden Substanz spielen.

References

- Adorjan, P., J. Distler, et al. (2002). "Tumour class prediction and discovery by microarray-based DNA methylation analysis." *Nucleic acids research* **30**(5): e21.
- Aggerholm, A., M. S. Holm, et al. (2006). "Promoter hypermethylation of p15INK4B, HIC1, CDH1, and ER is frequent in myelodysplastic syndrome and predicts poor prognosis in early-stage patients." *European journal of haematology* **76**(1): 23-32.
- Agrawal, S., W. K. Hofmann, et al. (2007). "The C/EBPdelta tumor suppressor is silenced by hypermethylation in acute myeloid leukemia." *Blood* **109**(9): 3895-3905.
- Agrelo, R., F. Setien, et al. (2005). "Inactivation of the lamin A/C gene by CpG island promoter hypermethylation in hematologic malignancies, and its association with poor survival in nodal diffuse large B-cell lymphoma." *Journal of clinical oncology : official journal of the American Society of Clinical Oncology* **23**(17): 3940-3947.
- Ahrendt, S. A., J. T. Chow, et al. (1999). "Molecular detection of tumor cells in bronchoalveolar lavage fluid from patients with early stage lung cancer." *J Natl Cancer Inst* **91**(4): 332-339.
- Ahringer, J. (2000). "NuRD and SIN3 histone deacetylase complexes in development." *Trends Genet* **16**(8): 351-356.
- Akashi, K., D. Traver, et al. (2000). "A clonogenic common myeloid progenitor that gives rise to all myeloid lineages." *Nature* **404**(6774): 193-197.
- Allfrey, V. G. and A. E. Mirsky (1964). "Structural Modifications of Histones and their Possible Role in the Regulation of RNA Synthesis." *Science* **144**(3618): 559.
- Altucci, L., N. Clarke, et al. (2005). "Acute myeloid leukemia: therapeutic impact of epigenetic drugs." *Int J Biochem Cell Biol* **37**(9): 1752-1762.
- Amara, K., M. Trimeche, et al. (2008). "Prognostic significance of aberrant promoter hypermethylation of CpG islands in patients with diffuse large B-cell lymphomas." *Annals of oncology : official journal of the European Society for Medical Oncology / ESMO* **19**(10): 1774-1786.
- Aparicio, A., C. A. Eads, et al. (2003). "Phase I trial of continuous infusion 5-aza-2'-deoxycytidine." *Cancer chemotherapy and pharmacology* **51**(3): 231-239.
- Asimakopoulos, F. A., P. J. Shteper, et al. (1999). "Prognostic significance of c-ABL methylation in chronic myelogenous leukemia: still an open question." *Blood* **94**(3): 1141.
- Asimakopoulos, F. A., P. J. Shteper, et al. (1999). "ABL1 methylation is a distinct molecular event associated with clonal evolution of chronic myeloid leukemia." *Blood* **94**(7): 2452-2460.
- Ateeq, B., A. Unterberger, et al. (2008). "Pharmacological inhibition of DNA methylation induces proinvasive and prometastatic genes in vitro and in vivo." *Neoplasia* **10**(3): 266-278.
- Balch, C., J. S. Montgomery, et al. (2005). "New anti-cancer strategies: epigenetic therapies and biomarkers." *Frontiers in bioscience : a journal and virtual library* **10**: 1897-1931.

- Ball, M. P., J. B. Li, et al. (2009). "Targeted and genome-scale strategies reveal gene-body methylation signatures in human cells." *Nature biotechnology* **27**(4): 361-368.
- Barker, D. J., J. G. Eriksson, et al. (2002). "Fetal origins of adult disease: strength of effects and biological basis." *International journal of epidemiology* **31**(6): 1235-1239.
- Baur, A. S., P. Shaw, et al. (1999). "Frequent methylation silencing of p15(INK4b) (MTS2) and p16(INK4a) (MTS1) in B-cell and T-cell lymphomas." *Blood* **94**(5): 1773-1781.
- Baylin, S. and T. H. Bestor (2002). "Altered methylation patterns in cancer cell genomes: cause or consequence?" *Cancer Cell* **1**(4): 299-305.
- Baylin, S. B., M. Esteller, et al. (2001). "Aberrant patterns of DNA methylation, chromatin formation and gene expression in cancer." *Hum Mol Genet* **10**(7): 687-692.
- Baylin, S. B., J. W. Hoppener, et al. (1986). "DNA methylation patterns of the calcitonin gene in human lung cancers and lymphomas." *Cancer Res* **46**(6): 2917-2922.
- Beadle, G. W. and E. L. Tatum (1941). "Genetic Control of Biochemical Reactions in Neurospora." *Proc Natl Acad Sci U S A* **27**(11): 499-506.
- Ben-Av, P., L. J. Crofford, et al. (1995). "Induction of vascular endothelial growth factor expression in synovial fibroblasts by prostaglandin E and interleukin-1: a potential mechanism for inflammatory angiogenesis." *FEBS letters* **372**(1): 83-87.
- Bender, C. M., M. L. Gonzalzo, et al. (1999). "Roles of cell division and gene transcription in the methylation of CpG islands." *Molecular and cellular biology* **19**(10): 6690-6698.
- Bentz, B. G., G. K. Haines, 3rd, et al. (2000). "Glutathione S-transferase pi in squamous cell carcinoma of the head and neck." *The Laryngoscope* **110**(10 Pt 1): 1642-1647.
- Berger, S. L., T. Kouzarides, et al. (2009). "An operational definition of epigenetics." *Genes & development* **23**(7): 781-783.
- Bernstein, B. E., T. S. Mikkelsen, et al. (2006). "A bivalent chromatin structure marks key developmental genes in embryonic stem cells." *Cell* **125**(2): 315-326.
- Bhagavathi, S. and M. Czader (2010). "MicroRNAs in benign and malignant hematopoiesis." *Arch Pathol Lab Med* **134**(9): 1276-1281.
- Bird, A. (2002). "DNA methylation patterns and epigenetic memory." *Genes Dev* **16**(1): 6-21.
- Bock, C., S. Reither, et al. (2005). "BiQ Analyzer: visualization and quality control for DNA methylation data from bisulfite sequencing." *Bioinformatics* **21**(21): 4067-4068.
- Bol, D. K., R. B. Rowley, et al. (2002). "Cyclooxygenase-2 overexpression in the skin of transgenic mice results in suppression of tumor development." *Cancer research* **62**(9): 2516-2521.
- Borchert, G. M., W. Lanier, et al. (2006). "RNA polymerase III transcribes human microRNAs." *Nat Struct Mol Biol* **13**(12): 1097-1101.
- Borde-Chiche, P., M. Diederich, et al. (2001). "Regulation of transcription of the glutathione S-transferase P1 gene by methylation of the minimal promoter in human leukemia cells." *Biochem Pharmacol* **61**(5): 605-612.

- Boultonwood, J. and J. S. Wainscoat (2007). "Gene silencing by DNA methylation in haematological malignancies." *British journal of haematology* **138**(1): 3-11.
- Bourc'his, D., G. L. Xu, et al. (2001). "Dnmt3L and the establishment of maternal genomic imprints." *Science* **294**(5551): 2536-2539.
- Boyum, A. (1976). "Isolation of lymphocytes, granulocytes and macrophages." *Scand J Immunol Suppl* **5**: 9-15.
- Bradbury, E. M. (1992). "Reversible histone modifications and the chromosome cell cycle." *Bioessays* **14**(1): 9-16.
- Bradford, M. M. (1976). "A rapid and sensitive method for the quantitation of microgram quantities of protein utilizing the principle of protein-dye binding." *Anal Biochem* **72**: 248-254.
- Brena, R. M., H. Auer, et al. (2006). "Accurate quantification of DNA methylation using combined bisulfite restriction analysis coupled with the Agilent 2100 Bioanalyzer platform." *Nucleic Acids Res* **34**(3): e17.
- Brena, R. M., H. Auer, et al. (2006). "Quantification of DNA methylation in electrofluidics chips (Bio-COBRA)." *Nat Protoc* **1**(1): 52-58.
- Brennecke, J., A. Stark, et al. (2005). "Principles of microRNA-target recognition." *PLoS Biol* **3**(3): e85.
- Brodzka, B., P. Otevrelva, et al. (2011). "Decitabine-induced apoptosis is derived by Puma and Noxa induction in chronic myeloid leukemia cell line as well as in PBL and is potentiated by SAHA." *Molecular and cellular biochemistry* **350**(1-2): 71-80.
- Bruserud, O., C. Stapnes, et al. (2006). "Protein lysine acetylation in normal and leukaemic haematopoiesis: HDACs as possible therapeutic targets in adult AML." *Expert Opin Ther Targets* **10**(1): 51-68.
- Bueno, M. J., I. Perez de Castro, et al. (2008). "Genetic and epigenetic silencing of microRNA-203 enhances ABL1 and BCR-ABL1 oncogene expression." *Cancer Cell* **13**(6): 496-506.
- Burbano (2006). "Epigenetics and genetic determinism." *História, Ciências, Saúde* **13**: 851-863.
- Burmeister, T., C. Meyer, et al. (2009). "The MLL recombinome of adult CD10-negative B-cell precursor acute lymphoblastic leukemia: results from the GMALL study group." *Blood* **113**(17): 4011-4015.
- Cairns, P., M. Esteller, et al. (2001). "Molecular detection of prostate cancer in urine by GSTP1 hypermethylation." *Clin Cancer Res* **7**(9): 2727-2730.
- Calin, G. A. and C. M. Croce (2006). "MicroRNA signatures in human cancers." *Nat Rev Cancer* **6**(11): 857-866.
- Calin, G. A., C. Sevignani, et al. (2004). "Human microRNA genes are frequently located at fragile sites and genomic regions involved in cancers." *Proc Natl Acad Sci U S A* **101**(9): 2999-3004.
- Cameron, E. E., K. E. Bachman, et al. (1999). "Synergy of demethylation and histone deacetylase inhibition in the re-expression of genes silenced in cancer." *Nat Genet* **21**(1): 103-107.
- Campos, E. I. and D. Reinberg (2009). "Histones: annotating chromatin." *Annual review of genetics* **43**: 559-599.
- Cao, D. L. and X. D. Yao (2010). "Advances in biomarkers for the early diagnosis of prostate cancer." *Chinese journal of cancer* **29**(2): 229-233.

- Chen, L., A. M. MacMillan, et al. (1991). "Direct identification of the active-site nucleophile in a DNA (cytosine-5)-methyltransferase." *Biochemistry* **30**(46): 11018-11025.
- Cheng, J. C., C. B. Yoo, et al. (2004). "Preferential response of cancer cells to zebularine." *Cancer cell* **6**(2): 151-158.
- Cheng, T., W. Cao, et al. (1998). "Prostaglandin E2 induces vascular endothelial growth factor and basic fibroblast growth factor mRNA expression in cultured rat Muller cells." *Investigative ophthalmology & visual science* **39**(3): 581-591.
- Chiam, K., M. M. Centenera, et al. (2011). "GSTP1 DNA Methylation and Expression Status Is Indicative of 5-aza-2'-Deoxycytidine Efficacy in Human Prostate Cancer Cells." *PLoS One* **6**(9): e25634.
- Chim, C. S., W. W. Chan, et al. (2008). "Epigenetic dysregulation of the DAP kinase/p14/HDM2/p53/Apaf-1 apoptosis pathway in acute leukaemias." *Journal of clinical pathology* **61**(7): 844-847.
- Chim, C. S., R. Liang, et al. (2001). "Methylation of p15 and p16 genes in acute promyelocytic leukemia: potential diagnostic and prognostic significance." *Journal of clinical oncology : official journal of the American Society of Clinical Oncology* **19**(7): 2033-2040.
- Chiorazzi, N., K. R. Rai, et al. (2005). "Chronic lymphocytic leukemia." *The New England journal of medicine* **352**(8): 804-815.
- Christensen, B. C., E. A. Houseman, et al. (2009). "Aging and environmental exposures alter tissue-specific DNA methylation dependent upon CpG island context." *PLoS genetics* **5**(8): e1000602.
- Christman, J. K. (2002). "5-Azacytidine and 5-aza-2'-deoxycytidine as inhibitors of DNA methylation: mechanistic studies and their implications for cancer therapy." *Oncogene* **21**(35): 5483-5495.
- Clark, S. J., J. Harrison, et al. (1994). "High sensitivity mapping of methylated cytosines." *Nucleic Acids Res* **22**(15): 2990-2997.
- Cohen, S. M., J. Brennecke, et al. (2006). "Denoising feedback loops by thresholding--a new role for microRNAs." *Genes Dev* **20**(20): 2769-2772.
- Conerly, M. L., S. S. Teves, et al. (2010). "Changes in H2A.Z occupancy and DNA methylation during B-cell lymphomagenesis." *Genome research* **20**(10): 1383-1390.
- Corn, P. G., B. D. Smith, et al. (2000). "E-cadherin expression is silenced by 5' CpG island methylation in acute leukemia." *Clinical cancer research : an official journal of the American Association for Cancer Research* **6**(11): 4243-4248.
- Costa, F. F. (2010). "Epigenomics in cancer management." *Cancer management and research* **2**: 255-265.
- Costello, J. F., M. C. Fruhwald, et al. (2000). "Aberrant CpG-island methylation has non-random and tumour-type-specific patterns." *Nature genetics* **24**(2): 132-138.
- Coughlin, S. S. and I. J. Hall (2002). "Glutathione S-transferase polymorphisms and risk of ovarian cancer: a HuGE review." *Genet Med* **4**(4): 250-257.
- Coughlin, S. S. and I. J. Hall (2002). "A review of genetic polymorphisms and prostate cancer risk." *Ann Epidemiol* **12**(3): 182-196.
- Cress, W. D. and E. Seto (2000). "Histone deacetylases, transcriptional control, and cancer." *J Cell Physiol* **184**(1): 1-16.

- Dahiya, N., C. A. Sherman-Baust, et al. (2008). "MicroRNA expression and identification of putative miRNA targets in ovarian cancer." PLoS One **3**(6): e2436.
- Dawson, D. W., J. S. Hong, et al. (2007). "Global DNA methylation profiling reveals silencing of a secreted form of EphA7 in mouse and human germinal center B-cell lymphomas." Oncogene **26**(29): 4243-4252.
- Deininger, M. (2005). "Resistance to imatinib: mechanisms and management." Journal of the National Comprehensive Cancer Network : JNCCN **3**(6): 757-768.
- Delhommeau, F., S. Dupont, et al. (2009). "Mutation in TET2 in myeloid cancers." The New England journal of medicine **360**(22): 2289-2301.
- Deneberg, S., M. Grovdal, et al. (2010). "Gene-specific and global methylation patterns predict outcome in patients with acute myeloid leukemia." Leukemia : official journal of the Leukemia Society of America, Leukemia Research Fund, U.K **24**(5): 932-941.
- Deng, S., G. A. Calin, et al. (2008). "Mechanisms of microRNA deregulation in human cancer." Cell Cycle **7**(17): 2643-2646.
- Di Croce, L., V. A. Raker, et al. (2002). "Methyltransferase recruitment and DNA hypermethylation of target promoters by an oncogenic transcription factor." Science **295**(5557): 1079-1082.
- Diederichs, S. and D. A. Haber (2006). "Sequence variations of microRNAs in human cancer: alterations in predicted secondary structure do not affect processing." Cancer Res **66**(12): 6097-6104.
- Dodge, J. E., C. Munson, et al. (2001). "KG-1 and KG-1a model the p15 CpG island methylation observed in acute myeloid leukemia patients." Leukemia research **25**(10): 917-925.
- Doi, A., I. H. Park, et al. (2009). "Differential methylation of tissue- and cancer-specific CpG island shores distinguishes human induced pluripotent stem cells, embryonic stem cells and fibroblasts." Nature genetics **41**(12): 1350-1353.
- dos Santos, N. R., R. Torensma, et al. (2000). "Heterogeneous expression of the SSX cancer/testis antigens in human melanoma lesions and cell lines." Cancer Res **60**(6): 1654-1662.
- Drexler, H. G. (1998). "Review of alterations of the cyclin-dependent kinase inhibitor INK4 family genes p15, p16, p18 and p19 in human leukemia-lymphoma cells." Leukemia : official journal of the Leukemia Society of America, Leukemia Research Fund, U.K **12**(6): 845-859.
- Druker, B. J., S. Tamura, et al. (1996). "Effects of a selective inhibitor of the Abl tyrosine kinase on the growth of Bcr-Abl positive cells." Nature medicine **2**(5): 561-566.
- DuBois, R. N., J. Shao, et al. (1996). "G1 delay in cells overexpressing prostaglandin endoperoxide synthase-2." Cancer research **56**(4): 733-737.
- Duffy, M. J., R. Napieralski, et al. (2009). "Methylated genes as new cancer biomarkers." Eur J Cancer.
- Dulaimi, E., I. Ibanez de Caceres, et al. (2004). "Promoter hypermethylation profile of kidney cancer." Clinical cancer research : an official journal of the American Association for Cancer Research **10**(12 Pt 1): 3972-3979.

- Durland-Busbice, S. and D. Reisman (2002). "Lack of p53 expression in human myeloid leukemias is not due to mutations in transcriptional regulatory regions of the gene." Leukemia : official journal of the Leukemia Society of America, Leukemia Research Fund, U.K **16**(10): 2165-2167.
- Duvoix, A., M. Schnekenburger, et al. (2004). "Expression of glutathione S-transferase P1-1 in leukemic cells is regulated by inducible AP-1 binding." Cancer Lett **216**(2): 207-219.
- Eaton, D. L. and T. K. Bammler (1999). "Concise review of the glutathione S-transferases and their significance to toxicology." Toxicol Sci **49**(2): 156-164.
- Eberhart, C. E., R. J. Coffey, et al. (1994). "Up-regulation of cyclooxygenase 2 gene expression in human colorectal adenomas and adenocarcinomas." Gastroenterology **107**(4): 1183-1188.
- Eden, S., M. Constanica, et al. (2001). "An upstream repressor element plays a role in Igf2 imprinting." Embo J **20**(13): 3518-3525.
- Ehrich, M., J. Turner, et al. (2008). "Cytosine methylation profiling of cancer cell lines." Proceedings of the National Academy of Sciences of the United States of America **105**(12): 4844-4849.
- Eiring, A. M., J. G. Harb, et al. (2010). "miR-328 functions as an RNA decoy to modulate hnRNP E2 regulation of mRNA translation in leukemic blasts." Cell **140**(5): 652-665.
- Ekmekci, C. G., M. I. Gutierrez, et al. (2004). "Aberrant methylation of multiple tumor suppressor genes in acute myeloid leukemia." American journal of hematology **77**(3): 233-240.
- Elder, D. J., D. E. Halton, et al. (2000). "Apoptosis induction and cyclooxygenase-2 regulation in human colorectal adenoma and carcinoma cell lines by the cyclooxygenase-2-selective non-steroidal anti-inflammatory drug NS-398." International journal of cancer. Journal international du cancer **86**(4): 553-560.
- Ellis, L., P. W. Atadja, et al. (2009). "Epigenetics in cancer: targeting chromatin modifications." Molecular cancer therapeutics **8**(6): 1409-1420.
- Esquela-Kerscher, A. and F. J. Slack (2006). "Oncomirs - microRNAs with a role in cancer." Nat Rev Cancer **6**(4): 259-269.
- Esteller, M. (2002). "CpG island hypermethylation and tumor suppressor genes: a booming present, a brighter future." Oncogene **21**(35): 5427-5440.
- Esteller, M. (2003). "Relevance of DNA methylation in the management of cancer." Lancet Oncol **4**(6): 351-358.
- Esteller, M. (2006). "Epigenetics provides a new generation of oncogenes and tumour-suppressor genes." British journal of cancer **94**(2): 179-183.
- Esteller, M. (2008). "Epigenetics in cancer." The New England journal of medicine **358**(11): 1148-1159.
- Esteller, M. (2011). "Epigenetic changes in cancer." F1000 biology reports **3**: 9.
- Esteller, M., P. G. Corn, et al. (1998). "Inactivation of glutathione S-transferase P1 gene by promoter hypermethylation in human neoplasia." Cancer research **58**(20): 4515-4518.
- Esteller, M., G. Gaidano, et al. (2002). "Hypermethylation of the DNA repair gene O(6)-methylguanine DNA methyltransferase and survival of patients with diffuse large B-cell lymphoma." J Natl Cancer Inst **94**(1): 26-32.

- Esteller, M., M. Guo, et al. (2002). "Hypermethylation-associated Inactivation of the Cellular Retinol-Binding-Protein 1 Gene in Human Cancer." *Cancer research* **62**(20): 5902-5905.
- Esteller, M., S. R. Hamilton, et al. (1999). "Inactivation of the DNA repair gene O6-methylguanine-DNA methyltransferase by promoter hypermethylation is a common event in primary human neoplasia." *Cancer research* **59**(4): 793-797.
- Esteller, M. and J. G. Herman (2002). "Cancer as an epigenetic disease: DNA methylation and chromatin alterations in human tumours." *J Pathol* **196**(1): 1-7.
- Esteller, M., M. Sanchez-Cespedes, et al. (1999). "Detection of aberrant promoter hypermethylation of tumor suppressor genes in serum DNA from non-small cell lung cancer patients." *Cancer Res* **59**(1): 67-70.
- Evron, E., W. C. Dooley, et al. (2001). "Detection of breast cancer cells in ductal lavage fluid by methylation-specific PCR." *Lancet* **357**(9265): 1335-1336.
- Fatemi, M., A. Hermann, et al. (2002). "Dnmt3a and Dnmt1 functionally cooperate during de novo methylation of DNA." *Eur J Biochem* **269**(20): 4981-4984.
- Feinberg, A. P. (2005). "Cancer epigenetics is no Mickey Mouse." *Cancer cell* **8**(4): 267-268.
- Feinberg, A. P. and B. Vogelstein (1983). "Hypomethylation distinguishes genes of some human cancers from their normal counterparts." *Nature* **301**(5895): 89-92.
- Feinberg, A. P. and B. Vogelstein (1983). "Hypomethylation of ras oncogenes in primary human cancers." *Biochem Biophys Res Commun* **111**(1): 47-54.
- Fiedler, W., H. Serve, et al. (2005). "A phase 1 study of SU11248 in the treatment of patients with refractory or resistant acute myeloid leukemia (AML) or not amenable to conventional therapy for the disease." *Blood* **105**(3): 986-993.
- Figuroa, M. E., S. Lugthart, et al. (2010). "DNA methylation signatures identify biologically distinct subtypes in acute myeloid leukemia." *Cancer cell* **17**(1): 13-27.
- Fosslien, E. (2001). "Review: molecular pathology of cyclooxygenase-2 in cancer-induced angiogenesis." *Annals of clinical and laboratory science* **31**(4): 325-348.
- Fraga, M. F., E. Ballestar, et al. (2005). "Loss of acetylation at Lys16 and trimethylation at Lys20 of histone H4 is a common hallmark of human cancer." *Nat Genet* **37**(4): 391-400.
- Friedman, R. C., K. K. Farh, et al. (2009). "Most mammalian mRNAs are conserved targets of microRNAs." *Genome Res* **19**(1): 92-105.
- Frommer, M., L. E. McDonald, et al. (1992). "A genomic sequencing protocol that yields a positive display of 5-methylcytosine residues in individual DNA strands." *Proc Natl Acad Sci U S A* **89**(5): 1827-1831.
- Furley, A. J., B. R. Reeves, et al. (1986). "Divergent molecular phenotypes of KG1 and KG1a myeloid cell lines." *Blood* **68**(5): 1101-1107.
- Furukawa, Y., K. Sutheesophon, et al. (2005). "Methylation silencing of the Apaf-1 gene in acute leukemia." *Molecular cancer research : MCR* **3**(6): 325-334.
- Galm, O., J. G. Herman, et al. (2006). "The fundamental role of epigenetics in hematopoietic malignancies." *Blood Rev* **20**(1): 1-13.

- Galm, O., S. Wilop, et al. (2005). "Clinical implications of aberrant DNA methylation patterns in acute myelogenous leukemia." Annals of hematology **84 Suppl 1**: 39-46.
- Garcia-Manero, G., J. Daniel, et al. (2002). "DNA methylation of multiple promoter-associated CpG islands in adult acute lymphocytic leukemia." Clinical cancer research : an official journal of the American Association for Cancer Research **8(7)**: 2217-2224.
- Garcia-Manero, G., H. Yang, et al. (2009). "Epigenetics of acute lymphocytic leukemia." Seminars in hematology **46(1)**: 24-32.
- Gardiner-Garden, M. and M. Frommer (1987). "CpG islands in vertebrate genomes." J Mol Biol **196(2)**: 261-282.
- Gebhard, C., L. Schwarzfischer, et al. (2006). "Rapid and sensitive detection of CpG-methylation using methyl-binding (MB)-PCR." Nucleic acids research **34(11)**: e82.
- Gebhard, C., L. Schwarzfischer, et al. (2006). "Genome-wide profiling of CpG methylation identifies novel targets of aberrant hypermethylation in myeloid leukemia." Cancer research **66(12)**: 6118-6128.
- Ghoshal, K., J. Datta, et al. (2005). "5-Aza-deoxycytidine induces selective degradation of DNA methyltransferase 1 by a proteasomal pathway that requires the KEN box, bromo-adjacent homology domain, and nuclear localization signal." Mol Cell Biol **25(11)**: 4727-4741.
- Giles, F. J., H. M. Kantarjian, et al. (2002). "Bone marrow cyclooxygenase-2 levels are elevated in chronic-phase chronic myeloid leukaemia and are associated with reduced survival." British journal of haematology **119(1)**: 38-45.
- Giotopoulos, G., C. McCormick, et al. (2006). "DNA methylation during mouse hemopoietic differentiation and radiation-induced leukemia." Experimental hematology **34(11)**: 1462-1470.
- Glaser, K. B., M. J. Staver, et al. (2003). "Gene expression profiling of multiple histone deacetylase (HDAC) inhibitors: defining a common gene set produced by HDAC inhibition in T24 and MDA carcinoma cell lines." Mol Cancer Ther **2(2)**: 151-163.
- Glover, A. B., B. R. Leyland-Jones, et al. (1987). "Azacitidine: 10 years later." Cancer Treat Rep **71(7-8)**: 737-746.
- Goessl, C., H. Krause, et al. (2000). "Fluorescent methylation-specific polymerase chain reaction for DNA-based detection of prostate cancer in bodily fluids." Cancer Res **60(21)**: 5941-5945.
- Goessl, C., M. Muller, et al. (2001). "DNA-based detection of prostate cancer in blood, urine, and ejaculates." Ann N Y Acad Sci **945**: 51-58.
- Goldberg, A. D., C. D. Allis, et al. (2007). "Epigenetics: a landscape takes shape." Cell **128(4)**: 635-638.
- Gonzalgo, M. L., M. Nakayama, et al. (2004). "Detection of GSTP1 methylation in prostatic secretions using combinatorial MSP analysis." Urology **63(2)**: 414-418.
- Goto, S., T. Iida, et al. (1999). "Overexpression of glutathione S-transferase pi enhances the adduct formation of cisplatin with glutathione in human cancer cells." Free radical research **31(6)**: 549-558.

- Grady, W. M., A. Rajput, et al. (2001). "Detection of aberrantly methylated hMLH1 promoter DNA in the serum of patients with microsatellite unstable colon cancer." *Cancer Res* **61**(3): 900-902.
- Graff, J. R., J. G. Herman, et al. (1997). "Mapping patterns of CpG island methylation in normal and neoplastic cells implicates both upstream and downstream regions in de novo methylation." *J Biol Chem* **272**(35): 22322-22329.
- Green, J. A., L. J. Robertson, et al. (1993). "Glutathione S-transferase expression in benign and malignant ovarian tumours." *British journal of cancer* **68**(2): 235-239.
- Greger, V., E. Passarge, et al. (1989). "Epigenetic changes may contribute to the formation and spontaneous regression of retinoblastoma." *Hum Genet* **83**(2): 155-158.
- Griffith, J. S. and H. R. Mahler (1969). "DNA ticketing theory of memory." *Nature* **223**(5206): 580-582.
- Grimson, A., K. K. Farh, et al. (2007). "MicroRNA targeting specificity in mammals: determinants beyond seed pairing." *Mol Cell* **27**(1): 91-105.
- Grimwade, D., H. Walker, et al. (1998). "The importance of diagnostic cytogenetics on outcome in AML: analysis of 1,612 patients entered into the MRC AML 10 trial. The Medical Research Council Adult and Children's Leukaemia Working Parties." *Blood* **92**(7): 2322-2333.
- Guenther, M. G., S. S. Levine, et al. (2007). "A chromatin landmark and transcription initiation at most promoters in human cells." *Cell* **130**(1): 77-88.
- Guil, S. and M. Esteller (2009). "DNA methylomes, histone codes and miRNAs: tying it all together." *Int J Biochem Cell Biol* **41**(1): 87-95.
- Guo, J., M. Burger, et al. (2005). "Differential DNA methylation of gene promoters in small B-cell lymphomas." *American journal of clinical pathology* **124**(3): 430-439.
- Haaf, T. (2006). "Methylation dynamics in the early mammalian embryo: implications of genome reprogramming defects for development." *Curr Top Microbiol Immunol* **310**: 13-22.
- Hagiwara, K., H. Nagai, et al. (2007). "Frequent DNA methylation but not mutation of the ID4 gene in malignant lymphoma." *Journal of clinical and experimental hematopathology : JCEH* **47**(1): 15-18.
- Haig, D. (2004). "The (dual) origin of epigenetics." *Cold Spring Harb Symp Quant Biol* **69**: 67-70.
- Hall, B. K. (1992). "Evolutionary developmental biology."
- Hansen, R. S., C. Wijmenga, et al. (1999). "The DNMT3B DNA methyltransferase gene is mutated in the ICF immunodeficiency syndrome." *Proc Natl Acad Sci U S A* **96**(25): 14412-14417.
- Harrington, M. A., P. A. Jones, et al. (1988). "Cytosine methylation does not affect binding of transcription factor Sp1." *Proc Natl Acad Sci U S A* **85**(7): 2066-2070.
- Harris, R. C. and M. D. Breyer (2001). "Physiological regulation of cyclooxygenase-2 in the kidney." *American journal of physiology. Renal physiology* **281**(1): F1-11.
- Harris, R. E., J. Beebe-Donk, et al. (2007). "Reduced risk of human lung cancer by selective cyclooxygenase 2 (COX-2) blockade: results of a case control study." *International journal of biological sciences* **3**(5): 328-334.

- Hauptstock, V., S. Kuriakose, et al. (2011). "Glutathione-S-transferase pi 1(GSTP1) gene silencing in prostate cancer cells is reversed by the histone deacetylase inhibitor depsipeptide." Biochemical and biophysical research communications.
- Hayashi, M., Y. Tokuchi, et al. (2001). "Reduced HIC-1 gene expression in non-small cell lung cancer and its clinical significance." Anticancer research **21**(1B): 535-540.
- Hayatsu, H. (2008). "Discovery of bisulfite-mediated cytosine conversion to uracil, the key reaction for DNA methylation analysis--a personal account." Proc Jpn Acad Ser B Phys Biol Sci **84**(8): 321-330.
- Hazar, B., M. Ergin, et al. (2004). "Cyclooxygenase-2 (Cox-2) expression in lymphomas." Leukemia & lymphoma **45**(7): 1395-1399.
- He, H., K. Jazdzewski, et al. (2005). "The role of microRNA genes in papillary thyroid carcinoma." Proc Natl Acad Sci U S A **102**(52): 19075-19080.
- He, L. and G. J. Hannon (2004). "MicroRNAs: small RNAs with a big role in gene regulation." Nat Rev Genet **5**(7): 522-531.
- Hegi, M. E., L. Liu, et al. (2008). "Correlation of O6-methylguanine methyltransferase (MGMT) promoter methylation with clinical outcomes in glioblastoma and clinical strategies to modulate MGMT activity." Journal of clinical oncology : official journal of the American Society of Clinical Oncology **26**(25): 4189-4199.
- Henrique, R. and C. Jeronimo (2004). "Molecular detection of prostate cancer: a role for GSTP1 hypermethylation." European urology **46**(5): 660-669; discussion 669.
- Herceg, Z. and A. Paliwal (2011). "Epigenetic mechanisms in hepatocellular carcinoma: How environmental factors influence the epigenome." Mutation research **727**(3): 55-61.
- Herman, J. G. and S. B. Baylin (2003). "Gene silencing in cancer in association with promoter hypermethylation." N Engl J Med **349**(21): 2042-2054.
- Herman, J. G., C. I. Civin, et al. (1997). "Distinct patterns of inactivation of p15INK4B and p16INK4A characterize the major types of hematological malignancies." Cancer research **57**(5): 837-841.
- Herman, J. G., J. R. Graff, et al. (1996). "Methylation-specific PCR: a novel PCR assay for methylation status of CpG islands." Proc Natl Acad Sci U S A **93**(18): 9821-9826.
- Herman, J. G., J. Jen, et al. (1996). "Hypermethylation-associated inactivation indicates a tumor suppressor role for p15INK4B." Cancer research **56**(4): 722-727.
- Hideshima, T., P. L. Bergsagel, et al. (2004). "Advances in biology of multiple myeloma: clinical applications." Blood **104**(3): 607-618.
- Hirst, M. and M. A. Marra (2009). "Epigenetics and human disease." Int J Biochem Cell Biol **41**(1): 136-146.
- Hochedlinger, K., R. Blelloch, et al. (2004). "Reprogramming of a melanoma genome by nuclear transplantation." Genes & development **18**(15): 1875-1885.
- Hollenbach, P. W., A. N. Nguyen, et al. (2010). "A comparison of azacitidine and decitabine activities in acute myeloid leukemia cell lines." PLoS one **5**(2): e9001.

- Holler, M., G. Westin, et al. (1988). "Sp1 transcription factor binds DNA and activates transcription even when the binding site is CpG methylated." *Genes Dev* **2**(9): 1127-1135.
- Holliday (2006). "A Historical Overview." *Epigenetics* **1**:2: 76-80.
- Holliday, R. and J. E. Pugh (1975). "DNA modification mechanisms and gene activity during development." *Science* **187**(4173): 226-232.
- Hopkins, T. G., P. A. Burns, et al. (2007). "DNA methylation of GSTP1 as biomarker in diagnosis of prostate cancer." *Urology* **69**(1): 11-16.
- Hopkins-Donaldson, S., A. Ziegler, et al. (2003). "Silencing of death receptor and caspase-8 expression in small cell lung carcinoma cell lines and tumors by DNA methylation." *Cell death and differentiation* **10**(3): 356-364.
- Hornstein, E. and N. Shomron (2006). "Canalization of development by microRNAs." *Nat Genet* **38 Suppl**: S20-24.
- Hortshemke (2005). "Was ist Epigenetik?" *Medizinische Genetik* **3**: 251-253.
- Hsu, S. D., C. H. Chu, et al. (2008). "miRNAMap 2.0: genomic maps of microRNAs in metazoan genomes." *Nucleic Acids Res* **36**(Database issue): D165-169.
- Hughes, L. A., P. A. van den Brandt, et al. (2009). "Early life exposure to famine and colorectal cancer risk: a role for epigenetic mechanisms." *PloS one* **4**(11): e7951.
- Huntly, B. J. and D. G. Gilliland (2005). "Leukaemia stem cells and the evolution of cancer-stem-cell research." *Nat Rev Cancer* **5**(4): 311-321.
- Irizarry, R. A., C. Ladd-Acosta, et al. (2009). "The human colon cancer methylome shows similar hypo- and hypermethylation at conserved tissue-specific CpG island shores." *Nature genetics* **41**(2): 178-186.
- Ismail, E. A., M. I. El-Mogy, et al. (2011). "Methylation Pattern of Calcitonin (CALCA) Gene in Pediatric Acute Leukemia." *Journal of pediatric hematology/oncology : official journal of the American Society of Pediatric Hematology/Oncology*.
- Issa, J. P., S. B. Baylin, et al. (1997). "DNA methylation changes in hematologic malignancies: biologic and clinical implications." *Leukemia : official journal of the Leukemia Society of America, Leukemia Research Fund, U.K* **11 Suppl 1**: S7-11.
- Issa, J. P., G. Garcia-Manero, et al. (2004). "Phase 1 study of low-dose prolonged exposure schedules of the hypomethylating agent 5-aza-2'-deoxycytidine (decitabine) in hematopoietic malignancies." *Blood* **103**(5): 1635-1640.
- Issa, J. P. and H. M. Kantarjian (2009). "Targeting DNA methylation." *Clinical cancer research : an official journal of the American Association for Cancer Research* **15**(12): 3938-3946.
- Issa, J. P., B. A. Zehnbaauer, et al. (1997). "HIC1 hypermethylation is a late event in hematopoietic neoplasms." *Cancer research* **57**(9): 1678-1681.
- Iwai, M., H. Kiyoi, et al. (2005). "Expression and methylation status of the FHIT gene in acute myeloid leukemia and myelodysplastic syndrome." *Leukemia : official journal of the Leukemia Society of America, Leukemia Research Fund, U.K* **19**(8): 1367-1375.
- Iwasaki, H. and K. Akashi (2007). "Hematopoietic developmental pathways: on cellular basis." *Oncogene* **26**(47): 6687-6696.
- Jaenisch, R. and A. Bird (2003). "Epigenetic regulation of gene expression: how the genome integrates intrinsic and environmental signals." *Nat Genet* **33 Suppl**: 245-254.

- Jelinek, J., V. Gharibyan, et al. (2011). "Aberrant DNA methylation is associated with disease progression, resistance to imatinib and shortened survival in chronic myelogenous leukemia." *PloS one* **6**(7): e22110.
- Jeltsch, A. (2002). "Beyond Watson and Crick: DNA methylation and molecular enzymology of DNA methyltransferases." *Chembiochem* **3**(4): 274-293.
- Jenal, M., C. Britschgi, et al. (2010). "Inactivation of the hypermethylated in cancer 1 tumour suppressor--not just a question of promoter hypermethylation?" *Swiss medical weekly* **140**: w13106.
- Jeronimo, C., R. Henrique, et al. (2004). "A quantitative promoter methylation profile of prostate cancer." *Clinical cancer research : an official journal of the American Association for Cancer Research* **10**(24): 8472-8478.
- Jeronimo, C., H. Usadel, et al. (2002). "Quantitative GSTP1 hypermethylation in bodily fluids of patients with prostate cancer." *Urology* **60**(6): 1131-1135.
- Jhaveri, M. S. and C. S. Morrow (1998). "Methylation-mediated regulation of the glutathione S-transferase P1 gene in human breast cancer cells." *Gene* **210**(1): 1-7.
- Jiemjit, A., T. E. Fandy, et al. (2008). "p21(WAF1/CIP1) induction by 5-azacytosine nucleosides requires DNA damage." *Oncogene* **27**(25): 3615-3623.
- Jirtle, R. L. (1999). "Genomic imprinting and cancer." *Exp Cell Res* **248**(1): 18-24.
- John, A. and G. Tuszynski (2001). "The role of matrix metalloproteinases in tumor angiogenesis and tumor metastasis." *Pathology oncology research : POR* **7**(1): 14-23.
- Jones, P. A. (1985). "Altering gene expression with 5-azacytidine." *Cell* **40**(3): 485-486.
- Jones, P. A. (1999). "The DNA methylation paradox." *Trends Genet* **15**(1): 34-37.
- Jones, P. A. and S. B. Baylin (2002). "The fundamental role of epigenetic events in cancer." *Nat Rev Genet* **3**(6): 415-428.
- Jones, P. A. and S. B. Baylin (2007). "The epigenomics of cancer." *Cell* **128**(4): 683-692.
- Jones, P. A. and D. Takai (2001). "The role of DNA methylation in mammalian epigenetics." *Science* **293**(5532): 1068-1070.
- Jones, P. A. and S. M. Taylor (1980). "Cellular differentiation, cytidine analogs and DNA methylation." *Cell* **20**(1): 85-93.
- Jones, P. A., S. M. Taylor, et al. (1982). "Cell cycle-specific reactivation of an inactive X-chromosome locus by 5-azadeoxycytidine." *Proc Natl Acad Sci U S A* **79**(4): 1215-1219.
- Jones, P. L., G. J. Veenstra, et al. (1998). "Methylated DNA and MeCP2 recruit histone deacetylase to repress transcription." *Nat Genet* **19**(2): 187-191.
- Juttermann, R., E. Li, et al. (1994). "Toxicity of 5-aza-2'-deoxycytidine to mammalian cells is mediated primarily by covalent trapping of DNA methyltransferase rather than DNA demethylation." *Proceedings of the National Academy of Sciences of the United States of America* **91**(25): 11797-11801.
- Kantarjian, H., J. P. Issa, et al. (2006). "Decitabine improves patient outcomes in myelodysplastic syndromes: results of a phase III randomized study." *Cancer* **106**(8): 1794-1803.
- Kantarjian, H. M., S. O'Brien, et al. (2003). "Results of decitabine (5-aza-2'deoxycytidine) therapy in 130 patients with chronic myelogenous leukemia." *Cancer* **98**(3): 522-528.

- Katzenellenbogen, R. A., S. B. Baylin, et al. (1999). "Hypermethylation of the DAP-kinase CpG island is a common alteration in B-cell malignancies." Blood **93**(12): 4347-4353.
- Kawamata, T., H. Seitz, et al. (2009). "Structural determinants of miRNAs for RISC loading and slicer-independent unwinding." Nat Struct Mol Biol **16**(9): 953-960.
- Kawano, S., C. W. Miller, et al. (1999). "Loss of p73 gene expression in leukemias/lymphomas due to hypermethylation." Blood **94**(3): 1113-1120.
- Kawasaki, H., L. Schiltz, et al. (2000). "ATF-2 has intrinsic histone acetyltransferase activity which is modulated by phosphorylation." Nature **405**(6783): 195-200.
- Kennedy, J. A. and F. Barabe (2008). "Investigating human leukemogenesis: from cell lines to in vivo models of human leukemia." Leukemia **22**(11): 2029-2040.
- Ketterer, B. (1998). "Glutathione S-transferases and prevention of cellular free radical damage." Free Radic Res **28**(6): 647-658.
- Kim, V. N. and J. W. Nam (2006). "Genomics of microRNA." Trends Genet **22**(3): 165-173.
- Kimura, A. and M. Horikoshi (1998). "How do histone acetyltransferases select lysine residues in core histones?" FEBS Lett **431**(2): 131-133.
- Kinzler, K. W. and B. Vogelstein (1997). "Cancer-susceptibility genes. Gatekeepers and caretakers." Nature **386**(6627): 761, 763.
- Knudson, A. G., Jr. (1971). "Mutation and cancer: statistical study of retinoblastoma." Proceedings of the National Academy of Sciences of the United States of America **68**(4): 820-823.
- Ko, M., Y. Huang, et al. (2010). "Impaired hydroxylation of 5-methylcytosine in myeloid cancers with mutant TET2." Nature **468**(7325): 839-843.
- Kondo, M., I. L. Weissman, et al. (1997). "Identification of clonogenic common lymphoid progenitors in mouse bone marrow." Cell **91**(5): 661-672.
- Kornberg, R. D. and Y. Lorch (1999). "Twenty-five years of the nucleosome, fundamental particle of the eukaryote chromosome." Cell **98**(3): 285-294.
- Koshland, D. and A. Strunnikov (1996). "Mitotic chromosome condensation." Annu Rev Cell Dev Biol **12**: 305-333.
- Kouzarides, T. (2007). "Chromatin modifications and their function." Cell **128**(4): 693-705.
- Koyama, M., T. Oka, et al. (2003). "Activated proliferation of B-cell lymphomas/leukemias with the SHP1 gene silencing by aberrant CpG methylation." Laboratory investigation; a journal of technical methods and pathology **83**(12): 1849-1858.
- Kumaki, Y., M. Oda, et al. (2008). "QUMA: quantification tool for methylation analysis." Nucleic Acids Res **36**(Web Server issue): W170-175.
- Kurdistani, S. K., S. Tavazoie, et al. (2004). "Mapping global histone acetylation patterns to gene expression." Cell **117**(6): 721-733.
- Kwak, P. B., S. Iwasaki, et al. (2010). "The microRNA pathway and cancer." Cancer science **101**(11): 2309-2315.
- Kwak, P. B., S. Iwasaki, et al. (2010). "The microRNA pathway and cancer." Cancer Sci **101**(11): 2309-2315.
- Lacroix, M. (2009). "MDA-MB-435 cells are from melanoma, not from breast cancer." Cancer chemotherapy and pharmacology **63**(3): 567.

- Ladetto, M., S. Vallet, et al. (2005). "Cyclooxygenase-2 (COX-2) is frequently expressed in multiple myeloma and is an independent predictor of poor outcome." *Blood* **105**(12): 4784-4791.
- Lai, A. Y., M. Fatemi, et al. (2010). "DNA methylation prevents CTCF-mediated silencing of the oncogene BCL6 in B cell lymphomas." *The Journal of experimental medicine* **207**(9): 1939-1950.
- Lakshmikuttyamma, A., S. A. Scott, et al. (2010). "Reexpression of epigenetically silenced AML tumor suppressor genes by SUV39H1 inhibition." *Oncogene* **29**(4): 576-588.
- Lasabova, Z., P. Tilandyova, et al. (2010). "Hypermethylation of the GSTP1 promoter region in breast cancer is associated with prognostic clinicopathological parameters." *Neoplasma* **57**(1): 35-40.
- Lavelle, D., J. DeSimone, et al. (2003). "Decitabine induces cell cycle arrest at the G1 phase via p21(WAF1) and the G2/M phase via the p38 MAP kinase pathway." *Leukemia research* **27**(11): 999-1007.
- Lee, R. C., R. L. Feinbaum, et al. (1993). "The *C. elegans* heterochronic gene *lin-4* encodes small RNAs with antisense complementarity to *lin-14*." *Cell* **75**(5): 843-854.
- Lee, W. H., W. B. Isaacs, et al. (1997). "CG island methylation changes near the GSTP1 gene in prostatic carcinoma cells detected using the polymerase chain reaction: a new prostate cancer biomarker." *Cancer Epidemiol Biomarkers Prev* **6**(6): 443-450.
- Lee, W. H., R. A. Morton, et al. (1994). "Cytidine methylation of regulatory sequences near the *pi*-class glutathione S-transferase gene accompanies human prostatic carcinogenesis." *Proc Natl Acad Sci U S A* **91**(24): 11733-11737.
- Lee, Y., K. Jeon, et al. (2002). "MicroRNA maturation: stepwise processing and subcellular localization." *EMBO J* **21**(17): 4663-4670.
- Lee, Y., M. Kim, et al. (2004). "MicroRNA genes are transcribed by RNA polymerase II." *EMBO J* **23**(20): 4051-4060.
- Lehmann, U., B. Hasemeier, et al. (2008). "Epigenetic inactivation of microRNA gene *hsa-mir-9-1* in human breast cancer." *J Pathol* **214**(1): 17-24.
- Lennartsson, A. and K. Ekwall (2009). "Histone modification patterns and epigenetic codes." *Biochimica et biophysica acta* **1790**(9): 863-868.
- Leone, G., F. D'Alo, et al. (2008). "Epigenetic treatment of myelodysplastic syndromes and acute myeloid leukemias." *Curr Med Chem* **15**(13): 1274-1287.
- Levine, J. J., K. M. Stimson-Crider, et al. (2003). "Effects of methylation on expression of TMS1/ASC in human breast cancer cells." *Oncogene* **22**(22): 3475-3488.
- Lewis, B. P., C. B. Burge, et al. (2005). "Conserved seed pairing, often flanked by adenosines, indicates that thousands of human genes are microRNA targets." *Cell* **120**(1): 15-20.
- Ley, T. J., L. Ding, et al. (2010). "DNMT3A mutations in acute myeloid leukemia." *The New England journal of medicine* **363**(25): 2424-2433.
- Li, E., T. H. Bestor, et al. (1992). "Targeted mutation of the DNA methyltransferase gene results in embryonic lethality." *Cell* **69**(6): 915-926.
- Li, L. C. and R. Dahiya (2002). "MethPrimer: designing primers for methylation PCRs." *Bioinformatics* **18**(11): 1427-1431.

- Li, Y., H. Nagai, et al. (2002). "Aberrant DNA methylation of p57(KIP2) gene in the promoter region in lymphoid malignancies of B-cell phenotype." *Blood* **100**(7): 2572-2577.
- Lin, X. and W. G. Nelson (2003). "Methyl-CpG-binding domain protein-2 mediates transcriptional repression associated with hypermethylated GSTP1 CpG islands in MCF-7 breast cancer cells." *Cancer research* **63**(2): 498-504.
- Lin, X., M. Tascilar, et al. (2001). "GSTP1 CpG island hypermethylation is responsible for the absence of GSTP1 expression in human prostate cancer cells." *Am J Pathol* **159**(5): 1815-1826.
- Liu, J., M. A. Carmell, et al. (2004). "Argonaute2 is the catalytic engine of mammalian RNAi." *Science* **305**(5689): 1437-1441.
- Liu, X. H. and D. P. Rose (1996). "Differential expression and regulation of cyclooxygenase-1 and -2 in two human breast cancer cell lines." *Cancer research* **56**(22): 5125-5127.
- Liu, X. H., S. Yao, et al. (1998). "NS398, a selective cyclooxygenase-2 inhibitor, induces apoptosis and down-regulates bcl-2 expression in LNCaP cells." *Cancer research* **58**(19): 4245-4249.
- Lo, H. W., L. Stephenson, et al. (2008). "Identification and functional characterization of the human glutathione S-transferase P1 gene as a novel transcriptional target of the p53 tumor suppressor gene." *Mol Cancer Res* **6**(5): 843-850.
- Lujambio, A., S. Ropero, et al. (2007). "Genetic unmasking of an epigenetically silenced microRNA in human cancer cells." *Cancer Res* **67**(4): 1424-1429.
- Lutsik, P., L. Feuerbach, et al. (2011). "BiQ Analyzer HT: locus-specific analysis of DNA methylation by high-throughput bisulfite sequencing." *Nucleic acids research* **39** **Suppl 2**: W551-556.
- Ma, X., Q. Yang, et al. (2004). "Promoter methylation regulates cyclooxygenase expression in breast cancer." *Breast cancer research : BCR* **6**(4): R316-321.
- Mahlknecht, U. and D. Hoelzer (2000). "Histone acetylation modifiers in the pathogenesis of malignant disease." *Mol Med* **6**(8): 623-644.
- Margison, G. P., A. C. Povey, et al. (2003). "Variability and regulation of O6-alkylguanine-DNA alkyltransferase." *Carcinogenesis* **24**(4): 625-635.
- Marino-Ramirez, L., J. L. Spouge, et al. (2004). "Statistical analysis of over-represented words in human promoter sequences." *Nucleic Acids Res* **32**(3): 949-958.
- Marsit, C. J., E. A. Houseman, et al. (2007). "Promoter hypermethylation is associated with current smoking, age, gender and survival in bladder cancer." *Carcinogenesis* **28**(8): 1745-1751.
- McDonald, H. L., R. D. Gascoyne, et al. (2000). "Involvement of the X chromosome in non-Hodgkin lymphoma." *Genes, chromosomes & cancer* **28**(3): 246-257.
- Meiers, I., J. H. Shanks, et al. (2007). "Glutathione S-transferase pi (GSTP1) hypermethylation in prostate cancer: review 2007." *Pathology* **39**(3): 299-304.
- Meissner, A., T. S. Mikkelsen, et al. (2008). "Genome-scale DNA methylation maps of pluripotent and differentiated cells." *Nature* **454**(7205): 766-770.
- Melki, J. R. and S. J. Clark (2002). "DNA methylation changes in leukaemia." *Seminars in cancer biology* **12**(5): 347-357.
- Melki, J. R., P. C. Vincent, et al. (1999). "Cancer-specific region of hypermethylation identified within the HIC1 putative tumour suppressor gene in acute myeloid

- leukaemia." Leukemia : official journal of the Leukemia Society of America, Leukemia Research Fund, U.K **13**(6): 877-883.
- Melki, J. R., P. C. Vincent, et al. (1999). "Concurrent DNA hypermethylation of multiple genes in acute myeloid leukemia." Cancer research **59**(15): 3730-3740.
- Melo, S. A. and M. Esteller (2010). "Dysregulation of microRNAs in cancer: Playing with fire." FEBS Lett.
- Meng, X. Y., S. T. Zhu, et al. (2010). "Promoter hypermethylation of cyclooxygenase-2 gene in esophageal squamous cell carcinoma." Diseases of the esophagus : official journal of the International Society for Diseases of the Esophagus / I.S.D.E.
- Meyer, C., E. Kowarz, et al. (2009). "New insights to the MLL recombinome of acute leukemias." Leukemia : official journal of the Leukemia Society of America, Leukemia Research Fund, U.K **23**(8): 1490-1499.
- Millar, D. S., C. L. Paul, et al. (2000). "A distinct sequence (ATAAA)_n separates methylated and unmethylated domains at the 5'-end of the GSTP1 CpG island." J Biol Chem **275**(32): 24893-24899.
- Miller, T. A., D. J. Witter, et al. (2003). "Histone deacetylase inhibitors." Journal of medicinal chemistry **46**(24): 5097-5116.
- Minucci, S., C. Nervi, et al. (2001). "Histone deacetylases: a common molecular target for differentiation treatment of acute myeloid leukemias?" Oncogene **20**(24): 3110-3115.
- Minucci, S. and P. G. Pelicci (2006). "Histone deacetylase inhibitors and the promise of epigenetic (and more) treatments for cancer." Nat Rev Cancer **6**(1): 38-51.
- Mitelman, F., B. Johansson, et al. (2007). "The impact of translocations and gene fusions on cancer causation." Nat Rev Cancer **7**(4): 233-245.
- Mitsiades, C. S., N. S. Mitsiades, et al. (2004). "Transcriptional signature of histone deacetylase inhibition in multiple myeloma: biological and clinical implications." Proc Natl Acad Sci U S A **101**(2): 540-545.
- Mizuno, S., T. Chijiwa, et al. (2001). "Expression of DNA methyltransferases DNMT1, 3A, and 3B in normal hematopoiesis and in acute and chronic myelogenous leukemia." Blood **97**(5): 1172-1179.
- Moch, K. (2004). "Das überholte Paradigma der Gentechnik." Öko-Institut e.V.
- Momparler, R. L. and D. Derse (1979). "Kinetics of phosphorylation of 5-aza-2'-deoxycytidine by deoxycytidine kinase." Biochem Pharmacol **28**(8): 1443-1444.
- Momparler, R. L., G. E. Rivard, et al. (1985). "Clinical trial on 5-aza-2'-deoxycytidine in patients with acute leukemia." Pharmacol Ther **30**(3): 277-286.
- Moore, A., C. J. Donahue, et al. (1998). "Simultaneous measurement of cell cycle and apoptotic cell death." Methods Cell Biol **57**: 265-278.
- Morceau, F., A. Duvoix, et al. (2004). "Regulation of glutathione S-transferase P1-1 gene expression by NF-kappaB in tumor necrosis factor alpha-treated K562 leukemia cells." Biochem Pharmacol **67**(7): 1227-1238.
- Mori, N., H. Inoue, et al. (2001). "Constitutive expression of the cyclooxygenase-2 gene in T-cell lines infected with human T cell leukemia virus type I." International journal of cancer. Journal international du cancer **94**(6): 813-819.

- Mulero-Navarro, S., J. M. Carvajal-Gonzalez, et al. (2006). "The dioxin receptor is silenced by promoter hypermethylation in human acute lymphoblastic leukemia through inhibition of Sp1 binding." *Carcinogenesis* **27**(5): 1099-1104.
- Mullis, K., F. Faloona, et al. (1986). "Specific enzymatic amplification of DNA in vitro: the polymerase chain reaction." *Cold Spring Harb Symp Quant Biol* **51 Pt 1**: 263-273.
- Mullis, K. B. and F. A. Faloona (1987). "Specific synthesis of DNA in vitro via a polymerase-catalyzed chain reaction." *Methods Enzymol* **155**: 335-350.
- Murata, H., S. Tsuji, et al. (2004). "Promoter hypermethylation silences cyclooxygenase-2 (Cox-2) and regulates growth of human hepatocellular carcinoma cells." *Laboratory investigation; a journal of technical methods and pathology* **84**(8): 1050-1059.
- Murray, P. G., G. H. Qiu, et al. (2004). "Frequent epigenetic inactivation of the RASSF1A tumor suppressor gene in Hodgkin's lymphoma." *Oncogene* **23**(6): 1326-1331.
- Murrell, A., S. Heeson, et al. (2001). "An intragenic methylated region in the imprinted Igf2 gene augments transcription." *EMBO Rep* **2**(12): 1101-1106.
- Mutallip, M., N. Nohata, et al. (2011). "Glutathione S-transferase P1 (GSTP1) suppresses cell apoptosis and its regulation by miR-133alpha in head and neck squamous cell carcinoma (HNSCC)." *International journal of molecular medicine* **27**(3): 345-352.
- Nakayama, M., C. J. Bennett, et al. (2003). "Hypermethylation of the human glutathione S-transferase-pi gene (GSTP1) CpG island is present in a subset of proliferative inflammatory atrophy lesions but not in normal or hyperplastic epithelium of the prostate: a detailed study using laser-capture microdissection." *The American journal of pathology* **163**(3): 923-933.
- Nan, X., H. H. Ng, et al. (1998). "Transcriptional repression by the methyl-CpG-binding protein MeCP2 involves a histone deacetylase complex." *Nature* **393**(6683): 386-389.
- Neff, T. and S. A. Armstrong (2009). "Chromatin maps, histone modifications and leukemia." *Leukemia : official journal of the Leukemia Society of America, Leukemia Research Fund, U.K* **23**(7): 1243-1251.
- Nelkin, B. D., D. Przepiorka, et al. (1991). "Abnormal methylation of the calcitonin gene marks progression of chronic myelogenous leukemia." *Blood* **77**(11): 2431-2434.
- Nelson, J. D., O. Denisenko, et al. (2006). "Protocol for the fast chromatin immunoprecipitation (ChIP) method." *Nat Protoc* **1**(1): 179-185.
- Nguyen, C., G. Liang, et al. (2001). "Susceptibility of nonpromoter CpG islands to de novo methylation in normal and neoplastic cells." *J Natl Cancer Inst* **93**(19): 1465-1472.
- Nieto, M., E. Samper, et al. (2004). "The absence of p53 is critical for the induction of apoptosis by 5-aza-2'-deoxycytidine." *Oncogene* **23**(3): 735-743.
- Niwa, T., T. Tsukamoto, et al. (2010). "Inflammatory processes triggered by Helicobacter pylori infection cause aberrant DNA methylation in gastric epithelial cells." *Cancer research* **70**(4): 1430-1440.

- Ohsawa, M., H. Fukushima, et al. (2006). "Expression of cyclooxygenase-2 in Hodgkin's lymphoma: its role in cell proliferation and angiogenesis." Leukemia & lymphoma **47**(9): 1863-1871.
- Okano, M., D. W. Bell, et al. (1999). "DNA methyltransferases Dnmt3a and Dnmt3b are essential for de novo methylation and mammalian development." Cell **99**(3): 247-257.
- Okano, M., S. Xie, et al. (1998). "Cloning and characterization of a family of novel mammalian DNA (cytosine-5) methyltransferases." Nat Genet **19**(3): 219-220.
- Okuno, Y., H. Iwasaki, et al. (2002). "Differential regulation of the human and murine CD34 genes in hematopoietic stem cells." Proc Natl Acad Sci U S A **99**(9): 6246-6251.
- Oshima, M., J. E. Dinchuk, et al. (1996). "Suppression of intestinal polyposis in Apc delta716 knockout mice by inhibition of cyclooxygenase 2 (COX-2)." Cell **87**(5): 803-809.
- Oswald, J., S. Engemann, et al. (2000). "Active demethylation of the paternal genome in the mouse zygote." Curr Biol **10**(8): 475-478.
- Ota, A., H. Tagawa, et al. (2004). "Identification and characterization of a novel gene, C13orf25, as a target for 13q31-q32 amplification in malignant lymphoma." Cancer Res **64**(9): 3087-3095.
- Ouaissi, M. and A. Ouaissi (2006). "Histone deacetylase enzymes as potential drug targets in cancer and parasitic diseases." J Biomed Biotechnol **2006**(2): 13474.
- Paixao, V. A., D. O. Vidal, et al. (2006). "Hypermethylation of CpG island in the promoter region of CALCA in acute lymphoblastic leukemia with central nervous system (CNS) infiltration correlates with poorer prognosis." Leukemia research **30**(7): 891-894.
- Palmisano, W. A., K. K. Divine, et al. (2000). "Predicting lung cancer by detecting aberrant promoter methylation in sputum." Cancer Res **60**(21): 5954-5958.
- Pan, G., S. Tian, et al. (2007). "Whole-genome analysis of histone H3 lysine 4 and lysine 27 methylation in human embryonic stem cells." Cell Stem Cell **1**(3): 299-312.
- Pandey, M., S. Shukla, et al. (2010). "Promoter demethylation and chromatin remodeling by green tea polyphenols leads to re-expression of GSTP1 in human prostate cancer cells." International journal of cancer. Journal international du cancer **126**(11): 2520-2533.
- Panning, B. and R. Jaenisch (1996). "DNA hypomethylation can activate Xist expression and silence X-linked genes." Genes Dev **10**(16): 1991-2002.
- Parasramka, M. A., E. Ho, et al. (2011). "MicroRNAs, diet, and cancer: New mechanistic insights on the epigenetic actions of phytochemicals." Molecular carcinogenesis.
- Parrett, M., R. Harris, et al. (1997). "Cyclooxygenase-2 gene expression in human breast cancer." International journal of oncology **10**(3): 503-507.
- Pasquale, E. B. (2010). "Eph receptors and ephrins in cancer: bidirectional signalling and beyond." Nature reviews. Cancer **10**(3): 165-180.
- Passegue, E., C. H. Jamieson, et al. (2003). "Normal and leukemic hematopoiesis: are leukemias a stem cell disorder or a reacquisition of stem cell characteristics?" Proc Natl Acad Sci U S A **100 Suppl 1**: 11842-11849.

- Paz, M. F., M. F. Fraga, et al. (2003). "A systematic profile of DNA methylation in human cancer cell lines." *Cancer research* **63**(5): 1114-1121.
- Peart, M. J., G. K. Smyth, et al. (2005). "Identification and functional significance of genes regulated by structurally different histone deacetylase inhibitors." *Proc Natl Acad Sci U S A* **102**(10): 3697-3702.
- Peng, D. F., M. Razvi, et al. (2009). "DNA hypermethylation regulates the expression of members of the Mu-class glutathione S-transferases and glutathione peroxidases in Barrett's adenocarcinoma." *Gut* **58**(1): 5-15.
- Phe, V., O. Cussenot, et al. (2010). "Methylated genes as potential biomarkers in prostate cancer." *BJU international* **105**(10): 1364-1370.
- Piimi, J. o., F. (1964). *Collection Czech. Chem. Commun.* **29**: 2576.
- Pískala, A. o., F. (1965). *Collection Czech. Chem. Commun* **30**: 2801.
- Portugal, J. and M. J. Waring (1988). "Assignment of DNA binding sites for 4',6'-diamidine-2-phenylindole and bisbenzimidazole (Hoechst 33258). A comparative footprinting study." *Biochim Biophys Acta* **949**(2): 158-168.
- Price, J. T., M. T. Bonovich, et al. (1997). "The biochemistry of cancer dissemination." *Critical reviews in biochemistry and molecular biology* **32**(3): 175-253.
- Pruthi, R. S., J. E. Derksen, et al. (2006). "Phase II trial of celecoxib in prostate-specific antigen recurrent prostate cancer after definitive radiation therapy or radical prostatectomy." *Clinical cancer research : an official journal of the American Association for Cancer Research* **12**(7 Pt 1): 2172-2177.
- Qin, T., J. Jelinek, et al. (2009). "Mechanisms of resistance to 5-aza-2'-deoxycytidine in human cancer cell lines." *Blood* **113**(3): 659-667.
- Qin, T., E. M. Youssef, et al. (2007). "Effect of cytarabine and decitabine in combination in human leukemic cell lines." *Clinical cancer research : an official journal of the American Association for Cancer Research* **13**(14): 4225-4232.
- Ramsay, R. G., A. Friend, et al. (2000). "Cyclooxygenase-2, a colorectal cancer nonsteroidal anti-inflammatory drug target, is regulated by c-MYB." *Cancer research* **60**(7): 1805-1809.
- Rasband, W. S. (1997-2008). "ImageJ."
- Raval, A., D. M. Lucas, et al. (2005). "TWIST2 demonstrates differential methylation in immunoglobulin variable heavy chain mutated and unmutated chronic lymphocytic leukemia." *Journal of clinical oncology : official journal of the American Society of Clinical Oncology* **23**(17): 3877-3885.
- Raval, A., S. M. Tanner, et al. (2007). "Downregulation of death-associated protein kinase 1 (DAPK1) in chronic lymphocytic leukemia." *Cell* **129**(5): 879-890.
- Reik, W. (2007). "Stability and flexibility of epigenetic gene regulation in mammalian development." *Nature* **447**(7143): 425-432.
- Reik, W. and J. Walter (2001). "Evolution of imprinting mechanisms: the battle of the sexes begins in the zygote." *Nat Genet* **27**(3): 255-256.
- Reik, W. and J. Walter (2001). "Genomic imprinting: parental influence on the genome." *Nature reviews. Genetics* **2**(1): 21-32.
- Reinhart, B. J., F. J. Slack, et al. (2000). "The 21-nucleotide let-7 RNA regulates developmental timing in *Caenorhabditis elegans*." *Nature* **403**(6772): 901-906.

- Rethmeier, A., A. Aggerholm, et al. (2006). "Promoter hypermethylation of the retinoic acid receptor beta2 gene is frequent in acute myeloid leukaemia and associated with the presence of CBFbeta-MYH11 fusion transcripts." British journal of haematology **133**(3): 276-283.
- Rice, K. L., I. Hormaeche, et al. (2007). "Epigenetic regulation of normal and malignant hematopoiesis." Oncogene **26**(47): 6697-6714.
- Rice, P., I. Longden, et al. (2000). "EMBOSS: the European Molecular Biology Open Software Suite." Trends Genet **16**(6): 276-277.
- Rideout, W. M., 3rd, K. Eggan, et al. (2001). "Nuclear cloning and epigenetic reprogramming of the genome." Science **293**(5532): 1093-1098.
- Riggs, A. D. (1975). "X inactivation, differentiation, and DNA methylation." Cytogenet Cell Genet **14**(1): 9-25.
- Ristimaki, A., N. Honkanen, et al. (1997). "Expression of cyclooxygenase-2 in human gastric carcinoma." Cancer research **57**(7): 1276-1280.
- Ristimaki, A., A. Sivula, et al. (2002). "Prognostic significance of elevated cyclooxygenase-2 expression in breast cancer." Cancer research **62**(3): 632-635.
- Ritchie, W., S. Flamant, et al. (2010). "mimiRNA: a microRNA expression profiler and classification resource designed to identify functional correlations between microRNAs and their targets." Bioinformatics **26**(2): 223-227.
- Rivard, G. E., R. L. Momparler, et al. (1981). "Phase I study on 5-aza-2'-deoxycytidine in children with acute leukemia." Leuk Res **5**(6): 453-462.
- Robertson, K. D., E. Uzvolgyi, et al. (1999). "The human DNA methyltransferases (DNMTs) 1, 3a and 3b: coordinate mRNA expression in normal tissues and overexpression in tumors." Nucleic Acids Res **27**(11): 2291-2298.
- Rodriguez, A., S. Griffiths-Jones, et al. (2004). "Identification of mammalian microRNA host genes and transcription units." Genome Res **14**(10A): 1902-1910.
- Rodriguez-Paredes, M. and M. Esteller (2011). "Cancer epigenetics reaches mainstream oncology." Nature medicine **17**(3): 330-339.
- Rolland, P. H., P. M. Martin, et al. (1980). "Prostaglandin in human breast cancer: Evidence suggesting that an elevated prostaglandin production is a marker of high metastatic potential for neoplastic cells." Journal of the National Cancer Institute **64**(5): 1061-1070.
- Roman, J., J. A. Castillejo, et al. (2001). "Hypermethylation of the calcitonin gene in acute lymphoblastic leukaemia is associated with unfavourable clinical outcome." British journal of haematology **113**(2): 329-338.
- Roman-Gomez, J., A. Jimenez-Velasco, et al. (2005). "Promoter hypomethylation of the LINE-1 retrotransposable elements activates sense/antisense transcription and marks the progression of chronic myeloid leukemia." Oncogene **24**(48): 7213-7223.
- Ropero, S., F. Setien, et al. (2004). "Epigenetic loss of the familial tumor-suppressor gene exostosin-1 (EXT1) disrupts heparan sulfate synthesis in cancer cells." Human molecular genetics **13**(22): 2753-2765.
- Rosas, S. L., W. Koch, et al. (2001). "Promoter hypermethylation patterns of p16, O6-methylguanine-DNA-methyltransferase, and death-associated protein kinase in tumors and saliva of head and neck cancer patients." Cancer Res **61**(3): 939-942.

- Rossi, D., D. Capello, et al. (2004). "Aberrant promoter methylation of multiple genes throughout the clinico-pathologic spectrum of B-cell neoplasia." *Haematologica* **89**(2): 154-164.
- Rozen, S. and H. Skaletsky (2000). "Primer3 on the WWW for general users and for biologist programmers." *Methods Mol Biol* **132**: 365-386.
- Ruan, K., X. Fang, et al. (2009). "MicroRNAs: novel regulators in the hallmarks of human cancer." *Cancer letters* **285**(2): 116-126.
- Rusco, J. E., L. A. Rosario, et al. (2001). "Pharmacologic or genetic manipulation of glutathione S-transferase P1-1 (GSTpi) influences cell proliferation pathways." *The Journal of pharmacology and experimental therapeutics* **298**(1): 339-345.
- Rush, L. J. and C. Plass (2002). "Alterations of DNA methylation in hematologic malignancies." *Cancer letters* **185**(1): 1-12.
- Ryan, E. P., S. J. Pollock, et al. (2006). "Constitutive and activation-inducible cyclooxygenase-2 expression enhances survival of chronic lymphocytic leukemia B cells." *Clinical immunology* **120**(1): 76-90.
- Sadri, R. and P. J. Hornsby (1996). "Rapid analysis of DNA methylation using new restriction enzyme sites created by bisulfite modification." *Nucleic Acids Res* **24**(24): 5058-5059.
- Sager, R. and R. Kitchin (1975). "Selective silencing of eukaryotic DNA." *Science* **189**(4201): 426-433.
- Saito, Y., G. Liang, et al. (2006). "Specific activation of microRNA-127 with downregulation of the proto-oncogene BCL6 by chromatin-modifying drugs in human cancer cells." *Cancer cell* **9**(6): 435-443.
- Sanchez-Cespedes, M., M. Esteller, et al. (1999). "Molecular detection of neoplastic cells in lymph nodes of metastatic colorectal cancer patients predicts recurrence." *Clin Cancer Res* **5**(9): 2450-2454.
- Sandler, R. S., S. Halabi, et al. (2003). "A randomized trial of aspirin to prevent colorectal adenomas in patients with previous colorectal cancer." *The New England journal of medicine* **348**(10): 883-890.
- Sassen, S., E. A. Miska, et al. (2008). "MicroRNA: implications for cancer." *Virchows Archiv : an international journal of pathology* **452**(1): 1-10.
- Sawaki, M., K. Enomoto, et al. (1990). "Phenotype of preneoplastic and neoplastic liver lesions during spontaneous liver carcinogenesis of LEC rats." *Carcinogenesis* **11**(10): 1857-1861.
- Schagdarsurengin, U., O. Gimm, et al. (2002). "Frequent epigenetic silencing of the CpG island promoter of RASSF1A in thyroid carcinoma." *Cancer research* **62**(13): 3698-3701.
- Schmelz, K., N. Sattler, et al. (2005). "Induction of gene expression by 5-Aza-2'-deoxycytidine in acute myeloid leukemia (AML) and myelodysplastic syndrome (MDS) but not epithelial cells by DNA-methylation-dependent and -independent mechanisms." *Leukemia : official journal of the Leukemia Society of America, Leukemia Research Fund, U.K* **19**(1): 103-111.
- Schotta, G., M. Lachner, et al. (2004). "A silencing pathway to induce H3-K9 and H4-K20 trimethylation at constitutive heterochromatin." *Genes & development* **18**(11): 1251-1262.

- Schulz, W. A. and W. Goering (2011). "Eagles report: Developing cancer biomarkers from genome-wide DNA methylation analyses." World journal of clinical oncology **2**(1): 1-7.
- Schwartsmann, G., M. S. Fernandes, et al. (1997). "Decitabine (5-Aza-2'-deoxycytidine; DAC) plus daunorubicin as a first line treatment in patients with acute myeloid leukemia: preliminary observations." Leukemia **11 Suppl 1**: S28-31.
- Sethupathy, P., B. Corda, et al. (2006). "TarBase: A comprehensive database of experimentally supported animal microRNA targets." RNA **12**(2): 192-197.
- Sevignani, C., G. A. Calin, et al. (2007). "MicroRNA genes are frequently located near mouse cancer susceptibility loci." Proc Natl Acad Sci U S A **104**(19): 8017-8022.
- Shea, T. C., S. L. Kelley, et al. (1988). "Identification of an anionic form of glutathione transferase present in many human tumors and human tumor cell lines." Cancer Res **48**(3): 527-533.
- Sheng, H., J. Shao, et al. (2000). "Transforming growth factor-beta1 enhances Ha-ras-induced expression of cyclooxygenase-2 in intestinal epithelial cells via stabilization of mRNA." The Journal of biological chemistry **275**(9): 6628-6635.
- Sheng, H., J. Shao, et al. (2001). "K-Ras-mediated increase in cyclooxygenase 2 mRNA stability involves activation of the protein kinase B1." Cancer research **61**(6): 2670-2675.
- Sheng, H., J. Shao, et al. (1998). "Modulation of apoptosis and Bcl-2 expression by prostaglandin E2 in human colon cancer cells." Cancer research **58**(2): 362-366.
- Shteper, P. J., Z. Siegfried, et al. (2001). "ABL1 methylation in Ph-positive ALL is exclusively associated with the P210 form of BCR-ABL." Leukemia : official journal of the Leukemia Society of America, Leukemia Research Fund, U.K **15**(4): 575-582.
- Si, J., Y. A. Bumber, et al. (2010). "Chromatin remodeling is required for gene reactivation after decitabine-mediated DNA hypomethylation." Cancer research **70**(17): 6968-6977.
- Siedlecki, P. and P. Zielenkiewicz (2006). "Mammalian DNA methyltransferases." Acta biochimica Polonica **53**(2): 245-256.
- Simic, T., J. Mimic-Oka, et al. (2005). "Glutathione S-transferase T1-1 activity upregulated in transitional cell carcinoma of urinary bladder." Urology **65**(5): 1035-1040.
- Sincic, N. and Z. Herceg (2011). "DNA methylation and cancer: ghosts and angels above the genes." Current opinion in oncology **23**(1): 69-76.
- Siu, L. L., J. K. Chan, et al. (2002). "Specific patterns of gene methylation in natural killer cell lymphomas : p73 is consistently involved." The American journal of pathology **160**(1): 59-66.
- Smit, A. F. and A. D. Riggs (1996). "Tiggers and DNA transposon fossils in the human genome." Proc Natl Acad Sci U S A **93**(4): 1443-1448.
- Song, J. Z., C. Stirzaker, et al. (2002). "Hypermethylation trigger of the glutathione-S-transferase gene (GSTP1) in prostate cancer cells." Oncogene **21**(7): 1048-1061.

- Stark, A., J. Brennecke, et al. (2005). "Animal MicroRNAs confer robustness to gene expression and have a significant impact on 3'UTR evolution." *Cell* **123**(6): 1133-1146.
- Stark, A., J. Brennecke, et al. (2003). "Identification of Drosophila MicroRNA targets." *PLoS Biol* **1**(3): E60.
- Stirzaker, C., J. Z. Song, et al. (2004). "Transcriptional gene silencing promotes DNA hypermethylation through a sequential change in chromatin modifications in cancer cells." *Cancer research* **64**(11): 3871-3877.
- Stone, R. M., D. J. DeAngelo, et al. (2005). "Patients with acute myeloid leukemia and an activating mutation in FLT3 respond to a small-molecule FLT3 tyrosine kinase inhibitor, PKC412." *Blood* **105**(1): 54-60.
- Strahl, B. D., P. A. Grant, et al. (2002). "Set2 is a nucleosomal histone H3-selective methyltransferase that mediates transcriptional repression." *Mol Cell Biol* **22**(5): 1298-1306.
- Strathdee, G. and R. Brown (2002). "Aberrant DNA methylation in cancer: potential clinical interventions." *Expert Rev Mol Med* **4**(4): 1-17.
- Strathdee, G., T. L. Holyoake, et al. (2007). "Inactivation of HOXA genes by hypermethylation in myeloid and lymphoid malignancy is frequent and associated with poor prognosis." *Clinical cancer research : an official journal of the American Association for Cancer Research* **13**(17): 5048-5055.
- Stresemann, C., I. Bokelmann, et al. (2008). "Azacytidine causes complex DNA methylation responses in myeloid leukemia." *Molecular cancer therapeutics* **7**(9): 2998-3005.
- Stresemann, C. and F. Lyko (2008). "Modes of action of the DNA methyltransferase inhibitors azacytidine and decitabine." *Int J Cancer* **123**(1): 8-13.
- Subbaramaiah, K., N. Altorki, et al. (1999). "Inhibition of cyclooxygenase-2 gene expression by p53." *The Journal of biological chemistry* **274**(16): 10911-10915.
- Suetake, I., F. Shinozaki, et al. (2004). "DNMT3L stimulates the DNA methylation activity of Dnmt3a and Dnmt3b through a direct interaction." *J Biol Chem* **279**(26): 27816-27823.
- Suzuki, H., E. Gabrielson, et al. (2002). "A genomic screen for genes upregulated by demethylation and histone deacetylase inhibition in human colorectal cancer." *Nature genetics* **31**(2): 141-149.
- Takahashi, T., N. Shivapurkar, et al. (2004). "DNA methylation profiles of lymphoid and hematopoietic malignancies." *Clinical cancer research : an official journal of the American Association for Cancer Research* **10**(9): 2928-2935.
- Tamaru, H. and E. U. Selker (2001). "A histone H3 methyltransferase controls DNA methylation in *Neurospora crassa*." *Nature* **414**(6861): 277-283.
- Tamm, I., M. Wagner, et al. (2005). "Decitabine activates specific caspases downstream of p73 in myeloid leukemia." *Annals of hematology* **84** Suppl 1: 47-53.
- Taylor, K. H., K. E. Pena-Hernandez, et al. (2007). "Large-scale CpG methylation analysis identifies novel candidate genes and reveals methylation hotspots in acute lymphoblastic leukemia." *Cancer research* **67**(6): 2617-2625.
- Team, R. D. C. (2010). "R: A language and environment for statistical computing."

- Terrier, P., A. J. Townsend, et al. (1990). "An immunohistochemical study of pi class glutathione S-transferase expression in normal human tissue." Am J Pathol **137**(4): 845-853.
- Teschendorff, A. E., U. Menon, et al. (2010). "Age-dependent DNA methylation of genes that are suppressed in stem cells is a hallmark of cancer." Genome research **20**(4): 440-446.
- Toyota, M., K. J. Kopecky, et al. (2001). "Methylation profiling in acute myeloid leukemia." Blood **97**(9): 2823-2829.
- Toyota, M., L. Shen, et al. (2000). "Aberrant methylation of the Cyclooxygenase 2 CpG island in colorectal tumors." Cancer research **60**(15): 4044-4048.
- Trachte, A. L., S. E. Suthers, et al. (2002). "Increased expression of alpha-1-antitrypsin, glutathione S-transferase pi and vascular endothelial growth factor in human pancreatic adenocarcinoma." American journal of surgery **184**(6): 642-647; discussion 647-648.
- Trifan, O. C., R. M. Smith, et al. (1999). "Overexpression of cyclooxygenase-2 induces cell cycle arrest. Evidence for a prostaglandin-independent mechanism." The Journal of biological chemistry **274**(48): 34141-34147.
- Tsujii, M. and R. N. DuBois (1995). "Alterations in cellular adhesion and apoptosis in epithelial cells overexpressing prostaglandin endoperoxide synthase 2." Cell **83**(3): 493-501.
- Tsujii, M., S. Kawano, et al. (1997). "Cyclooxygenase-2 expression in human colon cancer cells increases metastatic potential." Proceedings of the National Academy of Sciences of the United States of America **94**(7): 3336-3340.
- Turner, B. M. and L. P. O'Neill (1995). "Histone acetylation in chromatin and chromosomes." Semin Cell Biol **6**(4): 229-236.
- Uhm, K. O., E. S. Lee, et al. (2009). "Differential methylation pattern of ID4, SFRP1, and SHP1 between acute myeloid leukemia and chronic myeloid leukemia." Journal of Korean medical science **24**(3): 493-497.
- Uphoff, C. C., S. A. Denkmann, et al. (2010). "Detection of EBV, HBV, HCV, HIV-1, HTLV-I and -II, and SMRV in human and other primate cell lines." Journal of biomedicine & biotechnology **2010**: 904767.
- Vaissiere, T., C. Sawan, et al. (2008). "Epigenetic interplay between histone modifications and DNA methylation in gene silencing." Mutat Res **659**(1-2): 40-48.
- Villar-Garea, A. and M. Esteller (2003). "DNA demethylating agents and chromatin-remodelling drugs: which, how and why?" Curr Drug Metab **4**(1): 11-31.
- Visone, R. and C. M. Croce (2009). "MiRNAs and cancer." The American journal of pathology **174**(4): 1131-1138.
- Waddington (1942). "Canalisation of development and the inheritance of acquired characters. ." Nature **150**: 563-564.
- Wadhwa, P., A. K. Goswami, et al. (2005). "Cyclooxygenase-2 expression increases with the stage and grade in transitional cell carcinoma of the urinary bladder." International urology and nephrology **37**(1): 47-53.
- Wang, B. C., C. Q. Guo, et al. (2005). "Mechanism and clinical significance of cyclooxygenase-2 expression in gastric cancer." World journal of gastroenterology : WJG **11**(21): 3240-3244.
- Wang, J., T. Hoshino, et al. (1998). "ETO, fusion partner in t(8;21) acute myeloid leukemia, represses transcription by interaction with the human N-

- CoR/mSin3/HDAC1 complex." Proc Natl Acad Sci U S A **95**(18): 10860-10865.
- Wang, J., Y. Sauntharajah, et al. (1999). "Inhibitors of histone deacetylase relieve ETO-mediated repression and induce differentiation of AML1-ETO leukemia cells." Cancer Res **59**(12): 2766-2769.
- Wang, Q. Z., W. Xu, et al. (2009). "Potential uses of microRNA in lung cancer diagnosis, prognosis, and therapy." Curr Cancer Drug Targets **9**(4): 572-594.
- Warner, J. K., J. C. Wang, et al. (2004). "Concepts of human leukemic development." Oncogene **23**(43): 7164-7177.
- Waskewich, C., R. D. Blumenthal, et al. (2002). "Celecoxib exhibits the greatest potency amongst cyclooxygenase (COX) inhibitors for growth inhibition of COX-2-negative hematopoietic and epithelial cell lines." Cancer research **62**(7): 2029-2033.
- Weber, M. J. (2005). "New human and mouse microRNA genes found by homology search." FEBS J **272**(1): 59-73.
- Wightman, B., I. Ha, et al. (1993). "Posttranscriptional regulation of the heterochronic gene lin-14 by lin-4 mediates temporal pattern formation in *C. elegans*." Cell **75**(5): 855-862.
- Wijermans, P., M. Lubbert, et al. (2000). "Low-dose 5-aza-2'-deoxycytidine, a DNA hypomethylating agent, for the treatment of high-risk myelodysplastic syndrome: a multicenter phase II study in elderly patients." Journal of clinical oncology : official journal of the American Society of Clinical Oncology **18**(5): 956-962.
- Wijermans, P. W., J. W. Krulder, et al. (1997). "Continuous infusion of low-dose 5-Aza-2'-deoxycytidine in elderly patients with high-risk myelodysplastic syndrome." Leukemia **11 Suppl 1**: S19-23.
- Wild, L. and J. M. Flanagan (2010). "Genome-wide hypomethylation in cancer may be a passive consequence of transformation." Biochimica et biophysica acta **1806**(1): 50-57.
- Wilson, A. S., B. E. Power, et al. (2007). "DNA hypomethylation and human diseases." Biochimica et biophysica acta **1775**(1): 138-162.
- Winter, J., S. Jung, et al. (2009). "Many roads to maturity: microRNA biogenesis pathways and their regulation." Nature cell biology **11**(3): 228-234.
- Wolff, C. F. (1759). "Theoria generioris."
- Wolff, H., K. Saukkonen, et al. (1998). "Expression of cyclooxygenase-2 in human lung carcinoma." Cancer research **58**(22): 4997-5001.
- Wolffe, A. P. and J. J. Hayes (1999). "Chromatin disruption and modification." Nucleic Acids Res **27**(3): 711-720.
- Wong, I. H., M. H. Ng, et al. (2000). "Aberrant p15 promoter methylation in adult and childhood acute leukemias of nearly all morphologic subtypes: potential prognostic implications." Blood **95**(6): 1942-1949.
- Wossidlo, M., T. Nakamura, et al. (2011). "5-Hydroxymethylcytosine in the mammalian zygote is linked with epigenetic reprogramming." Nature communications **2**: 241.
- Wu, J. C. and D. V. Santi (1987). "Kinetic and catalytic mechanism of HhaI methyltransferase." J Biol Chem **262**(10): 4778-4786.
- Wu, X. M., J. Z. Shen, et al. (2009). "[Detection of APC gene promoter methylation in hematological malignant cell lines by nested-methylation specific polymerase

- chain reaction]." Zhongguo shi yan xue ye xue za zhi / Zhongguo bing li sheng li xue hui = Journal of experimental hematology / Chinese Association of Pathophysiology **17**(4): 957-960.
- Wu, Y., Y. Fan, et al. (2006). "Human glutathione S-transferase P1-1 interacts with TRAF2 and regulates TRAF2-ASK1 signals." Oncogene **25**(42): 5787-5800.
- Wun, T., H. McKnight, et al. (2004). "Increased cyclooxygenase-2 (COX-2): a potential role in the pathogenesis of lymphoma." Leukemia research **28**(2): 179-190.
- Xiao, C., L. Srinivasan, et al. (2008). "Lymphoproliferative disease and autoimmunity in mice with increased miR-17-92 expression in lymphocytes." Nat Immunol **9**(4): 405-414.
- Yang, J., F. Zhou, et al. (2008). "Analysis of sequence variations in 59 microRNAs in hepatocellular carcinomas." Mutat Res **638**(1-2): 205-209.
- Yang, X., D. L. Phillips, et al. (2001). "Synergistic activation of functional estrogen receptor (ER)-alpha by DNA methyltransferase and histone deacetylase inhibition in human ER-alpha-negative breast cancer cells." Cancer research **61**(19): 7025-7029.
- Yang, X. J. and E. Seto (2007). "HATs and HDACs: from structure, function and regulation to novel strategies for therapy and prevention." Oncogene **26**(37): 5310-5318.
- Yao, J., Q. Huang, et al. (2009). "Promoter CpG methylation of oestrogen receptors in leukaemia." Bioscience reports **29**(4): 211-216.
- Yoda, M., T. Kawamata, et al. (2010). "ATP-dependent human RISC assembly pathways." Nat Struct Mol Biol **17**(1): 17-23.
- Yuan, Y., Z. R. Qian, et al. (2008). "Reduction of GSTP1 expression by DNA methylation correlates with clinicopathological features in pituitary adenomas." Modern pathology : an official journal of the United States and Canadian Academy of Pathology, Inc **21**(7): 856-865.
- Zhang, B. L., T. Sun, et al. (2011). "Polymorphisms of GSTP1 is associated with differences of chemotherapy response and toxicity in breast cancer." Chinese medical journal **124**(2): 199-204.
- Zhang, G. S., D. S. Liu, et al. (2006). "Antitumor effects of celecoxib on K562 leukemia cells are mediated by cell-cycle arrest, caspase-3 activation, and downregulation of Cox-2 expression and are synergistic with hydroxyurea or imatinib." American journal of hematology **81**(4): 242-255.
- Zhang, H., Y. Li, et al. (2010). "The microRNA network and tumor metastasis." Oncogene **29**(7): 937-948.
- Zheng, T., J. Wang, et al. (2010). "Role of microRNA in anticancer drug resistance." International journal of cancer. Journal international du cancer **126**(1): 2-10.
- Zippo, A., R. Serafini, et al. (2009). "Histone crosstalk between H3S10ph and H4K16ac generates a histone code that mediates transcription elongation." Cell **138**(6): 1122-1136.

Websites

www.abcam.com/technical
<http://biq-analyzer.bioinf.mpi-sb.mpg.de>

www.calb.org
www.caymanchem.com/app/template/Artivle.vm/article/2136
<http://diana.pcbi.upenn.edu/CGi-bin/TargetCombo.cgi>
www.ebi.ac.uk/Tools/emboss/cpgblot/index.html
www.ensembl.org
www.life.umd.edu
www.ma.uni-heidelberg.de/apps/zmf/mirwalk/
<http://mirnamap.mbc.nctu.edu.tw/human/>
<http://mimirna.centenary.org.au/mep/formulaire.html>
www.mirz.unibas.ch/EIMMo3/
www.targetscan.org
www.refgene.com
rsbweb.nih.gov/ij/
www.russell.embl-heidelberg.de/miRNAs/

List of abbreviations

5-hmc	5-hydroxymethylcytosine
ABCB1	ATP-binding cassette. Sub-family B (MDR/TAP)
ABL1	c-Abelson oncogene 1 non-receptor tyrosine kinase
Ac	acetylation
AcH	Acetyl histone
ADP	Adenosine diphosphate
Ago	Argonaute
AHR	Aryl hydrocarbon receptor
ALL	Acute lymphoid leukemia
AML	Acute myeloid leukemia
AML1-ETO	Fusion gene
Anneal.	Annealing
AP-1	Activator protein-1
APAF-1	Apoptotic peptidase activating factor 1
APC	Adenomatosis polyposis coli
APS	Ammonium persulfate
ATP	Adenosine triphosphate
AR	Androgen receptor
AZA	Azacytidine
BCL	B-cell CLL/lymphoma
BCR/ABL1	Fusion gene
Bi	Bisulfite water control
Bio-CoBRA	Bioanalyzer Combined bisulfite restriction assay
BL	Burkitt's lymphoma
bp	Base pair
BRCA1	Breast cancer 1
BSA	Bovine serum albumin
BSP	Bisulfite sequencing
CAGR	Cancer-associated genomic region
CALCA	Calcitonin-related polypeptide alpha
CASP	Caspase
CBP	CREB binding protein
Ct	Threshold cycle
CDH1	E-cadherin
CDK	Cyclin-dependent kinase
CDKN1A (p57 ^{KIP2})	Cyclin-dependent kinase inhibitor 1A
CDKN2A (p16 ^{INK4A} , p14 ^{ARF})	Cyclin-dependent kinase 4 inhibitor A
CDKN2B (p15 ^{INK4B})	Cyclin-dependent kinase inhibitor 2B
cDNA	Complementary DNA
CDS	Coding sequence
CEBP	CCAAT/enhancer binding protein
CFSE	Carboxyfluorescein diacetate
CGi	CpG island

CHFR	Checkpoint with forkhead and ring finger domains
CLL	Chronic lymphoid leukemia
CLP	Common lymphoid progenitor
CML	Chronic myeloid leukemia
CMP	Common myeloid progenitor
CpG	CG dioligonucleotide
CR	Red cross
CRBP1	Cellular retinol-binding protein 1
CREB	cAMP response element binding
CXCR7	Scavenger chemokine receptor 7
DAB2IBA	DAB2 interacting protein
DAC	5-aza-2'-deoxycytidine
DAPK1	Death-associated protein kinase 1
DCR1	Decoy receptor 1
DEPC	Diethylpyrocarbonate
DGCR8	DiGeorge syndrom critical region 8
DLBCL	Diffuse large B-cell lymphoma
DLC1	Deleted in liver cancer 1
DMR	Differential methylation region
DMSO	Dimethyl sulfoxide
DNA	Deoxyribonucleic acid
DNMT	DNA methyltransferase
Drosha	Double strand specific endoribonuclease
ds	double strand
DTT	Dithiotreitol
dNTP	Deoxyribonucleoside triphosphate
<i>E.coli</i>	<i>Escherichia coli</i>
<i>e.g.</i>	exempli gratia (for example)
E-cadherin	Epithelial cadherin
ECL	Enhanced Chemiluminescence
EDTA	Ethylene diamine tetra acetic acid
EFNA1	Ephrin A7
EGTA	Ethylene glycol tetra acetic acid
EPHA7	EPH receptor A7
ESR1 (ER)	Estrogen receptor 1
EYA4	Eyes absent homolog 4
EXT1	Exostosin 1
FACS	Fluorescence assisted cell sorting
FBS	Fetal bovine serum
FDA	Food and drug administration
FGFBP1	Fibroblast growth factor binding protein
FHIT	Fragile histidine triad gene
FL	Follicular lymphoma
FLT	FMS-related tyrosine kinase
FU	Fluorescence units
FSC	Forward scatter

GATA-1	Erythroid transcription factor
Gcn5	General control non-derepressible 5
GFP	Green fluorescent protein
GM-CSF	Granulocyte macrophage colony-stimulating factor
GSH	Glutathione
GSTP1	Glutathione S-transferase
GS-X	Glutathione-conjugated electrophilic compound
GTP	Guanosine triphosphate
H2A, 2B, 3, 4, 1	Histone protein 2A, 2B, 3, 4, 1
H3K4	Histone 3 lysine 4
H3K9	Histone 3 lysine 9
H3K27	Histone 3 lysine 27
H4K12	Histone 4 lysine 12
H4K16	Histone 4 lysine 16
H4K20	Histone 4 lysine 20
H3S10	Histone 3 serine 10
H ₂ O	Water
H19	Imprinted gene
HAT	Histoneacetyltransferase
HDAC	Histonedeaceetylase
HDACi	Histonedeaceetylase inhibitor
HERV	Human endogenous retrovirus
HIC1	Hypermethylated in cancer 1
HL	Histiocytic lymphoma
HMT	Histonemethyltransferase
HOXA4	Homeobox A4
HP1	Heterochromatin protein 1
HPLC	High pressure liquid chromatography
H-RAS	Harvey rat sarcoma viral oncogene homolog
HSC	Human stem cells
hMLH1	human MutL protein homolog 1
ID4	Inhibitor of DNA binding 4
i.e.	<i>id est</i>
IGF2	Insulin-like growth factor 2
IGSF4	Cell adhesion molecule 1
IgG	Immunoglobulin G
IMDM	Iscove's modified Dulbecco's medium
IPTG	Isopropyl-beta-D-thio-galacto-pyranosid
JNK	c-jun NH2-terminal kinase
K	Lysine
kb	kilo base pairs
kDa	kilo Dalton

KLF4	Krüppel-like factor 4
KO	Knock out
K-RAS	Kirsten rat sarcoma viral oncogene homolog
lacZ	β -galactosidase gene
LB	Luria bertani
LINE1	Long interspersed nuclear element 1
LMNA	Lamin A/C
LSC	Leukemia stem cell
M	Methylated
M13	Phage gene
MAPK	Mitogen activated protein kinase
MBD	Methyl-CpG-binding-domain
MC	Methylated converted DNA
MCB	monochlorobimane
MCL	Mantle cell lymphoma
MDS	Myelodysplastic Syndrome
^{me} CpG	Methylated CpG
MeCP2	Methyl CpG binding protein 2
MFI	Mean fluorescence intensity
MGD	Methylation analysis of the distal GSTP1 region
MGMT	O6-methylguanine–DNA methyltransferase
MGP	Methylation analysis of the proximal GSTP1 region
ML	Multiple lymphoma
MLL1	Myeloid/lymphoid (mixed lineage) leukemia
MM	Multiple myeloma
MMP	metalloproteinase
MMSET	Multiple Myeloma SET domain
mRNA	Messenger RNA
miRNA (*), miR	Micro RNA (passenger strand)
MLH1	Micronuclear linker histone 1
MRP	Multidrug resistance protein
MSP	Methylation sensitive PCR
MSRA	Methylation sensitive restriction assay
MYOD1	Myogenic differentiation 1
MYST	MYST histone acetyltransferase
n.a.	Not available
NF-kB	Nuclear factor kappa-light-chain-enhancer of activated B cells
NHL	Non Hodgkin's lymphoma
nm	Nanometer
Noxa	NADPH oxidase activator 1
NURD	Nucleosome remodelling and histone deacetylase

OD	Optic density
O/E	Observed vs expected
OSCP1	Organic solute carrier partner 1
OSMR	Oncostatin M receptor
p14Arf	p14 alternate reading frame
p15INK4B	p15 inhibits CDK4
p16INK4A	p16 inhibits CDK4
p50	Nuclear factor NF-kappa-B p50 subunit
P57KIP2	Cycline dependent kinase inhibitor 1C
p65	Nuclear factor NF-kappa-B p65 subunit
p73 (TP73)	Tumor protein p73
p300	Histone acetyltransferase p300
PAA	Polyacrylamide
PACT	PKR activator
PBS (-T)	Phosphate buffered saline (-Tween)
P-body	Processing body
PBMC	Peripheral blood mononuclear cells
PCR	Polymerase chain reaction
PI	Propidium iodid
Pi	Phosphate
PIN	Prostatic intraepithelial neoplasia
PIPES	Piperazine-1,4-bis (ethanesulfonic acid)
PITX2	Paired-like homeodomain 2
PKR	Serin / threonine protein kinase R
PLZF-RAR	Fusion proteins
PMA	Phorbol myristate acetate
PML-RARB	Fusion proteins
PMSF	Phenylmethylsulfonylfluorid
POI	Protein of interest
Pol	Polymerase
pre-/pri-miRNA	Intermediate RNA
PROX1	prospero homeobox
ptch	patched
PTEN	Phosphatase and Tensin homolog
PTGS2	Prostaglandin-endoperoxide synthase 2
PTM	Post translational modification
Puma	p53 upregulated modulator of apoptosis
QUMA	Quantification tool for methylation analysis
R	Arginine
RB1	Retinoblastoma 1
RC	Transcriptional repressive complex
RARB2	Retinoic acid receptor- β 2
RASSF1A	Ras association domain family protein 1A

RASSF5 (NORE1A)	Ras association domain family 5
RISC	RNA-induced silencing complex
RNA	Ribonucleic acid
RNA polII	RNA polymerase II
ROS	Reactive Oxygen Species
RPMI	Rapid Prototyping & Manufacturing Institute
rRNA	ribosomal RNA
RT	Reverse transcription
S	Serine
SAH	S-adenosylhomocysteine
SAHA	Suberoylanilide hydroxamic acid
SAM	S adenosyl-L-methionine
SD	Standard deviation
SDC4	Syndecan 4
SDS	Sodium dodecyl sulfate
SET8	SET domain containing lysine methyltransferase
SHP1	Protein-tyrosine phosphatase
SIN3	Histone deacetylase complex subunit
SINE1	Short interspersed nuclear element 1
SIRT	Silent mating type information regulation 2 homolog 1
SOC	Super Optimal broth with catabolite repression
SOCS1	STAT induced SH3 protein 1
SNP	Single nucleotide polymorphism
SP	Specificity protein
SRBC	CD2 molecule
STAT	Signal Transducers and Activators of Transcription
SUV39H1	Suppressor of variegation 3-9 homolog 1
t	translocation
<i>Taq</i>	<i>Thermus aquaticus</i>
TBE	Tris Borate EDTA
TCF4	T-cell specific transcription factor 4
TCL1	T-cell leukemia/lymphoma 1
TE	Tris EDTA
TEMED	N,N,N',N'-Tetramethylethylenediamin
temp	temperature
TET	tet oncogene
THBS1	Thrombospondin 1
TIMP3	TIMP metalloproteinase inhibitor
TF	Transcription factor
TP73	tumor protein p73
TRAF2	Tumor necrosis factor receptor-associated factor 2

TRBP	Trans-activator responsive RNA-binding protein
TRE	AP1 binding site
tRNA	transfer RNA
TSA	Trichostatin A
TSG	Tumor suppressor gene
TSS	Transcription start site
U	Unmethylated
Ub	ubiquitylation
UC	Unconverted DNA
UMC	Unmethylated converted DNA
UTR	Untranslated region
VEGF	Vascular growth factor
VPA	Valproic acid
vs	verses
wnt	Wingless-type MMTV integration site family
X	X-Chromosome
X-Gal	5-Brom-4-Chloro-3-indoyl-beta-D-galactopyranosid
X-ChIP	Cross-linked chromatin immunoprecipitation
XIAP	X-linked inhibitor of apoptosis protein

Table of figures

FIGURE 1: CONRAD HAL WADDINGTON'S CLASSICAL EPIGENETIC LANDSCAPE.	2
FIGURE 2: SCHEMATIC REPRESENTATION OF POST-TRANSLATIONAL MODIFICATIONS WITHIN N- TERMINAL TAIL DOMAINS OF THE CORE HISTONE OCTAMER.	4
FIGURE 3: POSSIBLE MECHANISMS OF DNA METHYLATION-MEDIATED GENE SILENCING.	9
FIGURE 4: SCHEMATIC REPRESENTATION OF THE DNA METHYLTRANSFERASE-CATALYZED ENDOCYCLIC CYTOSINE METHYLATION.	11
FIGURE 5: MICRORNA BIOGENESIS.	14
FIGURE 6: SCHEMATIC VIEW OF TRANSCRIPTIONALLY ACTIVE AND EPIGENETICALLY SILENCED CHROMATIN REGIONS.	17
FIGURE 7: HEMATOPOIESIS IN ADULT MAMMALIAN ORGANISMS.	19
FIGURE 8: CLASSIFICATION OF HEMATOLOGICAL MALIGNANCIES.	20
FIGURE 9: CONSEQUENCES OF CANCER-SPECIFIC METHYLATION ALTERATIONS IN TUMOR DEVELOPMENT.	23
FIGURE 10: APPLICATION RANGE FOR CpG ISLAND HYPERMETHYLATION IN CANCER DIAGNOSTIC AND TREATMENT ROUTINE.	33
FIGURE 11: INTRACELLULAR METABOLIC PATHWAYS OF AZACYTIDINE AND 5-AZA-2'-DEOXYCYTIDINE.	37
FIGURE 12: SCHEMATIC REPRESENTATION OF GST-MEDIATED CELLULAR DETOXIFICATION.	40
FIGURE 13: ORGANIZATION OF GSTP1 GENE PROMOTER IN HUMAN.	41
FIGURE 14: CONFIGURATION OF PTGS2 PROMOTER.	44
FIGURE 15: IMPLICATION OF PTGS2/PGE2 SIGNALING IN THE HALLMARKS OF CANCER.	45
FIGURE 16: SEDIMENTATION PROFILE OF WHOLE BLOOD CELLS SEPARATED BY FICOLL.	76
FIGURE 17: SCHEMATIC REPRESENTATION OF FLOW CYTOMETRY PRINCIPLE.	84
FIGURE 18: METHYLATION-SPECIFIC PCR PRINCIPAL.	93
FIGURE 19: CHEMICAL PROCESS OF THE BISULFITE-INDUCED DEAMINATION OF CYTOSINE TO URACIL.	98
FIGURE 20: SCHEMATIC OVERVIEW OF CROSS-LINKED CHROMATIN IMMUNOPRECIPITATION PROCEDURE.	101
FIGURE 21: ANALYSIS OF BASAL GSTP1 EXPRESSION IN HUMAN LEUKEMIA AND LYMPHOMA CELL LINES.	106
FIGURE 22: EFFECT OF DAC TREATMENT ON GSTP1 EXPRESSION IN LEUKEMIA/LYMPHOMA CELL LINES.	108
FIGURE 23: ANALYSIS OF GSTP1 EXPRESSION IN CONTROL AND DAC-TREATED K-562, RAJI AND MEG-01 CELLS BY IMMUNOFLUORESCENCE.	110
FIGURE 24: QUANTIFICATION OF GSTP1 EXPRESSION IN DAC-TREATED K-562, MEG-01 AND RAJI CELLS.	112
FIGURE 25: TOTAL GLUTATHIONE S-TRANSFERASE ACTIVITY IN DAC-TREATED LEUKEMIA CELL LINES.	114
FIGURE 26: EFFECTS OF HDAC INHIBITORS ON GSTP1 EXPRESSION IN LEUKEMIA AND LYMPHOMA CELL LINES AND ON TOTAL HISTONE H4 ACETYLATION.	116
FIGURE 27: CpG ISLAND ANALYSIS OF THE GSTP1 PROMOTER REGION.	117
FIGURE 28: BSP ANALYSIS OF GSTP1 PROMOTER REGION IN K-562 AND RAJI CELLS.	120
FIGURE 29: BIO-CoBRA ANALYSIS OF GSTP1 PROMOTER METHYLATION STATUS.	122
FIGURE 30: MSP ANALYSIS OF GSTP1 PROMOTER METHYLATION STATUS IN VARIOUS LEUKEMIA AND LYMPHOMA CELL LINES.	123
FIGURE 31: KINETIC ANALYSIS OF DAC-INDUCED DEMETHYLATION OF GSTP1 PROMOTER IN VARIOUS LEUKEMIA AND LYMPHOMA CELL LINES.	125
FIGURE 32: CHARACTERIZATION OF GSTP1 CHROMATIN STRUCTURE IN K-562, RAJI AND MEG-01 LEUKEMIA CELL LINES BY X-CHIP ANALYSIS.	127
FIGURE 33: ANALYSIS OF THE EVOLUTION OF GSTP1 CHROMATIN STRUCTURE AFTER DAC TREATMENT OF K-562, RAJI AND MEG-01 LEUKEMIA CELL LINES BY X-CHIP ASSAY.	129
FIGURE 34: IMMUNOBLOT DETECTION OF PROTEINS ANALYZED IN X-CHIP EXPERIMENTS.	132
FIGURE 35: PREDICTION OF miRNA-GSTP1 mRNA INTERACTION.	135
FIGURE 36: EXPRESSION PATTERN OF POTENTIAL GSTP1 SILENCING miRNAs IN LEUKEMIA CELL LINES WITH HIGH, MODERATE AND LOW GSTP1 EXPRESSION LEVELS.	136

FIGURE 37: PTGS2 EXPRESSION IN VARIOUS LEUKEMIA/LYMPHOMA CELL LINES AND IN HEALTHY DONOR BLOOD CELLS.	138
FIGURE 38: CPG ISLAND PREDICTION FOR PTGS2 PROMOTER REGION.	140
FIGURE 39: ANALYSIS OF PTGS2 PROMOTER METHYLATION IN LEUKEMIA AND LYMPHOMA CELL LINES.	142
FIGURE 40: KINETIC ANALYSIS OF THE DAC-MEDIATED DEMETHYLATION OF PTGS2 PROMOTER IN LEUKEMIA AND LYMPHOMA CELL LINES.	143
FIGURE 41: KINETIC ANALYSIS OF PTGS2 EXPRESSION AFTER DAC TREATMENT.	144
FIGURE 42: FREQUENCY OF PTGS2 PROMOTER METHYLATION IN SAMPLES OF PATIENTS WITH A HEMATOLOGICAL MALIGNANCY.	146
FIGURE 43: DISTRIBUTION OF PTGS2 mRNA EXPRESSION LEVELS IN BLOOD CELLS FROM HEALTHY DONORS AND PATIENTS WITH HEMATOLOGICAL MALIGNANCIES.	147
FIGURE 44: ANALYSIS OF PTGS2 mRNA EXPRESSION IN RELATION TO THE PROMOTER METHYLATION STATE.	148
FIGURE 45: UNIQUE METHYLATION SIGNATURE OF LEUKEMIA AND LYMPHOMA CELL LINES.	150
FIGURE 46: ANALYSIS OF DAC EXPOSURE ON CELL VIABILITY.	153
FIGURE 47: EFFECT OF DAC ON LEUKEMIA AND LYMPHOMA CELL GROWTH AND VIABILITY.	154
FIGURE 48: MORPHOLOGY ANALYSIS OF CELL DEATH IN DAC-TREATED LEUKEMIA AND LYMPHOMA CELL LINES.	156
FIGURE 49: EVALUATION OF GLOBAL METHYLATION IN VARIOUS LEUKEMIA CELL LINES BY MSRA. .	158
FIGURE 50: ANALYSIS OF THE EFFECT OF DAC ON DNMT1 EXPRESSION.	159
FIGURE 51: KINETIC ANALYSIS OF THE GLOBAL DAC-INDUCED DNA DEMETHYLATION BY MSRA. .	161
FIGURE 52: EVALUATION OF THE INFLUENCE OF DAC TREATMENT ON RAJI CELL PROLIFERATION. .	163
FIGURE 53: EFFECT OF DAC TREATMENT ON THE DOUBLING TIME OF RAJI CELLS.	164
FIGURE 54: ANALYSIS OF THE LINK BETWEEN CELL DIVISION AND GSTP1 EXPRESSION IN DAC-TREATED RAJI CELLS.	165
FIGURE 55: ANALYSIS OF GSTP1 PROMOTER METHYLATION AFTER CELL SORTING BASED ON GSTP1 EXPRESSION IN DAC-TREATED RAJI CELLS.	167
FIGURE 56: METHYLATION ANALYSIS OF VARIOUS GENES IN CONTROL AND DAC-TREATED RAJI CELLS.	169
FIGURE 57: ANALYSIS OF GSTP1 PROMOTER METHYLATION PATTERN AFTER DAC RECOVERY. ...	173

List of tables

TABLE 1: GENES FOUND FREQUENTLY HYPERMETHYLATED IN HEMATOPOIETIC MALIGNANCIES.....	25
TABLE 2: LIST OF CHEMICAL PRODUCTS AND THEIR SUPPLIERS.	50
TABLE 3: COMMON BUFFERS AND SOLUTIONS.	52
TABLE 4: GEL ELECTROPHORETIC MIGRATION OF DNA MOLECULES.	52
TABLE 5: BUFFERS AND SOLUTIONS USED FOR THE WESTERN BLOT.	52
TABLE 6: BUFFERS USED FOR THE EXTRACTION OF NUCLEAR FACTORS.	53
TABLE 7: BUFFER USED FOR HISTONE ISOLATION.	53
TABLE 8: BUFFERS USED FOR CROSS-LINKING CHROMATIN IMMUNOPRECIPITATION (X-CHIP).	53
TABLE 9: KITS FOR THE EXTRACTION AND PURIFICATION OF PCR PRODUCTS, DNA, RNA AND PROTEINS.	54
TABLE 10: SOLUTIONS USED FOR BISULFITE CONVERSION OF GENOMIC DNA FOR DEEP SEQUENCING ANALYSIS ON THE GS FLX-PLATFORM.	54
TABLE 11: DNA AND RNA CAPILLARY ELECTROPHORESIS.....	55
TABLE 12: IMMUNODETECTION OF BLOTTED PROTEINS.	55
TABLE 13: MEDIUM AND ADDITIVES TO CULTURE MAMMALIAN SUSPENSION CELLS.	56
TABLE 14: MEDIUM AND THEIR ADDITIVES USED IN BACTERIAL CULTURE.	56
TABLE 15: MAMMALIAN CELL LINES USED IN CELL CULTURE	57
TABLE 16: BACTERIAL CELL CLONES AND THEIR SUPPLIERS.	57
TABLE 17: ENDONUCLEASES USED FOR RESTRICTION ASSAYS.	58
TABLE 18: DNA-SPECIFIC DNA POLYMERASES USED FOR VARIOUS PCR APPLICATIONS.	58
TABLE 19: RNA-SPECIFIC DNA POLYMERASES USED FOR EXPRESSION ANALYSIS.	59
TABLE 20: NUCLEASES, PROTEASES AND PROTEINS.....	59
TABLE 21: OLIGONUCLEOTIDES USED FOR BSP AND BIO-COBRA ANALYSIS.	59
TABLE 22: OLIGONUCLEOTIDES USED FOR MSP ASSAYS.....	60
TABLE 23: OLIGONUCLEOTIDES USED FOR BISULFITE DEEP SEQUENCING ANALYSIS.	62
TABLE 24: OLIGONUCLEOTIDES USED FOR EXPRESSION ANALYSIS.	64
TABLE 25: OLIGONUCLEOTIDES USED FOR X-CHIP ANALYSIS.	64
TABLE 26: OLIGONUCLEOTIDES USED FOR miRNA EXPRESSION PROFILE ANALYSIS.	64
TABLE 27: PRIMARY ANTIBODIES USED FOR WESTERN BLOT ANALYSIS.	66
TABLE 28: ANTIBODIES USED FOR X-CHIP.....	66
TABLE 29: HORSE RADISH PEROXIDASE-CONJUGATED SECONDARY ANTIBODIES USED FOR WESTERN BLOT ANALYSIS.	67
TABLE 30: SECONDARY ANTIBODIES USED FOR IMMUNODETECTION BY CYTOMETRY OR MICROSCOPY ANALYSES.....	68
TABLE 31: DNA MARKERS USED IN ELECTROPHORETIC MIGRATIONS.	68
TABLE 32: PROTEIN MARKER USED IN WESTERN BLOT.....	68
TABLE 33: PLASMID VECTORS AND MODIFIED DNA.	68
TABLE 34: DEVICES AND INSTRUMENTS.....	68
TABLE 35: TOOLS AND RESOURCES FOR GSTP1 miRNA TARGET PREDICTION.	72
TABLE 36: COMPOSITION OF THE BISULFITE SEQUENCING AND BISULFITE DEEP SEQUENCING PCR MASTER MIXTURE.	91
TABLE 37: CYCLING CONDITIONS FOR THE BISULFITE SEQUENCING PCR WITH THE HOT START <i>TAQ</i> POLYMERASE.	91
TABLE 38: CYCLING CONDITIONS FOR THE BISULFITE PCR WITH THE HOT FIRE POLYMERASE.	91
TABLE 39: CYCLING CONDITIONS FOR THE BISULFITE PCR WITH THE PLATINUM <i>TAQ</i> POLYMERASE.	91
TABLE 40: COMPOSITION OF COLONY PCR MASTER MIX.	92
TABLE 41: CYCLING PROGRAM FOR COLONY PCR.	92
TABLE 42: COMPOSITION OF THE MSP MASTER MIX.....	94
TABLE 43: CYCLING CONDITIONS FOR METHYLATION-SPECIFIC PCR.	94
TABLE 44: COMPOSITION OF THE REAL-TIME PCR MASTER MIX.	96
TABLE 45: CYCLING PROGRAM FOR THE REAL-TIME PCR.	96
TABLE 46: COMPOSITION OF THE REAL-TIME PCR MASTER MIX FOR miRNA EXPRESSION ANALYSIS.	96
TABLE 47: CYCLING PROGRAM FOR THE REAL-TIME PCR FOR miRNA EXPRESSION ANALYSIS.	97
TABLE 48: ANALYSIS OF THE GSTP1 METHYLATION STATUS IN LEUKEMIA AND LYMPHOMA PATIENT SAMPLES.	133

Appendix

Appendix 1: List of patient samples used for this study.

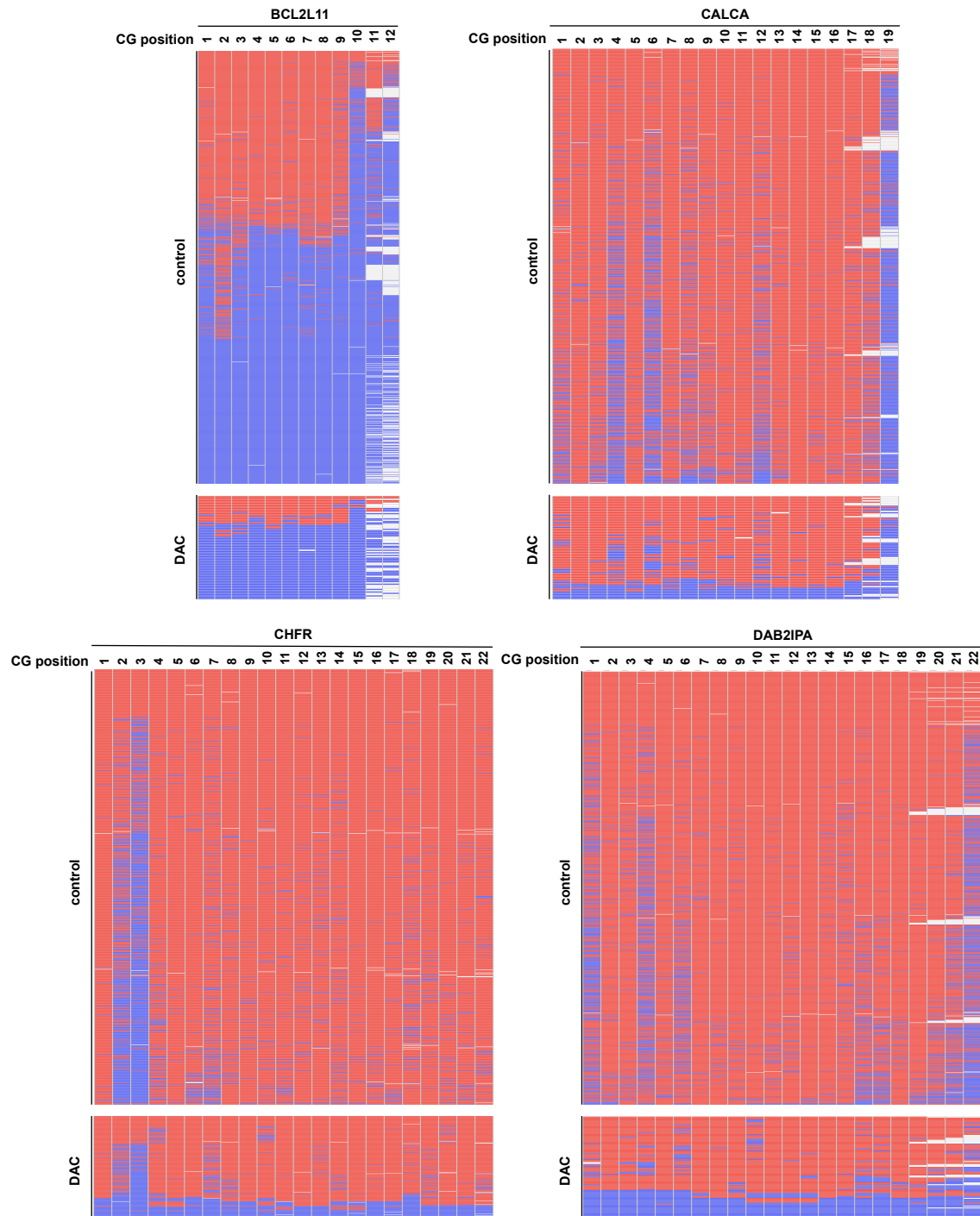
Anonymization	Age (years)	Organ	Diagnosis	Origin
CLL1	57	lymph node	CLL	Liège
CLL2	77	lymph node	CLL	Liège
CLL3	69	lymph node	CLL	Liège
CLL4	60	lymph node	CLL	Liège
CLL5	73	lymph node	CLL	Liège
CLL6	78	lymph node	CLL	Liège
CLL7	69	lymph node	CLL	Liège
CLL8	64	lymph node	CLL	Liège
CLL9	88	lymph node	CLL	Liège
CLL10	83	lymph node	CLL	Liège
CLL11	75	lymph node	CLL	Liège
CLL12	81	Parotid gland	CLL	Liège
CLL13	41	lymph node	CLL	Liège
CLL14	31	lymph node	CLL	Liège
DLBCL1	68	lymph node	DLBCL	Liège
DLBCL2	65	lymph node	DLBCL	Liège
DLBCL3	40	lymph node	DLBCL	Liège
DLBCL4	71	spleen	DLBCL	Liège
DLBCL5	72	lymph node	DLBCL	Liège
DLBCL6	42	lymph node	DLBCL	Liège
DLBCL7	67	stomach	DLBCL	Liège
DLBCL8	74	lymph node	DLBCL	Liège
DLBCL9	78	lymph node	DLBCL	Liège
DLBCL10	52	lymph node	DLBCL	Liège
DLBCL11	46	lymph node	DLBCL	Liège
DLBCL12	76	subcutaneous tissue	DLBCL	Liège
FL1	47	lymph node	FL	Liège
FL2	55	lymph node	FL	Liège
FL3	64	lymph node	FL	Liège
FL4	58	retroperitoneum	FL	Liège
FL5	65	lymph node	FL	Liège

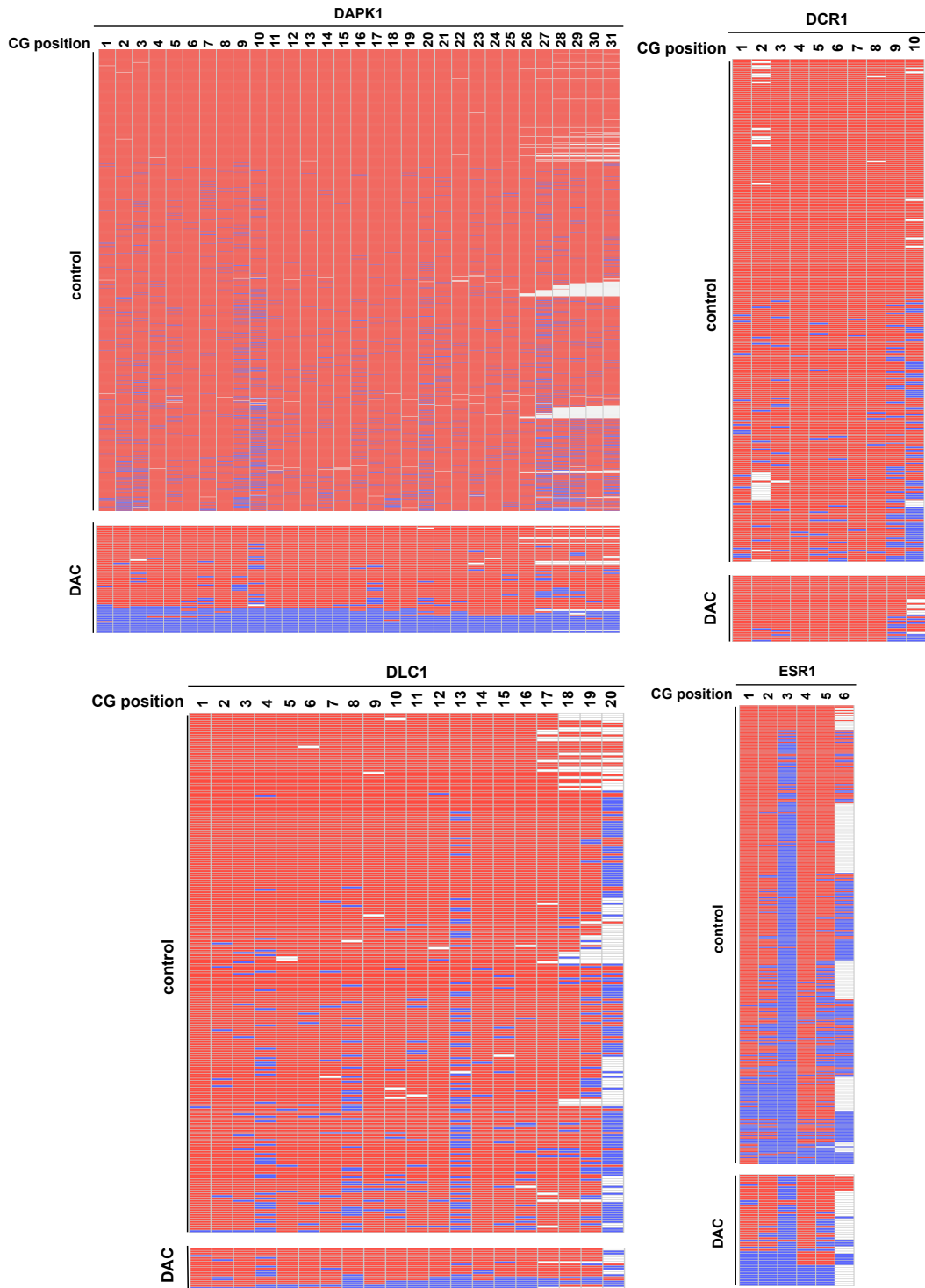
Anonymization	Age (years)	Organ	Diagnosis	Origin
FL6	44	lymph node	FL	Liège
FL7	65	lymph node	FL	Liège
FL8	50	lymph node	FL	Liège
FL9	78	lymph node	FL	Liège
FL10	66	lymph node	FL	Liège
FL11	40	lymph node	FL	Liège
FL12	57	lymph node	FL	Liège
MCL1	72	lymph node	MCL	Liège
MCL2	72	lymph node	MCL	Liège
MCL3	50	lymph node	MCL	Liège
MCL4	47	lymph node	MCL	Liège
MCL5	50	bronchus	MCL	Liège
MCL6	77	tonsil	MCL	Liège
MCL7	72	eye socket	MCL	Liège
MCL8	78	lymph node	MCL	Liège
MCL9	80	lymph node	MCL	Liège
MCL10	73	lymph node	MCL	Liège
MCL11	73	lymph node	MCL	Liège
MCL12	53	lymph node	MCL	Liège
BL1	64	lymph node	BL	Liège
BL2	34	liver	BL	Liège
BL3	58	lymph node	BL	Liège
LP1	n.a.	bone marrow	ALL	Nancy
LP2	n.a.	n.a.	AML	Nancy
LP3	n.a.	bone marrow	AML	Nancy
LP4	n.a.	bone marrow	AML	Nancy
LP5	n.a.	blood	CLL	Nancy
LP6	n.a.	n.a.	CLL	Nancy
LP7	n.a.	n.a.	AML	Nancy
LP10	n.a.	n.a.	CLL	Nancy
LP11	n.a.	bone marrow	AML	Nancy
LP35	n.a.	bone marrow	AML	Nancy
LP37	n.a.	bone marrow	ALL	Nancy
LP39	n.a.	bone marrow	AML	Nancy
LP40	n.a.	n.a.	ALL	Nancy
LP41	n.a.	bone marrow	ALL	Nancy

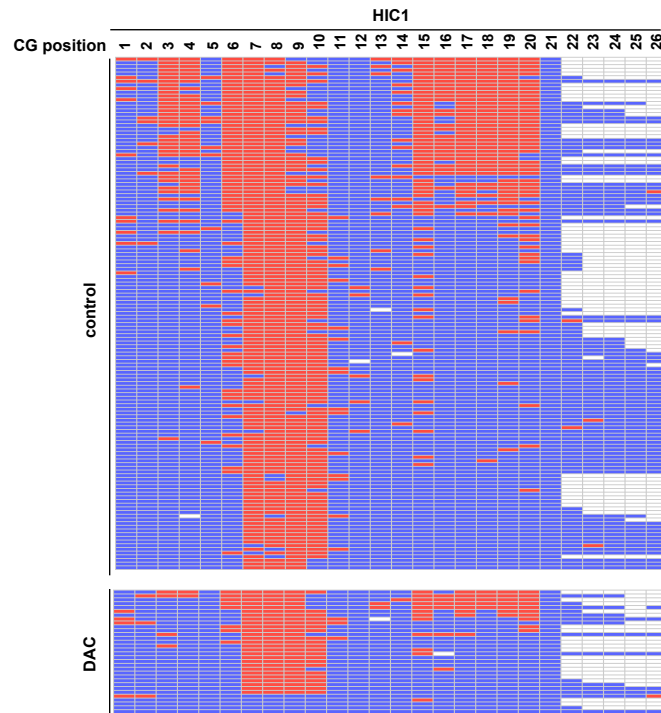
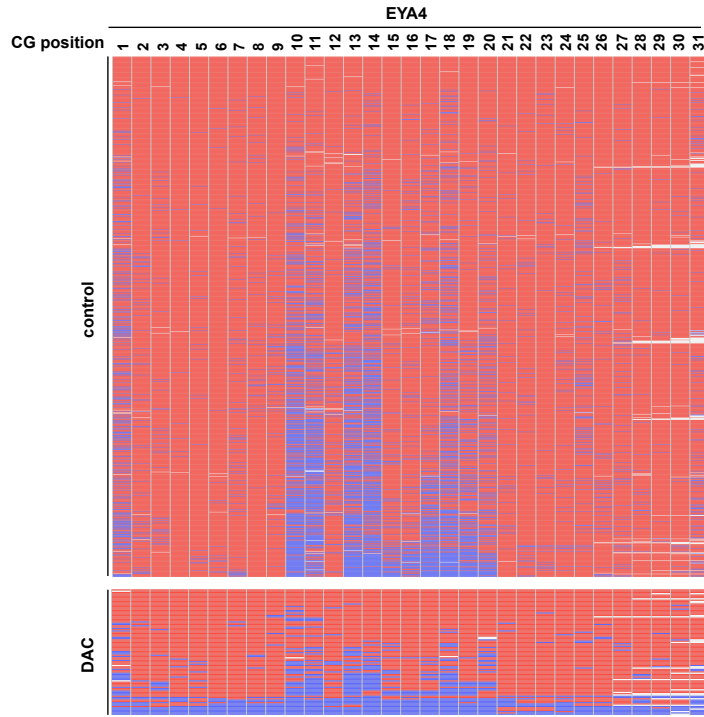
Anonymization	Age (years)	Organ	Diagnosis	Origin
LP43	n.a.	n.a.	ALL	Nancy
LP46	n.a.	n.a.	ALL	Nancy
LP48	n.a.	n.a.	ALL	Nancy
LP50	n.a.	bone marrow	AML	Nancy
LP54	n.a.	n.a.	AML	Nancy
601866	n.a.	blood	CML	Marseille
602393	n.a.	blood	BL	Marseille
603112	n.a.	blood	AML	Marseille
701757	n.a.	blood	AML	Marseille
702082	n.a.	blood	AML	Marseille
602519	n.a.	blood	AML	Marseille
700711	n.a.	blood	AML	Marseille
600389	n.a.	blood	AML	Marseille
603558	n.a.	blood	AML	Marseille
800563	n.a.	blood	AML	Marseille
703142	n.a.	blood	AML	Marseille
703821	n.a.	blood	MDS	Marseille
703821	n.a.	Bone marrow	MDS	Marseille
CHL1	n.a.	Blood	CML	CHL Luxembourg
CHL2	n.a.	Blood	CML	CHL Luxembourg
CHL3	n.a.	Blood	CML	CHL Luxembourg

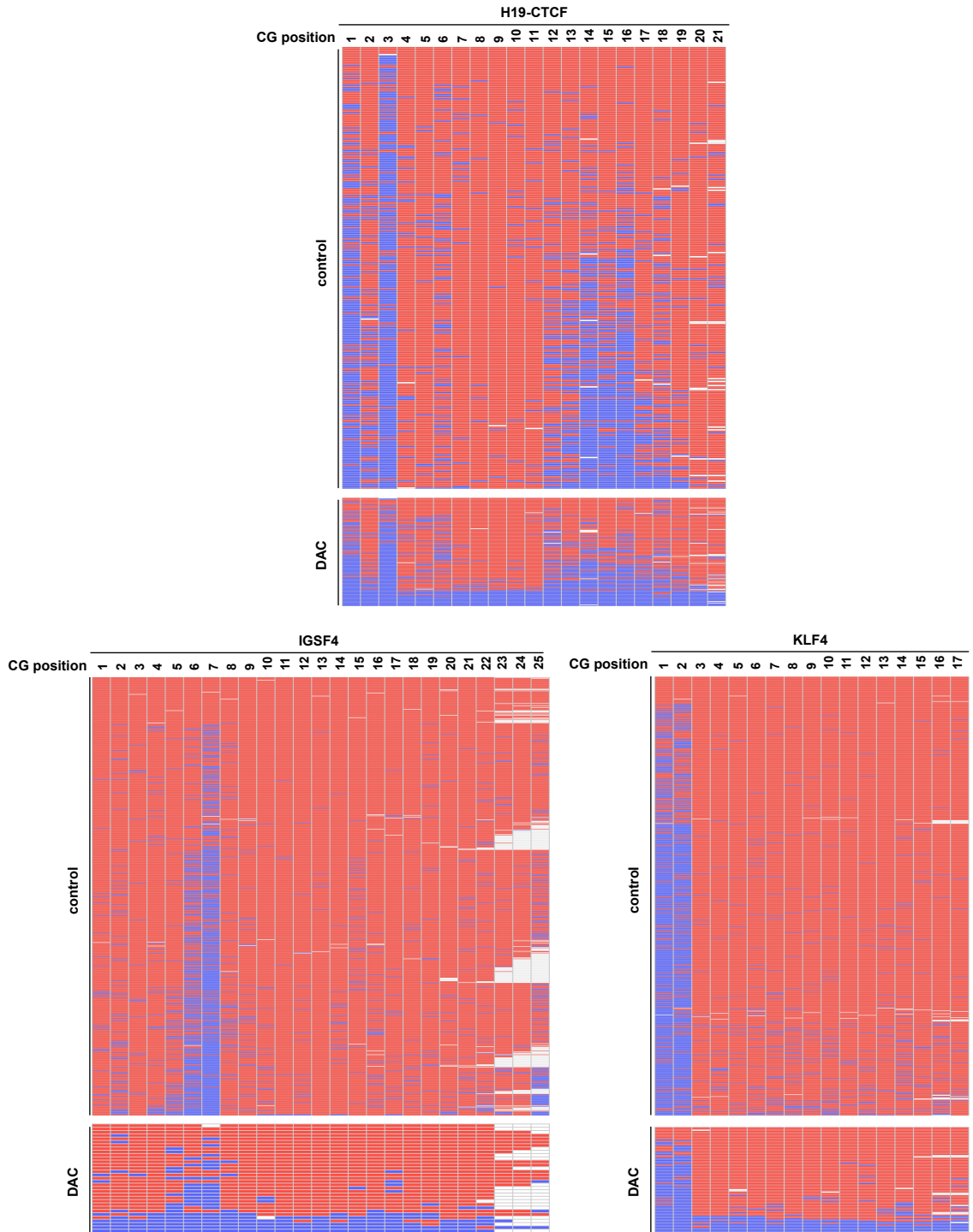
ALL: acute lymphoblastic leukemia, AML: acute myeloid leukemia, CLL: chronic lymphocytic leukemia, CML: chronic myeloid leukemia, DLBCL: diffuse large B-cell lymphoma, MCL: mantle cell lymphoma, FL: follicular lymphoma, BL: Burkitt's lymphoma, MDS: myelodysplastic syndrome, n.a.: information not available.

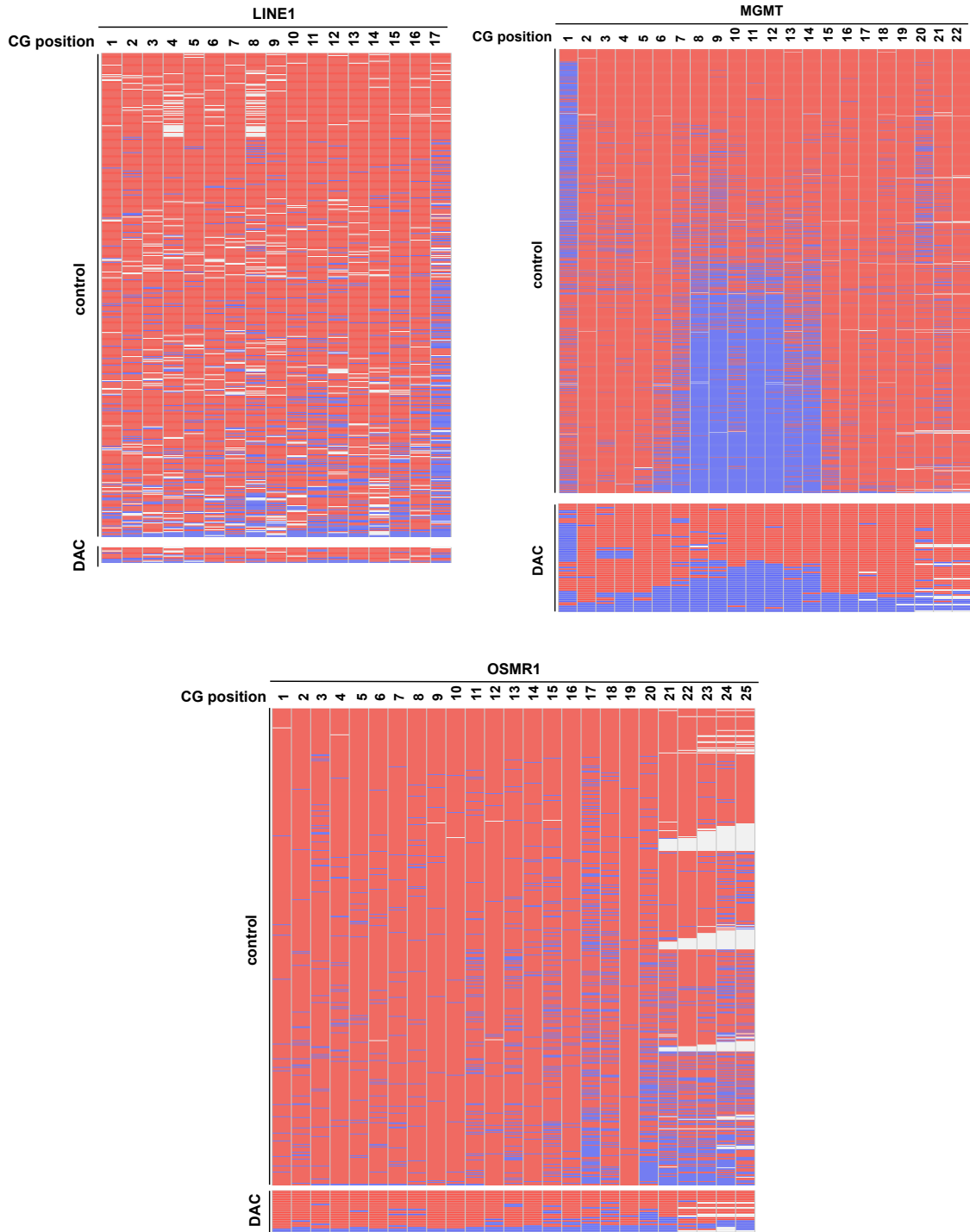
Appendix 2: Genomic DNA from RAJI cells treated for 3 days with 2 μ M DAC was bisulfite converted and regions of interest amplified by PCR. Methylation pattern was determined by next generation sequencing on a GS FLX platform. Detailed view on the sequence reads of *BCL2L11*, *CALCA*, *CHFR*, *DAB2IPA*, *DAPK1*, *DCR1*, *DLC1*, *ESR1*, *EYA4*, *HIC1*, *H19*, *IGSF4*, *KLF4*, *LINE1*, *MGMT*, *OSMR1*, *PTGS2*, *RARB*, *THBS1*, *TIMP3* and *TP73*. Red bars indicate methylated and blue bars unmethylated CpGs.

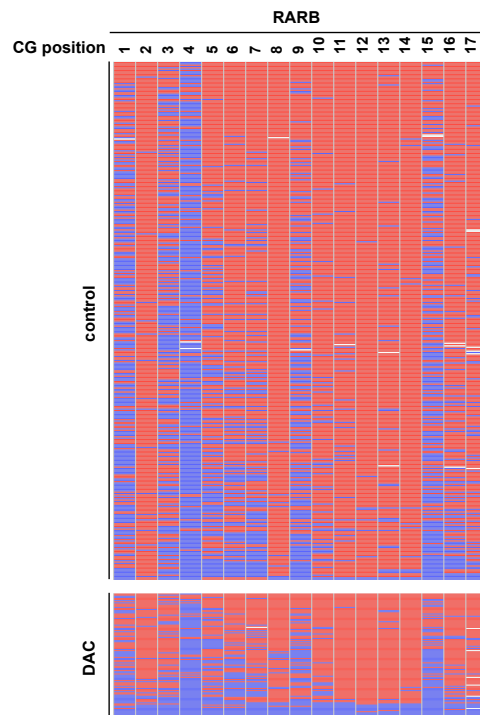
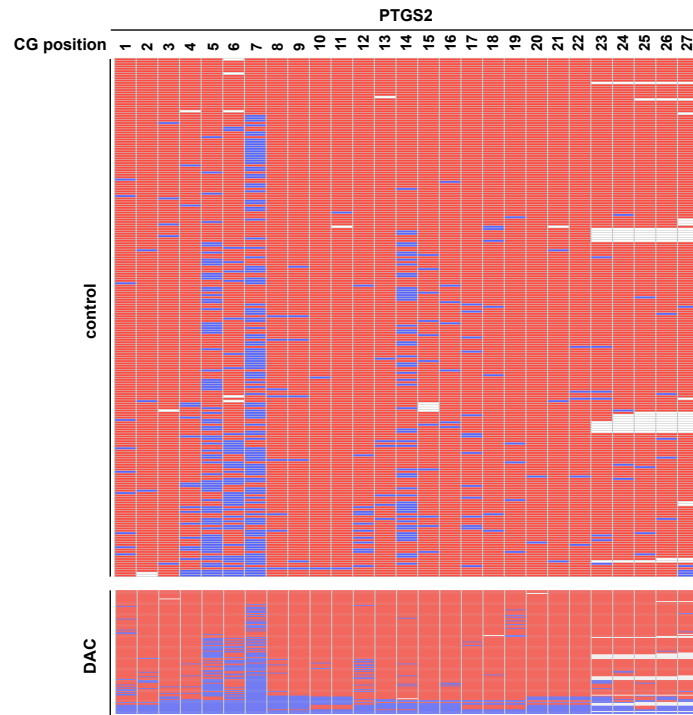


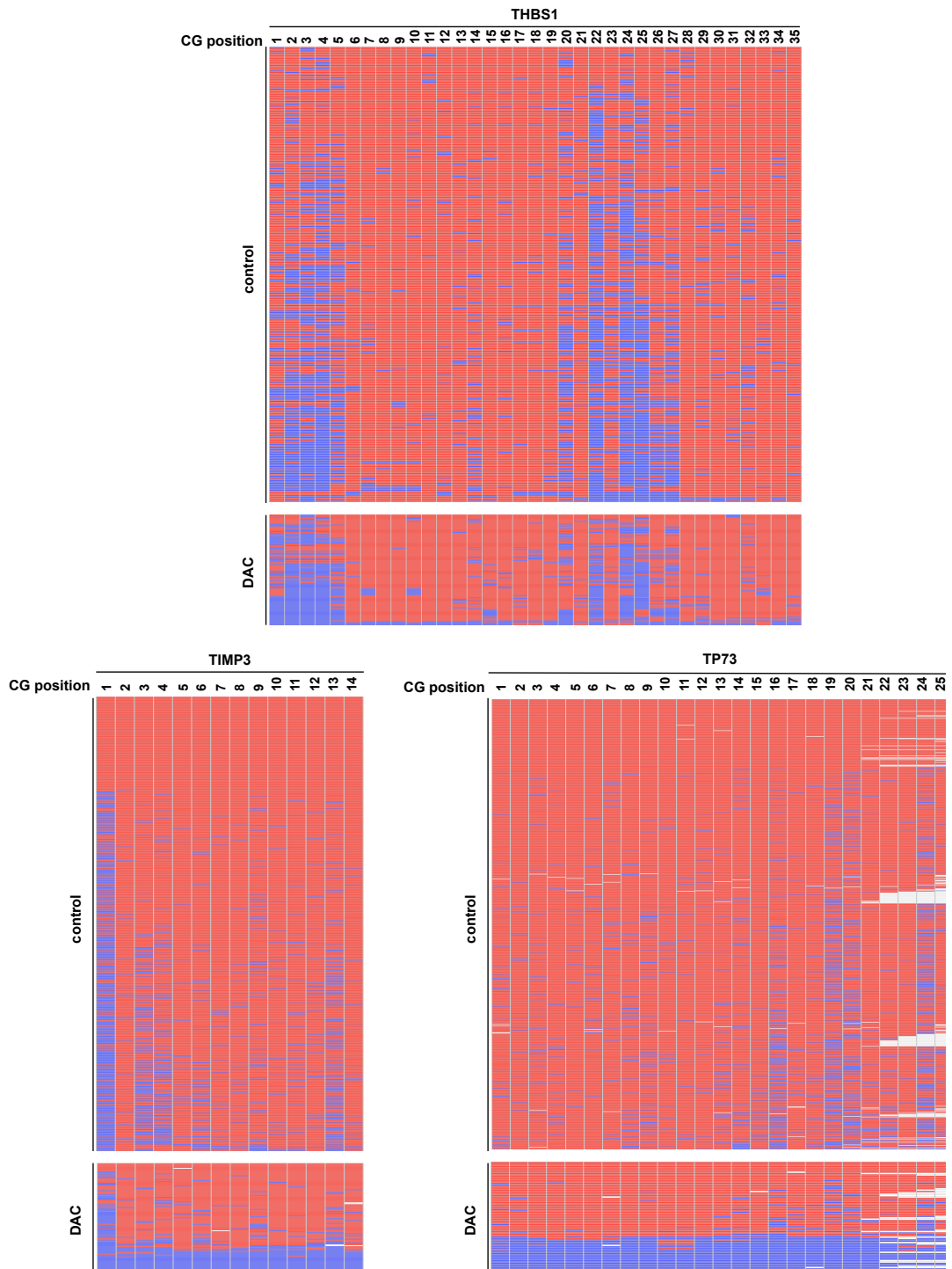












Curriculum vitae

KARIUS Tommy

25B, rue d'Iltzig
L-5231 Sandweiler
Luxembourg

Mobile phone: +352 621390095

E-mail: tommy.karius@lbmcc.lu, temschen@googlemail.com

Date of birth: 20 march 1980 at Luxembourg

Marital status: single

Nationality: Luxembourgian

Formation

- 2004 – 2007 Diplombiologie mit Schwerpunkt Human und Molekularbiologie
Universität des Saarlandes, Saarbrücken
2007 Diplombiologie mit Schwerpunkt Human und Molekularbiologie
- 2002 – 2004 Diplombiologie mit Schwerpunkt Human und Molekularbiologie
Universität des Saarlandes, Saarbrücken
2004 Diplom-Vorprüfung für Studierende der Biologie
- 2000 - 2002 Sciences biologiques
Université catholique de Louvain
- 1994 – 2000 Lycée de garçons Luxembourg
2000 Diplôme de fin d'études secondaires
- 1992 - 1994 École privée Notre-Dame Sainte-Sophie, Luxembourg
- 1986 - 1992 École primaire Commune de Lenningen

Languages

German, English, French	Spoken and written
Luxembourgish	Mother tongue

Computer skills

Microsoft Office, Vector NTI, Oligo, Finch TV, CLC Free Workbench, GeneSnap, FlowJo, ImageJ, Quantity One, End Note, BiQ Analyzer HT, MethMarker

Work experiences

- 2008 – 2011 Ph.D. thesis
Laboratoire de biologie moléculaire et cellulaire du cancer Luxembourg (Dr. M. Schnekenburger, Dr. M. Diederich), Universität des Saarlandes (Prof. J. Walter)
Subject: Mapping the unique epigenetic signature of hematological malignancies
- 2008 Student research assistant at the genetic/epigenetic institute
Universität des Saarlandes Saarbrücken (Prof. J. Walter)
- 2007 Diploma thesis at the genetic /epigenetic institute
Universität des Saarlandes, Saarbrücken (Prof. J. Walter)
Subject: Establishment of an hairpin bisulfite PCR assay to analyse the complementary methylation pattern of repetitive elements in mouse.
Activity analysis of a chimeric methyltransferase.
- 2006 Skilled work at the genetic /epigenetic institute (Prof. J. Walter)
Universität des Saarlandes, Saarbrücken
Subject: Construction of a chimeric methyltransferase out of M.BssHII and Dnmt1.
- 1996-1999 Student-job, Téléphonie S.A.
- 1995 Student-job, Administration communale de Lenningen

Practical trainings and workshops

- 2011 3130 Genetic analyzer (ABI), GS-FLX deep sequencing (Roche)
- 2010 Incucyte (Essen instruments), Imagequant LAS4000 (GE)
- 2009 Operator training FACSCalibur 4 colours (BD), healthcare Gel 2D (GE)
- 2008 CellR fluorescent microscopy imaging system (Olympus)
- 2006 *Seminars:* « Aktuelle Themen der Entwicklungsbiologie », « Neue Entwicklungen in der molekularen Zellbiologie », « Genom Evolution »
Practical training virology / immunology, developmental biology
- 2005 *Advanced practical training: genetics*
Practical trainings: humane genetics, physiology, pharmacology und toxicology, molecular biology, structure biology, biophysics, biochemistry, microbiology
- 2004 *Practical training: molecular cell biology*
Basic practical trainings: genetics, microbiology, molecular biology, biochemistry, biophysics, developmental biology
- 2003 *Basic practical trainings:* molecular cell biology, histology

Meetings

- 2011 Cell Signalomics 2011, Kirchberg, Luxembourg; CLEPSO meeting 2011, Homburg, Germany; Annual Mini-Symposium, Namur, Belgium
- 2010 Inflammation 2010, Kirchberg, Luxembourg; Epigenetic mechanisms in health and disease meeting 2010, Bruxelles, Belgium; Seminaire des jeunes chercheurs 2010, Louvain Woluwé, Belgium
- 2009 First LCA Summer course 2009, Strassen, Luxembourg; Lucilinx 2009, Limpertsberg, Luxembourg; Chromatin: Structure and Function 2009, Guanacaste, Costa Rica; 4th Luxembourgish Cytometry meeting 2009, Strassen, Luxembourg; Seminaire des jeunes chercheurs 2009, Gembloux, Belgium
- 2008 3rd Luxembourgish Cytometry meeting 2008, Strassen, Luxembourg; ImageJ User and Developer Conference 2008, Kirchberg, Luxembourg; Seminaire des jeunes chercheurs 2008, Liège, Belgium
-

Publications:
Reversible epigenetic fingerprint-mediated glutathione-S-transferase P1 gene silencing in human leukemia cell lines

Tommy Karius, Michael Schnekenburger, Jenny Gelfi, Jörn Walter, Mario Dicato, Marc Diederich

Biochemical pharmacology, 2011 Jun 1;81 (11):1329-42

Targeting inflammatory cell signaling mechanisms: a promising road to new therapeutic agents in chemoprevention and cancer therapy

Michael Schnekenburger, **Tommy Karius**, Claudia Cerella, Marc Diederich

Journal of experimental therapeutics & oncology, 2011; 9(1):1-4.

Sustained exposure to the DNA demethylating agent; 2'-deoxy-5-azacytidine; leads to apoptotic cell death in chronic myeloid leukemia by promoting differentiation; senescence; and autophagy

Michael Schnekenburger, Cindy Grandjette, Jenny Ghelfi, **Tommy Karius**, Bernard Foliguet, Mario Dicato, Marc Diederich

Biochemical Pharmacology, 2011 Feb 1;81 (3):364–378

In vivo control of CpG and CpA methylation at repetitive elements by DNA methyltransferases

Julia Arand, David Spieler, **Tommy Karius**, Daniela Meilinger, Alexander Meissner, Thomas Jenuwein, Guo-Liang Xu, Heinrich Leonhardt, Verena Wolf, Jorn Walter
Submitted

Aberrant epigenetic silencing and reduced expression of prostaglandin-endoperoxide synthase 2 gene are common events in human hematological malignancies

Tommy Karius*, Michael Schnekenburger*, Mario Dicato, Marc Diederich
Manuscript in preparation * Contribute equally to this work

Apoptosis in human leukemia cells exposed to the DNA demethylating agent 5-aza-2'-deoxycytidine

Michael Schnekenburger, **Tommy Karius**, Guillaume Yettou, Claudia Cerella, Mario Dicato, Marc Diederich
Manuscript in preparation

Presentations:

- 28/11/2008 **FNR Journal Club**, University of Luxembourg and the Laboratoire de biologie moléculaire et cellulaire du cancer, Kirchberg, Luxembourg
Subject: Gene silencing in cancer by histone H3 lysine 27 trimethylation independent of promoter DNA methylation, Yutaka Kondo et al., Nature Genetics 06/2008; 40(6)
- 13/03/2009 **Laboratory meeting**, Laboratoire de biologie moléculaire et cellulaire du cancer, Kirchberg, Luxembourg
29/06/2009
27/08/2009 Subject: Presentation of the actual research results
19/04/2010
07/06/2010
11/11/2010
- 27/04/2009 **Laboratory evaluation**, Laboratoire de biologie moléculaire et cellulaire du cancer, Kirchberg, Luxembourg
27/09/2009
05/03/2010 Subject: Presentation of the actual projects
20/09/2010
- 09/02/2010 **Project presentation** (Rudy Balling, University of Luxembourg), Laboratoire de biologie moléculaire et cellulaire du cancer, Kirchberg, Luxembourg
- 09/02/2010 **Project presentation** (Bob Phillips, Integrated Biobank Luxembourg), Laboratoire de biologie moléculaire et cellulaire du cancer, Kirchberg, Luxembourg
- 13/09/2011 **Annual Mini-symposium**, Ecole Doctorale Thematique en cancerologie experimentale, Groupe de contact FNRS „miRNA and Cancer, Faculté de medecin, Namur, Belgium
Subject: Reversible epigenetic fingerprint-mediated glutathione-S-transferase P1 gene silencing in human leukemia cell lines

Poster presentations:

- 16/11/2009-19/11/2009 Conference: Chromatin: Structure and Function, Guanacaste, Costa Rica
Poster: Prediction of cell sensitivity and response to 5-aza-2'-deoxycytidine in leukemia cells
- 10/06/2010 Conference: Epigenetic mechanisms in health and disease meeting, Bruxelles, Belgium
Poster: Reversible epigenetic fingerprint-mediated glutathione-S-transferase P1 gene silencing in human leukemia cell lines
- 07/12/2010 Conference: Séminaire des jeunes chercheurs (Télévie), Louvain Woluvé, Belgium
Poster: Reversible epigenetic fingerprint-mediated glutathione-S-transferase P1 gene silencing in human leukemia cell lines
- 12/03/2011-13/03/2011 Conference: CLEPSO, Clinical epigenetics international meeting, Homburg, Germany
Poster: Reversible epigenetic fingerprint-mediated glutathione-S-transferase P1 gene silencing in human leukemia cell lines
- 13/09/2011 Conference: Annual Mini-symposium, Ecole doctorale thématique en cancérologie expérimentale, Groupe de contact FNRS „miRNA and Cancer, Faculté de médecine, Namur, Belgium
Poster: Reversible epigenetic fingerprint-mediated glutathione-S-transferase P1 gene silencing in human leukemia cell lines

Conference staff:

- 27/01/2010-30/01/2010 Inflammation 2010 conference, Inflammation cell signalling mechanisms as therapeutic targets, Kirchberg, Luxembourg
- 26/01/2011-28/01/2011 Cell-Signalomics 2011 conference, Integrated cellular pathology – Systems biology of human disease, Kirchberg, Luxembourg

Internships:

- 2010 LOUREIRO Camilo Maria Helena, Job discovery, Lycée Esch, Luxembourg
- 2011 FRENGER Elodie, Etude des altérations du profil de méthylation de gènes suppresseurs de tumeur dans les leucémies: le cas des leucémies myeloïdes et lymphoblastiques aiguës
MASTER « ingénierie de la santé et sciences du médicament » parcours « Bio-ingénierie et médicaments », Nancy-Université Henri Poincaré